MOLECULAR DIAGNOSTICS, EPIDEMIOLOGY, AND POPULATION GENETICS OF THE SOYBEAN SUDDEN DEATH SYNDROME PATHOGEN, *FUSARIUM VIRGULIFORME*

By

Jie Wang

A DISSERTATION

Submitted to
Michigan State University
in partial fulfillment of the requirements
for the degree of

Plant Pathology - Doctor of Philosophy
Ecology, Evolutionary Biology and Behavior – Dual Major

2016

ABSTRACT

MOLECULAR DIAGNOSTICS, EPIDEMIOLOGY, AND POPULATION GENETICS OF THE SOYBEAN SUDDEN DEATH SYNDROME PATHOGEN, *FUSARIUM VIRGULIFORME*

By

Jie Wang

Soybean sudden death syndrome (SDS), caused by *Fusarium virguliforme*, is one of the most devastating diseases of soybean, responsible for yield losses in both North America and South America. In the United States, *F. virguliforme* is the predominant SDS causal pathogen, while four *Fusarium* species including *F. virguliforme* can cause SDS in South America. All four SDS-causing *Fusarium* species are located in clade2 of the *Fusarium solani* species complex (FSSC) along with three bean root rot (BRR) *Fusarium* pathogens. It is difficult to identify this group of fungi to species level based on morphological traits. In order to address this issue, we developed a specific and sensitive diagnostic real-time quantitative PCR assay (qPCR) for detection and quantification of *F. virguliforme* from plant or environmental samples. This assay was applied in characterization of temporal dynamics of *F. virguliforme* infection and colonization of soybean roots. The quantity of *F. virguliforme* increased over time and reached a plateau at the end of the season. The severity or appearance of SDS foliar symptoms was not associated with quantity of *F. virguliforme* infection, and cultivars with varied SDS resistance levels did not differ in their quantity of *F. virguliforme* in roots.

The fungicide fluopyram has been demonstrated to be effective in reducing SDS foliar symptoms in field trials as a seed treatment; however, *in vitro* evaluation of fungicide baseline sensitivity of *F. virguliforme* had not been determined. In this study, 185 *F. virguliforme* isolates collected from multiple locations in the United States were selected for estimation of fungicide

sensitivity to fluopyram. Overall, the US *F. virguliforme* population appears to be sensitive to fluopyram. The effective concentration to inhibit 50% growth for 95.1% of isolates was determined to be between 0.81 to 5 µg/ml, while only nine isolates were determined to be less sensitive.

Since the first report of SDS in Arkansas in 1971, SDS had been reported in surrounding states with an apparent pattern of dispersal. To date, although SDS has been reported in most soybean producing areas in the United States, limited research has been conducted to date to study the population biology of *F. virguliforme*. We utilized 539 isolates from North and South America in a population genetics study to test the hypothesis that Arkansas was the center of introduction within the United States, and investigate possible intercontinental movement. The Arkansas population demonstrated the highest genotypic diversity and most diverse population structure. Coalescence based migration analysis also supported a directional migration model from Arkansas to Indiana and Michigan. Within the United States, there was a weak positive correlation ($P = 0.08$) between genetic dissimilarity and geographical distance, suggesting a mixed dispersal pattern of *F. virguliforme* in the United States. Although South America has been proposed as the center of origin in previous studies, this hypothesis was only supported in the migrate analysis, and the genotypic diversity and population structure compositions detected in the United States cannot be explained by this hypothesis. Therefore, Arkansas as the center of origin in the United States hypothesis is supported by the population genetic analyses, but the South America as the center of origin hypothesis does not have strong support in our analysis.

I would like to dedicate this dissertation to my parents and to world peace.

ACKNOWLEDGEMENTS

I would like to acknowledge my advisor, Dr. Martin Chilvers, for his persistent support and guidance throughout my graduate study.

I would like to thank my committee members Drs. Frances Trail, Dechun Wang, Jim Smith, and Jan Byrne for their support and encouragement throughout of research. I would also like to thank Dr. Kerry O'Donnell for giving suggestions and providing isolates. Finally, I would like to thank Dr. Tyre Proffer, Dr. George Sundin for their suggestions on my research project.

I would like to acknowledge my funding sources, project GREEEN, Michigan soybean promotion committee, North Central soybean research program, A. L. Rogers scholarship, Beneke's award, and Carter Harrison student award. This research would not have been possible without their funding support.

I would like to thank my lab mates for their help throughout the past years including Janette Jacobs, Alejandro Rojas, Adam Byrne, Devon Rossman, Zach Noel, Mitch Roth, and Olivia Stenzel.

PREFACE

This dissertation includes six chapters: one literature review and five research articles. The research topics in this dissertation covered qPCR diagnostic assay development, temporal dynamics of *Fusarium virguliforme* in root colonization, screening *F. virguliforme* fungicide sensitivity to fluopyram, development of microsatellite markers for *F. virguliforme*, and population genetics of *F. virguliforme* to predict the demographic history of this pathogen.

TABLE OF CONTENTS

LIST OF TABLES

LIST OF FIGURES

CHAPTER 1 LITERATURE REVIEW

Host Plant: Soybean

Soybean (*Glycine max* (L.) Merr.), an annual legume of the Fabaceae family native to East Asia, is widely grown for its edible seeds. Soybean is one of the most important crops in the United States and worldwide. With its versatile uses and wide distribution, soybean has become an important food source for human beings and livestock. It has been estimated that soybean provides ca. 35% of total protein consumed by human directly and indirectly, and soybean is also an important source of oil (Ren and Michael, 2010), accounting for about 90% of oilseed production in the United States (USDA-ERS, 2012). In 2015, soybeans were the second-most planted field crop in the United States after corn, with 82 million acres planted and 81 million acres harvested (USDA-NASS, 2015). More than 80 percent of soybean acreage is concentrated in the Midwest, although significant amount of soybeans are still planted in southern states where soybean was historically grown (Doupnik, 1993; USDA-ERS, 2012). In Michigan, 2.03 million acres were planted in 2015 and 2.02 million acres were harvested with estimated yield of 98.98 million bushels, which is equivalent to $851 million farm-gate values (USDA-NASS, 2015).

Soybean Sudden Death Syndrome

Soybean sudden death syndrome (SDS), caused by the hemibiotrophic fungus, *Fusarium virguliforme*, is responsible for devastating yield reductions in both North and South America (Aoki et al., 2005). A survey conducted from 2003 to 2014 demonstrated that SDS was estimated to be one of the top five most damaging soybean diseases in the United States (Wrather and Koenning, 2009; Bradley and Allen, 2014). From 2010 to 2014, the average annual yield loss caused by SDS was approximately 45 million bushels, which is equivalent to approximately

$450 million cash value (Wrather and Koenning, 2006; Koenning and Wrather, 2010; Bradley and Allen, 2014).

SDS foliar symptoms usually start to develop in the early reproductive stage of soybean (Rupe, 1989; Roy et al., 1997). At this stage, the leaf symptoms begin as pale green to small chlorotic interveinal spots with a diameter of 1-3 millimeters scattered on leaves. With the development of disease, leaves may also demonstrate slight marginal cupping, and a wrinkled or puckered texture. The spots may enlarge or coalesce and eventually become necrotic, and only the region close to the leaf vein will remain green (Figure 1-1B-C). As the disease symptoms progress, severely diseased leaves may drop; only the petioles remained attached to the stem (Figure 1-1A). The most severe SDS symptoms may result in abortion of flowers and pods (Roy et al., 1989; Rupe, 1989). Although foliar symptoms are the most prominent, the causal pathogens have never been isolated from SDS symptomatic leaf tissues (Rupe, 1989). Additionally, molecular mechanism of the SDS pathogenicity proves that the toxins produced by *F. virguliforme* in the root and translocated to the leaves cause foliar symptoms (Ji et al., 2006).

Root symptoms of SDS include severe taproot and lateral root necrosis, internal root discoloration and root biomass reduction. Soybean root infection by *F. virguliforme* occurrs as early as seed germination stage (Gao et al., 2006a). Infected taproots have brownish vascular discoloration expanding from the inner part of the taproot to the lower part of the stem, but the stem pith of the soybean plant remains white in color (Hartman et al., 1999; Hartman et al., 2015). The *F. virguliforme* infected soybean plants showed reduced number of lateral or hairy roots (Roy et al., 1997), so that the infected plants can be easily pulled from soil. Occasionally, the fungus produces blue sporulation structure (sporodochia, Figure 1-1D) on the surface of

taproots or lower part of the stem, which is one of the characteristic diagnostic features for SDS (Roy, 1997).

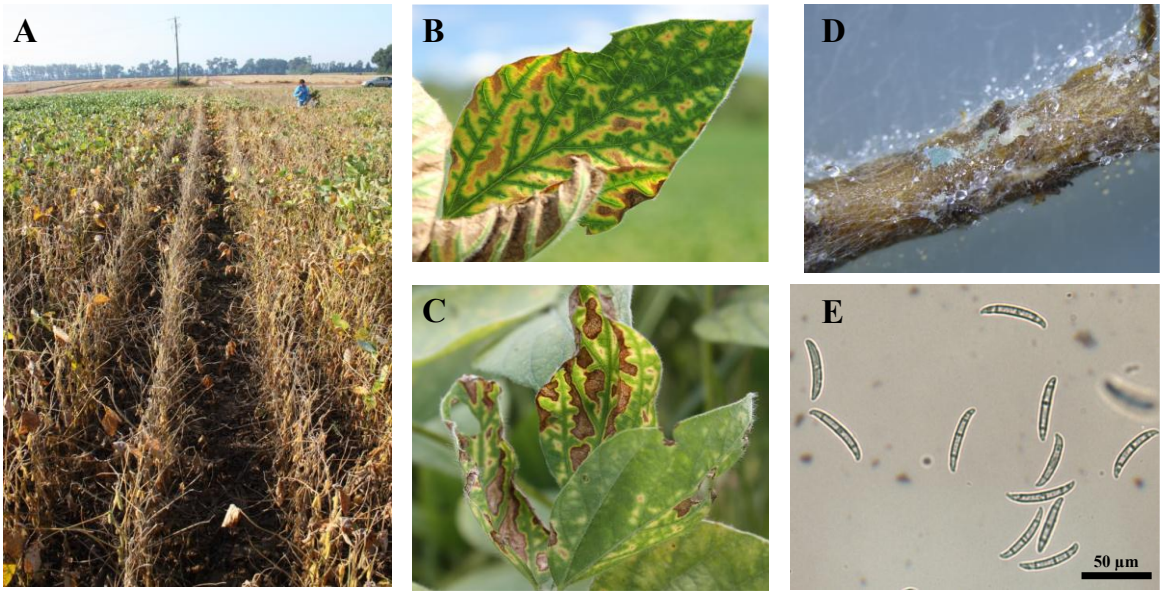

Figure 1-1 Foliar symptoms of soybean sudden death syndrome (SDS) shown in the field: (A) soybean premature defoliation, but petioles remain attached to the stem; (B-C) SDS foliar symptoms developed in the field; (D) asexual sporodochia reproductive structure form on the soybean root, when the infected roots are incubated on water agar for 7 days; (E) *Fusarium virguliforme* macroconidia, scale bar: 50 µm. Figures A-C photo credit to Dr. Martin Chilvers.

Abiotic and biotic factors affecting SDS

SDS severity and incidence in the field can be affected by both abiotic and biotic factors including soil type (Rupe et al., 1993; Scherm and Yang, 1996; Scherm et al., 1998), interactions with soybean cyst nematodes (SCN, *Heterodera glycines*) (Roy et al., 1989; Roy et al., 1997; Roy et al., 2000), environmental conditions (Scherm and Yang, 1996), soybean cultivars (Rupe et al., 2000; Vick et al., 2006), and field management (Vick et al., 2003; Paulitz et al., 2010). Compact soil, low soil temperature at planting, and high soil moisture favors SDS occurrences in the field (Rupe, 1989; McLean and Lawrence, 1993b; Scherm and Yang, 1996; Scherm et al., 1998). Furthermore, severe SCN pressure along with these soil and environmental conditions in the same field will exacerbate the severity and incidence of SDS (Roy et al., 1997). SDS is often

associated with SCN presence, though *F. virguliforme* alone can also cause severe SDS (Hirrel, 1983; Roy et al., 1989; Roy et al., 1997). The role of SCN in the development of SDS is still not clear, results from field (Xing and Westphal, 2006; Westphal et al., 2014) and greenhouse studies (Gao et al., 2006b) are not always in agreement. Field experiments demonstrated a synergistic relationship between SCN and *F. virguliforme* in SDS disease development (Xing and Westphal, 2006; Westphal et al., 2014); however, results from the greenhouse experiment contradicted the findings in the field experiment (McLean and Lawrence, 1993a; Gao et al., 2006b). Additionally, high soil fertility and well-managed soybean fields with high yield potential tend to favor SDS occurrences (Rupe, 1989; Rupe et al., 1993; Scherm et al., 1998).

Distribution of *Fusarium virguliforme*

Fusarium virguliforme is widely distributed in North America with sporadic reports of *F. virguliforme* discovered in Argentina, South Africa, Iran, and Malaysia (Figure 1-2). In the United States, since the first report of SDS in Arkansas in 1971 (Hirrel, 1983), SDS has been reported in the surrounding states with a spreading trend from southern to the northern part of the United States (Figure 1-3). Currently, SDS has been reported in most of the soybean producing states (Roy et al., 1997; Hartman et al., 1999; Pennypacker, 1999; Kurle et al., 2003; Ziems et al., 2006; Bernstein et al., 2007; Chilvers and Brown-Rytlewski, 2010; Tande et al., 2014). The climate in the Midwest is conducive for *F. virguliforme* infection of soybeans, cold and moist weather at planting exacerbates the disease occurrence and severity (Scherm and Yang, 1999). In the early 1990s, SDS was reported in Brazil and Argentina (Nakajima et al., 1996; Scandiani et al., 2003; Scandiani et al., 2004), which are the two major soybeans producing countries in South America (USDA-FAS, 2015). In addition to the Americas, *F. virguliforme* was also isolated

from soybean and soil samples collected in Africa and Asia, respectively (Tewoldemedhin et al., 2013; Chehri et al., 2014; Chehri, 2015).

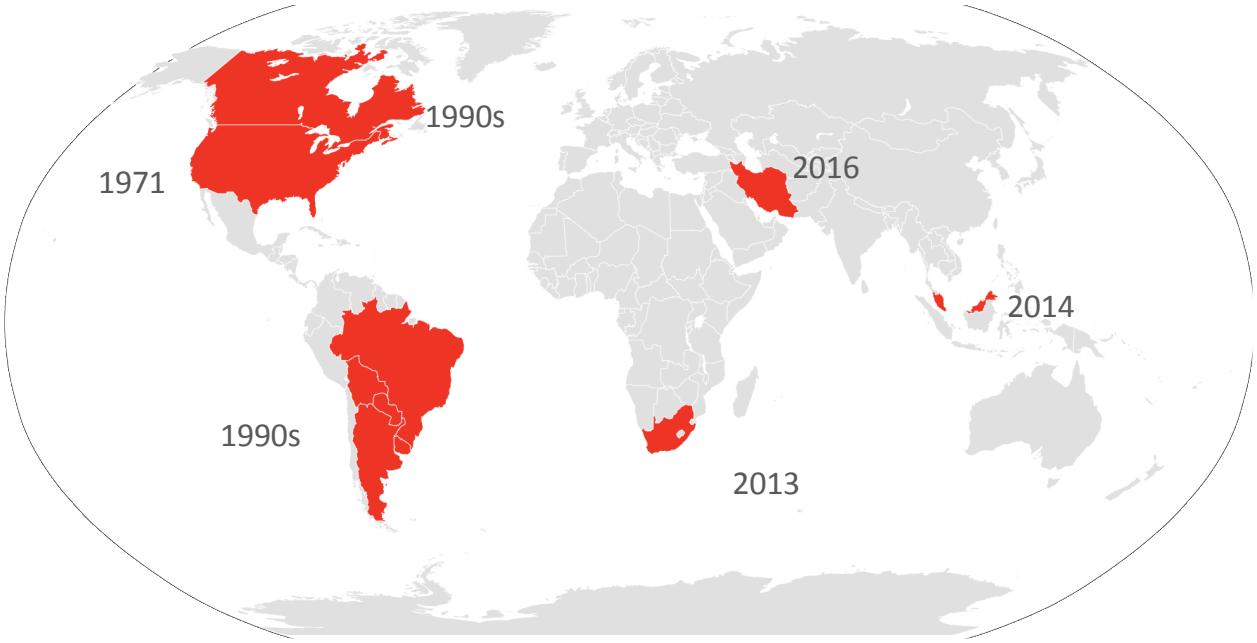

Figure 1-2 SDS or *F. virguliforme* distribution in the world. SDS was first reported in 1970 in Arkansas, United States. In the 1990s, SDS was reported in most soybean producing countries in North and South Americas. In South Africa, SDS was reported and confirmed in 2013. In 2014 and 2016, *F. virguliforme* was isolated from soil collected in Malaysia and Iran.

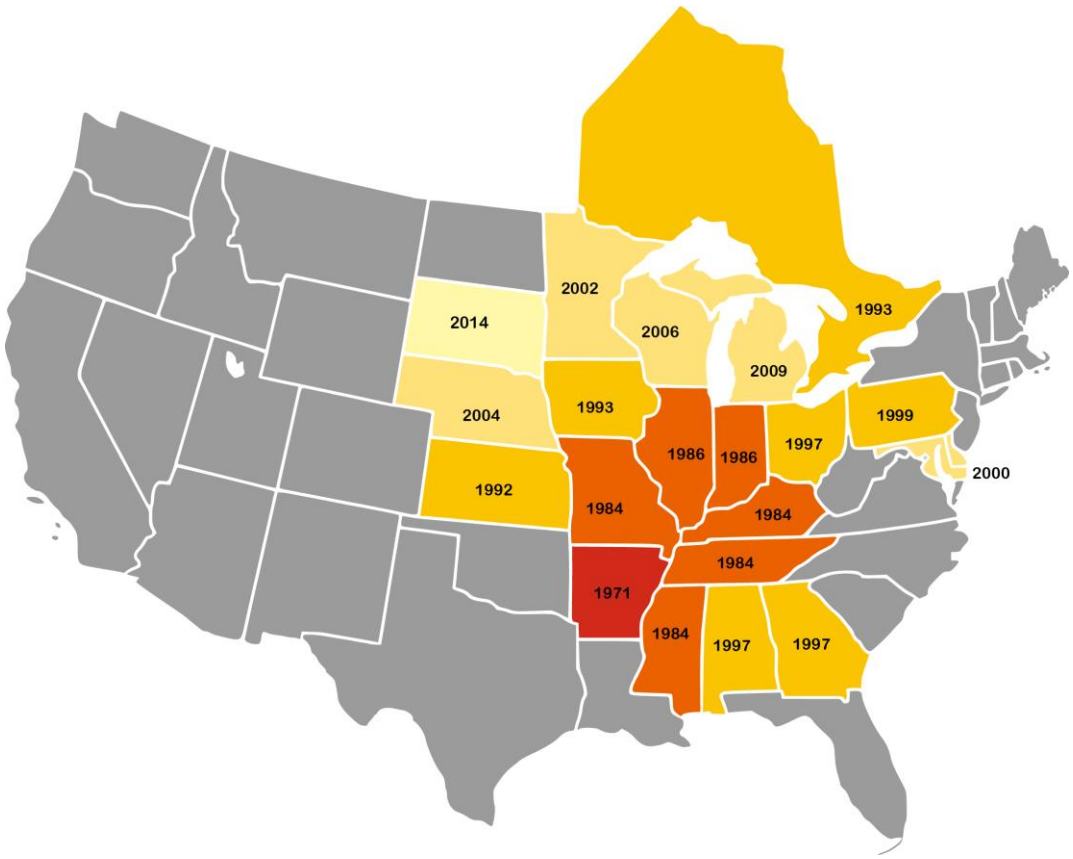

Figure 1-3 Distribution of SDS reported in the United States and Canada as the date of publication on the first report in Plant Disease, number in the map indicates the year SDS was reported to be present in the state.

SDS in Michigan

SDS was confirmed to be present in Michigan in 2009 (Chilvers and Brown-Rytlewski, 2010), but SDS-like symptoms were observed by local county agents and soybean growers in the early 2000s (Karen Zuaver and Martin Chilvers, personal communication). In 2009, SDS was confirmed in five counties located in the south west part of Michigan. Since then, SDS has been confirmed in an additional 21 Michigan countries (Figure 1-4). These diagnoses were confirmed by a PCR diagnostic assay (Wang et al., 2015).

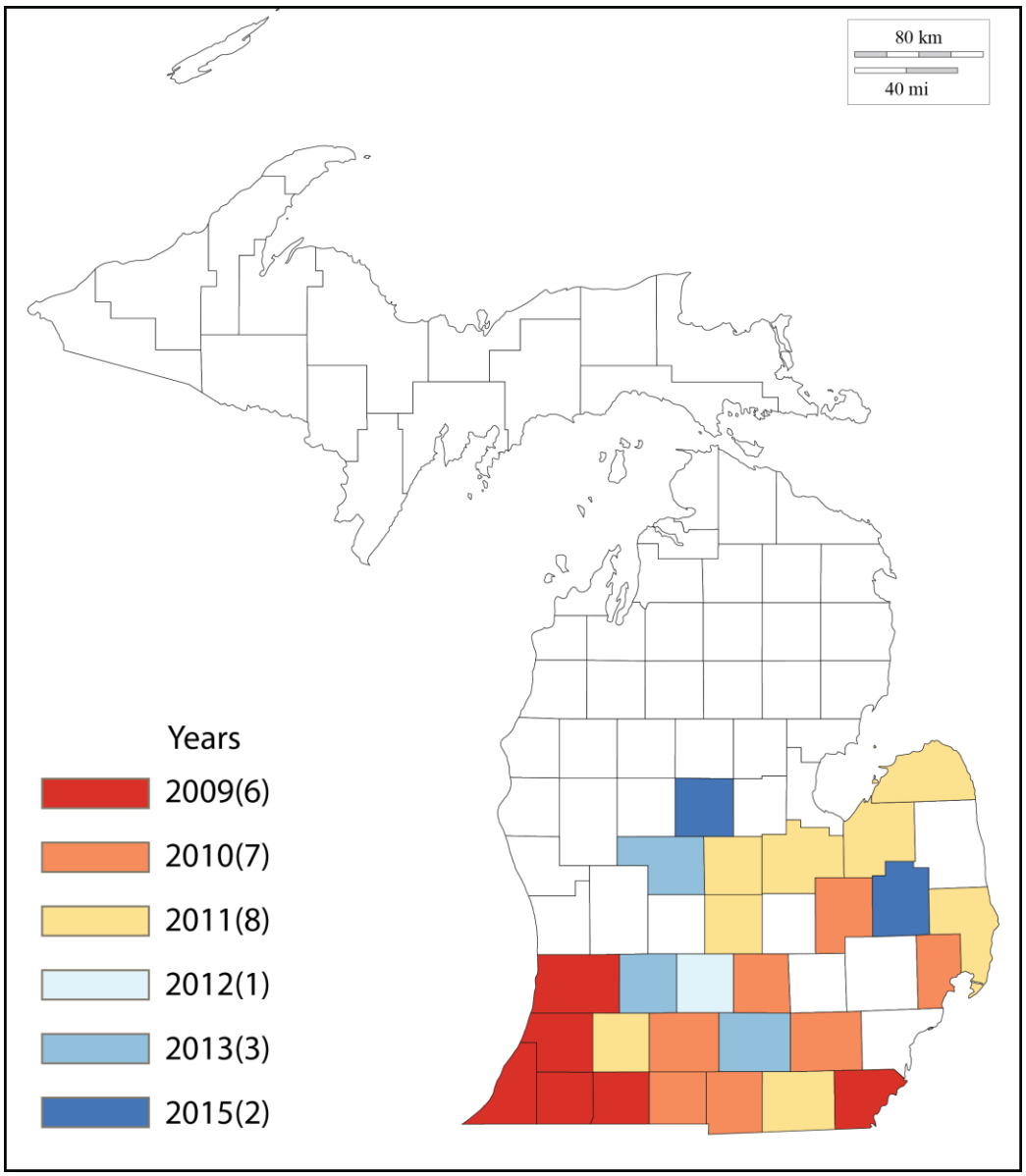

Figure 1-4 SDS distribution in Michigan as confirmed by qPCR assay or isolation of *F. virguliforme*

Taxonomy

The species taxonomy in the *Fusarium* genus has been revised numerous times with additional sampling efforts and DNA sequence data. The morphological species *Fusarium solani* was first described by C.F.P. Von Martius in 1842 as *Fusisporium solani* from rotted potato tubers, *Solanum tuberosum* (Booth, 1975). This species was then reclassified into the *Fusarium* genus by Piers A. Saccardo in 1881 (Saccardo, 1901). The genus *Fusarium* (Family =

Nectriaceae, Order = Hypocreales, Division = Ascomycetes) was divided into 12 sections based on conidia and colony morphology. *Fusarium solani* (Mart.) Appel & Wollenweber (teleomorph = *Nectria haematococca* Berk. & Br.) was categorized within the section *Martiella*, which was first described by Wollenweber and Reinking (1935), comprised 5 species, 10 varieties, and 4 forms. Snyder and Hansen (1941) collapsed the species in section *Martiella* into a single species by deleting the other four species as synonyms of *F. solani*. Booth (1971) and then Gerlach and Nirenberg (1982) proposed the incorporation of four and six species in the section *Martiella*, respectively. Morphological identification of species in section *Martiella* is difficult, because most *Martiella* fusaria were usually reported as polytypic species: *F. solani*, f. sp. or mating populations of *N. haematococca*. Species found within the taxonomy of *F. solani* are now known as the *Nectria haematococca-Fusarium solani* species complex (O'Donnell, 2000). Using sequence based phylogenetic analyses, O'Donnell (2000) proposed that 26 phylogenetically distinct ingroup species are identified in the *Nectria haematococca-Fusarium solani* species complex, of which *F. solani* f. sp. *glycines* was reported as a putative mitosporic species. *Fusarium solani* species complex (FSSC) comprises species that are widely present in soil and responsible for many economically-important plant, animal, and human diseases (O'Donnell, 2000; Zhang et al., 2006), including the soybean SDS causal pathogen *F. virguliforme* (former name: *F. solani* f. sp. *glycines*) (Aoki et al., 2003). Currently, at least 60 phylogenetically distinct species have been documented or characterized within the *Fusarium solani* species complex (O'Donnell et al., 2013), so that the species name *F. solani* should be avoided when referring to a species within the *Fusarium solani* specie complex.

The SDS causing *Fusarium* species have been reclassified numerous times with additional sampling efforts and introduction of new phylogenetic tools. The SDS-causing pathogen was

first described as blue masses of *Fusarium solani* species formed on the surface of roots and lower stems of soybean, causing severe foliar chlorosis symptoms (Roy et al., 1988; Rupe, 1989). The *Fusarium* isolates recovered from soybean roots were then designated as two forms, FS-A and FS-B, based on distinct morphology and varied pathogenicity on soybean. Eventually, Koch's postulate suggested FS-A was the causal pathogen for SDS (Roy et al., 1989), and further characterizations of FS-A isolates supported the designation of forma specialis, *F. solani* (Mart.) Sacc. f. sp. *glycines* (Roy, 1997).

SDS-causing *Fusarium* species were first characterized in a systemic study using isolates collected from the United States and Argentina. Both morphology and phylogenetic analysis suggested that isolates collected from South America possessed characteristics that are distinct from the SDS-causing *Fusarium* species collected in North American (Aoki et al., 2003). Therefore, Aoki et al. (2003) proposed two SDS-causing *Fusarium* species, *Fusarium tucumaniae* T. Aoki, O'Donnell, Yos. Homma et Lattanzi and *Fusarium virguliforme* O'Donnell & T. Aoki (syn. *F. solani* f. sp. *glycines*). Additional studies included isolates from Brazil, added two more new SDS-causal *Fusarium* species, *Fusarium brasiliense* T. Aoki & O'Donnell and *Fusarium cuneirostrum* O'Donnell & T. Aoki, which made a total of four SDS-causing *Fusarium* species clustered within the clade2 *Fusarium solani* species complex (Aoki et al., 2005). Besides the phylogenetic and morphological evidences, Covert et al. (2007) also demonstrated biological species evidence for the distinction between *F. tucumaniae* and *F. virguliforme* using a fertility crossing test, which demonstrated that fertile crosses occurred within *F. tucumaniae* but no fertile crosses between *F. tucumaniae* and *F. virguliforme*. In addition to the SDS-causing species, clade2 *Fusarium solani* species complex also include species (*F. cuneirostrum, F. phaseoli, F. azukicola*) that cause bean root rot (BRR) on dry bean

(*Phaseolus vulgaris* L.), mung beans (*Vigna radiata* (L.) R. Wilczek), and azuki beans (*Vigna angularis*) in the U.S., Canada, and Japan (Aoki et al., 2005; O'Donnell et al., 2010), which has classified *F. cuneirostrum* as a pathogen that causes disease on both soybean and dry bean (Table1-1). However, one of the *F. cuneirostrum* isolates collected from Brazil possessed distinct morphological and phylogenetic differences to the other isolates of *F. cuneirostrum* recovered from dry bean and mung bean (Aoki et al., 2005). Multilocus genotyping (MLGT) (O'Donnell et al., 2010) combined with morphological evidence indicated that the divergent *F. cuneirostrum* isolate (NRRL 31949) is a phylogenetically and morphologically distinct species, which was then renamed as *F. crassistipitatum* (Aoki et al., 2012a).

Table 1-1 Distribution and host specification of SDS-BRR clade *Fusarium* spp.

Species	Hosts	Countries	Causing Disease
F. virguliforme	*Glycine max*	USA, Canada, and Argentina	SDS
F. tucumaniae	*G. max*	Argentina and Brazil	SDS
F. braziliense	*G. max*	Brazil and USA	SDS
F. crassistipitatum	*G. max*	Brazil and Argentina	SDS
F. cuneirostrum	*Phaseolus vulgaris*	USA, Japan, Brazil, and Canada	BRR
F. phaseoli	*P. vulgaris*	USA	BRR
F. azukicola	*Vigna angularis*	Japan	BRR

SA: South America; NA: North America; SDS: Sudden death syndrome; and BRR: Bean root rot

Other SDS causal pathogens

Besides *F. virguliforme*, there are three additional *Fusarium* species (i.e., *F. tucumaniae, F. brasiliense,* and *F. crassistipitatum*) causing SDS on soybean in South America (Aoki et al., 2003; Aoki et al., 2005). The known reproductive cycle for *F. virguliforme* is asexual reproduction by forming asexual reproductive structure sporodochia on the taproot surface bearing asexual propagule conidia (Figure 1-1D, E). Genetic analysis of the mating type genes

within *F. virguliforme* indicated that only one mating type gene (*MAT1-1*) was present in the *F. virguliforme* populations with a survey of 138 isolates collected from both North and South America. Contrary to the strict asexual reproduction, the other two SDS causal pathogens, *F. tucumaniae* and *F. brasiliense,* have both mating type genes (*MAT1-1* and *MAT1-2*) present in their populations (Hughes et al., 2014). Additionally, the sexual reproductive structure perithecia of *F. tucumaniae* were observed in both lab and field conditions (Covert et al., 2007; Scandiani et al., 2010), which demonstrated strong potential to generate higher genetic diversity in the field. Given the facts that four SDS causal species and both mating types are found in South America, it was hypothesized that South America was the center of origin for the SDS causing pathogens, and *F. virguliforme* diverged from South America or Mesoamerica and spread to North America (Covert et al., 2007; Hughes et al., 2014).

SDS foliar symptoms are not caused by *Fusarium* pathogens direct infection or colonization on soybean leaves, but by secreted toxins. One of the fungal toxins produced by SDS causing pathogens is FvTox1, which is a small protein with an approximate molecular weight of 13.5 kDa (Brar et al., 2011). FvTox1 was first discovered in *F. virguliforme* culture filtrate and shown to induce chlorosis and necrosis in susceptible soybean leaves (Brar et al., 2011). Light is essential for developing SDS foliar symptoms (Ji et al., 2006). When the toxin is translocated to the foliage, it can cause the degradation of rubisco large subunit and subsequent accumulation of free radicals, triggering the programmed cell death causing SDS foliar symptoms (Ji et al., 2006). The FvTox1 gene is not only conservative within the SDS causing *Fusarium* pathogens, but also shares homologs with many clade2 *Fusarium solani* species complex species, and even some *Fusarium* species outside of *Fusarium solani* species complex (Mbofung 2011; Wang and Chilvers unpublished data). The wide presence of FvTox1 gene present in the non-SDS causing

Fusarium species may indicate that development of SDS foliar symptoms should be synergistic with multiple toxins or proteins. In addition, several other toxins have been found and verified to induce SDS foliar symptoms on soybean leaves (Brar et al., 2011; Chang et al., 2015). Therefore, there is a consortium of fungal toxins secreted by SDS-causing *Fusarium* species working synergistically to induce foliar chlorosis and necrosis.

Interaction between *F. virguliforme* and SCN

The relationship between soybean cyst nematodes (SCN) and *F. virguliforme* has been studied for decades; however, results from different studies are not always consistent with the effect of SCN on SDS development. In the early observation of SDS, Hirrel (1983) reported the dual presence of SDS symptoms and SCN in an SDS affected field. Also, he noted SCN was associated with 70% to 80% of plants displaying SDS symptoms. In 2000, Roy et al. isolated *F. virguliforme* from surface disinfested SCN cysts collected from the rhizosphere of SDS symptomatic soybean plants. They found the fungus can survive in SCN cysts for at least 8 months, and remain pathogenic (McLean and Lawrence, 1995; Roy et al., 2000). In addition, *F. virguliforme* can attach and get into the eggs and cysts of SCN which can possibly cause reduced SCN cysts or second stage juvenile during the field interactions (McLean and Lawrence, 1993b; Gao et al., 2006b).

In greenhouse and micro plot studies, soil inoculated with both *F. virguliforme* and SCN can cause more severe SDS foliar symptoms than *F. virguliforme* inoculum alone, but SCN is not required to induce *F. virguliforme* root infections (Roy et al., 2000). A synergistic relationship between SCN and *F. virguliforme* has been observed to exacerbate the SDS foliar symptoms in some greenhouse and field trials (McLean and Lawrence, 1993a, b; Xing and Westphal, 2006; Westphal et al., 2014); however, non-significant or negative correlation

between SCN and SDS disease severities were reported in both greenhouse and field experiments (Gao et al., 2006b; Marburger et al., 2014). As both sides of the argument presented convincing evidences for their argument, the relationship between SDS and SCN is still controversial.

SDS field management strategies

Soybean SDS has been present in the United State for over 40 years, but effective disease managements for SDS are still lacking. Common disease management strategies for SDS include planting SDS resistance soybean cultivars, disease escape, managing SCN, and seed treatment with fungicides (Roy et al., 1997; Hartman et al., 2015). Among these management practices, no single tactic will completely control SDS; however, yield losses can be minimized if several management practices are combined (Roy et al., 1997). In the past, there were no fungicides that could be used to effectively manage SDS in the field, and agronomic practices were not always effective in reducing SDS impact (Rupe et al., 1997; Navi and Yang, 2016). Soybean SDS resistance is controlled by many genes and is highly heritable (Iqbal et al., 2001; Njiti et al., 2002). There are 58 quantitative trait loci (QTL) associated with reactions to *F. virguliforme* infection (http://www.soybase.org; access date: Apr. 2016). Many of those loci were identified based on SDS foliar symptoms, while only a small portion of them were associated with root disease ratings (Hnetkovsky et al., 1996; Prabhu et al., 1999; Kazi et al., 2008; Abdelmajid et al., 2012). Collecting soybean SDS root disease ratings is not as easy as collecting SDS foliar disease ratings; as root disease rating requires digging and processing roots to examine root symptom severity. Thus, soybean root resistance to *F. virguliforme* infection traits were seldom examined (Njiti et al., 1997; Kazi et al., 2008). The identified SDS resistance QTL were mostly identified in the linkage mapping with the bi-parental populations, which determined the

mapping resolution is not precise enough to find specific genes associated with SDS resistance. There was only one resistance gene (*GmRLK18-1*) tagged and cloned (Srour et al., 2012). A genome wide association study (GWAS) was used to seek genomic regions associated with SDS resistance, and 20 genomic regions, including *GmRLK18-1*, were found to be associated with SDS resistance (Wen et al., 2014). The genomic regions strongly associated with SDS resistance will serve as candidates for searching SDS resistance genes to improve SDS resistance cultivar breeding. Furthermore, disease ratings on SDS root symptoms or root susceptibility to *F. virguliforme* should be considered as phenotypes in future breeding projects, since *F. virguliforme* root infection is the initial and direct cause of SDS.

Besides the breeding effort, seed treatments with chemical fungicides and bio-control microbes has been promising in reducing *F. virguliforme* root colonization and increasing yield in both greenhouse and field experiments. Seed treatment with fungicides for control SDS was first evaluated in the field, and then verified with greenhouse and seed germination assays in the lab (Mueller et al., 2011). Seed treatment with fungicide fluopyram was particularly effective in reducing *F. virguliforme* root colonization and SDS foliar symptoms. Field experiments in multiple states also verified the effect of fluopyram seed treatment in managing SDS and benefiting yield (Wang et al., 2014; Kandel et al., 2016). In addition to fluopyram, a Syngenta fungicide A10466G controlling SDS by improving root health and reducing SDS foliar symptoms (Olaya et al., 2014); however, varied efficacies in SDS management were observed in additional field trials.

Methods for detection of *F. virguliforme*

The success of field disease management relies on accurate and quick disease diagnostics, and thus a proper diagnostic assay for detection of *F. virguliforme* is vital for SDS management.

Numerous diagnostic assays have been developed for detection and quantification of *F. virguliforme* from plant and soil samples (Cho et al., 2001; Li and Hartman, 2003; Gao et al., 2006b; Li et al., 2008). Diagnostic assays for *F. virguliforme* can be categorized into two types: culture-based methods and DNA-based methods. The culture-based method includes plating root tissue or soil samples on the semi-selective media (i.e., modified Nash and Snyder's medium), to enumerate the colonies formed on the surface of the agar media (Cho et al., 2001). The application of this detection method is limited by its poor sensitivity and specificity, as *F. virguliforme* colony growth may be out-competed by other fast growing fungi and the colony morphology of *F. virguliforme* is not distinct from the other closely related fungal species. Furthermore, the microscopic method was used to identify *F. virguliforme* from pure culture, but microscopic characteristics of *F. virguliforme* are not distinct from closely related species (Roy, 1997; Li et al., 1998). For example, *F. virguliforme* macroconidia sizes overlapp with its closely related clade2 *Fusarium solani* species complex species (Aoki et al., 2005; Aoki et al., 2012a). Therefore, culture-based diagnostic of *F. virguliforme* is feasible, but may not be the best option.

Given the drawbacks of the culture-based diagnostic methods, molecular diagnostic assays that take advantage of the PCR technique improve both specificity and sensitivity for pathogen detection. The first molecular diagnostic assay developed for *F. virguliforme* was a conventional PCR assay that targets the ribosomal DNA (rDNA), which could specifically differentiate *F. virguliforme* (then named as: *F. solani* f. sp. *phaseoli*) from the other *Fusarium* species (O'Donnell and Gray, 1995). Li and Hartman (2003) developed another conventional PCR assay targeting the mitochondrial small-subunit rDNA, which was applied to detect and semi-quantify *F. virguliforme* from plant or soil samples. To accurately quantify *F. virguliforme* from environmental samples, quantitative real-time PCR (qPCR) assays were developed for

quantification of *F. virguliforme* from plant samples. The developed qPCR assays were specific to *F. virguliforme* and their lower limit of detection sensitivity was reported to be as low as 90 fg of genomic DNA (Gao et al., 2006b; Li et al., 2008; Mbofung et al., 2011). Based on the revised taxonomy of clade-2 FSSC, two of the published assays (i.e., Gao et al. (2006) and Li et al, (2008) assays) were no longer only specific to *F. virguliforme*, as these two assays may cross amplify with non-SDS causing *Fusarium* species due to lack of primer specificity (O'Donnell et al., 2010; Aoki et al., 2012a; Aoki et al., 2012b). Another qPCR assay developed by Mbofung et al. (2011) targets the single copy fungal toxin gene (*FvTox1*), which results in poor detection sensitivity. The qPCR assay detection sensitivity was determined to be 25 pg of *F. virguliforme* genomic DNA, which is significantly lower than the other qPCR assays. Collectively, qPCR is the method of choice for detection and quantification of *F. virguliforme* from plant or soil samples, but an improved qPCR assay with better sensitivity and optimized specificity is needed.

The choices of loci for qPCR assay design are the keys to qPCR diagnostic assay specificity, sensitivity, and consistency. Specificity to the target pathogen is a must for a plant pathogen diagnostic assay; otherwise the false positive rate would be hard to estimate. One of the common ways to select genetic loci for specific assay design is from the most recent phylogenetic studies. For instance, taxonomy of the clade 2 *Fusarium solani* species complex has been revised several times in the past years with possible further delineation in the future (Aoki et al., 2003; Aoki et al., 2005; O'Donnell et al., 2010; Aoki et al., 2012a). The design of a diagnostic qPCR assay should take advantage of the knowledge in the phylogenetic studies to select proper genetic locus for assay design based on the scope of the detection targets. Other ways to search for genetic loci specific to the target include searching genome-wide orthologs and the alignment-free BLAST-based method (Satya et al., 2010; Pritchard et al., 2012). These methods have been successfully

utilized for human pathogen PCR assay development, and should be easily adopted to design diagnostic assays for plant pathogens (Pritchard et al., 2013). In addition, qPCR assay sensitivity is directly correlated with the gene copy numbers per haploid genome in one pathogen cell. For one pathogen cell, different genes have varied gene copy numbers that can range between zero to hundreds copies, this can make a huge discrepancy in detection sensitivities among qPCR assays. The *F. virguliforme* qPCR assay designed on a single copy gene was less sensitive than the assay developed on the multiple copy genes, and the differences in detection sensitivities can be as large as three orders of magnitude (Gao et al., 2004; Mbofung et al., 2011). To improve specificity, genes present on the dispensable part of the pathogen genome can be targeted for assay design, especially if dispensable gene is associated with pathogenicity. The disadvantage of this method is lack of consistency, since the dispensable genes are not always present in pathogen cells (Coleman et al., 2009). Assay validation is also an important facet to evaluate a qPCR assay. A multi-lab round robin experiment has been conducted on *F. virguliforme* qPCR assays by focusing on testing assay specificity, sensitivity, and consistency among assays. The best qPCR assay was suggested to be the qPCR assay designed on the multi-copy rDNA intergenic spacer (IGS) region, which demonstrated good specificity and sensitivity (Kandel et al., 2015).

Population genetic structure of *F. virguliforme* and mating type gene

Selecting proper genetic markers is important to solve population biology questions. Molecular markers have been applied in many population genetic studies of plant pathogens for the purposes of detecting gene flow, identifying mating systems, locating the center of disease origin, and tracking pathogen adaptation to hosts (McDonald and Linde, 2002). To detect the genetic diversity of plant pathogens, there are three types of molecular markers as defined by the

nature of their molecular genetic marker: non-PCR based markers, PCR based markers that are not locus-specific, and locus specific markers (Milgroom, 2015). Before the advent of PCR technique, allozyme, restriction fragments length polymorphism (RFLP), and RFLP fingerprinting were the mainstream genetic markers used for population genetics of plant pathogens. After the advent of PCR, random amplified polymorphic DNA (RAPD), inter-simple sequence repeats (ISSR) and rep-PCR, and amplified fragment length polymorphism (AFLP) were developed and used widely in the population genetic studies of plant pathogens (Brown, 1996). Currently, the locus-specific molecular markers, such as microsatellite and single nucleotide polymorphism (SNP) markers are widely used for population genetic studies (Schlötterer, 2004). These two genetic markers were used for different population genetics analyses based on the topics of the biological questions, such as time of divergence, mating systems, and genes contributing to host adaptations. The microsatellite marker has a higher mutation rate than the SNP markers, which makes the microsatellite the marker of choice for studying a short time scale population genetic questions, such as a recent outbreak of plant disease or testing random mating of a local population. The SNP marker gained its popularity because of the advent of the next generation sequencing technology, which significantly decreased the cost and throughput for genotyping plant pathogen populations. Another benefit of SNP markers is the higher marker density than other markers, which can be not only used for population genetic study, but also can be utilized to identify genomic regions associated with the phenotypic traits (host specification, fungicide resistance, and thermal adaptation) of the pathogens using genome wide association study (GWAS).

To date, little genetic variability has been detected within *F. virguliforme* isolates collected in the United States. A survey based on 27 *F. virguliforme* isolates from northern US (i.e., IA, MN

and IL) suggested that DNA genetic loci including rDNA IGS, translation elongation factor 1α (EF-1α), and internal transcribed spacer (ITS) genes were identical among *F. virguliforme* isolates (Malvick and Bussey, 2008; O'Donnell et al., 2010). These results may suggest *F. virguliforme* isolates obtained from the north central US appear to be genetically identical or perhaps part of US clonal population (Malvick and Bussey, 2008). However, a pathogenicity and virulence study on *F. virguliforme* isolates demonstrated varying levels of root rot or SDS foliar symptoms (Li S. et al., 2009). For example, in pathogenicity tests the FSG14 and FSG 13 isolates cause very severe root symptoms, but less severe foliar symptoms (Li S. et al., 2009). Given the variations in aggressiveness of *F. virguliforme* isolates on soybeans, it is believed that *F. virguliforme* is not a clonal lineage in the US, and proper genetic markers with higher mutation rate may be needed to detect genetic diversity among *F. virguliforme* isolates. Using both RFLP and RAPD genetic markers, Mbofung ed al (2012) identified 25 genotypes from a collection of 72 *F. virguliforme* isolates; all the genotypes can be further grouped into four subgroups in a cluster analysis. Unfortunately, the lack of reproducibility has made the RAPD marker difficult to use between labs (Penner et al., 1993; McDonald, 1997). Therefore, genetic markers with higher reproducibility rate and polymorphism among *F. virguliforme* isolates are needed to improve current *F. virguliforme* genotyping.

Since the first report of SDS disease in Arkansas in 1970s, SDS has been reported in most soybean producing states in the United States in the past 40 years. If there was a spreading event from the one possible center of origin in Arkansas, the spreading event should be in a very short period of time scale. This implies that Sanger sequencing multi-locus sequencing typing genetic markers may not have enough evolutionary potential to create enough mutations to be detected in the previous sequencing genotyping efforts (Malvick and Bussey, 2008; O'Donnell et al., 2010).

The microsatellite markers with a higher mutation rate may become the ideal genetic marker for detecting genetic diversity for these types of population genetic questions in such a short time scale (Ellegren, 2004; Milgroom, 2015). Microsatellite genetic marker has been applied to multiple plant pathogens to study their population biology and demographic with narrow or wide geographical scales. It has been successfully used to predict plant pathogen center of origin, migration routes, and population structures (Berbegal et al., 2013; Ali et al., 2014; Goss et al., 2014; Everhart and Scherm, 2015; Kamvar et al., 2015). Therefore, to develop a set of microsatellite markers will facilitate the identification of population structure and demographic history for *F. virguliforme* in the United States.

The release of *F. virguliforme* draft genome enabled the rapid development of microsatellite markers for *F. virguliforme*. Using a 454 next generation sequencing (NGS) platform, the draft genome of *F. virguliforme* has been assembled and annotated (Srivastava et al., 2014). The genome has been assembled into 1386 scaffold with average scaffold length of 36 kb, which estimated the genome size to be ~50 Mb. Though the genome assembly quality is not as good as other model fungal organisms, the assembly quality was long enough for mining microsatellite markers. There are several bioinformatics tools been developed for mining microsatellite marker patterns from genomic sequences, such MISA, SSRIT, and SciRoKo (Thiel et al., 2003; Kofler et al., 2007). Given the size of *F. virguliforme* genome, most of the available software tools will be able to process the sequence data in a reasonable computing time. Collectively, microsatellite markers of *F. virguliforme* is ideal for study the population genetic question in such a short time scale, and the development of *F. virguliforme* microsatellite markers is feasible based on the genomic sequence data and bioinformatics tools.

Summary

Given the known knowledge about *F. virguliforme* and SDS, this review highlights the need for prioritized research in key areas. One critical need is for the development of improved qPCR assay for detect and quantify *F. virguliforme* from plant and soil samples. While the currently developed qPCR assays is specific or sensitive to *F. virguliforme*, qPCR assays that are both specific and sensitive are still not available. An improved qPCR assay can be used to study *F. virguliforme* temporal dynamics in soybean roots along the season, which greatly improve our understanding of soybean resistant to *F. virguliforme* root infections. Furthermore, *F. virguliforme* root colonization level is an index to represent trait that soybean root resistant to *F. virguliforme* infections, and these phenotypic data are quantitative and accurate than previous method. Besides the efforts for breeding SDS resistance cultivars, numerous fungicides showed potential to reduce *F. virguliforme* and SDS foliar symptoms, so that new research is also need to determine the baseline sensitivity of these fungicide chemicals and their performance in the field trials. At last, *F. virguliforme* has demonstrated diverse virulence on soybeans, and therefore molecular genetic markers with high mutation rate need to be developed for *F. virguliforme*. The microsatellite marker will help to profile the genetic diversity and population structure for *F. virguliforme*, and the center of origin hypothesis can also be tested with the *F. virguliforme* populations collected in the United States.

REFERENCES

REFERENCES

Abdelmajid, K. M., Ramos, L., Leandro, L., Mbofung, G., Hyten, D. L., Kantartzi, S. K., Grier, I., Robert, L., Njiti, V. N., and Meksem, K. 2012. The 'PI 438489B' by 'Hamilton' SNP-based genetic linkage map of soybean [*Glycine max* (L.) Merr.] identified quantitative trait loci that underlie seedling SDS resistance. Journal of Plant Genome Sciences 1:18-30.

Ali, S., Gladieux, P., Leconte, M., Gautier, A., Justesen, A.F., Hovmøller, M.S., Enjalbert, J., and de Vallavieille-Pope, C. 2014. Origin, migration routes and worldwide population genetic structure of the wheat yellow rust pathogen *Puccinia striiformis* f. sp. *tritici*. PLoS Pathog 10:e1003903.

Aoki, T., O'Donnell, K., Homma, Y., and Lattanzi, A.R. 2003. Sudden-death syndrome of soybean is caused by two morphologically and phylogenetically distinct species within the *Fusarium solani* species complex— *F. virguliforme* in North America and *F. tucumaniae* in South America. Mycologia 95:660-684.

Aoki, T., O'Donnell, K., and Scandiani, M.M. 2005. Sudden death syndrome of soybean in South America is caused by four species of *Fusarium*: *Fusarium brasiliense* sp. nov., *F. cuneirostrum* sp. nov., *F. tucumaniae*, and *F. virguliforme*. Mycoscience 46:162-183.

Aoki, T., Scandiani, M.M., and O'Donnell, K. 2012a. Phenotypic, molecular phylogenetic, and pathogenetic characterization of *Fusarium crassistipitatum* sp. nov., a novel soybean sudden death syndrome pathogen from Argentina and Brazil. Mycoscience 53:167-186.

Aoki, T., Tanaka, F., Suga, H., Hyakumachi, M., Scandiani, M.M., and O'Donnell, K. 2012b. *Fusarium azukicola* sp nov., an exotic azuki bean root-rot pathogen in Hokkaido, Japan. Mycologia 104:1068-1084.

Berbegal, M., Perez-Sierra, A., Armengol, J., and Grunwald, N.J. 2013. Evidence for Multiple Introductions and Clonality in Spanish Populations of *Fusarium circinatum*. Phytopathology 103:851-861.

Bernstein, E.R., Atallah, Z.K., Koval, N.C., Hudelson, B.D., and Grau, C.R. 2007. First report of sudden death syndrome of soybean in Wisconsin. Plant Dis 91:1201-1201.

Booth, C. 1971. The genus *Fusarium*. Commonwealth Mycological Institute, Surrey, England.

Booth, C. 1975. The Present Status of Fusarium Taxonomy. Annu. Rev. Phytopathol. 13:83-93.

Bradley, C., and Allen, T. (2014). Estimates of soybean yield reductions caused by diseases in the United States. (http://extension.cropsciences.illinois.edu/fieldcrops/diseases/yield_reductions.php) Access date: April 15, 2016

Brar, H.K., Swaminathan, S., and Bhattacharyya, M.K. 2011. The *Fusarium virguliforme* toxin fvtox1 causes foliar sudden death syndrome-like symptoms in soybean. Mol Plant Microbe Interact 24:1179-1188.

Brown, J.K.M. 1996. The choice of molecular marker methods for population genetic studies of plant pathogens. New Phytol. 133:183-195.

Chang, H.-X., Domier, L., Radwan, O., Yendrek, C., Hudson, M., and Hartman, G.L. 2015. Identification of multiple phytotoxins produced by *Fusarium virguliforme* including a phytotoxic effector (FvNIS1) associated with sudden death syndrome foliar symptoms. Mol Plant-Microbe Interact 29:96-108.

Chehri, K. 2015. First report on *Fusarium virguliforme* in Persian Gulf Beach soils. Journal of Mycology Research 2:55-61.

Chehri, K., Salleh, B., and Zakaria, L. 2014. *Fusarium virguliforme*, a soybean sudden death syndrome fungus in Malaysian soil. Australasian Plant Dis. Notes 9:1-7.

Chilvers, M.I., and Brown-Rytlewski, D.E. 2010. First report and confirmed distribution of soybean sudden death syndrome caused by *Fusarium virguliforme* in southern Michigan. Plant Dis 94:1164.

Cho, J.H., Rupe, J.C., Cummings, M.S., and Gbur, E.E. 2001. Isolation and identification of *Fusarium solani* f. sp *glycines* from soil on modified Nash and Snyder's medium. Plant Dis 85:256-260.

Coleman, J.J., Rounsley, S.D., Rodriguez-Carres, M., Kuo, A., Wasmann, C.C., Grimwood, J., Schmutz, J., Taga, M., White, G.J., Zhou, S., Schwartz, D.C., Freitag, M., Ma, L.J., Danchin, E.G., Henrissat, B., Coutinho, P.M., Nelson, D.R., Straney, D., Napoli, C.A., Barker, B.M., Gribskov, M., Rep, M., Kroken, S., Molnar, I., Rensing, C., Kennell, J.C., Zamora, J., Farman, M.L., Selker, E.U., Salamov, A., Shapiro, H., Pangilinan, J., Lindquist, E., Lamers, C., Grigoriev, I.V., Geiser, D.M., Covert, S.F., Temporini, E., and Vanetten, H.D. 2009. The genome of *Nectria haematococca*: contribution of supernumerary chromosomes to gene expansion. Plos Genet 5:e1000618.

Covert, S.F., Aoki, T., O'Donnell, K., Starkey, D., Holliday, A., Geiser, D.M., Cheung, F., Town, C., Strom, A., Juba, J., Scandiani, M., and Yang, X.B. 2007. Sexual reproduction in the soybean sudden death syndrome pathogen *Fusarium tucumaniae*. Fungal Genet Biol 44:799-807.

Doupnik, B. 1993. Soybean production and disease loss estimates for north central United States from 1989 to 1991. Plant Dis 77:1170-1171.

Ellegren, H. 2004. Microsatellites: simple sequences with complex evolution. Nat. Rev. Genet. 5:435-445.

Everhart, S.E., and Scherm, H. 2015. Fine-scale genetic structure of *Monilinia fructicola* during brown rot epidemics within individual peach tree canopies. Phytopathology 105:542-549.

Gao, X., Hartman, G., and Niblack, T. 2006a. Early infection of soybean roots by *Fusarium solani* f. sp *glycines*. Phytopathology 96:S38-S38.

Gao, X., Jackson, T.A., Hartman, G.L., and Niblack, T.L. 2006b. Interactions Between the Soybean Cyst Nematode and *Fusarium solani* f. sp. *glycines* Based on Greenhouse Factorial Experiments. Phytopathology 96:1409-1415.

Gao, X., Jackson, T.A., Lambert, K.N., Li, S., Hartman, G.L., and Niblack, T.L. 2004. Detection and quantification of *Fusarium solani* f. sp *glycines* in soybean roots with real-time quantitative polymerase chain reaction. Plant Dis 88:1372-1380.

Gerlach, W., Nirenberg, H., and Forstwirtschaft, B.B.f.L.-u. 1982. The genus *Fusarium*: a pictorial atlas. Kommissionsverlag P. Parey.

Goss, E.M., Tabima, J.F., Cooke, D.E.L., Restrepo, S., Fry, W.E., Forbes, G.A., Fieland, V.J., Cardenas, M., and Grunwald, N.J. 2014. The Irish potato famine pathogen *Phytophthora infestans* originated in central Mexico rather than the Andes. P Natl Acad Sci USA 111:8791-8796.

Hartman, G.L., Sinclair, J.B., and Rupe, J.C. 1999. Compendium of soybean diseases. American Phytopathological Society (APS Press).

Hartman, G.L., Chang, H.X., and Leandro, L.F. 2015. Research advances and management of soybean sudden death syndrome. Crop Protection 73:60-66.

Hirrel, M. 1983. Sudden-death syndrome of soybean-a disease of unknown etiology. Phytopathology 73:501-502.

Hnetkovsky, N., Chang, S.J.C., Doubler, T.W., Gibson, P.T., and Lightfoot, D.A. 1996. Genetic mapping of loci underlying field resistance to soybean sudden death syndrome (SDS). Crop Science 36:393-400.

Hughes, T.J., O'Donnell, K., Sink, S., Rooney, A.P., Scandiani, M.M., Luque, A., Bhattacharyya, M.K., and Huang, X. 2014. Genetic architecture and evolution of the mating type locus in fusaria that cause soybean sudden death syndrome and bean root rot. Mycologia 106:686-697.

Iqbal, M.J., Meksem, K., Njiti, V.N., Kassem, M.A., and Lightfoot, D.A. 2001. Microsatellite markers identify three additional quantitative trait loci for resistance to soybean sudden-death syndrome (SDS) in Essex × Forrest RILs. Theor Appl Genet 102:187-192.

Ji, J., Scott, M.P., and Bhattacharyya, M.K. 2006. Light is essential for degradation of ribulose-1.5-bisphosphate carboxylase-oxygenase large subunit during sudden death syndrome development in soybean. Plant Biology 8:597-605.

Kamvar, Z.N., Larsen, M.M., Kanaskie, A.M., Hansen, E.M., and Grunwald, N.J. 2015. Spatial and temporal analysis of populations of the sudden oak death pathogen in Oregon forests. Phytopathology 105:982-989.

Kandel, Y.R., Wise, K.A., Bradley, C., Chilvers, M.I., Tenuta, A., and Mueller, D.S. 2016. Fungicide and cultivar effects on sudden death syndrome and yield of soybean. Plant Dis *In press*.

Kandel, Y.R., Haudenshield, J., Srour, A.Y., Islam, K.T., Fakhoury, A.M., Santos, P., Wang, J., Chilvers, M.I., Hartman, G., Malvick, D., Floyd, C.M., Mueller, D., and Leandro, L. 2015. Multi-laboratory comparison of quantitative PCR assays for detection and quantification of *Fusarium virguliforme* from soybean roots and soil. Phytopathology 105:1601-1611.

Kazi, S., Shultz, J., Afzal, J., Johnson, J., Njiti, V.N., and Lightfoot, D.A. 2008. Separate loci underlie resistance to root infection and leaf scorch during soybean sudden death syndrome. Theor Appl Genet 116:967-977.

Koenning, S.R., and Wrather, J.A. 2010. Suppression of soybean yield potential in the continental United States by plant diseases from 2006 to 2009. Plant Health Progress Online.

Kofler, R., Schlotterer, C., and Lelley, T. 2007. SciRoKo: a new tool for whole genome microsatellite search and investigation. Bioinformatics 23:1683-1685.

Kurle, J., Gould, S., Lewandowski, S., Li, S., and Yang, X. 2003. First report of sudden death syndrome (*Fusarium solani* f. sp. *glycines*) of soybean in Minnesota. Plant Dis 87:449-449.

Li, S., and Hartman, G.L. 2003. Molecular detection of *Fusarium solani* f. sp *glycines* in soybean roots and soil. Plant Pathol 52:74-83.

Li, S., Hartman, G.L., Domier, L.L., and Boykin, D. 2008. Quantification of *Fusarium solani* f. sp *glycines* isolates in soybean roots by colony-forming unit assays and real-time quantitative PCR. Theor Appl Genet 117:343-352.

Li S., Hartman G.L., and Chen Y. 2009. Evaluation of aggressiveness of *Fusarium virguliforme* isolates that cause soybean sudden death. Journal of Plant Pathology 91:77-86.

Li, S.X., Hartman, G.L., and Gray, L.E. 1998. Chlamydospore formation, production, and nuclear status in *Fusarium solani* f. sp. *glycines* soybean sudden death syndrome-causing isolates. Mycologia 90:414-421.

Malvick, D.K., and Bussey, K.E. 2008. Comparative analysis and characterization of the soybean sudden death syndrome pathogen Fusarium virguliforme in the northern United States. Can J Plant Pathol 30:467-476.

Marburger, D., Conley, S., Esker, P., MacGuidwin, A., and Smith, D. 2014. Relationship between Fusarium virguliforme and Heterodera glycines in commercial soybean fields in Wisconsin. Plant Health Progress 15:11.

Mbofung, G., Harrington, T.C., Steimel, J.T., Navi, S.S., Yang, X.B., and Leandro, L.F. 2012. Genetic structure and variation in aggressiveness in *Fusarium virguliforme* in the Midwest United States. Canadian Journal of Plant Pathology 34:83-97.

Mbofung, G.C.Y., Fessehaie, A., Bhattacharyya, M.K., and Leandro, L.F.S. 2011. A new TaqMan real-time polymerase chain reaction assay for quantification of *Fusarium virguliforme* in soil. Plant Dis 95:1420-1426.

McDonald, B.A. 1997. The population genetics of fungi: tools and techniques. Phytopathology 87:448-453.

McDonald, B.A., and Linde, C. 2002. The population genetics of plant pathogens and breeding strategies for durable resistance. Euphytica 124:163-180.

McLean, K.S., and Lawrence, G.W. 1993a. Localized Influence of *Heterodera glycines* on Sudden Death Syndrome of Soybean. J Nematol 25:674-678.

McLean, K.S., and Lawrence, G.W. 1993b. Interrelationship of Heterodera glycines and Fusarium solani in Sudden Death Syndrome of Soybean. J Nematol 25:434-439.

McLean, K.S., and Lawrence, G.W. 1995. Development of Heterodera glycines as Affected by Fusarium solani, the Causal Agent of Sudden Death Syndrome of Soybean. J Nematol 27:70-77.

Milgroom, M.G. 2015. Population Biology of Plant Pathogens: Genetics, Ecology, and Evolution. American Phytopathological Society.

Mueller, T.A., Knake, R.P., and Riggs, J.L. 2011. Control of *Fusarium virguliforme* (sudden death syndrome) with a seed treatment. Phytopathology 101:S124-S124.

Nakajima, T., Mitsueda, T., and Charchar, M.J.D. 1996. First occurrence of sudden death syndrome of soybean in Brazil. Jarq-Jpn Agr Res Q 30:31-34.

Navi, S.S., and Yang, X. 2016. Impact of Crop Residue and Corn-soybean Rotation on the Survival of *Fusarium virguliforme* a Causal Agent of Sudden Death Syndrome of Soybean. Journal of Plant Pathology & Microbiology 2016.

Njiti, V.N., Suttner, R.J., Gray, L.E., Gibson, P.T., and Lightfoot, D.A. 1997. Rate-reducing resistance to *Fusarium solani* f. sp. *phaseoli* underlies field resistance to soybean sudden death syndrome. Crop Science 37:132-138.

Njiti, V.N., Meksem, K., Iqbal, M.J., Johnson, J.E., Kassem, M.A., Zobrist, K.F., Kilo, V.Y., and Lightfoot, D.A. 2002. Common loci underlie field resistance to soybean sudden death syndrome in Forrest, Pyramid, Essex, and Douglas. Theor Appl Genet 104:294-300.

O'Donnell, K. 2000. Molecular phylogeny of the *Nectria haematococca-Fusarium solani* species complex. Mycologia 92:919-938.

O'Donnell, K., and Gray, L.E. 1995. Phylogenetic relationships of the soybean sudden death syndrome pathogen *Fusarium solani* f. sp. *phaseoli* inferred from rDNA sequence data and PCR primers for its identification. Mol Plant Microbe Interact 8:709-716.

O'Donnell, K., Sink, S., Scandiani, M.M., Luque, A., Colletto, A., Biasoli, M., Lenzi, L., Salas, G., Gonzalez, V., Ploper, L.D., Formento, N., Pioli, R.N., Aoki, T., Yang, X.B., and Sarver, B.A. 2010. Soybean sudden death syndrome species diversity within North and South america revealed by multilocus genotyping. Phytopathology 100:58-71.

O'Donnell, K., Rooney, A.P., Proctor, R.H., Brown, D.W., McCormick, S.P., Ward, T.J., Frandsen, R.J., Lysoe, E., Rehner, S.A., Aoki, T., Robert, V.A., Crous, P.W., Groenewald, J.Z., Kang, S., and Geiser, D.M. 2013. Phylogenetic analyses of RPB1 and RPB2 support a middle Cretaceous origin for a clade comprising all agriculturally and medically important fusaria. Fungal Genet Biol 52:20-31.

Olaya, G., Ireland, D., Watrin, C., and Pedersen, P. 2014. Sudden death syndrome of soybeans caused by *Fusarium virguliforme* can be controlled by the Syngenta seed treatment fungicide A10466G. Phytopathology S104:86-86.

Paulitz, T.C., Schroeder, K.L., and Schillinger, W.F. 2010. Soilborne Pathogens of Cereals in an Irrigated Cropping System: Effects of Tillage, Residue Management, and Crop Rotation. Plant Dis 94:61-66.

Penner, G., Bush, A., Wise, R., Kim, W., Domier, L., Kasha, K., Laroche, A., Scoles, G., Molnar, S., and Fedak, G. 1993. Reproducibility of random amplified polymorphic DNA (RAPD) analysis among laboratories. Genome Res. 2:341-345.

Pennypacker, B.W. 1999. First report of sudden death syndrome caused by *Fusarium solani* f. sp. *glycines* on soybean in Pennsylvania. Plant Dis 83:879-879.

Prabhu, R.R., Njiti, V.N., Bell-Johnson, B., Johnson, J.E., Schmidt, M.E., Klein, J.H., and Lightfoot, D.A. 1999. Selecting soybean cultivars for dual resistance to soybean cyst nematode and sudden death syndrome using two DNA markers. Crop Science 39:982-987.

Pritchard, L., Holden, N.J., Bielaszewska, M., Karch, H., and Toth, I.K. 2012. Alignment-free design of highly discriminatory diagnostic primer sets for *Escherichia coli* O104:H4 outbreak strains. PloS one 7.

Pritchard, L., Humphris, S., Saddler, G.S., Parkinson, N.M., Bertrand, V., Elphinstone, J.G., and Toth, I.K. 2013. Detection of phytopathogens of the genus Dickeya using a PCR primer prediction pipeline for draft bacterial genome sequences. Plant Pathol 62:587-596.

Ren, S., and Michael, G.G. 2010. 108. GLYCINE Willdenow, Sp. Pl. 3: 854, 1053. 1802, nom. cons., not Linnaeus (1753). Flora of China 10:250-252.

Roy, K.W. 1997. *Fusarium solani* on soybean roots: nomenclature of the causal agent of sudden death syndrome and identity and relevance of *F. solani* form B. Plant Dis 81:259-266.

Roy, K.W., Patel, M.V., and Baird, R.E. 2000. Colonization of Heterodera glycines cysts by Fusarium solani form A, the cause of sudden death syndrome, and other fusaria in soybean fields in the midwestern and southern United States. Phytoprotection 81:57-67.

Roy, K.W., Hershman, D.E., Rupe, J.C., and Abney, T.S. 1997. Sudden death syndrome of soybean. Plant Dis 81:1100-1111.

Roy, K.W., Lawrence, G.W., Hodges, H.H., Mclean, K.S., and Killebrew, J.F. 1988. Etiology of sudden death syndrome of soybean. Proc. South. Soybean Dis, Work. Conf. 15:30.

Roy, K.W., Lawrence, G.W., Hodges, H.H., Mclean, K.S., and Killebrew, J.F. 1989. Sudden death syndrome of soybean: *Fusarium solani* as incitant and relation of *Heterodera glycines* to disease severity. Phytopathology 79:191-197.

Rupe, J.C. 1989. Frequency and pathogenicity of *Fusarium solani* recovered from soybeans with sudden death syndrome. Plant Dis 73:581-584.

Rupe, J.C., Robbins, R.T., and Gbur, E.E. 1997. Effect of crop rotation on soil population densities of *Fusarium solani* and *Heterodera glycines* and on the development of sudden death syndrome of soybean. Crop Protection 16:575-580.

Rupe, J.C., Sabbe, W.E., Robbins, R.T., and Gbur, E.E. 1993. Soil and Plant Factors Associated with Sudden-Death Syndrome of Soybean. J. Prod. Agric. 6:218-221.

Rupe, J.C., Widick, J.D., Sabbe, W.E., Robbins, R.T., and Becton, C.B. 2000. Effect of chloride and soybean cultivar on yield and the development of sudden death syndrome, soybean cyst nematode, and southern blight. Plant Dis 84:669-674.

Saccardo, P.A. 1901. Sylloge fungorum omnium hucusque cognitorum. sumptibus auctoris.

Satya, R.V., Kumar, K., Zavaljevski, N., and Reifman, J. 2010. A high-throughput pipeline for the design of real-time PCR signatures. BMC bioinformatics 11.

Scandiani, M., Ruberti, D., Pioli, R., Luque, A., and Giorda, L. 2003. First report of Koch's postulates completion of sudden death syndrome of soybean in Argentina. Plant Dis 87:447-447.

Scandiani, M., Ruberti, D., O'Donnell, K., Aoki, T., Pioli, R., Giorda, L., Luque, A., and Biasoli, M. 2004. Recent outbreak of soybean sudden death syndrome caused by *Fusarium virguliforme* and *F. tucumaniae* in Argentina. Plant Dis 88:1044-1044.

Scandiani, M.M., Aoki, T., Luque, A.G., Carmona, M.A., and O'Donnell, K. 2010. First report of sexual reproduction by the soybean sudden death syndrome pathogen *Fusarium tucumaniae* in nature. Plant Dis 94:1411-1416.

Scherm, H., and Yang, X.B. 1996. Development of sudden death syndrome of soybean in relation to soil temperature and soil water matric potential. Phytopathology 86:642-649.

Scherm, H., and Yang, X.B. 1999. Risk assessment for sudden death syndrome of soybean in the north-central United States. Agricultural Systems 59:301-310.

Scherm, H., Yang, X.B., and Lundeen, P. 1998. Soil variables associated with sudden death syndrome in soybean fields in Iowa. Plant Dis 82:1152-1157.

Schlötterer, C. 2004. The evolution of molecular markers—just a matter of fashion? Nat. Rev. Genet. 5:63-69.

Snyder, W.C., and Hansen, H.N. 1941. The species concept in Fusarium with reference to section Martiella. Am. J. Bot. 28:738-742.

Srivastava, S.K., Huang, X., Brar, H.K., Fakhoury, A.M., Bluhm, B.H., and Bhattacharyya, M.K. 2014. The genome sequence of the fungal pathogen *Fusarium virguliforme* that causes sudden death syndrome in soybean. PloS one 9:e81832.

Srour, A., Afzal, A.J., Blahut-Beatty, L., Hemmati, N., Simmonds, D.H., Li, W., Liu, M., Town, C.D., Sharma, H., Arelli, P., and Lightfoot, D.A. 2012. The receptor like kinase at Rhg1-a/Rfs2 caused pleiotropic resistance to sudden death syndrome and soybean cyst nematode as a transgene by altering signaling responses. BMC Genomics 13:368.

Tande, C., Hadi, B., Chowdhury, R., Subramanian, S., and Byamukama, E. 2014. First report of sudden death syndrome of soybean caused by *Fusarium virguliforme* in South Dakota. Plant Dis 98:1012-1012.

Tewoldemedhin, Y.T., Lamprecht, S.C., Geldenhuys, J.J., and Kloppers, F.J. 2013. First report of soybean sudden death syndrome caused by *Fusarium virguliforme* in South Africa. Plant Dis 98:569-569.

Thiel, T., Michalek, W., Varshney, R.K., and Graner, A. 2003. Exploiting EST databases for the development and characterization of gene-derived SSR-markers in barley (Hordeum vulgare L.). Theor Appl Genet 106:411-422.

USDA-ERS. (2012). Soybeans & Oil Crops. (http://www.ers.usda.gov/topics/crops/soybeans-oil-crops.aspx) Access date: Octurber 27, 2012

USDA-NASS. (2015). National Statistics for Soybeans. (http://www.nass.usda.gov/Statistics_by_Subject/index.php?sector=CROPS) Access date: Apr 27, 2015

Vick, C.M., Chong, S.K., Bond, J.P., and Russin, J.S. 2003. Response of soybean sudden death syndrome to subsoil tillage. Plant Dis 87:629-632.

Vick, C.M., Bond, J.P., Chong, S.K., and Russin, J.S. 2006. Response of soybean sudden death syndrome to tillage and cultivar. Canadian Journal of Plant Pathology 28:77-83.

Wang, J., Jacobs, J., and Chilvers, M. 2014. Management of soybean sudden death syndrome by seed treatment with fluopyram. Phytopathology 104 (Suppl.):127-127.

Wang, J., Jacobs, J.L., Byrne, J.M., and Chilvers, M.I. 2015. Improved diagnoses and quantification of *Fusarium virguliforme*, causal agent of soybean sudden death syndrome. Phytopathology 105:378-387.

Wen, Z., Tan, R., Yuan, J., Bales, C., Du, W., Zhang, S., Chilvers, M.I., Schmidt, C., Song, Q., Cregan, P.B., and Wang, D. 2014. Genome-wide association mapping of quantitative resistance to sudden death syndrome in soybean. BMC Genomics 15:809.

Westphal, A., Li, C., Xing, L., McKay, A., and Malvick, D. 2014. Contributions of *Fusarium virguliforme* and *Heterodera glycines* to the disease complex of sudden death syndrome of soybean. PloS one 9:e99529.

Wollenweber, H.W., and Reinking, O.A. 1935. Die fusarien ihre beschreibung, schadwirkung und bekämpfung. P. Parey, Berlin.

Wrather, J., and Koenning, S. 2006. Estimates of disease effects on soybean yields in the United States 2003 to 2005. Journal of Nematology 38:173-180.

Wrather, J., and Koenning, S. 2009. Effects of diseases on soybean yields in the United States 1996 to 2007. Plant Health Progress.

Xing, L., and Westphal, A. 2006. Interaction of *Fusarium solani* f. sp. *glycines* and *Heterodera glycines* in sudden death syndrome of soybean. Phytopathology 96:763-770.

Zhang, N., O'Donnell, K., Sutton, D.A., Nalim, F.A., Summerbell, R.C., Padhye, A.A., and Geiser, D.M. 2006. Members of the *Fusarium solani* species complex that cause infections in both humans and plants are common in the environment. J Clin Microbiol 44:2186-2190.

Ziems, A.D., Giesler, L.J., and Yuen, G.Y. 2006. First report of sudden death syndrome of soybean caused by *Fusarium solani* f. sp *glycines* in Nebraska. Plant Dis 90:109-109.

CHAPTER 2 IMPROVED DIAGNOSES AND QUANTIFICATION OF *FUSARIUM VIRGULIFORME*, CAUSAL AGENT OF SOYBEAN SUDDEN DEATH SYNDROME

This chapter was originally published in Phytopathology.

Wang, J., Jacobs, J.L., Byrne, J.M. and Chilvers, M.I., 2015. Improved diagnoses and quantification of *Fusarium virguliforme*, causal agent of soybean sudden death syndrome. *Phytopathology*, *105*(3):378-387.

Abstract

Fusarium virguliforme (syn. *F. solani* f. sp. *glycines*) is the primary causal pathogen responsible for soybean sudden death syndrome (SDS) in North America. Diagnosis of SDS is difficult because symptoms can be inconsistent or similar to several soybean diseases and disorders. Additionally, quantification and identification of *F. virguliforme* by traditional dilution plating of soil or ground plant tissue is problematic due to the slow growth rate and plastic morphology of *F. virguliforme*. Although several real-time quantitative PCR (qPCR) based assays have been developed for *F. virguliforme*, the performance of those assays does not allow for accurate quantification of *F. virguliforme* due to the reclassification of the *F. solani* species complex. In this study, we developed a TaqMan qPCR assay based on the ribosomal DNA (rDNA) intergenic spacer (IGS) region of *F. virguliforme*. Specificity of the assay was demonstrated by challenging it with genomic DNA of closely related *Fusarium* species and commonly encountered soilborne fungal pathogens. The detection limit of this assay was determined to be 100 fg of pure *F. virguliforme* genomic DNA or 100 macroconidia in 0.5 g of soil. An exogenous control was multiplexed with the assay to evaluate for PCR inhibition. Target locus copy number variation had minimal impact, with a range of rDNA copy number from 138 to 233 copies per haploid genome, resulting in a minor variation of up to 0.76 Ct values between strains. The qPCR assay is transferable across platforms, as validated on the primary real-time PCR platform used in the North Central region of the National Plant Diagnostic Network. A conventional PCR assay for *F. virguliforme* detection was also developed and validated for use in situations where qPCR is not possible.

Introduction

Within the United States, soybean (*Glycine max* (L.) Merr.) is the second most widely grown crop with more than 3 billion bushels produced per annum (USDA NASS, 2013). Numerous plant diseases threaten soybean production in the United States, including soybean sudden death syndrome (SDS) (Wrather and Koenning, 2010). In the past decade, SDS has ranked within the top five most yield damaging soybean diseases in the United States, with estimated yield losses of 70 million bushels in 2010 (Wrather and Koenning, 2011). In North America, the predominant causal agent of soybean SDS is the soilborne fungal pathogen, *Fusarium virguliforme* (Aoki et al., 2003). *Fusarium virguliforme* has been reported to colonize a wide range of host plant species (Kolander et al., 2012), and can survive in soil or debris by producing conidia or chlamydospores (Roy et al., 1997). Diagnosis of SDS in the field can be difficult as several other diseases can produce similar symptoms, such as brown stem rot caused by *Phialophora gregata* (≡*Cadophora gregata*) or red crown rot caused by *Cylindrocladium parasiticum* (Roy et al., 1997).

Studies suggest that early infection of soybean plants by *F. virguliforme* is essential for foliar SDS symptom development (Navi and Yang, 2008), infection by *F. virguliforme* was detected as early as the seedling stage (Gao et al., 2006). As a soilborne pathogen, *F. virguliforme* only colonizes the root and the lower stem of soybean plants (Rupe, 1989), phytotoxins produced by the fungus are translocated through the xylem to the foliage, causing SDS foliar symptoms (Brar and Bhattacharyya, 2012). Accurate detection and quantification of *F. virguliforme* in root and soil samples are essential to study the epidemiology of *F. virguliforme*. Both culture-based and molecular PCR-based methods have been developed for the detection of *F. virguliforme*. Culture-based methods utilize dilution plating or isolation from infected tissue on semi-selective media (Roy et al., 1989; Rupe, 1989; Luo et al., 1999; Cho et al., 2001). However, these culture-

based methods are time consuming and can be difficult to implement given the slow growth rate and plastic morphology of *F. virguliforme* (Cho et al., 2001; Aoki et al., 2003). These limitations of sensitivity and specificity led to the development of DNA-based molecular detection tools. Multiple conventional PCR assays have been developed for the detection of *F. virguliforme*, but they are not specific due to the revised taxonomy of the *F. solani* species complex (O'Donnell and Gray, 1995; Achenbach et al., 1996; Li and Hartman, 2003). Therefore, no specific conventional PCR assay is currently available for diagnosis of *F. virguliforme*.

Quantitative real-time PCR (qPCR) has been extensively applied in quantification and diagnosis of numerous plant pathogens. Compared to conventional PCR assay, qPCR assays can be more sensitive and specific and can detect multiple pathogens by multiplexing assays (Schaad and Frederick, 2002; Patrinos and Ansorge, 2010). Gao et al. (2004) and Li et al. (2008) reported two qPCR assays for quantification of *F. virguliforme* from plant samples using TaqMan probe assays designed against the mitochondrial SSU rDNA sequence. Due to the reclassification of the *Fusarium solani* species complex, the mtDNA region used for design of these two assays was too conserved to differentiate *F. virguliforme* from the dry bean root rot pathogens, *F. cuneirostrum* and *F. phaseoli* and other SDS causal agents such as *F. tucumaniae, F. crassistipitatum*, and *F. brasiliense*, which predominate in South America (O'Donnell et al., 2010; Aoki et al., 2012). Therefore, it is clear that qPCR assays for *F. virguliforme* need to be improved. O'Donnell et al. (2010) and Aoki et al. (2012) demonstrated that the intergenic spacer (IGS) region of the rDNA is one of the genetic loci that can resolve *F. virguliforme* from the other closely related *Fusarium* species in their multilocus genotyping studies of clade 2 *Fusarium solani* species complex. The rDNA IGS region is a multi-copy genetic locus in the eukaryotic genome (Long and Dawid, 1980), therefore the sensitivity of the assay based on IGS

rDNA region is greater than a single copy gene assay, and has been used for detection and quantification of numerous plant pathogens (Chilvers et al., 2007; Bilodeau et al., 2012; Gramaje et al., 2013). Although the rDNA IGS region seems an ideal region for qPCR assay design, large rDNA copy number variations were reported in many fungal organisms (Herrera et al., 2009; Bilodeau et al., 2012), and accuracy of the quantification may be affected in plants infected by fungal strains with varied rDNA copy numbers. In addition, PCR inhibitors in DNA samples can cause false negative results or low PCR amplification efficiencies. Strategies to deal with PCR inhibitors include dilution of DNA samples (Malvick and Impullitti, 2007), additional DNA purification steps or the use of PCR additives such as polyvinylpolypyrrolidone (Jiang et al., 2005; Malvick and Grunden, 2005) and bovine serum albumin (Haudenshield and Hartman, 2011). Despite attempts to reduce or remove PCR inhibitors, an internal or exogenous control is needed to monitor each reaction for PCR inhibition.

Soybean SDS is becoming one of the most devastating diseases threatening soybean production across most of the soybean production zones in the United States and its range continues to expand. Despite this, an accurate, robust and sensitive diagnostic and quantitative assay is not available. Therefore, development of such an assay will facilitate the diagnosis of SDS, and can be used to study the epidemiology of *F. virguliforme*, which will improve our understanding, and management of this pathogen. The objectives of this study were to: (i) develop a qPCR assay with the inclusion of an internal control for the sensitive and specific detection and quantification of *F. virguliforme*; (ii) determine the transferability of the qPCR assay between platforms; (iii) develop a complimentary conventional PCR assay for use in situations where qPCR is not possible; (iv) to thoroughly validate the qPCR and PCR assays with plant and soil samples.

Materials and Methods

Fungal isolates and DNA extraction

Thirty-six isolates of *Fusarium* species and other genera commonly found associated with soybeans were used in this study (Table2-1). Cultures of *Fusarium* species were grown on potato dextrose agar (PDA) media (Acumedia, Burton, MI) at room temperature for 14 d, agar plugs with conidia were collected and stored at -80 ℃ in 20% glycerol. To obtain mycelia for DNA extraction, seven to eight 4-mm^3 pieces of colonized PDA media were transferred to 50 mL potato dextrose broth (PDB) (Acumedia) in 250-mL Erlenmeyer flasks and shaken at room temperature on an orbital rotary shaker at 120 rpm for 3 to 4 d. Mycelia were collected by vacuum filtration on Miracloth (Calbiochem, Darmstadt, Germany) with a Buchner funnel, frozen and lyophilized in sterile 2-mL micro centrifuge tubes overnight. Lyophilized mycelia (20 mg) were disrupted in 2-mL screw-cap tubes with one 6-mm ceramic bead and five 2-mm glass beads in a FastPrep FP120 Bio101 Savant machine (Qbiogene, Carlsbad, CA) at the speed setting 6 for 40 s. Mycelia were used for DNA extraction using the DNeasy Plant Mini kit (Qiagen, Germantown, MD). DNA concentration was determined with a Quant-iT dsDNA high-sensitivity assay kit (Invitrogen, Carlsbad, CA) on a 96-well SAFIRE microplate reader (TECAN, Männedorf, Switzerland).

Table 2-1 Specificity test panel for qPCR assay validation. This panel includes the *Fusarium* species that are closely related to the SDS-causing *Fusarium* species and other commonly encountered soil fungal species. Ct values listed in the table indicate the specificity performance of the *F. virguliforme* qPCR assay when 100 pg genomic DNA were added to the reaction.

Species[a]	Ct[b]	NRRL[c]	Host[d]	Geographic Origin
Fusarium acuminatum[e]	35.75	-	*Solanum tuberosum*	Michigan, USA
F. avenaceum[e]	35.07	-	*S. tuberosum*	Michigan, USA
F. brasiliense	32.06	22678	*Glycine max*	California, USA
F. brasiliense	36.21	22743	*G. max*	Brasilia, Distrito Federal, Brazil
F. cerealis[e]	34.11	-	*S. tuberosum*	Michigan, USA

Table 2-1 (cont'd)

F. crassistipitatum	36.04	31949	*G. max*	Cristalina, Goias, Brazil
F. cuneirostrum	33.05	31157	*Phaseolus vulgaris*	Presque Isle, Michigan, USA
F. equiseti[e]	34.29	-	*S. tuberosum*	Michigan, USA
Fusarium sp.[*]	32.6	22574	*Coffea arabica*	Guatemala
Fusarium sp.[*]	35.54	22412	Bark	French Guiana
F. graminearum[e]	34.91	-	*S. tuberosum*	Michigan, USA
Fusarium sp.[*]	31.35	22387	Bark	French Guian
F. oxysporum[e]	36.07	-	*S. tuberosum*	Michigan, USA
F. phaseoli	37.18	22276	*P. vulgaris*	USA
F. phaseoli	36.47	31156	*P. vulgaris*	Michigan, USA
F. sambucinum[e]	37.36	-	*S. tuberosum*	Michigan, USA
F. solani	37.19	22395	Bark	Venezuela
F. solani[e]	35.21	-	*S. tuberosum*	Michigan, USA
F. torulosum[e]	34.58	-	*S. tuberosum*	Michigan, USA
F. tricinctum[e]	35.31	-	*S. tuberosum*	Michigan, USA
F. tucumaniae	38.57	31096	*G. max*	San Agustin, Tucuman, Argentina
F. tucumaniae	37.15	31773	*G. max*	Brazil, PR, Ponta Grossa
F. virguliforme	21.78	22823	*G. max*	Indiana, USA
F. virguliforme	20.88	31041	*G. max*	Illinois, USA
F. virguliforme	21.08	34551	*G. max*	San Pedrom, Buenos Aures, Argentina
F. virguliforme	20.53	22292	*G. max*	Illinois, USA
F. virguliforme	19.36	-	*G. max*	Counties across Michigan, USA
P. gregata (B)	34.84	-	*G. max*	-
Phialophora gregata (A)	33.82	-	*G. max*	-
Phytophthora sansomeana	34.9	-	*G. max*	-
Phytophthora sojae	35.98	-	*G. max*	-
Pythium svlvaticum	34.21	-	*G. max*	-
Pythium ultimum	34.93	-	*G. max*	-
Rhizoctonia solani AG-2-2IIIB	34.93	-	-	-
Rhizoctonia solani AG-4	34.99	-	-	-
Sclerotinia sclerotiorum	35.36	-	*G. max*	-

[a] unnamed *Fusarium* species nested within clade two of the *F. solani* species complex (O'Donnell et al., 2008)

[b] Ct values were determined by setting the threshold line at 0.1

[c] NRRL, The Agriculture Research Service Culture Collection, National Center for Agricultural Utilization Research, USDA/ARS

[d] Host plants for the microorganisms

[e] species isolates obtained from the study published by Gachango et al. (Gachango et al., 2012)

Real-time PCR primer and probe design for *F. virguliforme*

The multi-copy-number intergenic spacer (IGS) region of the ribosomal DNA (rDNA) was chosen to design primers and probes. IGS rDNA sequences of *Fusarium* species (Table2-1) were obtained from the National Center for Biotechnology Information (NCBI) GenBank database (FJ919498, FJ919499, FJ919507, FJ919510, FJ919511, FJ919512, FJ919515, and FJ919521). Eight IGS rDNA sequences from the soybean sudden death syndrome and bean root rot (SDS-BRR) clade of *Fusarium* species (i.e., *F. virguliforme, F. tucumaniae, F. cuneirostrum, F. crassistipitatum, F. brasiliense*, and *F. phaseoli*) were chosen for multiple sequence alignment to find the unique polymorphic regions of *F. virguliforme* using the MUltiple Sequence Comparison by Log- Expectation (MUSCLE) method (Edgar, 2004). In addition, the sequence self-repeat structure was viewed using the 'dottup' package in EMBOSS (Rice et al., 2000) to avoid cross amplification within the IGS rDNA region. Primers were designed to amplify PCR product sizes ranging from 50 to 150 bp. Polymorphic nucleotides unique to *F. virguliforme* were designed at the 3' end of the primers and the middle of probes. Melting temperatures for the primer oligos were predicted using the primer probe test tool in Primer Express 3.0 (Applied Biosystems, Carlsbad, CA). The secondary structure of the target amplicon was predicted with the 'mfold' software package (Zuker, 2003) at the temperature of PCR annealing step and with the final $[Mg^{2+}]$ = 2 mM and $[Na^{+}]$ = 50 mM. The free energy (ΔG) was used to evaluate the stability of the amplicon secondary structure, and the PCR product with a higher ΔG was selected as test candidates for further evaluation. For the probe design, the following rules were applied: probe Tm 10ºC higher than primer Tm; 15 to 30 nt in length; avoid G on the 5' end; and place the mismatching nucleotides in the middle of the probe instead of both ends. The 5' end of the TaqMan probe (Life Technologies) for *F. virguliforme* was labeled with 6FAM (fluorescein), and the 3' end was modified with a MGB (minor groove binder) and NFQ (non-fluorescent

quencher). Other PrimeTime dual-labeled probes (IDT, Coralville, Iowa) were labeled with 5' 6-FAM, internal ZEN quencher, and 3' Iowa Black FQ quencher. The exogenous control HHIC assay primers and probe were ordered from IDT as describe in Haudenshield and Hartman (2011).

qPCR amplification parameters

Real-time qPCR amplifications were performed on the ABI StepOnePlus thermocycler v2.3 (Applied Biosystems). Real-time qPCR was performed in a 20 µL total volume with at least two technical repeats. The qPCR mix consisted of 10 µL TaqMan Universal real-time PCR master mix (2X) (Applied Biosystems), 2 µL DNA template, 0.5 µL FvPrb-3 (10 µM), 0.5 µL for F6-3 and R6 primers (20 µM, Table2-2), 0.6 µL HHIC-F (20 µM) primer, 0.2 µL HHIC-R (20 µM), 0.4 µL HHIC-prb (10 µM), 0.5 µL linearized HHIC DNA plasmid (10 fg/ µL) (Haudenshield and Hartman, 2011), 0.4 µL of 10 mg/mL BSA and 4.4 µL distilled water (Gibco, Grand Island, NY). qPCR conditions were initialized with one cycle incubation at 50 ℃ for 2 min to activate uracil-N-glycosylase (UNG), one cycle at 95 ℃ for 10 min, 40 cycles at 95 ℃ for 15 s, 60 ℃ for 1 min, with fluorescent data collection in the annealing and extension step.

Table 2-2 Primers and probes used in the qPCR quantification assays.

Names	Sequences (5'-3')	Length (nt)	Tm (℃)[a]
F6-3[bde]	GTAAGTGAGATTTAGTCTAGGGTAGGTGAC	30	57.8
R6[be]	GGGACCACCTACCCTACACCTACT	24	59.6
FvPrb-3[be]	6FAM-TTTGGTCTAGGGTAGGCCG-MGBNFQ	19	70.0
R9[bd]	CCATCCGTCTGGGAATTTTAACTA	24	59.3
HHIC-F[c]	CTAGGACGAGAACTCCCACAT	21	54.6
HHIC-R[c]	CAATCAGCGGGTGTTTCA	18	55.0
HHIC-prb[c]	5HEX-TCGGTGTTGATGTTTGCCATGGT-3IABkFQ	23	65.2

[a] Tm values were calculated using ABI PrimerExpress 3.0 - Primer Probe Test Tool
[b] Primers and probes developed in this study
[c] Primers and probes developed by Haudenshield and Hartman (2011)
[d] Primers used for conventional PCR assay
[e] Primers and probes used for qPCR assay

Real-time PCR specificity and sensitivity tests

For the specificity tests, 100 pg of genomic DNA template of target and non-target species (listed in Table2-1) were tested against the designed assays. Only the assays with specificity to *F. virguliforme* were evaluated in the validation step. To determine the PCR efficiency and sensitivity, a ten-fold *F. virguliforme* genomic DNA serial dilution from 10 ng to 1 fg was tested with the specific qPCR assay. PCR efficiency was calculated with the formula: efficiency = $10^{(-1/slope)}-1$ (slope was calculated from the linear regression between DNA $\log_{10}$ (template DNA concentrations) and Ct values). *Fusarium virguliforme* genomic DNA serial dilutions were diluted with 1 ng/µL salmon sperm DNA (Invitrogen, Carlsbad, CA) to increase the stability of the low concentration DNA and protect against degradation or affinity to the plastic tubes.

Conventional PCR amplification parameters

Multiple primer sets were designed for the conventional PCR assay. To ensure ease of PCR amplification and product visualization in an agarose gel, the amplicon size was designed to be between 300 to 400 bp. Conventional PCR assays were performed with an ABI 2720 Thermal Cycler (Applied Biosystems). Conventional PCR was performed in a total volume of 25 µL, which included 2.5 µL 10X DreamTaq DNA buffer (Thermo Fisher Scientific, Waltham, MA), 0.2 µL 25 µM dNTPs (Promega, Madison, WI), 1 µL of 10 µM primers (Sigma-Aldrich, St. Louis, MO, Table2-2), 0.2 µL (5U/µl) DreamTaq DNA polymerase (Thermo Fisher Scientific), 0.5 µL 10 mg/mL BSA, 2 µL DNA template and distilled water to a total volume of 25 µL. PCR cycling conditions were set at one cycle at 94 ℃ for 3 min, followed by 35 cycles of 30 s at 94 ℃, 30 s at 65 ℃, 30 s at 72 ℃ and a final extension for 5 min at 72 ℃. PCR products were separated and visualized on a 1.5% agarose gel at 85 V for 45 min and stained with 1 µg/mL ethidium bromide. Genomic DNA of *F. virguliforme* was serially diluted 1:10 from 10 ng to 1 fg to test

the sensitivity of the conventional PCR assay. Also, 100 pg of genomic DNA from the specificity check panel (Table2-1) was tested against the conventional PCR assay.

DNA extraction from soil

To determine the applicability of the qPCR assay to soil samples, DNA was extracted from artificially inoculated and naturally infested soil samples. In artificially inoculated soil samples, 0.5 g of soil was inoculated with 100 µL 1:10 serially diluted *F. virguliforme* spore suspensions in sterile deionized water, with concentrations ranging from 10^8 spores/mL to 100 spores/mL. A half gram of moist Riddles-Hillsdale sandy loam soil was placed into a 2 mL lysing matrix E tube with the FastDNA SPIN kit for soil (MP Bio, Solon, OH). After adding 978 µL of sodium phosphate buffer and 122 µL of MT buffer, the tubes were placed in a FastPrep FP120 instrument (MP Bio) and homogenized twice at speed 6 for 40 s. Subsequent steps were performed according to the manufacturer's recommendations; DNA was eluted with a final volume of 100 µL of DES buffer (MP Biomedicals).

DNA extraction from soybean roots

Soybean roots with SDS-like foliar or root rot symptoms were collected from commercial fields and from samples submitted to the MSU Diagnostic Services Laboratory. Roots were washed with tap water, rinsed with deionized water, and patted dry with paper towel. Lateral or tap root tissues with obvious discoloration or lesions were preferred for DNA extraction; two technical replicates were made for each processed sample. One hundred milligrams of root tissue was added to a 2-mL lysing tube with five 1-mm diameter glass beads and one 2-mm diameter glass bead (except for samples processed in the Diagnostic Service Laboratory, where Lysing matrix A with two ceramic beads instead of the glass beads). Four hundred microliters of AP1 buffer from the Qiagen Plant DNeasy mini kit (Qiagen) was added to each of the 2-mL lysing

tubes and the mixture was homogenized in a FastPrep FP120 instrument (MP bio) twice at speed setting 6 for 40 s. After homogenization AP2 buffer (130 µL) was added to each tube and tubes were cooled on ice for 5 min, then spun at 16,000 g for 6 min. Subsequent DNA purification steps were performed as per the manufacturer's instruction. DNA concentration was measured using the Quant-iT dsDNA high-sensitivity assay kit (Invitrogen) on a 96-well SAFIRE microplate reader (TECAN).

Copy number of rDNA in *F. virguliforme*

Three single-copy genes (β-tubulin (HM453328.1), *G3PD* (glyceraldehyde 3-phosphate dehydrogenase), and *FvToxin-1* (JF440964.1)) were selected as single copy reference genes to determine the rDNA copy numbers among *F. virguliforme* isolates collected from multiple soybean fields. These genes were confirmed as single copy by BLASTn search against the *F. virguliforme* genome sequence (Srivastava et al., 2014). Primers specific to each of these three genes were designed using Primer Express 3.0 (Applied Biosystems) as listed in Table2-3. The PCR efficiency of these three primer sets was evaluated by running a five-fold serial dilution of *F. virguliforme* genomic DNA ranging from 10 ng to 1 pg. Quantification of the rDNA and the three single-copy genes was performed using SYBR green based qPCR, which consisted of 10 µL of 2X SYBR Green PCR Master Mix (Life Technologies), 0.5 µL of each primer (20 µM), 0.2 µL BSA (20 mg/mL) and distilled water (Gibco) to a total-volume of 20 µL in duplicate for each template DNA. Several genotypes were identified in a multilocus genotyping study of *F. virguliforme* (Wang and Chilvers, unpublished). Therefore, to maximize the genetic diversity among the tested *F. virguliforme* isolates, multiple isolates from different genotype groups were included in the rDNA copy number variation test. PCR cycling conditions were set at one cycle at 95 ℃ for 10 min, followed by 40 cycles of 15 s at 95 ℃, 60 s at 60 ℃ (fluorescent signal was

collected at this stage). After the qPCR cycling stage, the melt curve stage was performed to determine the specificity of each primer set. The melt curve stage parameter was set as: one step with 15 s at 95 ℃ for dissociation, 60 s at 60 ℃ for re-association, and increase the temperature from 60 ℃ to 95 ℃ with 0.3 ℃ increments using the step and hold method.

Table 2-3 Primers for determining rDNA IGS copy number variation

Names	Sequences (5'-3')	Length (nt)	Tm(℃)[a]	PCR efficiency	Amplicon size
gpd_F[b]	CTTGATGGCCTGCTTGATCTC	21	58.5	94.72%	74 bp
gpd_R[b]	ACGTCTCCGTTGTCGACCTTA	21	58.3		
b-tub_F[c]	CTGCAGCAGCTTCATCATGAG	21	58.4	99.36%	67 bp
b-tub_R[c]	CCGGTCTGGAGGTGAACCT	19	58.5		
FvTox1_F[d]	CAACAACACCCATCGCTAACG	21	60.0	95.12%	68 bp
FvTox1_R[d]	GGGAGGACCCCAGTTTTCC	19	59.2		

[a] Tm values were calculated using ABI PrimerExpress 3.0 (ABI) - Primer Probe Test Tool
[b] gpd: designed based on the *F. virguliforme* glyceraldehyde 3-phosphate dehydrogenase gene
[c] b-tub: designed based on the beta-tubulin gene
[d] FvTox1: designed based on the *FvTox1* gene, *FvTox1*: phytotoxin gene

Real-time PCR assay cross-laboratory and platform validation

Specificity and sensitivity of the qPCR assay was evaluated on a different platform, in collaboration with Michigan State University's Diagnostic Services Laboratory. The qPCR assay was performed on the Cepheid SmartCycler real-time PCR system (Cepheid, Sunnyvale, CA), in a 20 µL total volume with two technical repeats. The qPCR master mix and cycling conditions were the same as previously described and sensitivity was evaluated with serially diluted *F. virguliforme* genomic DNA from 10 ng to 10 fg with a 1:10 dilution factor. Specificity of this assay was tested against closely related *Fusarium* species (*F. tucumaniae, F. brasiliense, F. phaseoli, F. crassistipitatum*, and *F. cuneirostrum*). Additionally, soybean samples from commercial fields submitted for disease diagnosis were tested with this assay. DNA extraction from soybean samples was performed as described above.

Data analyses

Real-time PCR data were collected and analyzed using StepOne Software v2.3. qPCR standard curve plots and DNA concentration correlations were plotted using the R ggplot2 package (Wickham, 2009). The limit of detection was determined by 100% amplification of the lowest amount of target genomic DNA(Bustin et al., 2009). Statistical analysis was performed with the R stats package.

Results

Assay design and *in silico* screening

Based on the multiple sequence alignment conducted with MUSCLE, two polymorphic regions were identified as candidates for design of *F. virguliforme* specific assays. One of the polymorphic regions (from 481 to 777 bp) has a self-repeat (from 1736 to 2034 bp) in the IGS rDNA region (Figure 2-4). Primers designed on the self-repeat region were determined to be less specific to *F. virguliforme* because of the ambiguous nucleotide mismatches with the self-repeat region. Instead, the other polymorphic region (between 1.2 kb and 1.4 kb) of the IGS rDNA with moderate polymorphism did not have any self-repeats and was chosen as the target to design primers and probe for the final assay. Multiple primers (n=35) and dual-labeled probes (n=5) were designed on the polymorphic sites. Before testing primer sets, the secondary structure of the designed PCR assay amplicons were predicted using the mfold (Zuker, 2003) web server under PCR annealing conditions. The best amplicon candidates had higher free energy and fewer stem-loop structures as demonstrated in the assay (Figure 2-5).

Specificity and sensitivity of real-time PCR

A total of 30 primers and 6 probes were tested during assay development. One primer set (F6-3 and R6, Table 2-2) amplifying a 76-bp product from *F. virguliforme* and one TaqMan

probe (FvPrb-3, Table 2-2) were determined to be the most specific and sensitive primer and probe combination. The qPCR assay detected all tested target *F. virguliforme* strains at 100 pg of DNA with a Ct value range between 20.53 and 21.78, while the Ct value for the other non-target species were all above the preset Ct values of the lower limit of detection (LOD-Ct = 30, Table2-1). There was a linear relationship ($y = -3.3x + 36$ $R^2 = 0.996$) between *F. virguliforme* genomic DNA serial dilutions (log transformed) and Ct values, and the corresponding PCR efficiency was 99% (Figure 2-1). The genomic DNA serial dilution standard curve indicated that the qPCR assay consistently detected 10 fg of *F. virguliforme* genomic DNA (Ct = 33.2). The cut-off Ct value threshold for positive amplification was set at 100 fg of *F. virguliforme* genomic DNA to remove non-specific background amplifications (Figure 2-2). In the artificially inoculated soil samples, our qPCR assay consistently detected 100 conidia artificially inoculated in 0.5 g soil samples (Figure 2-3).

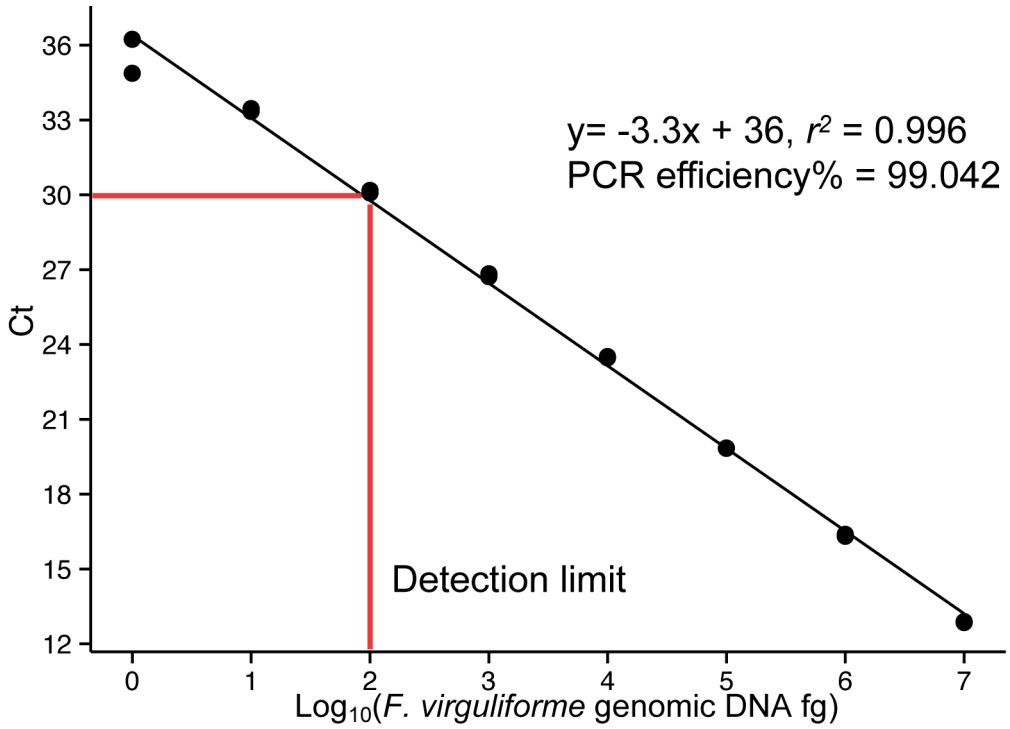

Figure 2-1 Standard curve for absolute quantification of *F. virguliforme* genomic DNA (fg). Genomic DNA samples were prepared from pure cultures grown in broth. The detection limit for pure culture genomic DNA was 100 fg. Two technical repeats for each *F. virguliforme* genomic DNA dilution level.

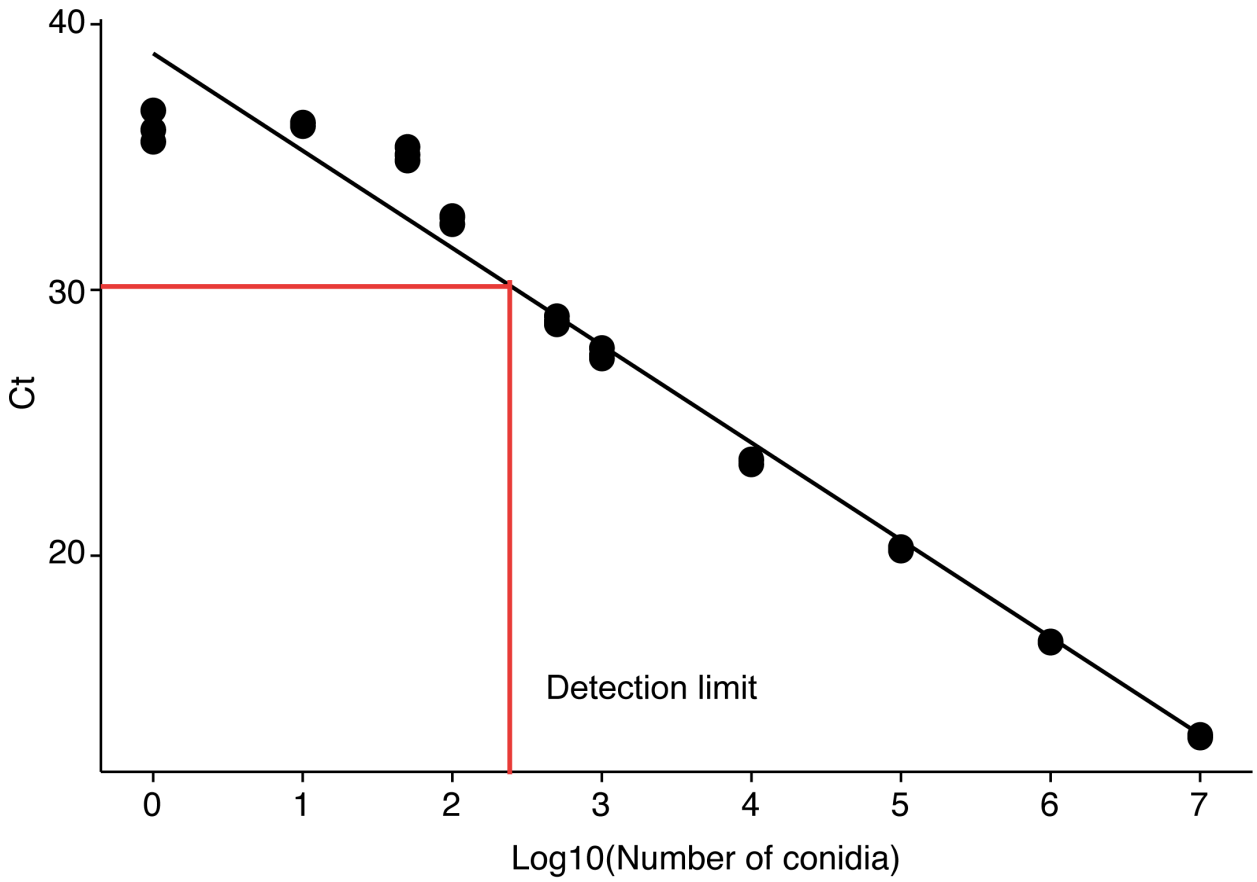

Figure 2-2 qPCR quantification of DNA samples isolated from artificially inoculated soil samples with serially diluted *F. virguliforme* macroconidia suspension. Detection limit was 100 macroconidia per 0.5 g soil. Total soil DNA were isolated from six soil sample replicates, and qPCR was run twice for each soil DNA sample.

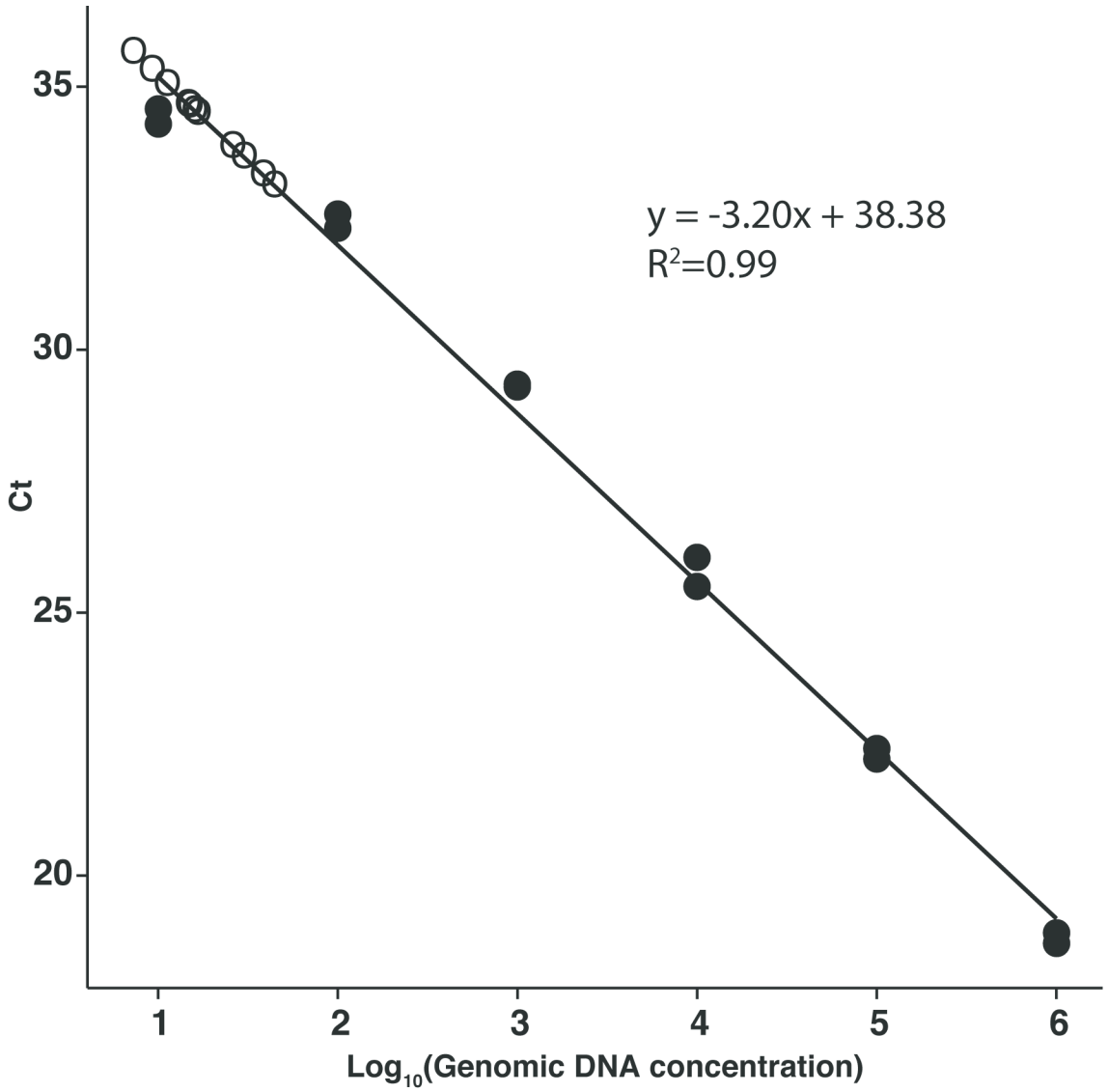

Figure 2-3 qPCR standard curve plotted with serially diluted genomic DNA (log transformed) in fg against Ct values with solid circles. Sensitivity of the assay was determined to be 100 fg of *F. virguliforme* genomic DNA.

Conventional PCR assay

The conventional PCR assay developed is specific to *F. virguliforme*, amplifying a 375 bp DNA fragment. The conventional PCR was specific to *F. virguliforme* except for weak amplification of two non-targets *Fusarium* species, *F. crassistipitatum* and *F. brasiliense* (product size = 375 bp). To overcome the nonspecific amplifications, the annealing temperature was raised from 60 ℃ to 65 ℃, which successfully eliminated amplification of these non-target species (Figure S2-4). The detection limit of the conventional PCR was determined to be 1 pg of *F. virguliforme* genomic DNA (Figure S2-3).

Validation of real-time PCR assay and conventional PCR assay

Both conventional PCR and real-time PCR were used to diagnose soybean plants collected from commercial soybean fields in Michigan from 2011 to 2013. Based on the diagnostic results (Table 2-5), SDS-like symptomatic soybean plants were not always associated with the positive detection of *F. virguliforme* DNA from soybean root tissues. For example, samples collected from Midland county Michigan (Midland-12-02) in 2012 were detected to be SDS negative, but tested positive for *Phialophora gregata* the causal agent of Brown Stem Rot (BSR) with the BSR diagnostic qPCR assay (Malvick and Impullitti, 2007). However, three plant samples with non-typical SDS foliar interveinal symptoms (MISO2-3, GR-12-02, and SA-11-2a) were determined to have positive *F. virguliforme* infection (Ct values < 30). Using the conventional PCR assay, most plant samples (27 out of 38) were diagnosed with definitive results, as indicated with intense bands. However, the sensitivity of the conventional PCR assay was limited, potentially causing false negative results for 11 out of 38 samples. In contrast, the qPCR assay gave unambiguous diagnostic results by simultaneously utilizing quantitative Ct values and a reliable exogenous control assay. In diagnostic samples with abundant *F. virguliforme* DNA the

exogenous control may perform abnormally (e.g. no exponential amplification or early amplifications). The exogenous control assay began to be affected when the *F. virguliforme* genomic DNA reached 1 pg or more in the diagnostic samples (Figure S2-5).

rDNA IGS copy number variation between isolates

Amplification efficiencies of the three single copy genes were all very similar at 95%, 99%, and 95% for the G3PD, β-tubulin, and FvTox1 assays, respectively. Less than 5% difference in efficiency exists between the qPCR assay and the single copy gene assays, indicating a valid rDNA copy number analysis. Melt curve analysis of the SYBR green PCR product, detected a single peak for each primer set, demonstrating amplification of a single product. The PCR efficiency of the qPCR assay was calculated using the formula: IGS copy = $(1+0.994)^{deltaCt}$, (e.g. deltaCt is the difference between Ct values of two amplified genes) given the PCR efficiency of 99.36%. The IGS rDNA copy numbers of *F. virguliforme* ranged from 138 to 233 with an average of 208 per haploid genome (Table 2-4).

Table 2-4 *Fusarium virguliforme* rDNA IGS copy number estimation using three single copy reference genes

	Mean Ct difference between IGS and single copy gene				
Isolates[a]	Btub[e]-IGS[b]	FvTox1[f]-IGS[b]	G3PD[g]-IGS[b]	Mean Ct diff[c]	Copy number[d]
INMO_A6	7.57	7.64	7.66	7.62	190
INMO_C5	7.69	7.53	7.76	7.66	195
KSSH_E5	7.83	7.54	7.84	7.74	205
MIBer_A6	7.59	7.51	7.71	7.60	187
MIBer_B7	7.76	7.56	7.83	7.72	202
MIBer_E1	7.99	7.76	8.02	7.92	233
MIIN_B7	7.89	7.67	7.93	7.83	219
MISA_C4	7.30	7.26	7.50	7.36	158
MISTJ_E4a	7.80	7.71	8.06	7.86	223
MISTJ_G5	8.02	7.66	8.04	7.91	231
MITU_B4	7.90	7.79	8.03	7.91	231

Table 2-4 (cont'd)

MIVB_A5	7.21	7.02	7.25	7.16	138
22292-Mont1	7.54	7.56	7.87	7.66	194

[a] *Fusarium virguliforme* isolates collected from Indiana (INMO), Kansas (KSSH), and Michigan (MIBer, MIIN, MISA. MISTJ, MITU and MIVB)
[b] Ct differences between IGS rDNA assay and single copy gene assay
[c] Average Ct for all three single copy genes
[d] Copy number determined by mean Ct differences
[e] Btub: beta tubulin gene
[f] FvTox1: phytotoxin gene produced by *F. virguliforme*
[g] G3PD: glyceraldehyde 3-phosphate dehydrogenase gene

qPCR assay cross-laboratory and platform validation

The qPCR assay performed similarly on both platforms tested. Assay sensitivity was determined to be 100 fg of *F. virguliforme* DNA and the assay was determined to be specific to this species. PCR efficiency of the *F. virguliforme* qPCR assay on the SmartCycler real-time PCR system and the StepOnePlus real-time PCR system was 99.8% and 99.0%, respectively. Sixteen soybean and one dry bean diagnostic samples were submitted from 14 counties in Michigan; 8 samples were diagnosed as positive for *F. virguliforme* with the qPCR assay Table 2-6. Of the 17 diagnostic samples tested on the SmartCycler system, 4 were also tested on the StepOnePlus system, producing comparable results. Ct values of DNA samples extracted from taproot versus lateral root were not significantly different ($p > 0.05$).

Table 2-5 Soybean and dry beans samples submitted to Michigan State University Diagnostic Services Laboratory for diagnosis assayed on a SmartCycler real-time PCR system.

Sample ID	Root parts [a]	County [c]	Dilution [d]	Ct	Results
2192	Lateral	Branch	1	19.32	positive
	Lateral	Branch	1:10	22.74	
	Tap	Branch	1	14.12	
	Tap	Branch	1:10	18.48	
2193	Lateral	Branch	1	29.22	positive
	Lateral	Branch	1:10	33.25	
	Tap	Branch	1	26.31	
	Tap	Branch	1:10	29.73	

Table 2-5 (cont'd)

2198	Lateral	Lenawee	1	26.42	positive
	Lateral	Lenawee	1:10	30.19	
	Tap	Lenawee	1	23.24	
	Tap	Lenawee	1:10	27.11	
2371	Lateral	Hillsdale	1	19.44	positive
	Lateral	Hillsdale	1:10	23.17	
	Tap	Hillsdale	1	22.32	
	Tap	Hillsdale	1:10	26.09	
2905[b]	Lateral	Huron	1	37.99	negative
	Lateral	Huron	1:10	UD[e]	
	Tap	Huron	1	UD	
	Tap	Huron	1:10	UD	
3006	Lateral	Allegan	1	24.41	positive
	Lateral	Allegan	1:10	23.97	
	Tap	Allegan	1	19.66	
	Tap	Allegan	1:10	23.51	
2603	Lateral	Shiawasee	1	UD	negative
	Lateral	Shiawasee	1:10	UD	
	Tap	Shiawasee	1	UD	
	Tap	Shiawasee	1:10	UD	
2591	Lateral	Clinton	1	UD	negative
	Lateral	Clinton	1:10	UD	
	Tap	Clinton	1	UD	
	Tap	Clinton	1:10	UD	
3059	Lateral	Ingham	1	18.97	positive
	Lateral	Ingham	1:10	23.07	
	Tap	Ingham	1	19.36	
	Tap	Ingham	1:10	22.81	
3062	Lateral	Van Buren	1	32.22	negative
	Lateral	Van Buren	1:10	36.39	
	Tap	Van Buren	1	37.13	
	Tap	Van Buren	1:10	UD	
3240	Lateral	Tuscola	1	36.41	negative
	Lateral	Tuscola	1:10	UD	
	Tap	Tuscola	1	34.37	
	Tap	Tuscola	1:10	UD	
3415	Lateral	Tuscola	1	35.25	negative
	Lateral	Tuscola	1:10	38.65	
	Tap	Tuscola	1	37.56	
	Tap	Tuscola	1:10	UD	
3505	Lateral	Van Buren	1	18.98	positive
	Lateral	Van Buren	1:10	22.28	
	Tap	Van Buren	1	17.48	
	Tap	Van Buren	1:10	20.45	

Table 2-5 (cont'd)

3525	Lateral	Saginaw	1	UD	negative
	Lateral	Saginaw	1:10	UD	
	Tap	Saginaw	1	37.97	
	Tap	Saginaw	1:10	UD	
3851	Lateral	Lapeer	1	31.08	negative
	Lateral	Lapeer	1:10	35.28	
	Tap	Lapeer	1	31.48	
	Tap	Lapeer	1:10	34.21	
3872	Lateral	Arenac	1	UD	negative
	Lateral	Arenac	1:10	UD	
	Tap	Arenac	1	39.22	
	Tap	Arenac	1:10	UD	
4532	Lateral	Lenawee	1	26.73	positive
	Lateral	Lenawee	1:10	31.16	
	Tap	Lenawee	1	36.86	
	Tap	Lenawee	1:10	UD	

[a] Root portion used for DNA extraction;
[b] Dry bean samples;
[c] Michigan county;
[d] DNA dilution level from the original DNA extraction; and
[e] UD undetected

Table 2-6 Diagnostic results for commercial soybean samples on StepOnePlus real-time PCR system. Results include isolation on semi-selective media, conventional PCR, plant symptoms, and qPCR Ct values.

Sample ID	Sources[a] (County)	Isolation[b]	CPCR[c]	qPCR	Fv Ct1 [d]	Fv Ct2	HHIC Ct1[e]	HHIC Ct2	Description of symptoms
Coleman	Midland	NEG[f]	POS[g]	POS	15.64	14.90	UD[f]	UD	Foliar SDS symptoms, leaf chlorosis and necrosis
Razjer	Van Buren	NEG	NEG	NEG	UD	UD	UD	UD	Root rot
Avery	Van Buren	NEG	?[h]	POS	29.48	31.36	29.48	28.64	SDS-like foliar symptoms
EA-13-1	Eaton	POS	POS	POS	31.42	29.55	28.26	28.21	SDS-like foliar symptoms discoloration of taproot
MtC-13-1	Montcalm	POS	POS	POS	29.59	27.76	28.23	28.15	SDS-like foliar symptoms
IN-13-1	Ingham	NEG	NEG	NEG	32.78	31.31	28.10	28.09	White mold symptoms and chlorosis on leaves
MISO2-7	Midland	NEG	NEG	NEG	31.38	31.27	29.42	29.47	Foliar symptom on the lower part plant, possible herbicide
CL-12-01	Clinton	NEG	NEG	NEG	34.97	33.44	29.04	29.31	Foliar SDS-like symptom, but not typical
IO-12-01	Ionia	NEG	NEG	NEG	34.62	33.55	29.25	29.23	Foliar chlorosis symptom
EA-12-01	Eaton	NEG	?	NEG	32.33	32.28	29.08	29.21	no SDS foliar symptoms
TU-12-01	Tuscola	NEG	?	NEG	32.93	30.88	29.27	29.18	Manganese deficiency symptoms
GR-12-01	Gratiot	POS	POS	POS	31.34	24.15	29.34	28.93	Typical SDS-like symptoms, wilting
IS-12-01	Isabella	NEG	NEG	NEG	34.67	34.52	29.16	28.99	no SDS foliar symptoms
MISO2-3	Allegan	NEG	POS	POS	29.68	26.78	29.22	29.06	Both oomycete and fungal wilting symptom
IN-12-01	Ingham	NEG	NEG	NEG	33.18	35.22	29.20	29.39	Interveinal chlorosis, lack of hairy roots, may be BSR pith dark brown, but BSR assay negative
GR-12-02	Gratiot	NEG	POS	POS	33.09	27.96	29.22	28.95	Wilting and leaves chlorosis
Midland-12-02	Midland	NEG	?	NEG	35.52	34.88	29.29	29.13	SDS-like foliar symptoms, brown pith, BSR assay positive
DL201203875	Monroe	POS	POS	POS	18.59	-[i]	UD	-	Brown stem, leaves discoloration
EA-12-02	Eaton	NEG	?	NEG	32.71	31.7	29.13	29.236	Phytoplasma symptoms, but no SDS symptoms

Table 2-6 (cont'd)

SA-11-2a	Saginaw	POS	POS	POS	20.55	-	*23.24	-	Plant wilting, defoliation, and Dead
SA-11-2b	Saginaw	NEG	POS	POS	21.16	-	UD	-	Foliar SDS-like symptom
HU-11-1b	Huron	POS	POS	POS	21.50	-	UD	-	Foliar SDS-like symptom
HU-11-1 (DL-6)	Huron	POS	POS	POS	21.89	-	*23.90	-	Foliar SDS-like symptom
DL-5	Lenawee	POS	POS	POS	20.21	20.83	UD	UD	Foliar SDS-like symptom
SA-11-1	Saginaw	POS	POS	POS	24.32	25.84	28.18	27.766	Foliar SDS-like symptom
CL-11-1	Clinton	POS	POS	POS	24.00	-	*26.97	-	N/A
GR-11-2b	Gratiot	POS	POS	POS	28.22	-	28.2	-	Foliar SDS-like symptom
CL-11-2	Clinton	NEG	POS	POS	28.23	-	28.09	-	N/A
GR-11-2a	Gratiot	NEG	POS	POS	28.03	-	28.31	-	Plant Defoliation and Dead
IN-11-1	Ingham	NEG	POS	POS	29.75	-	29.29	-	Foliar SDS-like symptom
TUS-11-2a	Tuscola	NEG	?	NEG	33.58	-	28.43	-	Leaf burn/ herbicide/desiccant damage
TUS-11-2b	Tuscola	NEG	?	NEG	33.38	-	28.09	-	Foliar SDS-like symptom
TUS-11-1b	Tuscola	NEG	?	NEG	33.85	-	28.08	-	Stunted beans/yellowing/root rot
HU-11-2	Huron	NEG	?	NEG	32.55	-	28.34	-	SDS-like symptoms
TUS-11-1a	Tuscola	NEG	?	NEG	33.79	-	28.18	-	N/A
DL-4	Kalamazoo	NEG	?	NEG	34.71	33.94	28.32	28.476	Foliar SDS-like symptom
TUS-11-3	Tuscola	NEG	NEG	NEG	34.35	-	28.14	-	Foliar SDS-like symptom

[a] County in Michigan where samples were collected from;
[b] Positive isolation was identified by colony morphology;
[c] CPCR, conventional PCR assay results;
[d] Two DNA extractions were made for qPCR detection;
[e] Internal control to assess the potential PCR inhibitors, *abnormal Ct values affected by *F. virguliforme* assay competition;
[f] NEG: negative results;
[g] POS: positive results;
[h] ? unclear results, i.e. weak band
[i] not applicable

Discussion

Soybean SDS is a major threat to soybean production in the United States. Specific and sensitive molecular diagnostic assays are lacking, which hampers diagnosis, and limits epidemiological studies of the disease. To address this need, we developed a specific and sensitive qPCR assay to quantify *F. virguliforme* in soybean tissue, soil, and environmental samples. The assay was specific to *F. virguliforme* when tested against closely related *Fusarium* species and other commonly encountered fungi in soybean fields. The assay is very sensitive and can detect as little as 100 fg of *F. virguliforme* genomic DNA or 100 macroconidia per half gram of soil. An exogenous control was multiplexed with the *F. virguliforme* assay to detect false negatives and monitor for the presence of PCR inhibitors. In addition, the assay was validated with soybean samples collected from commercial soybean fields. The qPCR assay is transferable and successfully performed on a Cepheid SmarterCycler real-time PCR platform at the North Central region's hub laboratory of the National Plant Diagnostic Network.

The choice of genetic locus and *in silico* sequence analysis plays a pivotal role in development and performance of a qPCR assay. Revision of the taxonomy of *Fusarium* species that cause SDS or bean root rot has resulted in the obsolescence of previously developed assays. However, the taxonomic revision and loci used for phylogeny construction also provided an opportunity for the development of more specific diagnostic assays. The phylogenetic tree constructed with IGS rDNA sequences explicitly separated the *Fusarium* species in the SDS-BRR (bean root rot) clade with high branch support (O'Donnell et al., 2010). Therefore, the IGS rDNA was determined to be a suitable target locus to design an assay for the specific detection of *F. virguliforme*. The multi-copy nature of the IGS rDNA target was also desirable from the standpoint of assay specificity.

An optimized multiple sequence alignment is essential for identifying suitable polymorphic regions within a locus for species-specific primer and probe design. Different sequence alignment methods (MUSCLE, MAFFT, ClustalW, and T-Coffee) were used to align the IGS rDNA sequence of SDS-BRR clade *Fusarium* species. The multiple sequence alignments of the IGS rDNA loci required the insertion of a considerable number of gaps, which increased the complexity of the alignment. Alignments with ClustalW (Larkin et al., 2007) and T-Coffee (Notredame et al., 2000) resulted in alignments that were not optimal for locating polymorphic loci. However, the use of methods such as MUSCLE (Edgar, 2004) and MAFFT (Katoh and Standley, 2013) resulted in the identification and validation of polymorphisms suitable for specific species discrimination.

Sensitivity is also a significant factor that determines the applicability of a qPCR assay. For the previous qPCR assays designed for *F. virguliforme*, two targeted the small subunit of the mitochondrial DNA and the other was designed on the *FvTox1* toxin-coding gene (Gao et al., 2004; Li et al., 2008; Mbofung et al., 2011). Although the limit of detection for the mtDNA assays was 90 fg genomic DNA, these two assays are not specific to *F. virguliforme* based on the discovery of four SDS and three BRR *Fusarium* pathogens (Aoki et al., 2005; Aoki et al., 2012). The assay designed to the *FvTox1* is specific, however the assay is not as sensitive, because it requires 25 pg of genomic DNA. We designed our qPCR assay to the IGS rDNA region, and the limit of detection was determined to be 100 fg of genomic DNA (approximately equivalent to the DNA quantity of four haploid genomes of *F. virguliforme*), which is 100 times more sensitive than the single copy *FvTox1* gene assay.

Ribosomal DNA copy number variation and IGS rDNA sequence variation among isolates have been reported in several fungal species (Herrera et al., 2009; Akamatsu et al., 2012;

Bilodeau et al., 2012). Variation in rDNA copy number within species may cause variability in qPCR assay sensitivity. IGS rDNA sequence variation within species may affect the specificity of the qPCR assay as well. In this study, we tested our qPCR assay with numerous isolates of *F. virguliforme* obtained from isolates representing the primary genetic groups (Wang and Chilvers, unpublished) from geographically distant locations from within the United States. Although the rDNA copy number ranged from 138 to 233 with an average number of 208 copies per haploid genome, the largest difference in Ct value was 0.76 cycles, which is within the same order of magnitude. Therefore, the differences in rDNA IGS copy numbers did not cause significant differences in qPCR quantification or diagnostic detection.

Although improved sensitivity and specificity are ideal, consistent performance in dealing with 'real-world' diagnostic soybean samples was of primary concern. The molecular diagnostic assay results are strong evidence in determining a diagnostic conclusion, especially when the submitted plant samples lack other specific symptoms or signs. Because of PCR inhibitors in plant DNA or plant tissue sampling bias, the molecular diagnostic assay detection results can be inconsistent (Table 2-5). To avoid the potential inconsistent detection of *F. virguliforme* during diagnostics, we implemented PCR additives (e.g., BSA), which alleviated the PCR inhibition effects. Multiple (n>=2) biological and technical repeats are recommended to improve consistency in the diagnostic assay. Normally, without competition or inhibition, the HHIC exogenous control assay will produce a Ct value of 29. However, inhibitors in the DNA samples can prevent PCR amplification for the *F. virguliforme* assay and exogenous control assay. To overcome the PCR inhibition issues, magnetic bead based DNA sample purification can be used to reduce PCR inhibitors in DNA samples. Furthermore, PCR inhibitions are not the only cause for lack of amplification in the exogenous control assay. Too much *F. virguliforme* genomic

DNA in the sample can also cause no amplification or malfunction of the HHIC exogenous control assay. When the *F. virguliforme* genomic DNA reaches 1 pg in the reaction, the HHIC exogenous control assay is affected. Therefore, interpretations of the HHIC exogenous control results help evaluate the performance of the *F. virguliforme* assay.

Stable performance across labs is one of the most important criteria of a qPCR diagnostic assay. The performance of a qPCR assay can be vulnerable to changes in the PCR reagents or real-time PCR systems (Hayden et al., 2008). It may require efforts to optimize the qPCR conditions to perform a robust qPCR assay with the desired performance. Use of a qPCR assay on a new platform, change in PCR master mix, or use in a new lab should always be implemented with the appropriate validation. To explore the applicability of our qPCR assay on another real-time PCR systems, we collaborated with the Michigan State University Diagnostic Services Laboratory. Assay performance was tested on a Cepheid SmartCycler real-time PCR system, which is the most popular system in the North Central region of the National Plant Diagnostic Network. Without changing the reagents or cycling parameters, this assay successfully achieved the desired performance (specificity, sensitivity and PCR efficiency), demonstrating high transferability of this assay between platforms. In addition, the Michigan State University Diagnostic Services Laboratory used this assay for the diagnostic evaluation of soybean and dry bean plants with SDS and/or root rot symptoms (Table 2-6). Although both taproot and lateral root tissues were used for DNA extractions, the detection results (Ct values) were not significantly different.

The *F. virguliforme*-specific qPCR assay presented here allows for the rapid and accurate quantification of *F. virguliforme*, which will facilitate epidemiological studies and diagnosis of this pathogen in plant, soil and environmental samples. The assay may be used to screen for root

rot resistance where visual estimation or culture-based methods are difficult or not practical. In addition, the assay may be used to potentially predict the pre-plant risk of SDS development if *F. virguliforme* inoculum thresholds can be established.

Acknowledgement

We are grateful to Dr. James Haudenshield and Dr. Glen Hartman of the USDA-ARS at the University of Illinois at Urbana Champaign for generously providing the HHIC plasmid. We thank Esther Gachango and Dr. Willie Kirk for sharing *Fusarium* strains. This work was supported by grants from Project GREEEN (#GR10-113), the Michigan Soybean Promotion Committee, and the A.L. Rogers Endowed Research Scholarship.

APPENDIX

Supplementary figures

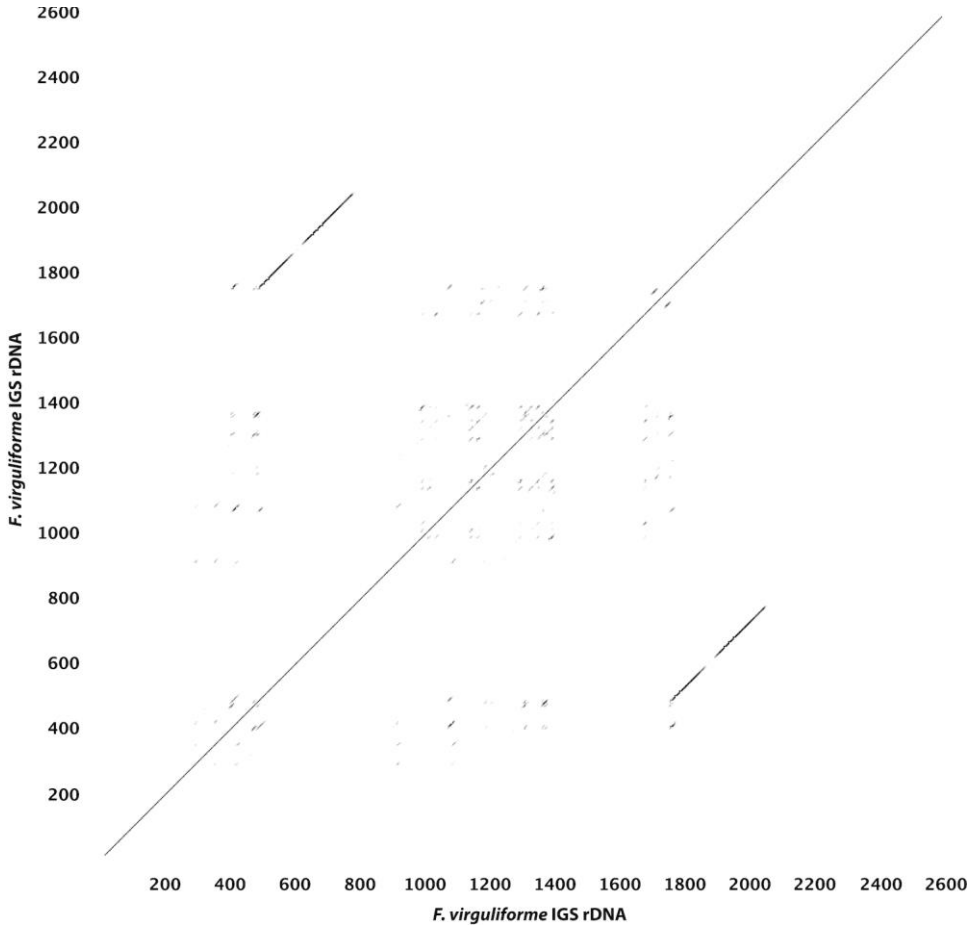

Figure S 2-1 Sequence self-dot plot of the IGS rDNA of *F. virguliforme*. Showing a repeat that may cause mis-binding in PCR assay. The plot was generated using the dottup package from EMBOSS.

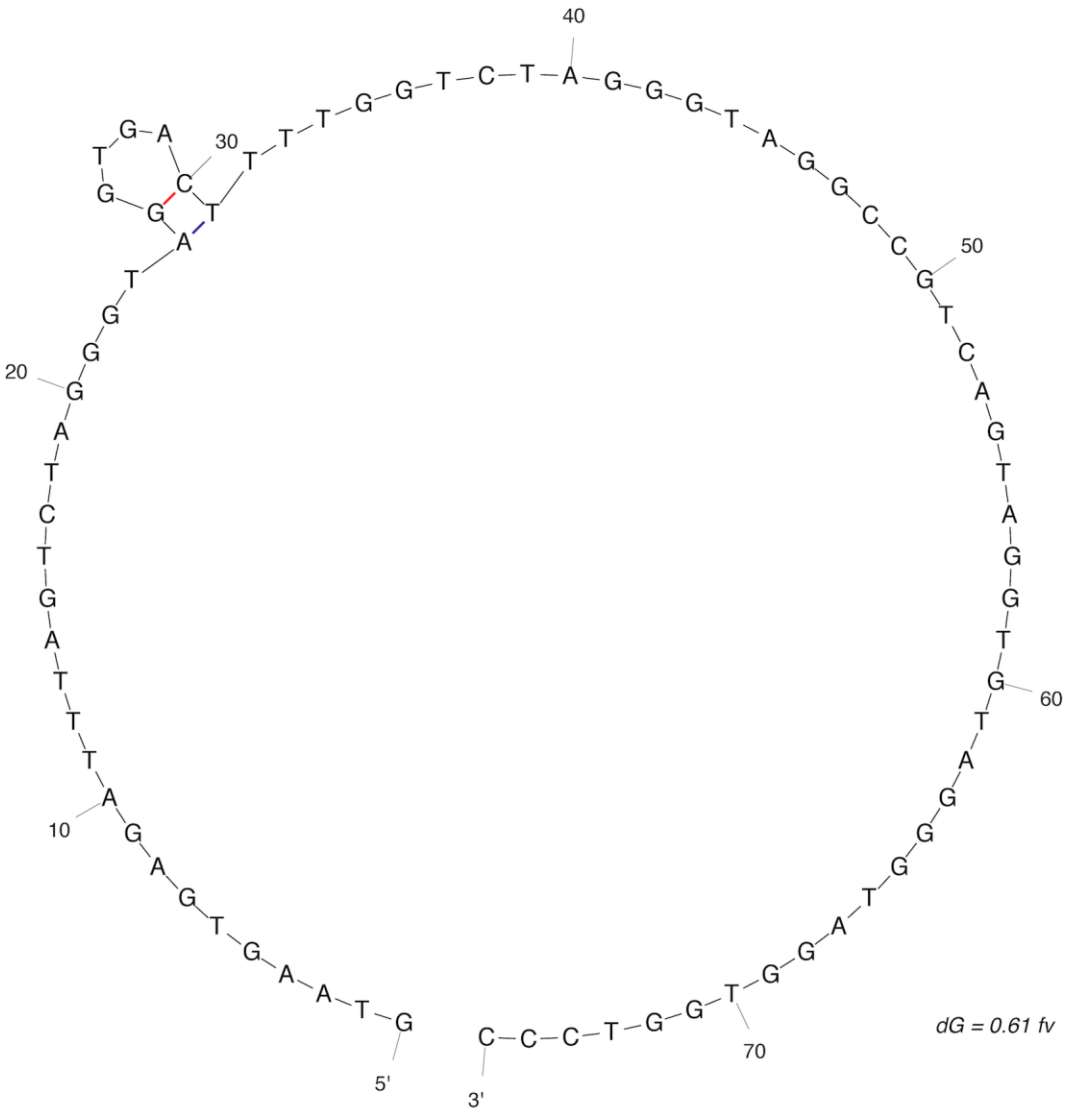

Figure S 2-2 Simulation of target amplicon secondary structure at annealing stage of the qPCR conducted using mfold

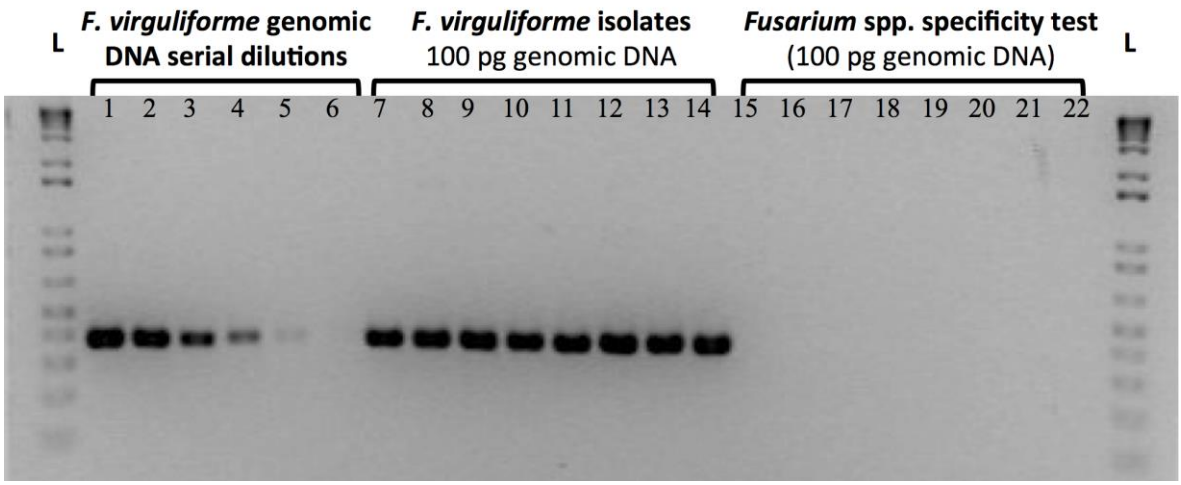

Figure S 2-3 Assay sensitivity and specificity test, L: 1 kb+ DNA ladder, lane1 – lane 6: 1 ng through 10 fg *F. virguliforme* genomic DNA, lane 7 – lane 14: panel of *F. virguliforme* isolates at 100 pg genomic DNA, lane 15 – lane 22: panel of other *Fusarium* spp. at 100 pg genomic DNA (*F. tucumaniae, F. brasiliense, F. phaseoli, F. phaseoli, F. crassistipitatum, F. cuneirostrum, F. tucumaniae*, and *F. brasiliense*)

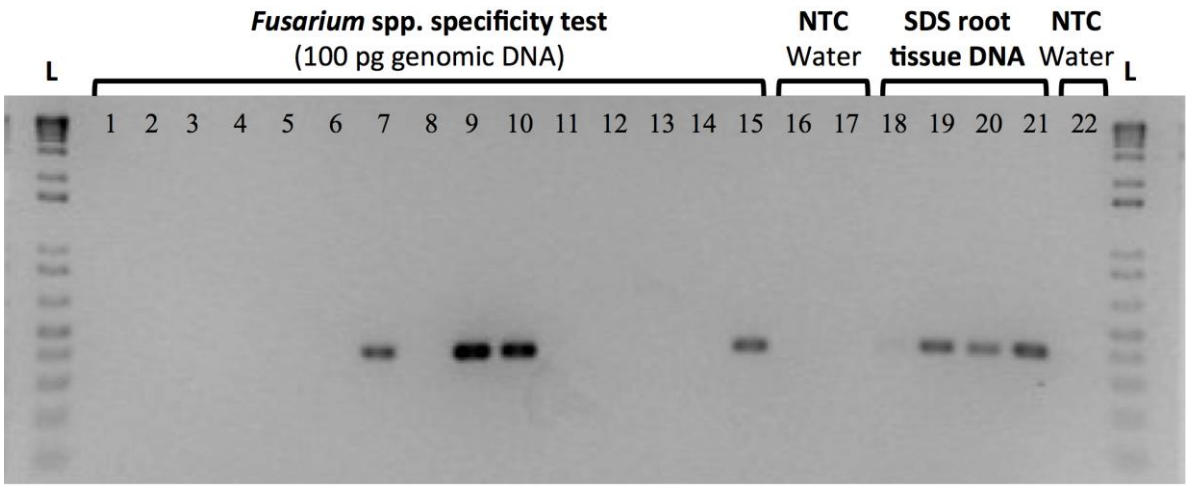

Figure S 2-4 Assay specificity test and validation, L: 1 kb+ DNA ladder, lane 1 – lane 6, lane 8, and lane 11 – lane 14: Other *Fusarium* spp.; lane 7, lane 9 – lane 10, and lane 15: *F. virguliforme* isolates; lane 18 – lane 21: SDS soybean root tissue DNA; lane 16, lane 17, and lane 22: NTC

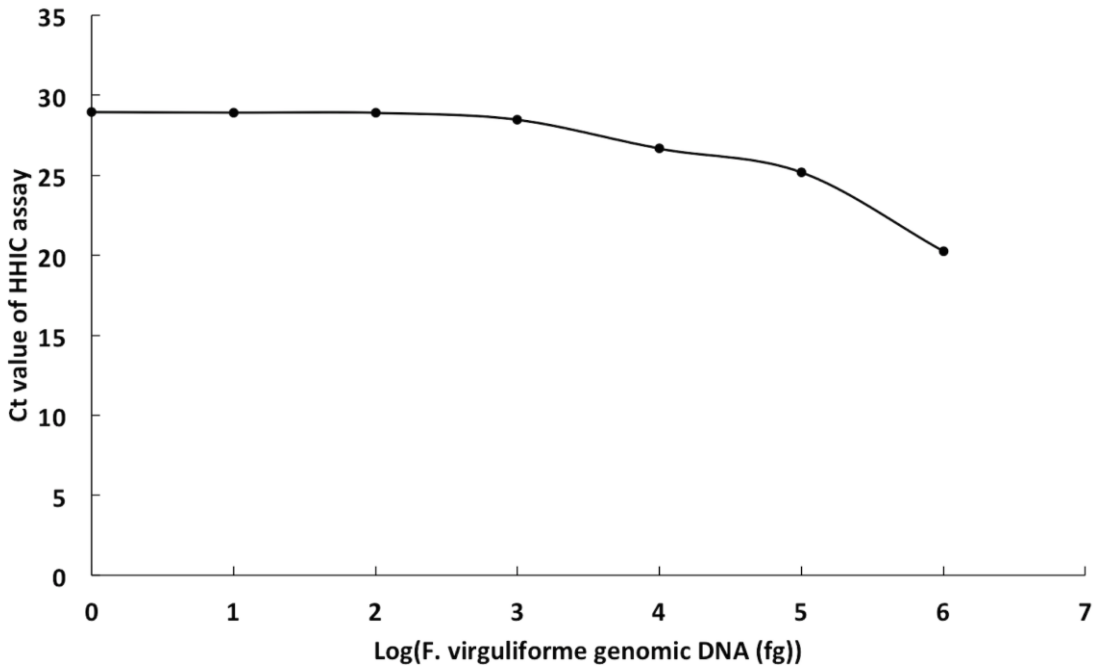

Figure S 2-5 Interference of the *F. virguliforme* qPCR assay to HHIC exogenous assay in the serially diluted genomic DNA samples. Ct values of exogenous control assay (y axis) were plotted with the log transformed genomic DNA concentration (x axis). With the increase of the genomic DNA concentration, the Ct value of the exogenous control assay was affected

REFERENCES

REFERENCES

Achenbach, L.A., Patrick, J.A., and Gray, L.E. 1996. Use of RAPD markers as a diagnostic tool for the identification of *Fusarium solani* isolates that cause soybean sudden death syndrome. Plant Dis 80:1228-1232.

Akamatsu, H.O., Chilvers, M.I., Kaiser, W.J., and Peever, T.L. 2012. Karyotype polymorphism and chromosomal rearrangement in populations of the phytopathogenic fungus, *Ascochyta rabiei*. Fungal Biol 116:1119-1133.

Aoki, T., O'Donnell, K., and Scandiani, M.M. 2005. Sudden death syndrome of soybean in South America is caused by four species of *Fusarium*: *Fusarium brasiliense* sp. nov., *F. cuneirostrum* sp. nov., *F. tucumaniae*, and *F. virguliforme*. Mycoscience 46:162-183.

Aoki, T., Scandiani, M.M., and O'Donnell, K. 2012. Phenotypic, molecular phylogenetic, and pathogenetic characterization of *Fusarium crassistipitatum* sp. nov., a novel soybean sudden death syndrome pathogen from Argentina and Brazil. Mycoscience 53:167-186.

Aoki, T., O'Donnell, K., Homma, Y., and Lattanzi, A. 2003. Sudden-death syndrome of soybean is caused by two morphologically and phylogenetically distinct species within the *Fusarium solani* species complex *F. virguliforme* in North America and *F. tucumaniae* in South America. Mycologia 95:660.

Bilodeau, G.J., Koike, S.T., Uribe, P., and Martin, F.N. 2012. Development of an assay for rapid detection and quantification of *Verticillium dahliae* in soil. Phytopathology 102:331-343.

Brar, H.K., and Bhattacharyya, M.K. 2012. Expression of a single-chain variable-fragment antibody against a *Fusarium virguliforme* toxin peptide enhances tolerance to sudden death syndrome in transgenic soybean plants. Mol Plant Microbe Interact 25:817-824.

Bustin, S.A., Benes, V., Garson, J.A., Hellemans, J., Huggett, J., Kubista, M., Mueller, R., Nolan, T., Pfaffl, M.W., Shipley, G.L., Vandesompele, J., and Wittwer, C.T. 2009. The MIQE guidelines: minimum information for publication of quantitative real-time PCR experiments. Clin Chem 55:611-622.

Chilvers, M.I., du Toit, L.J., Akamatsu, H., and Peever, T.L. 2007. A real-time, quantitative PCR seed assay for *Botrytis* spp. that cause neck rot of onion. Plant Dis 91:599-608.

Cho, J.H., Rupe, J.C., Cummings, M.S., and Gbur, E.E. 2001. Isolation and identification of *Fusarium solani* f. sp *glycines* from soil on modified Nash and Snyder's medium. Plant Dis 85:256-260.

Edgar, R.C. 2004. MUSCLE: multiple sequence alignment with high accuracy and high throughput. Nucleic Acids Res 32:1792-1797.

Gachango, E., Hanson, L.E., Rojas, A., Hao, J.J., and Kirk, W.W. 2012. *Fusarium* spp. causing dry rot of seed potato tubers in Michigan and their sensitivity to fungicides. Plant Dis 96:1767-1774.

Gao, X., Hartman, G., and Niblack, T. 2006. Early infection of soybean roots by *Fusarium solani* f. sp *glycines*. Phytopathology 96:S38-S38.

Gao, X., Jackson, T.A., Lambert, K.N., Li, S., Hartman, G.L., and Niblack, T.L. 2004. Detection and quantification of *Fusarium solani* f. sp *glycines* in soybean roots with real-time quantitative polymerase chain reaction. Plant Dis 88:1372-1380.

Gramaje, D., Perez-Serrano, V., Montes-Borrego, M., Navas-Cortes, J.A., Jimenez-Diaz, R.M., and Landa, B.B. 2013. A comparison of real-time PCR protocols for the quantitative monitoring of asymptomatic olive infections by *Verticillium dahliae* pathotypes. Phytopathology 103:1058-1068.

Haudenshield, J.S., and Hartman, G.L. 2011. Exogenous controls increase negative call veracity in multiplexed, quantitative PCR assays for *Phakopsora pachyrhizi*. Plant Dis 95:343-352.

Hayden, R.T., Hokanson, K.A., Pounds, S.B., Bankowski, M.J., Belzer, S.W., Carr, J., Diorio, D., Forman, M.S., Joshi, Y., Hillyard, D., Hodinka, R.L., Nikiforova, M.N., Romain, C.A., Stevenson, J., Valsamakis, A., Balfour, H.H., and Grp, U.E.W. 2008. Multicenter comparison of different real-time PCR assays for quantitative detection of Epstein-Barr virus. J Clin Microbiol 46:157-163.

Herrera, M.L., Vallor, A.C., Gelfond, J.A., Patterson, T.F., and Wickes, B.L. 2009. Strain-dependent variation in 18S ribosomal DNA Copy numbers in *Aspergillus fumigatus*. J Clin Microbiol 47:1325-1332.

Jiang, J.L., Alderisio, K.A., Singh, A., and Xiao, L.H. 2005. Development of procedures for direct extraction of *Cryptosporidium* DNA from water concentrates and for relief of PCR inhibitors. Appl Environ Microb 71:1135-1141.

Katoh, K., and Standley, D.M. 2013. MAFFT multiple sequence alignment software version 7: improvements in performance and usability. Mol Biol Evol 30:772-780.

Kolander, T.M., Bienapfl, J.C., Kurle, J.E., and Malvick, D.K. 2012. Symptomatic and asymptomatic host range of *Fusarium virguliforme*, the causal agent of soybean sudden death syndrome. Plant Dis 96:1148-1153.

Larkin, M.A., Blackshields, G., Brown, N.P., Chenna, R., McGettigan, P.A., McWilliam, H., Valentin, F., Wallace, I.M., Wilm, A., Lopez, R., Thompson, J.D., Gibson, T.J., and Higgins, D.G. 2007. Clustal W and Clustal X version 2.0. Bioinformatics 23:2947-2948.

Li, S., and Hartman, G.L. 2003. Molecular detection of *Fusarium solani* f. sp *glycines* in soybean roots and soil. Plant Pathol 52:74-83.

Li, S., Hartman, G.L., Domier, L.L., and Boykin, D. 2008. Quantification of *Fusarium solani* f. sp *glycines* isolates in soybean roots by colony-forming unit assays and real-time quantitative PCR. Theor Appl Genet 117:343-352.

Long, E.O., and Dawid, I.B. 1980. Repeated genes in eukaryotes. Annu Rev Biochem:727-764.

Luo, Y., Myers, O., Lightfoot, D., and Schmidt, M. 1999. Root colonization of soybean cultivars in the field by *Fusarium solani* f. sp. *glycines*. Plant Dis 83:1155-1159.

Malvick, D., and Impullitti, A. 2007. Detection and quantification of *Phialophora gregata* in soybean and soil samples with a quantitative, real-time PCR assay. Plant Dis 91:736-742.

Malvick, D.K., and Grunden, E. 2005. Isolation of fungal DNA from plant tissues and removal of DNA amplification inhibitors. Mol Ecol Notes 5:958-960.

Mbofung, G.C.Y., Fessehaie, A., Bhattacharyya, M.K., and Leandro, L.F.S. 2011. A new TaqMan real-time polymerase chain reaction assay for quantification of *Fusarium virguliforme* in soil. Plant Dis 95:1420-1426.

Navi, S.S., and Yang, X. 2008. Foliar symptom expression in association with early infection and xylem colonization by *Fusarium virguliforme* (formerly *F. solani* f. sp. *glycines*), the causal agent of soybean sudden death syndrome. Plant Health Progress 10.

Notredame, C., Higgins, D.G., and Heringa, J. 2000. T-Coffee: A novel method for fast and accurate multiple sequence alignment. J Mol Biol 302:205-217.

O'Donnell, K., and Gray, L.E. 1995. Phylogenetic relationships of the soybean sudden death syndrome pathogen *Fusarium solani* f. sp. *phaseoli* inferred from rDNA sequence data and PCR primers for its identification. Mol Plant Microbe Interact 8:709-716.

O'Donnell, K., Sutton, D.A., Fothergill, A., McCarthy, D., Rinaldi, M.G., Brandt, M.E., Zhang, N., and Geiser, D.M. 2008. Molecular phylogenetic diversity, multilocus haplotype nomenclature, and in vitro antifungal resistance within the *Fusarium solani* species complex. J Clin Microbiol 46:2477-2490.

O'Donnell, K., Sink, S., Scandiani, M.M., Luque, A., Colletto, A., Biasoli, M., Lenzi, L., Salas, G., Gonzalez, V., Ploper, L.D., Formento, N., Pioli, R.N., Aoki, T., Yang, X.B., and Sarver, B.A. 2010. Soybean sudden death syndrome species diversity within North and South america revealed by multilocus genotyping. Phytopathology 100:58-71.

Patrinos, G.P., and Ansorge, W. 2010. Molecular diagnostics. Elsevier Academic Press, Amsterdam, Boston.

Rice, P., Longden, I., and Bleasby, A. 2000. EMBOSS: The European molecular biology open software suite. Trends Genet 16:276-277.

Roy, K.W., Hershman, D.E., Rupe, J.C., and Abney, T.S. 1997. Sudden death syndrome of soybean. Plant Dis 81:1100-1111.

Roy, K.W., Lawrence, G.W., Hodges, H.H., Mclean, K.S., and Killebrew, J.F. 1989. Sudden death syndrome of soybean: *Fusarium solani* as incitant and relation of *Heterodera glycines* to disease severity. Phytopathology 79:191-197.

Rupe, J.C. 1989. Frequency and pathogenicity of *Fusarium solani* recovered from soybeans with sudden death syndrome. Plant Dis 73:581-584.

Schaad, N.W., and Frederick, R.D. 2002. Real-time PCR and its application for rapid plant disease diagnostics. Canadian Journal of Plant Pathology 24:250-258.

Srivastava, S.K., Huang, X., Brar, H.K., Fakhoury, A.M., Bluhm, B.H., and Bhattacharyya, M.K. 2014. The genome sequence of the fungal pathogen *Fusarium virguliforme* that causes sudden death syndrome in soybean. PloS one 9:e81832.

Wickham, H. 2009. ggplot2: elegant graphics for data analysis. Springer Science & Business Media.

Wrather, J., and Koenning, S. 2010. Suppression of soybean yield potential in the continental United States by plant diseases from 2006 to 2009. Plant Health Progress HP-2010:1122-1101.

Wrather, J., and Koenning, S. (2011). Soybean disease loss estimates for the United States, 1996-2010. (http://aes.missouri.edu/delta/research/soyloss.stm) Access date: Dec 2013 2013

Zuker, M. 2003. Mfold web server for nucleic acid folding and hybridization prediction. Nucleic Acids Res 31:3406-3415.

CHAPTER 3 TEMPORAL DYNAMICS OF *FUSARIUM VIRGULIFORME* IN SOYBEANS

Abstract

Sudden death syndrome (SDS) is one of the most yield limiting soybean diseases in the United States. SDS symptoms include two major components: root rot caused by *Fusarium virguliforme* infection and foliar symptoms induced by fungal toxins. Planting SDS resistant soybean cultivars is one of the most effective disease management options, but no cultivar displays full resistance. In breeding programs, SDS foliar symptoms are used as the major phenotype in screening for SDS resistant soybean germplasm. Disease severity rating for resistance to *F. virguliforme* seldom includes examination of root infection or colonization, partly due to the laborious nature of methods for quantification of *F. virguliforme*. In this study, two greenhouse and three field experiments were conducted to determine the temporal dynamics of *F. virguliforme* colonization of soybean roots using quantitative real-time PCR (qPCR). In addition, soybean cultivars with varied levels of SDS resistance were selected to identify their responses to *F. virguliforme* infection and colonization. In the greenhouse experiments, all soybean cultivars developed SDS foliar symptoms, but the *F. virguliforme* root colonization levels did not significantly correlate with SDS foliar symptoms. *Fusarium virguliforme* in soybean roots was detected as early as 7 days after planting (DAP) and quantification peaked at 14 DAP, and maintained a relatively stable quantity until 35 DAP. In the field experiments, varied levels of SDS foliar symptoms developed among soybean cultivars; however, the *F. virguliforme* infection coefficients across the cultivars were not significantly different between SDS foliar symptomatic and asymptomatic cultivars. In the 2014 field experiment where individual plants were rated, there was no significant correlation between SDS foliar symptoms and the *F. virguliforme* infection coefficient detected in roots. Starting from the initial V3 stage (25 DAP) sampling, *F. virguliforme* was detected in all soybean cultivars, with *F. virguliforme* infection coefficient increasing in roots over time, reaching a maximum level for all soybean

cultivars at the post-harvest stage (153 DAP). The area under the *F. virguliforme* infection coefficient curves was not significantly correlated with the SDS foliar symptoms in both greenhouse and field experiments. Collectively, appearance and disease severity ratings of SDS foliar symptoms were not associated with *F. virguliforme* infection coefficient in roots, thus it suggests a need to include *F. virguliforme* root colonization as a breeding trait to screen soybean germplasm for resistance to *F. virguliforme*.

Keywords: cultivar resistance, *Fusarium virguliforme*, root colonization, soybean sudden death syndrome, temporal dynamics

Introduction

The causal pathogen of sudden death syndrome (SDS) of soybean in North America is the soilborne fungus, *F. virguliforme* (Aoki et al., 2003). Soybean resistance to SDS is composed of two major components: resistance to foliar chlorosis and necrosis as a result of phytotoxins produced by *F. virguliforme*, and resistance to root infection by *F. virguliforme* (Kazi et al., 2008). SDS foliar symptoms have been extensively used as a phenotype in soybean breeding programs to evaluate soybean germplasm for resistance (Njiti et al., 1996; Clark et al., 2013; Wen et al., 2014), while soybean resistance to *F. virguliforme* root infection has seldom been evaluated (Njiti et al., 1997; Luckew et al., 2013). Evaluation of soybean root resistance to *F. virguliforme* has primarily relied on visual rating of percent root surface discoloration (Ortiz-Ribbing and Eastburn, 2004; Srour et al., 2012) or the number of *F. virguliforme* colonies formed on taproot slices (Njiti et al., 1997; Luo et al., 1999). These methods, are either irreproducible across labs or inaccurate in quantification of *F. virguliforme*. With increased interest in breeding soybeans that are resistant to *F. virguliforme* root infection, there is a critical

need to develop an accurate and reproducible disease rating method for evaluating soybean resistance to *F. virguliforme* root infection.

SDS disease symptoms include both root rot caused by fungal infection and interveinal leaf chlorosis and necrosis as a result of toxins produced by *F. virguliforme* (Ji et al., 2006; Brar et al., 2011; Chang et al., 2015). SDS root infections and foliar symptoms are not simultaneous. Root rot symptoms can be detected as early as the seedling stage (VC-V1), while the earliest foliar symptoms develop at the V3-V4 vegetative growth stage. The onset of full SDS foliar symptom development usually occurs at the early reproductive stage (R1) (Roy et al., 1997). Although the foliar symptoms are the key identification feature for SDS disease diagnosis, the pathogen has never been recovered from above ground tissues (Rupe, 1989).

Early in the growing season, *F. virguliforme* conidia germinate and form germ tubes to infect soybean taproots, and infections can be detected as early as 18 days after planting in field conditions (Njiti et al., 1997; Gao et al., 2006). In a greenhouse experiment, Huang and Hartman (1998) were able to recover *F. virguliforme* within 10 days after planting. The xylem plays an integral role in translocating fungal toxins from the roots to the leaves, and causing SDS foliar symptoms (Abeysekara and Bhattacharyya, 2014). Therefore, it was proposed that early infection at the seedling stage is necessary for *F. virguliforme* penetration into xylem tissues in order to induce foliar phytotoxic symptoms (Navi and Yang, 2008; Gongora-Canul and Leandro, 2011a). Unfavorable conditions for soybean seedling germination, such as low temperature, high precipitation, high soil moisture, and compacted soils may increase the risk of infection by *F. virguliforme,* by prolonging the soybean's time at the seedling stage (Scherm and Yang, 1996; Gongora-Canul and Leandro, 2011b). To avoid these unfavorable conditions during germination or emergence, delayed planting has been suggested as a possible SDS management strategy

(Hershman et al., 1990; Roy et al., 1997), however there are often yield penalties associated with late planted soybeans, and the short window for field operations mean that this is often not a viable management option (Kandel et al., 2016).

Soybean resistance to SDS is primarily determined by visual evaluation of foliar symptom development (Njiti et al., 1996; Clark et al., 2013). The examination of the roots for discoloration or rotting symptoms has been rarely used to resolve soybean resistance to *F. virguliforme* root infection (Kazi et al., 2008; Gongora-Canul et al., 2012). The relationship between SDS foliar symptom severity and *F. virguliforme* infection levels is not clear, as root infection by *F. virguliforme* does not necessarily cause SDS foliar symptoms. SDS foliar and root rot phenotypes have been mapped on separate quantitative trait loci (Kazi et al., 2008). In addition, yield loss due to *F. virguliforme* infection is difficult to estimate, due to the lack of effective tools for quantifying *F. virguliforme* colonized in soybean roots. Currently, two major root disease-rating methods (i.e., visual rating of percent root discoloration and counting colony forming units (CFU) of *F. virguliforme* from root tissues) have been utilized for screening soybean root resistance to *F. virguliforme* infection (Njiti et al., 1997; Gongora-Canul et al., 2012). The culture-based quantification methods provide a good estimation of viable *F. virguliforme* in soybean roots or soil samples, but it can be highly inaccurate, as *F. virguliforme* colony growth may be out-competed by other fast growing fungi and the *F. virguliforme* colony morphology is not distinct from other closely related fungal species (Njiti et al., 1997; Cho et al., 2001). Also, the visual estimation of root surface discoloration can be unspecific and subjective, as root surface discoloration may be caused by other soil-borne soybean pathogens, such as other *Fusarium* spp., *Rhizoctonia solani*, or *Phytophthora* spp. (Dorrance et al., 2003; Arias et al., 2013), which makes this method difficult to reproduce between labs. The low sensitivity and

non-specific nature of the culture-based or visual rating methods may limit the interpretation of the root disease ratings, so that a method that can effectively quantify *F. virguliforme* in root is needed.

Quantitative real-time PCR (qPCR) provides an alternative method to the culture-based or visual rating methods. qPCR has been widely used for diagnosing and quantifying plant pathogens from soil or plant tissues (Chilvers et al., 2007; Hughes et al., 2009; Bilodeau et al., 2012). There are several qPCR assays that have been developed for the quantification of *F. virguliforme* in plant tissues or soil (Gao et al., 2004; Li et al., 2008; Westphal et al., 2014; Wang et al., 2015). The performance of the *F. virguliforme* specific assays have been compared, and each assay showed distinct variations in regard to specificity and sensitivity, with assays developed based on the rDNA intergenic spacer region demonstrating the greatest potential for *F. virguliforme* quantification (Kandel et al., 2015). Based on the benchmark performance related to specificity, sensitivity, and consistency, the qPCR assay developed by Wang et al. (2015) was used in this study.

We set out to improve our understanding of the temporal dynamics of *F. virguliforme* in soybean roots and the variation of colonization across soybean cultivars in greenhouse and field conditions. The objectives of this study were to i) evaluate the colonization dynamics of *F. virguliforme* with qPCR in soybean root tissues throughout the growing season; ii) detect colonization differences among soybean cultivars; iii) determine the relationship between SDS foliar symptoms and root colonization by *F. virguliforme*.

Materials and Methods

Fusarium virguliforme inoculum preparation

Fusarium virguliforme isolates (VB2a and Mont-1) were transferred onto Nash Snyder (NS) medium (Leslie et al., 2008) and incubated at room temperature for 2-3 weeks to allow full plate colonization. Sorghum (milo maize) seeds were used as a growth substrate for *F. virguliforme* inoculum. Sorghum seeds were soaked overnight in deionized water, were drained to remove any excess water, and 1.8 kg of seeds were weighed out into mushroom spawn bags (Fungi Perfecti, Olympia, WA). Seeds were autoclaved at 121 ℃, 18 psi for 8 h and cooled at room temperature for 24 h. Five *F. virguliforme* colonized NS medium plates, five non-colonized NS medium plates, and 500 mL sterile deionized water were placed in a stainless steel sterile blender carafe and homogenized at low speed for 30 s. The homogenized inoculum slurry was evenly distributed across five mushroom bags containing autoclaved sorghum seeds, and bags were sealed with a heat sealer. Inoculum bags were incubated at room temperature with ambient light for 30 d and shaken every other day. After sorghum grains were completely colonized, the inoculum grains were spread onto kraft paper in trays and air dried at room temperature with the aid of a fan for 3-4 d.

Greenhouse experimental design

To study the temporal dynamics of *F. virguliforme* colonization on roots and determine the potential variability of root colonization across soybean cultivars with varied SDS susceptibility ratings, a five-week greenhouse experiment was conducted from planting to early vegetative growth stages and replicated twice. Plants were destructively sampled at each of the five time points to quantify *F. virguliforme* DNA. Four soybean cultivars (AG2107, AG2002, 92M82, and 92Y53) were selected by their commercial susceptibility rating to SDS based on foliar disease

symptom expression (Table 3-1). The greenhouse experimental protocol was modified from the SDS inoculated-layer technique developed by R. Bowen and G. Hartman (2011, unpublished). A soil mix was prepared by homogenizing pasturized sandy loam soil and SUREMIX (Sure, Galesburg, MI) at a ratio of 1:2. Trays (10.2 × 35.5 × 50.8 cm, catalog number: 14-3401 Hummert, Earth City, MO) with 16, 5 mm diameter holes drilled into the tray bottom for drainage were used to assemble the SDS inoculated-layer screening protocol. To assemble the trays, two paper towels were placed on the bottom of the tray to prevent soil mix loss, and 3.2 L of soil mix was placed over the paper towels and gently leveled. A second layer consisting of homogenized *F. virguliforme* inoculum (336 mL) and 1.26 L soil mix was added evenly across the tray. An additional 3.2 L of soil mix was spread over the inoculum layer. Seven furrows were created across the width of each tray using a form constructed with seven equally spaced 6.35 mm wood strips attached to a piece of plywood cut to fit the inside dimension of the tray. Two trays were planted for each of the five time points. Each of the seven furrows was planted with three cultivar replicates, which consisted of five seeds per replicate, each cultivar was replicated three times within a tray and planted in a completely randomized design. Finally, the seeds were uniformly covered with 1.6 L soil mix. Foliar SDS disease assessment at the 35 days after planting (DAP) followed the disease severity rating system prepared by R. Bowen and G. Hartman (2011, unpublished). A disease score '1' indicates a healthy plant without foliar symptoms, scores '2' to '5' indicate development of leaf interveinal chlorosis followed by necrosis with increased percentage of leaf area affected receiving higher scores; score '6' to '9' indicate developed symptoms of defoliation and premature death. Root rot SDS symptoms were assessed by estimating the percentage of discoloration and rot on the plant root system with a rating scale from 0 to 100%.

Table 3-1 Soybean cultivars used in this study. Soybean cultivars were selected based on seed industry SDS susceptibility rankings and maturity groups suitable for growing conditions in Michigan.

Varieties	Relative Maturity Group	SCN Resistance	SDS Resistance	Experiments*
AG2107	2.1	PI88788	Susceptible	Greenhouse and field 2012
AG2002	2.0	PI88788	Moderately resistant	Greenhouse and field 2012
92M82	2.8	No	Susceptible	Greenhouse and field 2012
92Y53/ P92Y53	2.5	Peking (PI548402)	Moderately resistant	Greenhouse, field 2012, and field 2014
P92Y11	2.1	Peking	Susceptible	Field 2014
P92Y51	2.5	PI88788	Moderately resistant	Field 2014
P92Y60	2.6	PI88788	Susceptible	Field 2014
P93M11	3.1	none	Moderately resistant	Field 2014

*: Soybean cultivars used for different research experiments.

Field experimental design

Field experiments were conducted at two locations: 1) research field site in Decatur, MI (42°7'35.86"N, 86°1'28.60"W) with sandy loam soil naturally infested with *F. virguliforme* and soybean cyst nematode, and 2) research field site at the Michigan State University (MSU) Agronomy Farm (42°42'40.08"N, 84°28'7.80"W) in East Lansing, MI with loam sandy soil artificially inoculated with *F. virguliforme*. Four soybean cultivars (AG2107, AG2002, 92M82, and 92Y53) as in the greenhouse study were planted at both locations in a randomized complete block design with five replicated plots. At the Decatur site, soybean plots were planted in six rows, 6.1 m (20 ft) long spaced 0.38 m (15 in) apart. At the East Lansing site, soybean plots were planted in two rows, 9.1 m (30 ft) long and spaced 0.76 m (30 in) apart. Planting dates were May 7 and May 11 2012 at Decatur and East Lansing, respectively. In 2014, a field experiment was conducted at the Decatur site with five soybean cultivars, P92Y53, P92Y11, P92Y51, P92Y60, and P93M11 (Table3-1). Each cultivar was replicated five times across 6-row plots in a randomized complete block design with 6.1 m (20 ft) long rows spaced 0.38 m (15 in) apart. The outer rows (i.e., first and sixth) were used for destructive root sampling, while the inner four rows were kept for harvest to estimate yield.

Disease evaluation – field trials

SDS foliar symptoms for each plot were rated for disease severity (DS) and disease incidence (DI) based on the SDS scoring method developed by C. Schmidt (2007) at Southern Illinois University. The DS scale ranges from 0 to 9, 0 representing a healthy plant and 9 representing premature defoliation of the whole plant. DI was estimated by estimating the percentage (0-100%) of SDS symptomatic plants in a plot. Disease index (DX) is a metric combining both DS and DI parameters to indicate the soybean SDS foliar symptoms present in a soybean plot; DX

was calculated using the formula: DX= (DI×DS)/9, where 9 represents the highest SDS disease severity rating possible.

In 2014, to gain a better understanding of the relationship between *F.virguliforme* colonization and foliar symptom expression, the severity of SDS foliar symptoms and root rot were rated on individual plants. Fifteen whole soybean plants were sampled at four time points Each plant was rated for SDS foliar symptom severity and root rot discoloration (percentage). Root tissue was processed for subsequent DNA extraction and qPCR quantification.

Sample collection and processing

In 2012, 15 roots were collected from each field plot five times from June 4 to October 9, 2014. Roots were dug with a shovel, and above ground tissues were removed. Roots were transported to the lab, rinsed under tap water to remove attached soil and debris, and oven dried at 50˚C for 48 h. Root dry weights per plot were measured. Dried soybean roots were ground in a Wiley mill (Thomas Scientific, Swedesboro, NJ) with a 2-mm pore size mesh screen.

Disease evaluation – greenhouse trials

Five soybean roots were collected and washed under tap water to remove the attached soil and oven dried at 50˚C for 48 h. Stems were removed by cutting at the soil line, and roots were oven dried at 50˚C for 48 h and root dry weight was collected. Soybean roots taken at V2 growth stage were dried and ground using FASTPREP tubes (MPBIO, Solon, OH) with a ceramic sphere (MPBIO) and five 2-mm glass beads. Roots collected after the V2 stage were ground using a coffee grinder (KRUPS). To avoid cross contamination between samples, the inside of the coffee grinder was rinsed with 70% ethanol and wiped dried with paper towel between samples.

For both field and greenhouse root tissues, an automated DNA extraction protocol was used in an AutoGenprep 850 Alpha system (AutoGen, Holliston, MA). One hundred milligrams of dried root tissue and 1 mL plant lysis solution (AutoGen) were added to a sample tube. Tubes were sealed with aluminum foil and incubated in a water bath for 1.5 h at 75˚C. Preprocessed samples were submitted to the Michigan State University genomics core for automated high-throughput phenol:chloroform DNA purification. The precipitated DNA pellet was dissolved in 150 µL 1X Tris-EDTA buffer. DNA was quantified using the Quant-iT dsDNA high-sensitivity assay kit (Invitrogen, Carlsbad, CA) on a 96-well SAFIRE microplate reader (TECAN, Männedorf, Switzerland).

***Fusarium virguliforme* root quantification**

qPCR was performed on the ABI StepOnePlus thermo cycler (Applied Biosystem, Carlsbad, CA) with a 20 µL total reaction volume and two technical repeats. The qPCR master mix for *F. virguliforme* consisted of 10 µL TaqMan Universal real-time PCR master mix (2X) (Applied Biosystems), 0.5 µL TaqMan dual labeled MGB probe FvProb3 (10 µM), 0.5 µL of each primer (20 µM, F6-3 and R6), 0.4 µL bovine serum albumin (10 mg/mL), 0.6 µL of HHIC-F primer (20 µM), 0.2 of HHIC-R primer (20 µM), 0.4 µL of HHIC-prb probe (10 µM), 0.5 µL linearized HHIC DNA plasmid (10 fg/µL) (Table 3-2) (Haudenshield and Hartman, 2011) , 4.4 µL molecular grade water (Gibco, Carlsbad, CA) and 2 µL DNA template (1:10 dilution with dH_2O). qPCR cycling conditions were initialized with one cycle incubation at 50 ℃ for 2 min, one cycle at 95 ℃ for 10 min for denaturing, 40 cycles at 95 ℃ for 15 s, 60 ℃ for 1 min, with fluorescent data collection at 60 ℃ step. A qPCR assay for quantification of soybean genomic DNA was designed on a single-copy beta tubulin gene from the soybean genome. The qPCR master mix for the soybean quantification assay consisted of 10 µL TaqMan Universal real-time PCR master

mix (2X) (Applied Biosystems), 0.5 µL TaqMan dual labeled MGB probe TUB-Prb-1 (10 µM), 0.5 µL for each primer (20 µM, TUB-F1 and TUB-R1), 0.4 µL bovine serum albumin (10 mg/mL), 6.1 µL of molecular grade dH_2O, and 2 µL DNA template (1:100 dilution with dH_2O). PCR efficiency for both quantification assays was determined by running a five-point standard curve ranging from 1 ng to 100 fg of genomic DNA. The qPCR conditions for the soybean genomic DNA quantification assay were optimized to be the same as the *F. virguliforme* qPCR assay, which makes it possible to run both assays on the same 96-well plate. Infection coefficient of *F. virguliforme* was calculated using the formula: CT_{Soy}/CT_{Fv}, where CT_{Soy} is the CT value of soybean real-time PCR assay and CT_{Fv} is the CT value of *F. virguliforme* real-time PCR assay. The infection coefficient (IC) is a measurement ratio between *F. virguliforme* and soybean, which is a normalized *F. virguliforme* infection value of soybean root tissue (Valsesia et al., 2005).

Data analysis

Real-time qPCR quantification data were collected from the real-time PCR thermal cycler using StepOnePlus software version 2.3 (Applied Biosystems). Analysis of variance (ANOVA) was performed using the "stat" package in R v3.2 (R Core Team, 2015). Figures were generated using "graphic" and "ggplot2" package (Wickham, 2009). The areas under infection coefficient curves (AUICC) was calculated using the function "audpc" in "agricolae" package (De Mendiburu, 2014) in R.

Table 3-2 Primers and probes used in this study.

Primer names	Sequences (w/ modifications)	Final concentration	Target	Source
F6-3	GTAAGTGAGATTTAGTCTAGGGTAGGTGAC	500nM	rDNA-IGS	Wang et al. 2015
R6	GGGACCACCTACCCTACACCTACT	500nM	rDNA-IGS	Wang et al. 2015
FvPrb3	6FAM-TTTGGTCTAGGGTAGGCCG-MGBNFQ	250nM	rDNA-IGS	Wang et al. 2015
TUB-F1	GCGGTGCTCATGGATCTAGAG	500nM	beta-tubulin	This study
TUB-R1	TGACCGTAGGGACCAGATCTG	500nM	beta-tubulin	This study
TUB-Prb-1	NED-AGGGACCATGGACAGC-MGBNFQ	250nM	beta-tubulin	This study
HHIC-F	CTAGGACGAGAACTCCCACAT	600 nM	pJSH-B14	Haudenshield et al. 2011
HHIC-R	CAATCAGCGGGTGTTTCA	200 nM	pJSH-B14	Haudenshield et al. 2011
HHIC-Prb	5HEX-TCGGTGTTGATGTTTGCCATGGT-3IABkFQ	200 nM	pJSH-B14	Haudenshield et al. 2011

Results

Greenhouse temporal dynamics of *F. virguliforme* colonization

In the first greenhouse experiment, *F. virguliforme* was detected at the initial sampling time point, 7 days after planting (DAP) in all soybean cultivars with an average infection coefficient (IC) ranging between 0.96 and 1.12 (Figure 3-1). The *F. virguliforme* root IC reached a maximum level of 1.19 at the second sampling time point (14 DAP). After 14 DAP, *F. virguliforme* relative quantities decreased for the subsequent sampling time points (21, 28, and 35 DAP), with the average IC ranged between 0.99 and 1.14. The IC of *F. virguliforme* colonized roots were significantly different among the four cultivars at two sampling time points (28, and 35 DAP, $P < 0.01$), but *F. virguliforme* relative quantities in the susceptible cultivars (AG2107 and 92M82) were not always significantly higher than the moderately resistant cultivars. All soybean cultivars developed foliar symptoms by 35 DAP (Figure 3-2), and foliar disease indices were not significantly different among the four cultivars ($P = 0.73$).

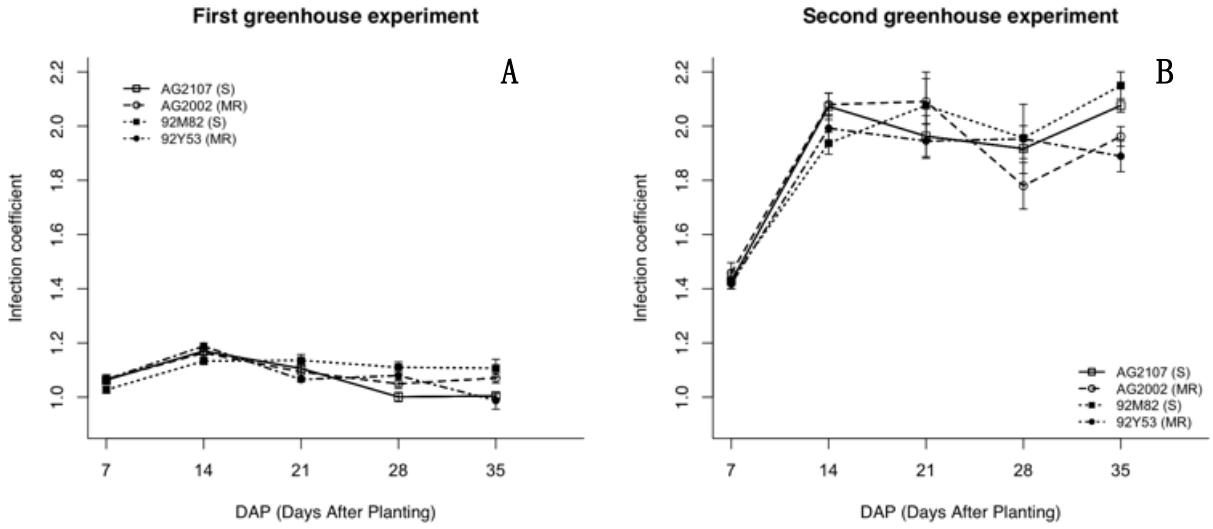

Figure 3-1 Temporal dynamics of *F. virguliforme* infection coefficient in soybean roots from two greenhouse experiments measured from 7 to 35 DAP. Four soybean cultivars were included in both greenhouse experiments, and resistance to SDS is indicated in the figure legend as susceptible (S) and moderately resistance (MR). Although significant root colonization levels were observed among cultivars at several sampling time points, no correlation between foliar symptoms and root colonization was detected. (A) Temporal dynamics of *F. virguliforme* infection coefficient at first experiment; (B) Temporal dynamics of *F. virguliforme* infection coefficient at second experiment.

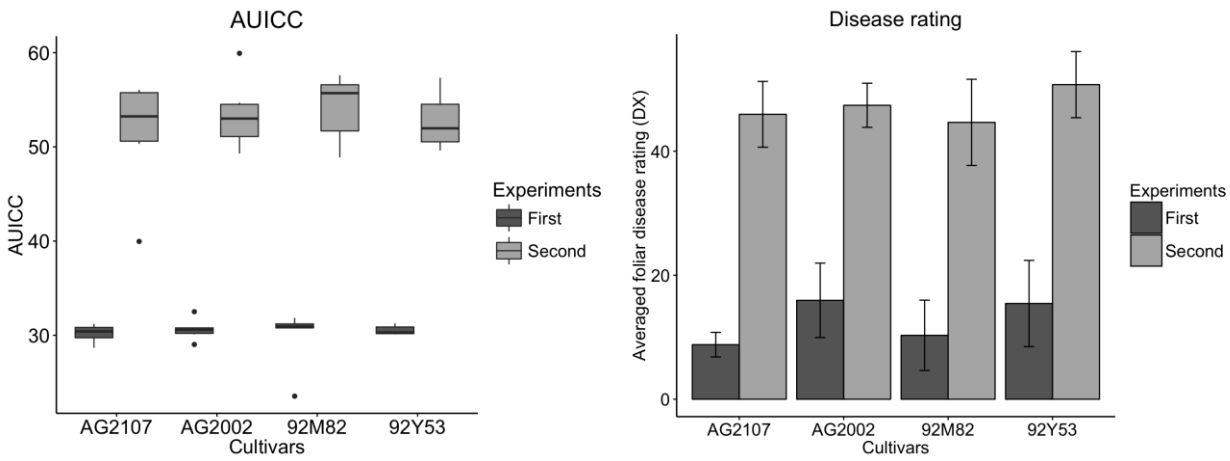

Figure 3-2 (A) Boxplot of the area under *Fusarium virguliforme* infection coefficient curve (AUICC) calculated based on the temporal data of four soybean cultivars in both greenhouse experiments. No significant differences were detected among cultivars within each experiment, however the second greenhouse experiment had a higher AUICC. Dots within the figure are the data outliers in the boxplot. (B) Bar plot of SDS foliar disease rating index (DX in a scale 0-100, where 0 indicates healthy plant and 100 indicates most severe SDS foliar symptoms). Disease ratings were taken at 35 DAP in both greenhouse experiments as shown in black (first experiment) and gray (second experiment). The second greenhouse experiment showed more severe SDS foliar symptoms, which aligned with the increased *F. virguliforme* infection coefficient detected in soybean roots between two greenhouse experiments.

In the second greenhouse experiment, the ICs of *F. virguliforme* colonized in roots were higher than the relative quantities of *F. virguliforme* detected in the first greenhouse experiment. At the first time point (7 DAP), *F. virguliforme* was detected in all cultivars with average IC ranging between 1.42 and 1.46. From 7 to 14 DAP, the mean of *F. virguliforme* relative quantities increased from 1.43 to 2.02 with a relative colonization rate of 0.08 IC per day. For the subsequent sampling time points (21, 28, and 35 DAP), the *F. virguliforme* IC fluctuated between 1.78 and 2.15. In the first four sampling time points, the *F. virguliforme* IC did not show significant differences among four soybean cultivars ($P > 0.05$). At the fifth sampling time point (35 DAP), the *F. virguliforme* IC were significantly higher in susceptible cultivar 92M82 than the moderately resistant cultivars 92M53 and AG2002 ($P < 0.01$), but IC in AG2107 was not significantly higher than IC in AG2107 ($P > 0.05$). All four soybean cultivars developed SDS

foliar symptoms at 35 DAP, and SDS foliar symptom disease indices were not significantly different among cultivars ($P = 0.87$, Figure 3-2B).

The overall *F. virguliforme* root colonization was estimated by calculating the area under infection coefficient curves (AUICC) for each cultivar. The AUICC in the second greenhouse experiment were greater than the AUICC in the first greenhouse experiment ($P < 0.01$) for all cultivars. Within each greenhouse experiment, there were no significant differences among cultivars ($P > 0.7$, Figure 3-2A). In the first greenhouse experiment, root dry weight increased over time and reached an average weight of 0.08 g/plant at 35 DAP, except for cultivar 92M82 (Figure S 3-1). Significant root dry weight differences among cultivars were observed at 28 and 35 DAP, with cultivar 92M82 root dry weight being significantly lower than the other three cultivars ($P < 0.05$). In the second greenhouse experiment, root dry weight increased over time but didn't reach the same levels as the first experiment. By 35 DAP, the average root dry weight was around 0.03 g/plant. Significant root dry weight differences were observed among the four cultivars at 14, 21, and 28 DAP, but there were no significant root dry weight differences among cultivars at time point 35 DAP.

Fusarium virguliforme colonization of field grown soybean roots

In 2012, *F. virguliforme* root colonization was similar at both field locations. Variation in *F. virguliforme* IC among soybean cultivars was greater at the East Lansing field location than the Decatur site (Figure 3-3). *Fusarium virguliforme* was detected in root tissue with qPCR at the V3 stage of all soybean cultivars, the average *F. virguliforme* IC ranged between 0.91 and 1.03. The *F. virguliforme* IC in soybean roots was significantly higher at the East Lansing site than the Decatur site ($P < 0.01$) for the first three sampling time points (25, 28, 56 DAP). From the V5 to R5 stage, the *F. virguliforme* IC increased over time at both locations, but the Decatur site had a

higher root colonization rate (0.007 IC/day) than at the East Lansing site (0.003 IC/day). At 96 and 99 DAP, the *F. virguliforme* IC decreased by 0.060 and 0.079 at the East Lansing site and Decatur site, respectively. For the later reproductive stages (R7, R8, and Post Harvest), *F. virguliforme* IC started to increase again and reached their maximum colonization level at either 124 DAP or 153 DAP (post-harvest). At the Decatur site, the first appearance of SDS foliar symptoms were recorded between 40 DAP, and gradually developed into most severe foliar symptoms at 96 DAP. At the Decatur site, the average SDS foliar disease indices were 3.33, 0.56, 63.9, and 0 for soybean cultivars AG2107, AG2002, 92M82, and 92Y53, respectively. Despite the significant differences in SDS foliar symptoms among cultivars, *F. virguliforme* IC in roots were not significantly different among cultivars over time, except 127 DAP at the Decatur site ($P < 0.05$, Figure3-3B). No SDS foliar symptoms were observed at the artificially inoculated East Lansing site.

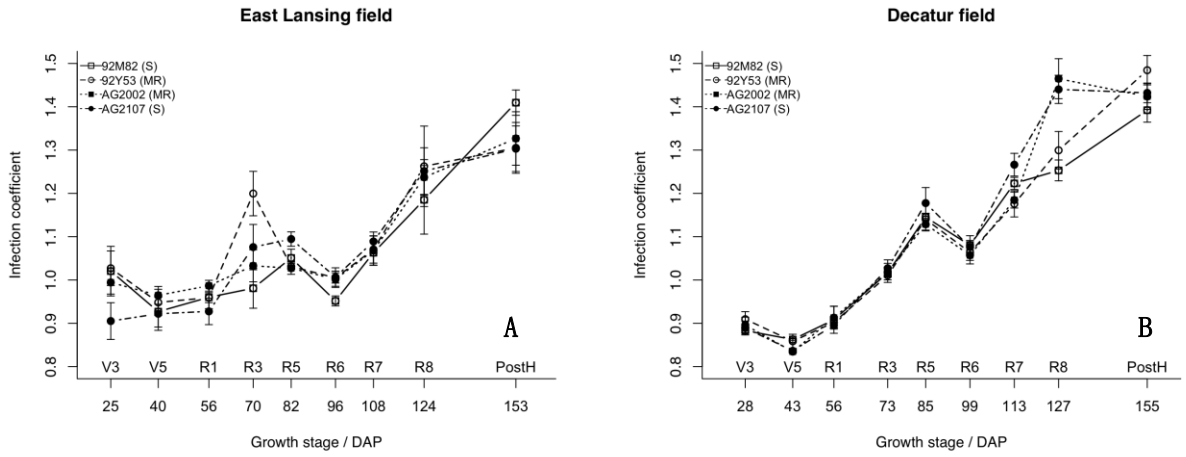

Figure 3-3 Temporal dynamics of the relative *Fusarium virguliforme* infection coefficient in soybean roots in 2012 field experiments in four soybean cultivars, two susceptible (S) and two moderately resistant (MR). Soybean cultivar susceptibility to SDS was based on industry rating on foliar symptom expression. Field locations: (A) an artificially inoculated field in East Lansing, MI; (B) a naturally infested field in Decatur, MI. The x-axis is represented by the days after planting (DAP) along with the corresponding soybean growth stage. The Y-axis is the *F. virguliforme* infection coefficient. *F. virguliforme* was detected in all soybean cultivars in both field locations from the first sampling point (V3 stage). By the end of the growing season at the post harvest stage (Post H), all cultivars in both field locations reached the same infection coefficient level.

The areas under infection coefficient curves (AUICC) was calculated to evaluate the season-long trends of *F. virguliforme* root colonization. In 2012, AUICCs were not significantly different among the four cultivars at both Decatur ($P = 0.08$) and the East Lansing site ($P = 0.70$) (Figure 3-4A). The AUICCs at the Decatur site were significantly higher than the East Lansing site ($P = 0.02$), and SDS foliar symptoms were only observed at the Decatur site (Figure 3-4B). The most severe SDS foliar symptoms (DX = 66.7) were detected on cultivar 92M82 at the Decatur site, its root colonization level was significantly lower than the other three soybean cultivars ($P = 0.046$, Figure 3-4A). On the contrary, the cultivars AG2002 and AG2107, that showed less severe SDS foliar symptoms (i.e., DX: 0.56 and 3.33), showed higher *F. virguliforme* AUICC over the season.

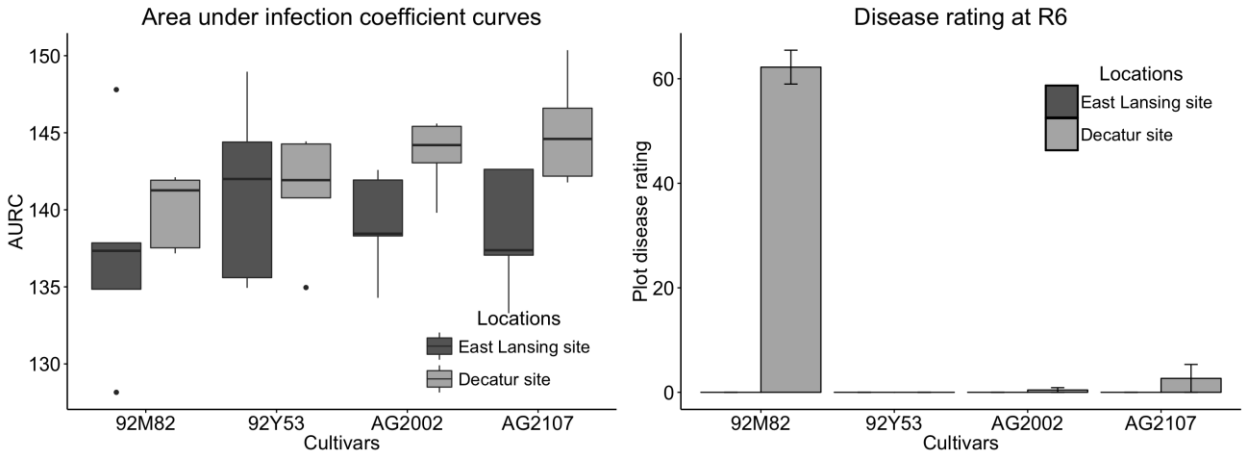

Figure 3-4 Boxplot of area under relative quantity curve (AURQC) calculated using the temporal data of *F. virguliforme* DNA quantified in soybean roots at both field locations. The East Lansing site is represented by dark gray, while the Decatur site with light gray. (B) Bar plot of SDS foliar disease rating at R6 growth stage for four soybean cultivars at both locations based on a plot scale disease rating. At both locations, *F. virguliforme* DNA was detected in considerable quantity across all soybean cultivars, however, not all soybean cultivars displayed SDS foliar symptoms. Soybean cultivar 92M82, showed the most severe foliar symptoms, but the AURQC was lower than the other three cultivars at both locations.

In 2014, *F. virguliforme* was detected in all five soybean cultivars with an average IC ranging between 0.92 and 1.00 at the first sampling time point at Decatur site. The *F. virguliforme* IC in roots slightly increased at 62 DAP, and remained stable until 93 DAP with the average IC ranging between 0.92 and 1.09 (Figure 3-5). *Fusarium virguliforme* root colonization was greatest at 107 DAP for all five cultivars. Three out of five cultivars developed SDS foliar symptoms at 93 DAP with disease indices: 23.0, 9.1, 0.0, 18.1, and 0.0, for cultivar P92Y11, P92Y51, P92Y53, P92Y60, and P93M11, respectively (Figure 3-6B). Although SDS foliar symptom disease indices were significantly different among cultivars ($P = 0.0062$), the *F. virguliforme* IC in soybean roots did not significantly correlate with plot SDS foliar symptoms (Spearman correlation test, $P = 0.143$). The AUICC did not align with the foliar symptoms at R6 growth stage (Figure 3-6).

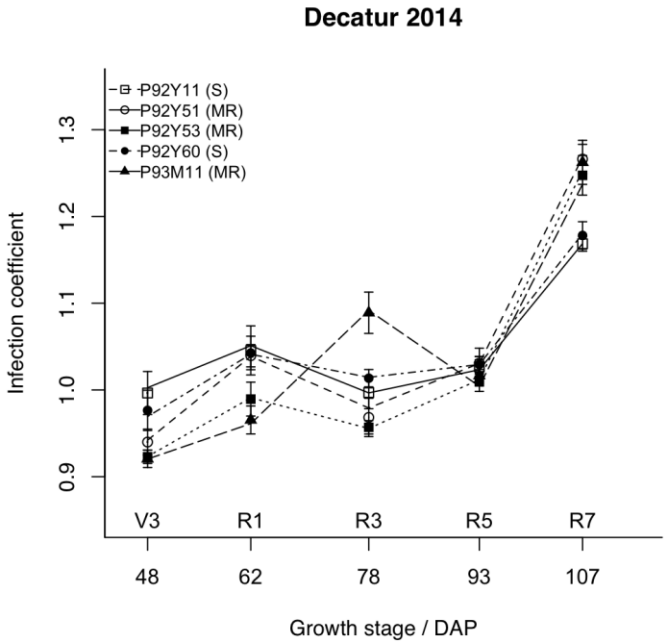

Figure 3-5 Infection coefficient of *F. virguliforme* (Ct_{Soy}/Ct_{Fv}) in the five soybean cultivars measured at five growth stages during 2014 in a naturally infected field in Decatur MI. *F. virguliforme* DNA was detected in all soybean cultivars starting at the V3 time point. The relative quantity of *F. virguliforme* DNA detected only slightly increased from the V3 to R5 stage, but a significant increase of relative *F. virguliforme* DNA quantity was observed between the R5 and R7 growth stages. At the R7 growth stage, two cultivars showed significantly higher *F. virguliforme* relative quantities in roots. *F. virguliforme* DNA quantities were not associated with foliar disease symptom ratings taken at the R5 growth stage.

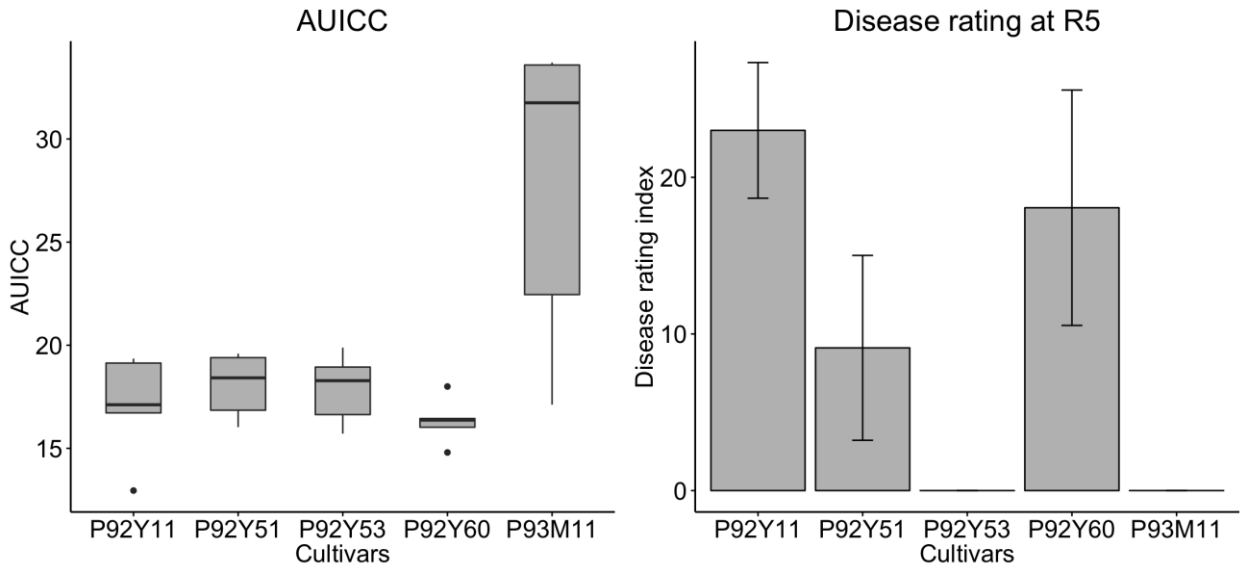

Figure 3-6 Area under the relative *Fusarium virguliforme* DNA quantity curve (AURQC) and soybean SDS foliar disease rating index for individual plants sampled at the R5.5 growth stage for five soybean cultivars in 2014 Decatur field experiment. (A) Boxplot of AURQC calculated for the temporal dynamics data of *F. virguliforme* DNA quantified in soybean roots. AURQC were not significantly different among five cultivars ($p=0.11$). (B) Bar plot of SDS foliar disease rating index at R5.5 growth stage for five soybean cultivars. Significant difference was detected among the five soybean cultivars ($p< 0.01$) for SDS foliar disease rating index, however the quantified *F. virguliforme* in roots was at a similar level for all cultivars.

In 2014, SDS foliar and root ratings were performed on individual plants to improve the precision of disease-rating compared to whole plot foliar disease ratings. Individual plant SDS root severity indices demonstrated a positive, but non-significant correlation with the *F. virguliforme* relative quantities in roots ($r^2 = 0.02$, Spearman correlation $p = 0.21$, Figure 3-7A). There was no correlation between individual plant SDS foliar disease indices with *F. virguliforme* relative quantities in roots ($r^2 < 0.001$, Spearman correlation $p = 0.80$, Figure 3-7B).

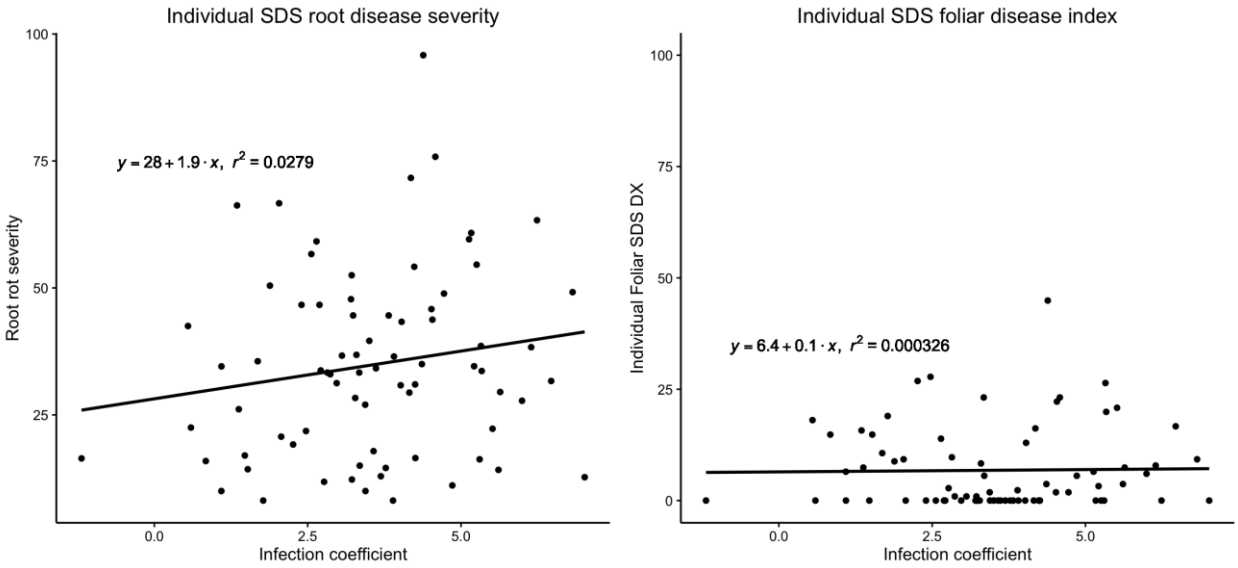

Figure 3-7 Correlation between individually rated soybean plants for SDS symptoms and *F. virguliforme* infection coefficient detected in soybean roots. (A) Root rot severity rated on 15 individual plants for each of the 25 plots, based on the percentage of root surface discoloration correlated with the *F. virguliforme* infection coefficient in soybean roots. The y-axis is the root rot severity, and the x-axis is the relative quantity of *F. virguliforme* in roots. (B) SDS foliar symptom disease rating index on the same 15 individual plants from each of the 25 plots, based on disease severity rating scale from 0-9 and the disease incidence correlated with *F. virguliforme* relative quantities. There was no significant correlation between SDS root or foliar disease ratings and the amount of *F. virguliforme* quantified in soybean roots.

Discussion

In this study, both field and greenhouse experiments were conducted to examine *F. virguliforme* colonization of soybean roots throughout the growing season using a qPCR based quantification method. Based on two years of field experiments, the quantities of *F. virguliforme* present in soybean roots were not significantly correlated with SDS foliar symptoms. Soybean cultivars with varied SDS disease susceptibility ratings based on foliar symptom development, were grown in field trials in the quantity of *F. virguliforme* in the roots. Therefore, screening soybean cultivars resistant to SDS based on SDS foliar symptom severity ranking does not equate to resistance to *F. virguliforme* root infection or colonization. Quantifying the amount of *F. virguliforme* present in soybean roots as infection coefficient provides a quantitative measurement to score soybean cultivars for resistance to *F. virguliforme* root infection or colonization. Compared to the previous culture-based methods, the qPCR method provides a fast and accurate means to quantify *F. virguliforme* in soybean roots. In the field experiments, the R5-R7 stages were determined to be the optimal sampling time point for *F. virguliforme* quantification in roots, this coincides with the full development of the foliar symptoms on soybean plants. Based on results of greenhouse experiment, the early time points are not recommended for quantification of *F. virguliforme*. Soybean plants grown in the greenhouse start developing SDS foliar symptoms at the V3/V4 stage or approximately 30 DAP, thereby providing an optimal time point for collecting roots for *F. virguliforme* quantification.

Greenhouse experiments

Greenhouse experiments were conducted twice to determine the temporal dynamics of *F. virguliforme* early infection and colonization in soybean roots. The infection coefficient of *F. virguliforme* quantified in the first greenhouse experiment was significantly lower than the

second greenhouse experiment, and the foliar SDS symptoms were less severe in the first greenhouse experiment (Figure1 and 2). The differences in the amount of *F. virguliforme* quantified in the roots can be caused by the batch effect between two greenhouse experiments impacted by numerous factors including: soil moisture, temperature, and different batches of steamed soil. Similar to the findings by Gongora-Canul et al. (2011b; 2012), soybean plants had less severe foliar symptoms and heavier root dry weight than the second experiment (Figure 3-2 and Figure S3-1), and *F. virguliforme* relative quantities were significantly higher in the second greenhouse experiment than the first greenhouse experiment (Figure 3-1and Figure 3-2). In addition, four soybean cultivars with varied levels of susceptibility to SDS foliar symptoms had similar amounts of *F. virguliforme* in their roots; foliar disease ratings among these four cultivars were not significantly different in both greenhouse experiments. The similar SDS foliar symptom among cultivars could be caused by the high inoculum level created in the greenhouse soil. Therefore, high inoculum pressure in the greenhouse experiment may have saturate the tolerance of both susceptible and moderate resistant cultivars.

SDS foliar symptoms and *F. virguliforme* root infection/colonization

SDS foliar symptom development requires root infection by *F. virguliforme*, but SDS foliar symptoms do not always develop after *F. virguliforme* root infection, and SDS foliar symptom severity is not correlated with the *F. virguliforme* IC detected in roots (Njiti et al., 1997; Prabhu et al., 1999, this study). SDS foliar symptoms are caused by the toxins produced by *F. virguliforme* that colonizes the roots; the severity or appearance of foliar symptoms should depend on the amounts of *F. virguliforme* toxins translocated to the leaves. Infected but SDS asymptomatic soybean plants and symptomatic plants had similar amount of *F. virguliforme* present in roots (Njiti et al., 1997, this study). There were no significant differences in *F.*

virguliforme quantities among plants that showed varied levels of SDS foliar symptoms (Figure 3-7). Based on these results, soybean cultivars may have different susceptibility to foliar symptoms, but do not differ in resistances to *F. virguliforme* root infections.

SDS foliar symptoms were consistently developed at the naturally infested site in this study, but not at the artificially infested site. At both sites, *F. virguliforme* was detected at all sampling points throughout the season, but the *F. virguliforme* IC detected between R5 to R7 stages were significantly higher ($P < 0.01$) at the naturally infested field than the artificially inoculated field. At R5 to R7 stages, soybean plants usually had fully developed SDS foliar symptoms (Roy et al., 1997). The significantly higher amount of *F. virguliforme* detected in the naturally infested field (Decatur site) than the artificially infested field may indicate the causing of SDS foliar symptoms on the susceptible soybean cultivars associated with amount of *F. virguliforme* colonized in roots. After R7 growth stage, when soybean starts to senesce, *F. virguliforme* root IC reached similar level at both sites (Figure 3-3). Because senescent soybean roots have less live tissue (Figure S3-3), the pathogen transitions from necrotrophic to saprophytic growth, possibly explaining the fast colonization of *F. virguliforme* in soybean roots after R7 growth stage.

It was proposed that soybean radical roots infected with *F. virguliforme* at the seedling stage were more likely to develop SDS foliar symptoms (Navi and Yang, 2008; Gongora-Canul and Leandro, 2011a). Early infection by *F. virguliforme* allowed the pathogen to grow into the root xylem ("effective infection zone") and secret toxins into the vascular systems causing SDS foliar symptoms (Navi and Yang, 2008). In our study, soybean plants at the artificially inoculated site had significantly higher *F. virguliforme* IC than the naturally infested site at the first sampling time points (25-28 DAP), however, only plants at naturally infested site developed foliar symptoms. Therefore, the amount of *F. virguliforme* quantified at the early vegetative growth

stage may not associate with later season SDS foliar symptoms development.

Serial sampling of soybean roots for quantifying *F. virguliforme*

Serial root sampling is not practical for soybean breeding projects, thus to select a proper time for root sampling is important to study the infection and colonization of *F. virguliforme* in soybean roots. In previous studies, there was no agreement on a certain time point for root sampling. For the initial root infection evaluation, Luo et al. (1999) arbitrarily used 45 DAP time point for comparing root infection levels, since they found some locations were difficult to obtain data at 30 DAP. Njiti et al. (1997) started root sampling at 8 DAP, both SDS susceptible and resistant cultivars were not detected with *F. virguliforme* infection until 15 or 24 DAP. In these previous studies, the inconsistent detection of *F. virguliforme* from soybean roots at the initial stage may have been caused by limited detection sensitivity of the culture-based methods. In this study, *F. virguliforme* was consistently detected in all soybean cultivars since the first sampling time point (25, 28 DAP in the field and 7 DAP in the greenhouse) using the qPCR based quantification method. Though no significant differences were detected in *F. virguliforme* quantity among soybean cultivars, detection sensitivity of the qPCR quantification method provided the ability to compare *F. virguliforme* infection at the early growth stage. In addition, Luo et al. (1999) were able to distinguish resistant and susceptible cultivars in the field study using area under population curve (AUPC) measurements. The AUPC method was also used in our study to obtain an overall estimation for *F. virguliforme* root colonization, because soybean cultivars showed inconsistent colonization levels at different sampling time points (Figure 3-1, Figure 3-3, and Figure 3-5). In our study, AUICCs were calculated for different soybean cultivars, AUICCs were not significantly different among soybean cultivars in the ANOVA test, thought varied levels of SDS foliar symptoms were developed on each cultivar. For example,

cultivar 92M82 had the most severe SDS foliar symptoms in the naturally infested field, but it it had the lowest AUICC of the soybean cultivars evaluated (Figure 3-4). On the other hand, AUICCs may not be practical measurement for soybean cultivars resistant to *F. virguliforme* root infections, especially in a breeding project, because of the multiple root samplings and processing are labor intensive.

Root samples collected at R6 and R8 stages were used for *F. virguliforme* quantification, and different QTL were associated with root quantification data collected at R6 and R8 growth stages (Kazi et al., 2008). In this study, significant differences in *F. virguliforme* root IC were observed among cultivars at R8 stages, but no significant differences were detected at R6 stage. At R8 stage, more than 95% of the plants reached full maturity, the differences in *F. virguliforme* relative quantities could possibly cause by different soybean maturity groups (Table 3-1). Early mature group cultivars tend to senescence earlier and root dry weights started to decrease earlier than the later maturity groups (Figure S3-2), so that *F. virguliforme* colonized well in the early matured soybean cultivar. When the soybean roots started to degrade, the life style of *F. virguliforme* may switch from necrotrophic stage into saprophytic stage for fast colonization, as has been observed in the *Colletotrichum* fungus (O'Connell et al., 2012). Therefore, root sampling between R5 to R7 stages is recommended to detect *F. virguliforme* as a measurement for soybean resistance to *F. virguliforme* root infection/colonization, but root samples from R8 or post-harvest stages are not recommended.

Quantification methods

Quantification of *F. virguliforme* in soybean roots using qPCR is more specific and accurate than the culture based methods. The culture-based methods are generally limited by the slow growth rate of *F. virguliforme* on semi-selective medium, and it takes 7-10 days for *F.*

virguliforme to form a recognizable colony morphology (Njiti et al., 1997; Luo et al., 1999). Also, it is difficult to count *F. virguliforme* colonies on the semi-selective medium, because other fast growing fungi will out-grow *F. virguliforme* colonies, and closely related *Fusarium* species may produce colonies with similar morphology (Cho et al., 2001). The qPCR quantification method can specifically detect *F. virguliforme* DNA from the total root DNA, and the amplification step increases the sensitivity level to quantify *F. virguliforme* from root samples. Therefore, the qPCR quantification methods utilized in this study provided accurate and precise quantification of *F. virguliforme* in soybean root.

The presentation of qPCR quantification data differs among studies, however, absolute and relative quantification are the two major methods used. Either absolute or relative quantification methods can be misleading if the underlying assumptions are not met. The result will be misinterpretation of the data. (Bustin et al., 2009). Absolute quantification is widely applied in many qPCR assays for plant pathogen quantification (Chilvers et al., 2007; Malvick and Impullitti, 2007; Bilodeau et al., 2012). The advantage of using absolute quantification is that the quantification results can be directly interpreted into the actual quantity of the target pathogen. The assumed conditions of the absolute quantification method are that PCR efficiencies between the standard and unknown samples should be within the same range and DNA concentration measurement for the standard must be accurate. The amplification efficiency of the serially diluted genomic DNA standards is not always consistent with the amplification efficiency of environmental or plant DNA samples, due to the presence of PCR inhibitors in environmental or plant DNA samples. Thus if PCR efficiency variances occur than the absolute quantification values will not be accurate. Also, the DNA concentration measurement methods (i.e. Spectrophotometer and fluorophotometer) are limited in the range of nucleic acid

concentration they accurately measure and are not always extremely accurate. The most common DNA concentration measurement methods (i.e., NanoDrop and Quant iT) are known to have biases ranging from -8.17% to +38.08% (English et al., 2006). Relative quantification of qPCR data for pathogen quantification is another common method. The relative quantity of a target pathogen can be presented as ΔCt (Gao et al., 2004; Li et al., 2008) or infection coefficient (Valsesia et al., 2005; Atallah et al., 2007). The advantage of the relative quantification method is that the relative quantity will include both host (endogenous control) and pathogen (target) components, which provide pathogen quantification in the context of host-pathogen interactions. The assumptions for valid relative quantification is to have equal PCR efficiencies for both plant host and pathogen qPCR assays (Livak and Schmittgen, 2001). Recovery rates of DNA in DNA extractions are known to be an issue in PCR-based quantification assays (Mumy and Findlay, 2004; Claassen et al., 2013), and maintaining a relative constant DNA endogenous control, such as plant tissue genomic DNA, will help to calibrate the DNA recovery rate variances. However, over the course of the growing season, plant genomic DNA versus plant biomass ratio in root tissues is not always constant over time (Figure S3-3). Taken together, there are advantages and disadvantages of using these two quantifications methods. In this study, relative quantification by collecting both plant and pathogen CT values was used to evaluate the *F. virguliforme* quantity in soybean roots. The PCR efficiencies between the *F. virguliforme* and soybean qPCR assay were within the range of 90-95%. Also, the relative quantification provided the ratio between *F. virguliforme* cells over the live root tissues, which demonstrated the possible interactions between soybean and *F. virguliforme*. One possible limitation of the qPCR based quantification method is that dead and live pathogen cells present in roots can both be quantified in the qPCR, this could result in overestimation of *F. virguliforme* in soybean roots.

In conclusion, both greenhouse and field experiments demonstrated that the appearance and severity of SDS foliar symptoms are independent of the relative quantities of *F. virguliforme* colonized in roots. Since the direct cause of SDS starts from root infection, screening soybean germplasm for resistance to *F. virguliforme* infection or colonization may confer the most effective SDS disease resistant trait for SDS management. In this study, we have developed an efficient and accurate method for quantification of *F. virguliforme* in soybean roots, which can be used in a breeding program as a phenotype for soybean root resistance to *F. virguliforme*. In addition, both SDS foliar symptomatic and asymptomatic plants showed similar levels of *F. virguliforme* relative quantities in roots, thus it would be worthwhile to evaluate the impact of *F. virguliforme* root infection on the SDS asymptomatic plants.

Acknowledgement

We would like to thank Adam Byrne and John Boyse for their assistance in fieldwork.

This research was funded by the Michigan Soybean Promotion Committee, the Carter Harrison Endowed Graduate Student Fund, and Pioneer Crop Sciences.

APPENDIX

Supplementary figures

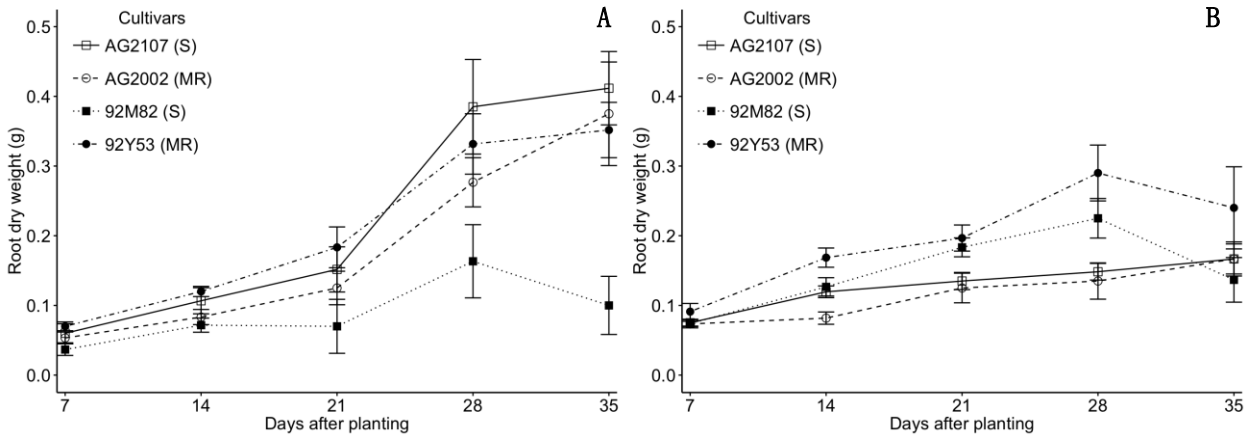

Figure S 3-1 Dry weight of four soybean cultivars in the greenhouse experiments. Each sampling time point represents the dry weight of six replicates of five individual plants per replicate. Root dry weights were collected to estimate the overall root health as affected by *F. virguliforme* under greenhouse conditions. (A) the first greenhouse experiment and (B) the second greenhouse experiment.

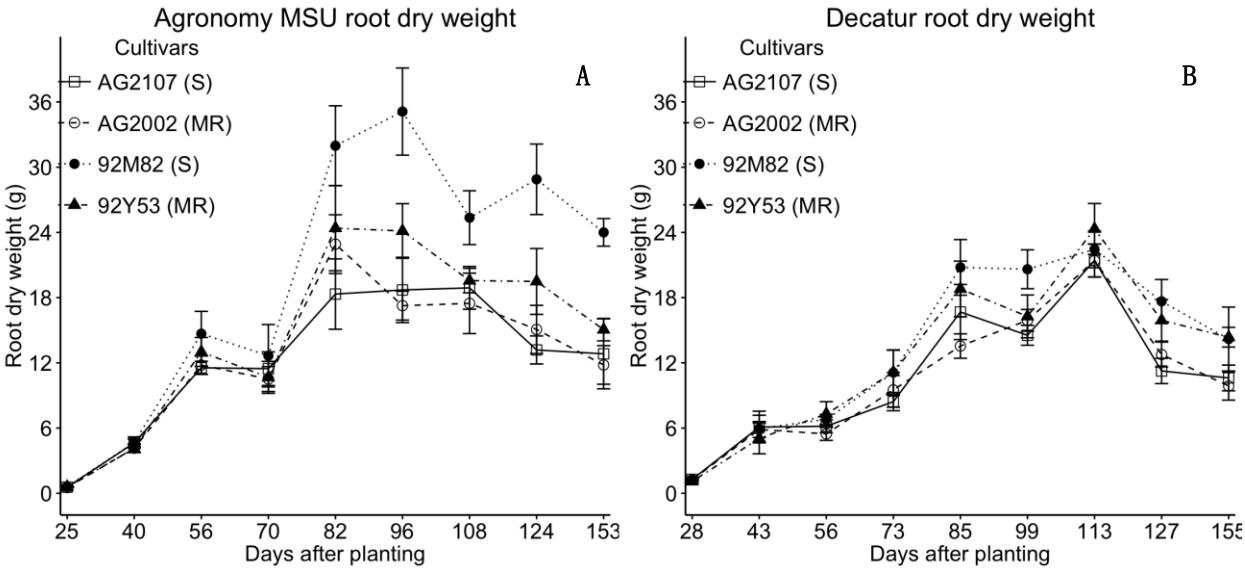

Figure S 3-2 Root dry weight of 15 plants collected from five replicated plots for each of the four soybean cultivars. (A) an artificially inoculated field in agronomy farm at East Lansing site. (B) a naturally infested field in Decatur site.

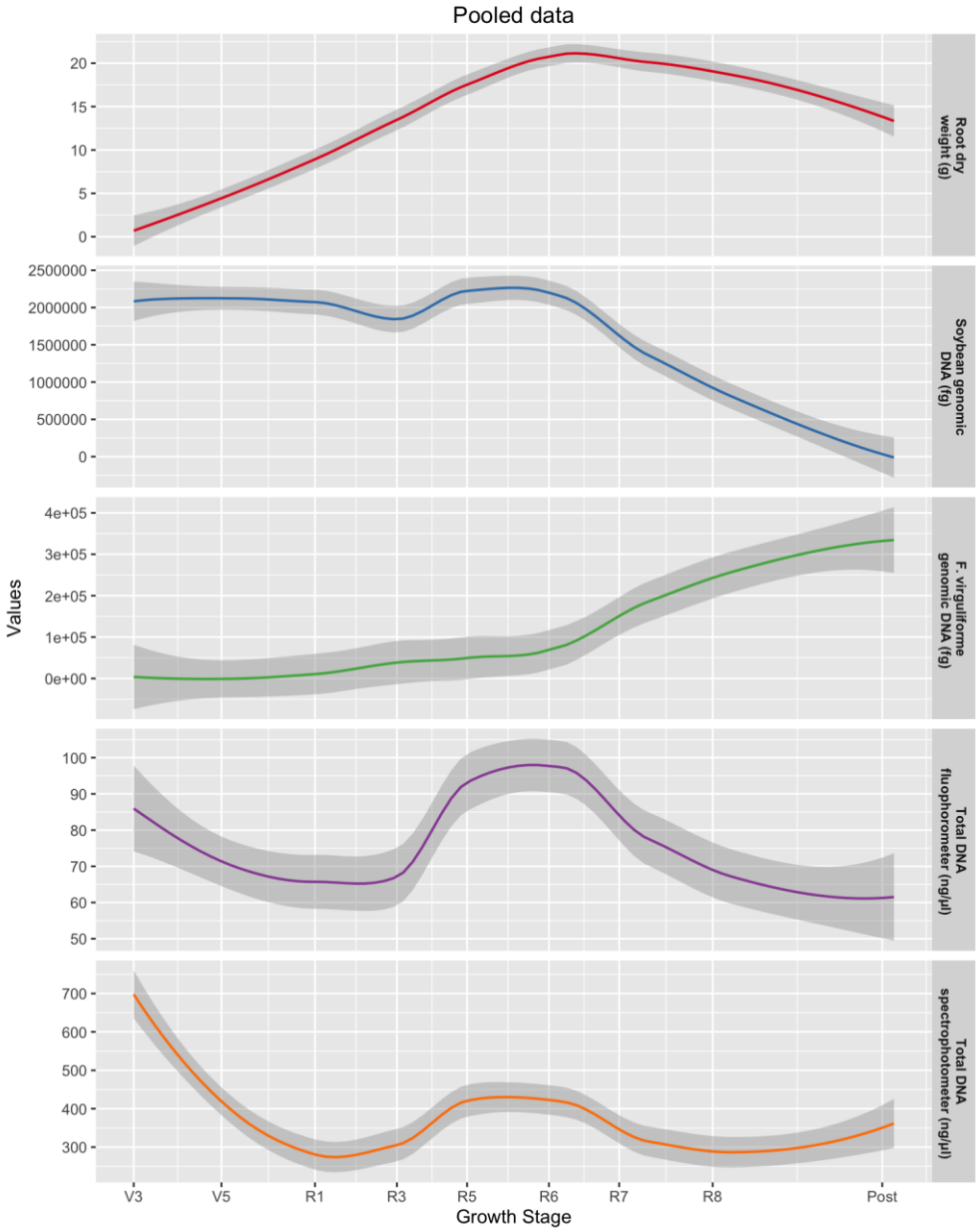

Figure S 3-3 Throughout the growth season soybean root dry weight, soybean genomic DNA quantity, *F. virguliforme* DNA quantity, total DNA extracted from root tissue from V3 to Post (post harvest). Soybean root dry weight increased until R6, and started to decrease until the post harvest stage. As root dry weight decreased after R6, soybean genomic DNA also decreased dramatically. *F. virguliforme* DNA quantified from root increased gradually from R6 to Post harvest, but increase rapidly after R8. The amount of total DNA extracted from 100 mg of root tissues peaks at R5-R6 stages.

REFERENCES

REFERENCES

Abeysekara, N.S., and Bhattacharyya, M.K. 2014. Analyses of the xylem sap proteomes identified candidate *Fusarium virguliforme* proteinacious toxins. PloS one 9:e93667.

Aoki, T., O'Donnell, K., Homma, Y., and Lattanzi, A.R. 2003. Sudden-death syndrome of soybean is caused by two morphologically and phylogenetically distinct species within the *Fusarium solani* species complex— *F. virguliforme* in North America and *F. tucumaniae* in South America. Mycologia 95:660-684.

Arias, M.M.D., Leandro, L.F., and Munkvold, G.P. 2013. Aggressiveness of *Fusarium* species and impact of root infection on growth and yield of soybeans. Phytopathology 103:822-832.

Atallah, Z.K., Bae, J., Jansky, S.H., Rouse, D.I., and Stevenson, W.R. 2007. Multiplex real-time quantitative PCR to detect and quantify *Verticillium dahliae* colonization in potato lines that differ in response to *Verticillium* wilt. Phytopathology 97:865-872.

Bilodeau, G.J., Koike, S.T., Uribe, P., and Martin, F.N. 2012. Development of an assay for rapid detection and quantification of *Verticillium dahliae* in soil. Phytopathology 102:331-343.

Brar, H.K., Swaminathan, S., and Bhattacharyya, M.K. 2011. The *Fusarium virguliforme* toxin fvtox1 causes foliar sudden death syndrome-like symptoms in soybean. Mol Plant Microbe Interact 24:1179-1188.

Bustin, S.A., Benes, V., Garson, J.A., Hellemans, J., Huggett, J., Kubista, M., Mueller, R., Nolan, T., Pfaffl, M.W., Shipley, G.L., Vandesompele, J., and Wittwer, C.T. 2009. The MIQE guidelines: minimum information for publication of quantitative real-time PCR experiments. Clin Chem 55:611-622.

Chang, H.-X., Domier, L., Radwan, O., Yendrek, C., Hudson, M., and Hartman, G.L. 2015. Identification of multiple phytotoxins produced by *Fusarium virguliforme* including a phytotoxic effector (FvNIS1) associated with sudden death syndrome foliar symptoms. Mol Plant-Microbe Interact 29:96-108.

Chilvers, M.I., du Toit, L.J., Akamatsu, H., and Peever, T.L. 2007. A real-time, quantitative PCR seed assay for *Botrytis* spp. that cause neck rot of onion. Plant Dis 91:599-608.

Cho, J.H., Rupe, J.C., Cummings, M.S., and Gbur, E.E. 2001. Isolation and identification of *Fusarium solani* f. sp *glycines* from soil on modified Nash and Snyder's medium. Plant Dis 85:256-260.

Claassen, S., du Toit, E., Kaba, M., Moodley, C., Zar, H.J., and Nicol, M.P. 2013. A comparison of the efficiency of five different commercial DNA extraction kits for extraction of DNA from faecal samples. Journal of Microbiological Methods 94:103-110.

Clark, W.D., Reyes-Valdes, M.H., Bond, J., and Kantartzi, S.K. 2013. Performance of LS97-1610×'Spencer' soybean recombinant inbred line population segregating for resistance to *Fusarium virguliforme*. Can J Plant Sci 93:1179-1185.

De Mendiburu, F. 2014. Agricolae: Statistical procedures for agricultural research. R package version 1:1-6.

Dorrance, A.E., Kleinhenz, M.D., McClure, S.A., and Tuttle, N.T. 2003. Temperature, moisture, and seed treatment effects on *Rhizoctonia solani* root rot of soybean. Plant Dis 87:533-538.

English, C.A., Merson, S., and Keer, J.T. 2006. Use of elemental analysis to determine comparative performance of established DNA quantification methods. Anal. Chem. 78:4630-4633.

Gao, X., Hartman, G., and Niblack, T. 2006. Early infection of soybean roots by *Fusarium solani* f. sp *glycines*. Phytopathology 96:S38-S38.

Gao, X., Jackson, T.A., Lambert, K.N., Li, S., Hartman, G.L., and Niblack, T.L. 2004. Detection and quantification of *Fusarium solani* f. sp *glycines* in soybean roots with real-time quantitative polymerase chain reaction. Plant Dis 88:1372-1380.

Gongora-Canul, C., Nutter Jr, F.W., and Leandro, L.F.S. 2012. Temporal dynamics of root and foliar severity of soybean sudden death syndrome at different inoculum densities. European journal of plant pathology 132:71-79.

Gongora-Canul, C.C., and Leandro, L.F.S. 2011a. Plant age affects root infection and development of foliar symptoms of soybean sudden death syndrome. Plant Dis 95:242-247.

Gongora-Canul, C.C., and Leandro, L.F.S. 2011b. Effect of soil temperature and plant age at time of inoculation on progress of root rot and foliar symptoms of soybean sudden death syndrome. Plant Dis 95:436-440.

Haudenshield, J.S., and Hartman, G.L. 2011. Exogenous controls increase negative call veracity in multiplexed, quantitative PCR assays for *Phakopsora pachyrhizi*. Plant Dis 95:343-352.

Hershman, D.E., Hendrix, J.W., Stuckey, R.E., Bachi, P.R., and Henson, G. 1990. Influence of planting date and cultivar on soybean sudden death syndrome in Kentucky. Plant Dis 74:761-766.

Huang, Y.H., and Hartman, G.L. 1998. Reaction of selected soybean genotypes to isolates of *Fusarium solani* f. sp. *glycines* and their culture filtrates. Plant Dis 82:999-1002.

Hughes, T.J., Atallah, Z.K., and Grau, C.R. 2009. Real-time PCR assays for the quantification of *Phialophora gregata* f. sp. *sojae* IGS genotypes A and B. Phytopathology 99:1008-1014.

Ji, J., Scott, M.P., and Bhattacharyya, M.K. 2006. Light is essential for degradation of ribulose-1.5-bisphosphate carboxylase-oxygenase large subunit during sudden death syndrome development in soybean. Plant Biology 8:597-605.

Kandel, Y.R., Wise, K.A., Bradley, C.A., Tenuta, A.U., and Mueller, D.S. 2016. Effect of planting date, seed treatment, and cultivar on plant population, sudden death syndrome, and yield of soybean. Plant Dis:PDIS-02-16-0146-RE.

Kandel, Y.R., Haudenshield, J., Srour, A.Y., Islam, K.T., Fakhoury, A.M., Santos, P., Wang, J., Chilvers, M.I., Hartman, G., Malvick, D., Floyd, C.M., Mueller, D., and Leandro, L. 2015. Multi-laboratory comparison of quantitative PCR assays for detection and quantification of *Fusarium virguliforme* from soybean roots and soil. Phytopathology 105:1601-1611.

Kazi, S., Shultz, J., Afzal, J., Johnson, J., Njiti, V.N., and Lightfoot, D.A. 2008. Separate loci underlie resistance to root infection and leaf scorch during soybean sudden death syndrome. Theor Appl Genet 116:967-977.

Li, S., Hartman, G.L., Domier, L.L., and Boykin, D. 2008. Quantification of *Fusarium solani* f. sp *glycines* isolates in soybean roots by colony-forming unit assays and real-time quantitative PCR. Theor Appl Genet 117:343-352.

Livak, K.J., and Schmittgen, T.D. 2001. Analysis of relative gene expression data using real-time quantitative PCR and the 2(T)(-Delta Delta C) method. Methods 25:402-408.

Luckew, A.S., Leandro, L.F., Bhattacharyya, M.K., Nordman, D.J., Lightfoot, D.A., and Cianzio, S.R. 2013. Usefulness of 10 genomic regions in soybean associated with sudden death syndrome resistance. Theor Appl Genet 126:2391-2403.

Luo, Y., Myers, O., Lightfoot, D., and Schmidt, M. 1999. Root colonization of soybean cultivars in the field by *Fusarium solani* f. sp. *glycines*. Plant Dis 83:1155-1159.

Malvick, D., and Impullitti, A. 2007. Detection and quantification of *Phialophora gregata* in soybean and soil samples with a quantitative, real-time PCR assay. Plant Dis 91:736-742.

Mumy, K.L., and Findlay, R.H. 2004. Convenient determination of DNA extraction efficiency using an external DNA recovery standard and quantitative-competitive PCR. J. Microbiol. Methods 57:259-268.

Navi, S.S., and Yang, X. 2008. Foliar symptom expression in association with early infection and xylem colonization by *Fusarium virguliforme* (formerly *F. solani* f. sp. *glycines*), the causal agent of soybean sudden death syndrome. Plant Health Progress 10.

Njiti, V.N., Shenaut, M.A., Suttner, R.J., Schmidt, M.E., and Gibson, P.T. 1996. Soybean response to sudden death syndrome: Inheritance influenced by cyst nematode resistance in Pyramid x Douglas progenies. Crop Science 36:1165-1170.

Njiti, V.N., Suttner, R.J., Gray, L.E., Gibson, P.T., and Lightfoot, D.A. 1997. Rate-reducing resistance to *Fusarium solani* f. sp. *phaseoli* underlies field resistance to soybean sudden death syndrome. Crop Science 37:132-138.

O'Connell, R.J., Thon, M.R., Hacquard, S., Amyotte, S.G., Kleemann, J., Torres, M.F., Damm, U., Buiate, E.A., Epstein, L., Alkan, N., Altmuller, J., Alvarado-Balderrama, L., Bauser, C.A., Becker, C., Birren, B.W., Chen, Z.H., Choi, J., Crouch, J.A., Duvick, J.P., Farman, M.A., Gan, P., Heiman, D., Henrissat, B., Howard, R.J., Kabbage, M., Koch, C., Kracher, B., Kubo, Y., Law, A.D., Lebrun, M.H., Lee, Y.H., Miyara, I., Moore, N., Neumann, U., Nordstrom, K., Panaccione, D.G., Panstruga, R., Place, M., Proctor, R.H., Prusky, D., Rech, G., Reinhardt, R., Rollins, J.A., Rounsley, S., Schardl, C.L., Schwartz, D.C., Shenoy, N., Shirasu, K., Sikhakolli, U.R., Stuber, K., Sukno, S.A., Sweigard, J.A., Takano, Y., Takahara, H., Trail, F., van der Does, H.C., Voll, L.M., Will, I., Young, S., Zeng, Q.D., Zhang, J.Z., Zhou, S.G., Dickman, M.B., Schulze-Lefert, P., van Themaat, E.V.L., Ma, L.J., and Vaillancourt, L.J. 2012. Lifestyle transitions in plant pathogenic Colletotrichum fungi deciphered by genome and transcriptome analyses. Nat Genet 44:1060-1067.

Ortiz-Ribbing, L.M., and Eastburn, D.M. 2004. Soybean root systems and sudden death syndrome severity: Taproot and lateral root infection. Plant Dis 88:1011-1016.

Prabhu, R.R., Njiti, V.N., Bell-Johnson, B., Johnson, J.E., Schmidt, M.E., Klein, J.H., and Lightfoot, D.A. 1999. Selecting soybean cultivars for dual resistance to soybean cyst nematode and sudden death syndrome using two DNA markers. Crop Science 39:982-987.

R Core Team. 2015. R: A language and environment for statistical computing. R Foundation for Statistical Computing, Vienna, Austria.

Roy, K.W., Hershman, D.E., Rupe, J.C., and Abney, T.S. 1997. Sudden death syndrome of soybean. Plant Dis 81:1100-1111.

Rupe, J.C. 1989. Frequency and pathogenicity of *Fusarium solani* recovered from soybeans with sudden death syndrome. Plant Dis 73:581-584.

Scherm, H., and Yang, X.B. 1996. Development of sudden death syndrome of soybean in relation to soil temperature and soil water matric potential. Phytopathology 86:642-649.

Srour, A., Afzal, A.J., Blahut-Beatty, L., Hemmati, N., Simmonds, D.H., Li, W., Liu, M., Town, C.D., Sharma, H., Arelli, P., and Lightfoot, D.A. 2012. The receptor like kinase at Rhg1-a/Rfs2 caused pleiotropic resistance to sudden death syndrome and soybean cyst nematode as a transgene by altering signaling responses. BMC Genomics 13:368.

Valsesia, G., Gobbin, D., Patocchi, A., Vecchione, A., Pertot, I., and Gessler, C. 2005. Development of a high-throughput method for quantification of *Plasmopara viticola* DNA in grapevine leaves by means of quantitative real-time polymerase chain reaction. Phytopathology 95:672-678.

Wang, J., Jacobs, J.L., Byrne, J.M., and Chilvers, M.I. 2015. Improved diagnoses and quantification of *Fusarium virguliforme*, causal agent of soybean sudden death syndrome. Phytopathology 105:378-387.

Wen, Z., Tan, R., Yuan, J., Bales, C., Du, W., Zhang, S., Chilvers, M.I., Schmidt, C., Song, Q., Cregan, P.B., and Wang, D. 2014. Genome-wide association mapping of quantitative resistance to sudden death syndrome in soybean. BMC Genomics 15:809.

Westphal, A., Li, C., Xing, L., McKay, A., and Malvick, D. 2014. Contributions of *Fusarium virguliforme* and *Heterodera glycines* to the disease complex of sudden death syndrome of soybean. PloS one 9:e99529.

Wickham, H. 2009. ggplot2: elegant graphics for data analysis. Springer Science & Business Media.

CHAPTER 4 BASELINE SENSITIVITY OF *FUSARIUM VIRGULIFORME* TO FLUOPYRAM FUNGICIDE

Abstract

Fluopyram, a succinate dehydrogenase inhibitor (SDHI) fungicide, was recently registered for use as a soybean seed treatment for management of sudden death syndrome (SDS) caused by *Fusarium virguliforme*. Although registered and now used commercially, baseline fungicide sensitivity of *F. virguliforme* to fluopyram has not yet been established. In this study, the baseline sensitivity of *F. virguliforme* to fluopyram was determined using mycelium growth and conidia germination with two collections of *F. virguliforme* isolates. A total of 130 and 75 *F. virguliforme* isolates were tested using the mycelial growth and conidia germination assays, respectively, including a core set of isolates that were tested with both assays. In the mycelial growth inhibition assay, 113 out of 130 isolates (86.9%) were determined to have effective concentrations that inhibited 50% of growth (EC_{50}) at less than 5 µg/ml with a mean EC_{50} of 3.35 µg/ml. For the conidia germination assay, 73 out of 75 isolates (97%) were determined to have an estimated EC_{50} of less than 5 µg/ml with a mean EC_{50} value of 2.28 µg/ml. In a subset of 20 common isolates that were phenotyped with both assays, conidia germination of *F. virguliforme* was also determined to be more sensitive to fluopyram (mean EC_{50} = 2.28 µg/ml) than mycelial growth (mean EC_{50} = 3.35 µg/ml). Hormetic effects were observed in the mycelial growth inhibition assay, 19.2% of the isolates demonstrated more growth on medium amended with the lowest fluopyram concentration (1 µg/ml), as compared to the non-fluopyram amended control. Nine out of 185 isolates (4.8%) were less sensitive to fluopyram, as those isolates did not reach 50% growth or conidia germination inhibition at the highest fluopyram concentrations (100 µg/ml and 20 µg/ml for mycelial growth and conidia germination inhibition assays, respectively) tested. On the whole, the *F. virguliforme* population appears to be sensitive to fluopyram, and this study enables future monitoring of fungicide sensitivity.

Introduction

Sudden death syndrome (SDS) is a major yield limiting disease in soybean (*Glycine max*) production. SDS is primarily caused by *Fusarium virguliforme* within North America. Crop rotation with common field crops, especially corn, is ineffective in reducing SDS, due to the broad host range of *F. virguliforme* (Kolander et al. 2012; Navi and Yang 2016). Increased soil porosity or reduced soil moisture through tillage have been reported to reduce SDS severity (Vick et al. 2003); however, consistency of response, long term benefit, and associated costs are still not clear (Hartman et al. 2015). Planting partially resistant soybean cultivars can significantly reduce foliar SDS severity (Njiti et al. 1997). However, the *F. virguliforme* colonization of partially resistant soybean cultivars may not be significantly different to those of susceptible cultivars (Wang et al. 2013), possibly resulting in hidden yield loss and enabling maintenance of *F. virguliforme* inoculum in the soil. Thus, there is a critical need to develop additional SDS disease management tools, including protection from root rot and root colonization.

Soybean fungicide seed treatments are primarily used to manage soilborne pathogens that cause seed rot, damping-off, seedling blight, and root rot (Mueller et al. 2013; Munkvold 2009). Although SDS is known for its typical foliar symptoms late in the season, root infections by *F. virguliforme* are essential for the development of SDS symptoms. *Fusarium virguliforme* can infect soybean roots shortly after germination (Gao et al. 2006). Early infection events also appear to be essential for severe SDS symptom development (Navi and Yang 2008). Therefore, an effective method to inhibit early infection may assist in SDS management. Fungicides seed treatments have been examined for their management of soybean SDS, however to date only fluopyram appears to have any efficacy (Kandel et al. 2016; Mueller et al. 2011; Wang et al.

2014; Weems et al. 2015). However, the baseline sensitivity of *F. virguliforme* to fluopyram has not yet been determined.

Fluopyram is a succinate dehydrogenase inhibitor (SDHI) that targets the ubiquinone binding site to block energy metabolism in mitochondria (Kuhn 1984). SDHI fungicides have been successfully utilized to manage a broad range of plant pathogens causing diseases on various fruits and vegetables (Avenot et al. 2008; Vega and Dewdney 2015). SDHI fungicides are categorized by the Fungicide Resistance Action Committee (FRAC) to have a medium to high risk for the selection of SDHI-resistant fungal isolates (FRAC 2015). This medium to high risk is due to the single-site mode of action of SDHI fungicides, and many registered SDHI fungicide are in the same cross-resistance group (Avenot and Michailides 2010; 2015). Examples of resistance to SDHI fungicides (carboxin, fluotolanil, and boscalid) were reported shortly after their introduction to the market, and have been linked to point mutations in one subunit of succinate dehydrogenase coding genes (Avenot et al. 2008; Broomfield and Hargreaves 1992; Gunatilleke et al. 1975). The recently developed SDHI fungicide, fluopyram, showed a lack of cross-resistance to the other SDHI fungicide resistant fungal strains (Amiri et al. 2014; Ishii et al. 2011). The low cross-resistance feature of fluopyram was demonstrated at the molecular level, by showing that the fluopyram molecule binds to a different cavity on the succinate dehydrogenase molecule that also requires a lower binding energy than other SDHI fungicides (Fraaije et al. 2012).

The fungicide testing method will affect the estimation of fungal sensitivity (Vega and Dewdney 2015). Fungicide-amended agar medium for the characterization of fungal mycelial growth inhibition is one of the most common methods to determine fungicide sensitivity (Liang et al. 2015; Saville et al. 2015). Spore germination rates on fungicide amended agar medium

have also been used to calculate fungicide sensitivities (Bradley and Pedersen 2011; Chiocchio et al. 2000). SDHI fungicides have been reported to have species-specific differential inhibition effects on mycelial growth and conidia germination (Vega and Dewdney 2015). Therefore, both mycelial growth and spore germination assays were included in this study to obtain a complete evaluation of *F. virguliforme* sensitivity to fluopyram.

To determine the efficacy of fluopyram in the field, and to prolong the product life of fluopyram, it is essential to monitor for shifts in sensitivity by conducting a fungicide baseline sensitivity study. Thus the objectives of this study were: 1) to determine the baseline sensitivity of *F. virguliforme* against the SDHI fungicide, fluopyram; 2) to compare the inhibition efficacy of fluopyram on *F. virguliforme* mycelia growth and conidia germination rate.

Materials and methods

Fungal isolation collection and storage

A total of 130 *F. virguliforme* isolates were tested in mycelial growth inhibition assay at Michigan State University (MSU). Isolates were recovered from soybean roots showing typical SDS foliar and root symptoms from 2009 to 2014 from five states (Table 4-1): 8 Arkansas isolates, 13 Illinois isolates, 11 Kansas isolates, 80 Michigan isolates, and 18 Indiana isolates. The conidia germination fungicide sensitivity assay was conducted on a collection of 75 *F. virguliforme* isolates at the University of Illinois. These isolates were collected from seven states (Table 4-2): 2 Arkansas isolates, 47 Illinois isolates, 6 Iowa isolates,1 Kansas isolate, 1 Kentucky isolate, 10 Michigan isolates, 1 Minnesota isolate, and 7 unknown sources.

Table 4-1 EC_{50} of *F. virguliforme* isolates used in the mycelial growth inhibition assay against the SDHI fungicide, fluopyram. A total of 130 isolates were collected from five states in the United States from 2009 to 2014.

State	N	Years	EC_{50} [a] (µg/ml)
Arkansas	8	2012	2.34 - 4.07*
Illinois	13	2013 - 2014	2.15 - 6.92
Kansas	11	2012	1.76 - 3.73*
Michigan	80	2009 - 2013	1.53 - 9.28*
Indiana	18	2012	2.22 - 4.47*
Total	130		

[a]: range of EC_{50} estimation for the isolates from each state

* Does not include the isolates from Arkansas (n=1), Kansas (n=2), Michigan (n=10), and Indiana (n=1) that did not reach 50% growth inhibition at the highest concentration of fluopyram (100 µg/ml) or non-significant EC_{50} estimation at non-linear regression.

Table 4-2 EC_{50} of *F. virguliforme* isolates used in the conidia germination inhibition assay testing against SDHI fungicide fluopyram. Isolates were collected from seven states in the United States from 2009 to 2014.

State	N	Years	EC_{50}[b] (μg/ml)
Arkansas	2	2012	2.41 - 2.94
Illinois	47	2010 - 2014	0.81 - 5.57
Iowa	6	2013	2.18 - 4.07
Kansas	1	2012	3.31
Kentucky	1	2014	2.54
Michigan	10	2009 - 2012	1.34 - 4.08
Minnesota	1	Unknown	3.41
Unknown [a]	7	2012 - 2013	1.24 - 2.38*
Total	75		

[a]: indicates isolates with unknown source of origin
[b]: range of EC_{50} estimation for the isolates from each state
* not include the isolates with unknown source that did not reach 50% growth inhibition at the highest concentration of fluopyram (100 μg/ml)

All isolates were derived from a single-conidium culture. Isolates at MSU were selected to ensure genetic diversity by genotyping with microsatellite markers (Wang and Chilvers 2016; Wang and Chilvers, unpublished). Isolates were stored by allowing mycelia to colonize pieces of sterile Whatman #1 qualitative filter paper, which was placed on the surface of potato dextrose agar (PDA) (Acumedia, Lansing, MI) in a petri plate. Once filter papers were fully colonized with mycelia, filter papers were taken from the media, and air dried for storage at -20 ℃. Additionally, macroconidia suspensions were added to equal volume of 30% glycerol for long term storage at -80 ℃. Isolates used at MSU were identified to be *F. virguliforme* using a species specific PCR assay (Wang et al. 2015).

Determination of baseline EC_{50} values – mycelial growth inhibition assay

The inhibition effect of fluopyram on *F. virguliforme* mycelia growth was evaluated using fungicide amended half-strength PDA (Acumedia). Formulated fluopyram (Luna Privilege; Bayer CropScience, Research Triangle Park, NC) (containing 43% active ingredient) was used to

prepare stock solutions at concentrations of 1, 5, 10, 25, 50, and 100 mg/ml in sterilized water. One liter of culture media included 12 g of potato dextrose broth powder (Acumedia), 15 g of agar (Sigma Aldrich, St. Louis, MO), and 1 liter of deionized water (dH_2O). After the media was autoclaved and cooled to 55 ℃, 1 ml of fluopyram stock solution was added to the media to make a final concentration of 0, 1, 5, 10, 25, 50, and 100 µg/ml (ppm) fluopyram. Isolates were divided into 11 sets tested in different experimental runs. To validate the reproducibility of this experiment, two isolates from each set of the experiment were randomly selected to verify the reproducibility of this assay (Figure S4-1).

Mycelial plugs (2 mm^3 cubes) cut from the edge of 10 day-old fungal colonies were placed mycelia side down on the center of each petri dish plate. Three replicate plates were used for each fungicide concentration. Plates were incubated at 24 ℃ for 10 days in the dark, and a culture of each isolate was scanned at 3 and 10 days after inoculation (DAI) with 300 dpi image quality, using a Perfection V600 scanner (EPSON, Long Beach, CA). On each scanned image, a photographic reference scale (http://web.ncf.ca/jim/scale/) was included to calibrate the ratio between image digital pixel and physical length for the subsequent image analysis. Dark blue background card (Hobby Lobby, hex color code: #1E2E4D) was used at the scanning step to create strong contrast to facilitate image analysis.

Image analysis and model selection

All images were analyzed using Assess v2.0 software (American Phytopathological Society, St. Paul, MN) using the manual panel option, and the HSV color space was used to analyze the selected colony area using hue value between 0 and 195. Relative mycelial growth rate was calculated by subtracting the 3 DAI colony areas from the 10 DAI colony area and divided by seven days to get the colony area increase per day. The growth rate of the colony area was

converted to calculate the mycelial growth rate (mm/d). The R (R Core Team 2015) package 'drc' (Ritz and Streibig 2005) was used to select the best fitting non-linear dose-response curve model. The 'mselect' function was used to determine the fittest non-linear model for the fungal mycelial growth inhibition dose response curves. The tested non-linear models include: the three-parameter log-logistic model (LL.3), the four-parameter log-logistic model (LL.4), the four-parameter Weibull models (W2.4), the Cedergreen-Ritz-Streibig model (CRS.4a), and the Brain-Cousens hormesis models (BC.4). The best fitting model was determined based on the lowest Akaike's Information Criterion (AIC) value.

Determine baseline EC_{50} values – conidia germination inhibition assay

Macroconidia were plated on fungicide amended agar media to determine the inhibitory effect of fluopyram on *F. virguliforme* spore germination. A conidia spore suspension was prepared from a 6-day old *F. virguliforme* colony grown on PDA by collecting conidia from *F. virguliforme* sporodochia. Sterilized water (5 µl) was added to a sporodochium and a pipette was used to homogenize the water and conidia by pipetting up and down, and a 5 µl condial suspension was collected and diluted into 1 ml sterilized water in a 1.5-ml eppendorf tube. Technical grade fluopyram (Bayer CropScience) was dissolved in dimethyl sulfoxide (DMSO) to make a stock solution for making medium. Based on a preliminary experiment, five fluopyram final concentrations (0.1, 1, 5, 10, and 20 µg/ml including a 0 µg/ml control) were used in the conidia germination experiment. A conidia suspension (20 µl) was transferred and evenly spread with a bent glass rod onto PDA amended with different concentrations of fluopyram. Cultures were incubated in ambient light at 20 ℃ for 20 h. After incubation, 50 conidia on two replicates plates were evaluated under a microscope to determine the conidia germination rate. A conidium in which the germination tube grew to the length of the conidium was counted as germinated.

Data analyses

The effective concentration to reduce mycelial growth or conidia germination rate by 50% (EC_{50}) for the isolates were calculated by fitting the mycelial relative growth rate against the log transformed fungicide concentrations using the best fitting model (LL.4) in the R package 'drc' v2.5 (Ritz and Streibig 2005). The calculated EC_{50} values were filtered through two thresholds: 1) relative growth inhibition at highest fluopyram concentration was more than 50% of the zero-control; 2) *P* value of the EC_{50} parameter estimation less than 0.05. ANOVA was performed to determine the significance level with the 'car' package using type II sum of square to determine the sources of variances in EC_{50} values comparisons. Figures were prepared with "ggplot2" package (Wickham 2009) in R. The estimated EC_{50} values all the isolates were listed in Table S4-1 and Table S4-2. The R scripts used for data analysis was made to be accessible through Zenodo (DOI: 10.5281/zenodo.53939)

Comparison of the mycelial and spore germination assays

To compare the fungicide sensitivity testing methods, 20 isolates were selected for testing with both methods (). To determine the differences between these two methods, EC_{50} values calculated for each of these methods were compared using a paired t-test, and the EC_{50} mean contrasts were plotted in a forest plot using R package 'latticeExtra' (Sarkar 2008). The EC_{50} values calculated using these two methods were regressed over each other in a linear model, and the Spearman correlation was used to determine the level of correlation significance using base R package 'stats' (R Core Team 2015).

Results

Model selection and data validation for the mycelial growth inhibition assay

The 4-parameter-log-logistic model (LL.4) was determined to be the best fitting model based on the lowest AIC for most of isolates (78%) tested in the mycelial growth inhibition assay (Figure 4-1). The remaining 22% of the isolates in the mycelial growth assay showed a hormetic effect, where mycelial growth rate was higher in the low concentration fungicide treatment (1 µg/ml) than the non-fluopyram control treatment. The models specialized describing the "u-shape" hormesis were included in the model selection, and the Brain-Cousins modified log-logistic model (BC.4) was determined to be the best fitting model for the hormetic effect isolates. To keep a parsimonious summary for EC_{50} calculation, the 4-parameter log-logistic model was used consistently for all the mycelial growth inhibition assay data.

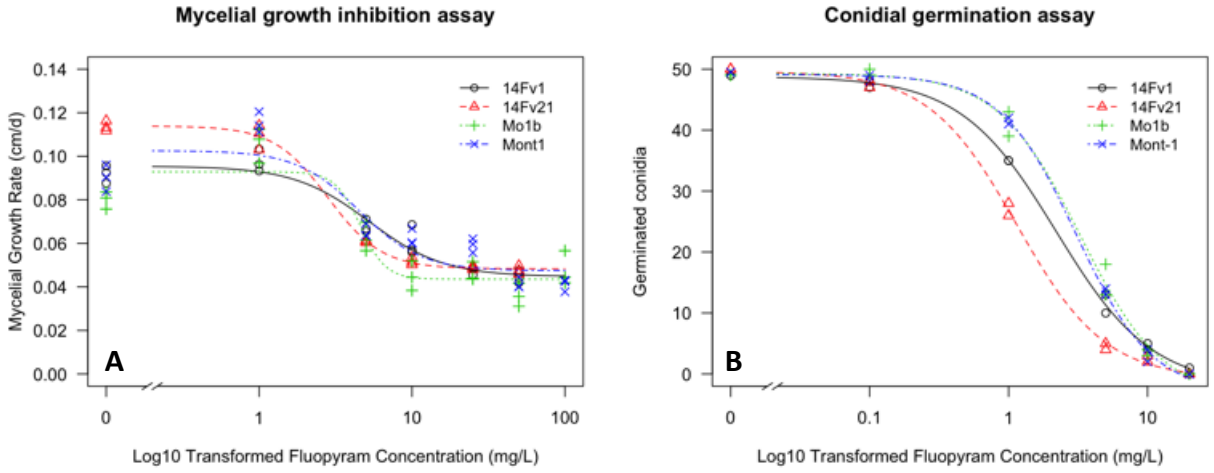

Figure 4-1 Dose response curve fitting for (A) mycelial growth and (B) conidia germination at different concentrations of fluopyram amended in the agar media for the *F. virguliforme* isolates: 14Fv1, 14Fv21, Mo1b, and Mont1, as represented by "o", "Δ", "+", and "x" symbols, respectively.

To validate the robustness of the mycelial growth inhibition assays, two *F. virguliforme* isolates were randomly selected from each of the 11 batch runs to repeat the mycelial growth inhibition assay. The estimation of EC_{50} using mycelial growth inhibition was reproducible, as EC_{50} value replicates calculated for the 21 out of 22 isolates overlapped with their means confidence interval (Figure 4-5).

Mycelial growth sensitivity against fluopyram

In the mycelial growth inhibition assay, 116 out of 130 *F. virguliforme* isolates demonstrated mycelial growth inhibition by 50% on the media amended with fluopyram, while the other eight isolates (6.1%) did not reach a 50% mycelial growth inhibition even at the highest fluopyram concentration (100 µg/ml), where a reduction in growth rate by 0 and 43.8% was observed; five isolates were filtered at non-linear regression step; and one isolate failed at image analysis step possibly due to heavily pigmented background. The calculated EC_{50} values for 116 isolates ranged from 1.53 to 9.28 µg/ml, with mean and median EC_{50} of 3.35 and 3.25 µg/ml, respectively (Figure 4-2 and Table 4-4). EC_{50} values for most isolates (78.5%) were within a range between 2 and 4 µg/ml. There were no significant differences in EC_{50} values among the isolates collected from five states ($P = 0.41$) in the US. The frequency distribution of EC_{50} values for the 116 isolates was a unimodal curve, with a right tail distribution indicating the presence of few less sensitive *F. virguliforme* isolates to fluopyram, not including those 14 isolates for which we could not calculate EC_{50}.

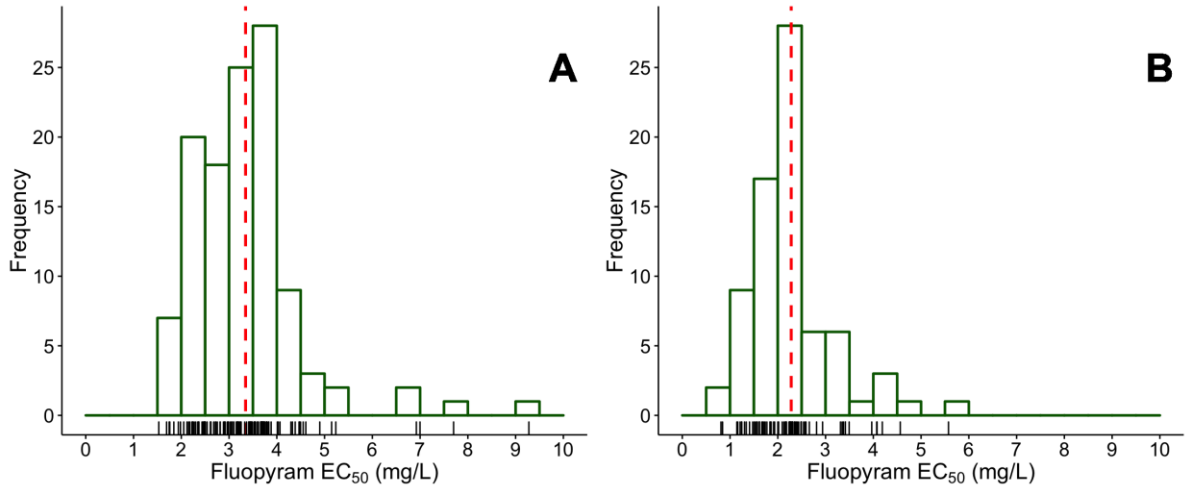

Figure 4-2 Frequency distribution of effective fungicide concentration that inhibits growth by 50% for both (A) mycelial growth inhibition assay and (B) conidia germination inhibition assay. The mean EC_{50} value was indicated as the dotted vertical lines with the mean EC_{50} values: 3.35 and 2.28 µg/ml for the mycelial growth inhibition assay and conidia germination assay, respectively.

Mycelial growth hormetic effects

A hormetic effect was solely observed in the mycelial growth inhibition assay at the concentrations of 1 µg/ml and 0.5 µg/ml (data not shown) amended in the media. Twenty-two percent (n=29) of the isolates tested in the mycelial growth inhibition assay demonstrated a hormetic effect. The best fitting model for these isolates was determined to be the Brain-Cousens hormesis model (BC.4) based on the lowest AIC values (Figure 4-4 and Table 4-3). The calculated EC_{50} values with the BC.4 model were significantly higher than the EC_{50} values calculated using the LL.4 model (P = 0.006, Table 4-3). On average, the BC.4 model estimated EC_{50} values were higher than the LL.4 model estimated EC_{50} values by 10 µg/ml. Between these two models, 22 out of 29 EC_{50} values estimated using the BC.4 model fell within the concentration range where the 50% growth inhibition was reached, while 3 of the 29 EC_{50} values estimated using the LL.4 model fell the concentration range where the 50% growth inhibition was reached. Neither of these two models fell within the concentration range where 50% growth

inhibition was reach for the rest of the four isolates (Table 4-3). Overall, the LL.4 model underestimated the EC_{50} for the isolates showed hermetic effect, and BC.4 had a more accurate estimation of EC_{50} for the isolates showed hormetic effect.

Table 4-3 Comparison of EC_{50} values calculated using 4-parameter log-logistic model (LL.4) and the Brain-Cousens model (BC.4) for the *F. virguliforme* isolates that showed hormetic effect in the mycelial growth inhibition assay. At model selection, the AIC values calculated for LL.4 and BC.4 models were -4148 and -3926 (lower is better), respectively.

Strain	Set [a]	LL.4		BC.4		Difference	Relative growth ratio[e]				Better Model [d]
		EC50	StdErr [b]	EC50	StdErr	in EC_{50}	5 µg/ml	10 µg/ml	50 µg/ml	100 µg/ml	
AL1a	2	3.10	0.49	5.14	0.60	2.04	**0.45**	**0.38**	**0.22**	- [f]	LL.4
ARLE-A1	1	3.73	0.98	5.77	1.13	2.04	**0.47**	**0.44**	**0.18**	-	LL.4
Mo4a	1	2.91	0.74	5.17	0.97	2.26	**0.45**	**0.38**	**0.22**	-	LL.4
MIVB-A5	2	1.21	0.11	3.67	0.41	2.47	0.51	**0.35**	**0.25**	**0.30**	None
MIVB-C1	10	3.79	0.50	9.14	1.47	5.35	0.53	**0.43**	**0.29**	**0.29**	BC.4
MITU-B1	12	4.01	1.46	9.98	2.46	5.97	0.54	**0.49**	**0.32**	**0.33**	BC.4
MISTJ-A1	3	4.12	1.03	10.44	4.13	6.32	0.55	**0.43**	**0.26**	**0.38**	None
STJ-7P2ss	1	3.59	1.18	9.93	3.66	6.33	0.54	**0.47**	**0.33**	-	BC.4
MIBer-E6	3	3.74	0.79	11.13	3.78	7.39	0.49	**0.43**	**0.23**	**0.34**	None
Mo1a-2	10	3.71	0.50	12.21	2.18	8.50	0.56	0.51	**0.30**	**0.33**	BC.4
MIBer-F3	10	3.75	0.55	13.38	2.78	9.63	0.57	0.52	**0.30**	**0.38**	BC.4
KSSH-G2	10	3.73	0.61	14.66	3.03	10.93	0.58	0.52	**0.36**	**0.36**	BC.4
MISA-A1	7	4.46	1.12	20.16	5.09	15.69	0.64	0.58	**0.36**	**0.38**	BC.4
Mo3a	9	4.38	0.92	23.83	6.94	19.45	0.69	0.59	**0.38**	**0.42**	BC.4
INMO-A6	10	4.47	0.82	26.09	5.92	21.62	0.70	0.60	**0.39**	**0.43**	BC.4
MIVB-A6	1	4.61	1.58	27.38	11.10	22.77	0.79	0.68	**0.47**	-	BC.4
Mont1	14	9.34	2.00	34.10	7.64	24.76	0.77	0.75	**0.43**	**0.45**	BC.4
MISTJ-F6	11	4.50	1.06	30.45	8.89	25.96	0.75	0.67	**0.43**	**0.49**	BC.4
14Fv1	13	5.24	0.87	33.39	6.49	28.16	0.74	0.66	**0.49**	-	BC.4
MISTJ-E4	11	4.00	1.48	36.19	13.25	32.19	0.59	0.54	**0.42**	**0.42**	BC.4
Mont1	7	4.51	1.39	42.01	11.40	37.51	0.77	0.75	**0.43**	**0.45**	BC.4
Ca2a	4	4.30	1.66	117.88	96.28	113.58	0.87	0.70	0.64	0.72	BC.4 [g]
MIBer-E4	8	7.70	3.00	231.42	170.19	223.72	1.11	1.00	0.69	0.81	BC.4 [g]
ARLE-C3a	11	NA [c]	NA	270.18	187.66	NA	1.09	1.00	0.70	0.62	BC.4 [g]

Table 4-3 (cont'd)

KSSH-A4	1	NA [c]	NA	11.46	4.18	NA	0.53	0.51	**0.38**	-	BC.4
LE-11-1	3	NA [c]	NA	154.55	130.28	NA	1.01	0.92	0.59	0.76	BC.4 [g]
MIBer-A5	11	NA [c]	NA	22.29	9.16	NA	0.61	0.51	**0.43**	**0.39**	BC.4
MIBer-D1	2	NA [c]	NA	7.78	1.37	NA	NA	0.43	NA	-	BC.4
MITU-B1	2	NA [c]	NA	11.85	3.76	NA	0.54	**0.49**	**0.32**	**0.33**	None

[a]: batch number for different sets of testing isolates

[b]: standard error

[c]: the EC_{50} parameter estimation in the LL.4 model does not have a significant *P* value.

[d]: EC_{50} estimated using either LL.4 or BC.4 falls within the range of relative growth inhibition by 50%

[e]: relative germination ratio at these concentrations to the 0 μg/ml control, the percentage values lower than 50% are in bold font

[f]: missing data

[g]: EC_{50} estimation out of tested concentration range

Model selection and data validation for the conidia germination inhibition assay

For the conidia germination assay, conidia germination rate decreased as fluopyram concentrations increased. The best fitting model selected for the conidia germination assay dose response data was the 4-parameter-log-logistic model, less than 10% of the isolates showed a better fit with other non-linear models (e.g., Weibull, Cedergreen-Ritz-Streibig model, or Brain-Cousens hormesis models). To keep a parsimonious summary for EC_{50} and to be able to compare amongst isolates, the 4-parameter-log-logistic model was used for all isolates (Figure 4-1).

To validate the reproducibility of the conidia germination inhibition assay, 51 isolates were tested in two separate runs to compare their EC_{50} estimations. The confidence intervals of the EC_{50} estimation were calculated for the replicated isolates, and 40 out of 51 replicated isolates were determined to be not significantly different between two replicates, as indicated by overlapped EC_{50} mean confidence interval (Figure S4-2).

Conidia germination sensitivity against fluopyram

Most of the *F. virguliforme* isolates were sensitive to fluopyram in the conidia germination inhibition assay. In total, 74 out of 75 *F. virguliforme* isolates showed a conidia germination rate reduction by 50% on medium amended with fluopyram, with one isolate not reaching a 50% conidia germination rate reduction even at the highest fluopyram concentration (20 μg/ml). The calculated EC_{50} values for the 74 isolates ranged between 0.81 and 5.57 μg/ml, with mean and median EC_{50} of 2.28 and 2.24 μg/ml, respectively (Figure 4-2 and Table S4-2). EC_{50} values for most of the isolates (89%) fell within a range of 1 and 3.5 μg/ml with a right-tailed unimodal distribution indicating that most isolates were sensitive to fluopyram, not including one isolate for which we could not calculate EC_{50}.

Differences between two fungicide sensitivity testing methods

There is a fundamental difference in fungicide sensitivity tests between the mycelial growth inhibition assay and the conidia germination inhibition assay, including starting fungal materials and experiment durations. The EC_{50} values estimated using the mycelial growth inhibition assay were significantly higher than the EC_{50} values calculated with the conidia germination assay ($P < 0.01$). Of the 20 cross-validated *F. virguliforme* isolates, 15 isolates showed higher EC_{50} estimates for the mycelial growth inhibition assay than the conidia germination inhibition assay (Figure 4-3, $P < 0.01$). Between the EC_{50} values calculated from both of the fungicide sensitivity testing methods, there was no statistically significant correlation between those two sets of EC_{50} estimation data (Spearman correlation was non-significant at $P = 0.4$, Figure 4-3).

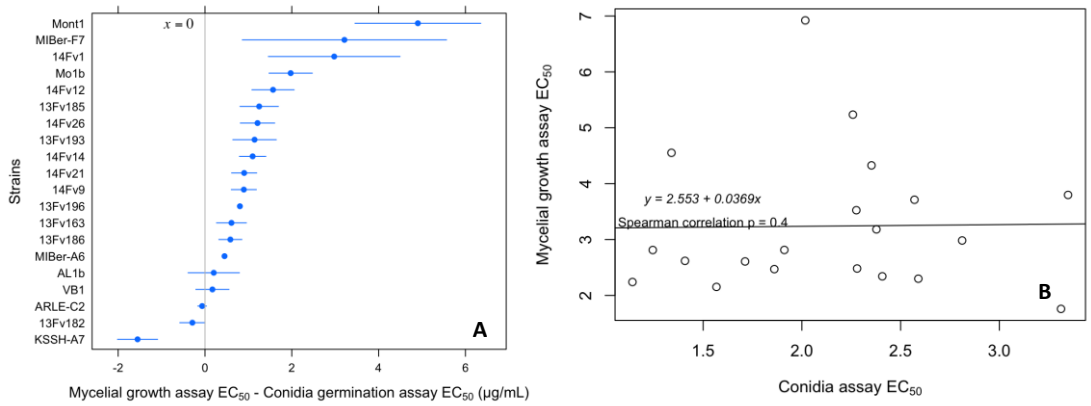

Figure 4-3 (**A**) Comparison of the difference in EC_{50} values estimated using mycelial growth inhibition assay and conidia germination inhibition assay. The differences in EC_{50} estimation between the mycelial growth inhibition and conidia germination assay were plotted for 20 *F. virguliforme* isolates. (**B**) Correlations between the EC_{50} estimations using mycelial growth inhibition assay and conidia germination inhibition assay. There was no significant correlation between those two methods (Spearman correlation $P = 0.40$).

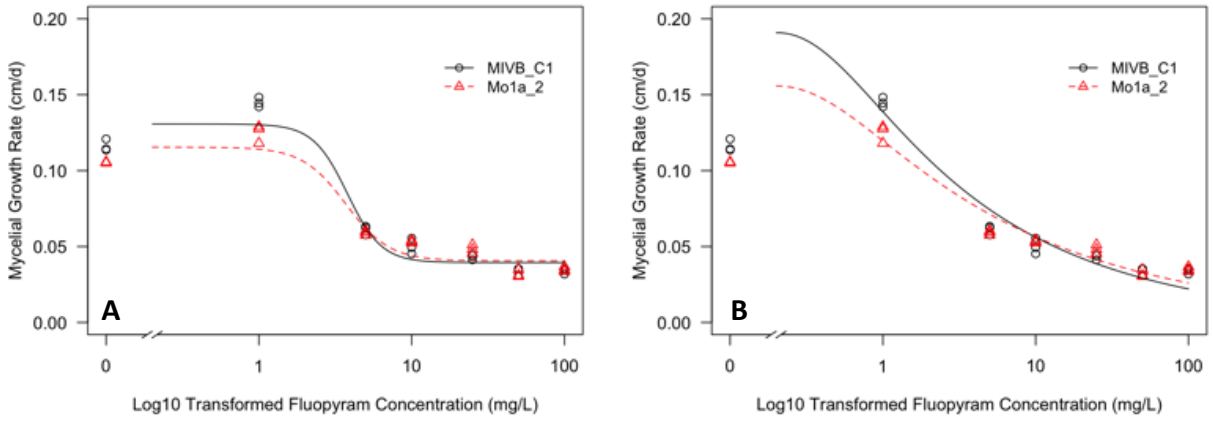

Figure 4-4 Dose response curve fitting the isolates showed hormetic effect using (A) 4-parameter logistic model and (B) Brain-Cousens model. The hormetic effect isolates showed faster growth rate at 1 µg/ml concentration than the zero-control. The non-linear regression BC.4 model (AIC = -271) fits better than the LL.4 (AIC = -259) model for the isolates showed hormesis.

Discussion

Most of the isolates tested in this study were sensitive to fluopyram, but a small fraction of isolates (~5%) were insensitive to fluopyram treatment. The presence of fluopyram insensitive *F. virguliforme* isolates may imply the risk to accumulate less sensitive isolates in the field populations, and result in possible disease management failure. Based on this survey, there is no significant difference in EC_{50} values among sampling locations or years of collections, which is perhaps expected since this pathogen was most likely not previously exposed to fluopyram. Although one of the major fluopyram product, Luna Privilege, is registered on horticultural crops that could have been in rotation with soybean, most of the *F. virguliforme* isolates in this study were collected from the fields, which were predominantly in corn-soybean rotation. Additionally, other SDHI fungicides may have been applied in soybean seed treatments, but fluopyram binds to a different cavity than the other SDHI's possibly reducing cross-resistance (Fraaije et al. 2012).

Fungicide sensitivity EC_{50}s evaluated using the mycelial growth inhibition assay was significantly higher than the fungicide sensitivity EC_{50}s calculated using the conidia germination

inhibition assay by 1 μg/ml. The difference in EC_{50} estimation using different methods was reported in a previous study (Vega and Dewdney 2015) with *Alternaria alternata* isolates tested against another SDHI fungicide, boscalid. Contrary to their findings that mycelial growth of *A. alternata* was more sensitive to boscalid than conidia germination, fluopyram was more effective in inhibiting conidia germination for *F. virguliforme* than mycelia growth. The difference in EC_{50} estimations from these two methods could be explained by a fundamental difference in transferring starting materials: conidia and mycelia. Before transferring to the fungicide amended media agar, the conidia were in a "dormant" condition, while the mycelia were taken from the actively growing part of a colony (Gougouli and Koutsoumanis 2013). The different onset of metabolic levels (Cochrane and Cochrane 1966; Liu et al. 2015) may affect the dose response to fungicide treatment. Thus, it may not be surprising to observe the difference in EC_{50} estimations using these two methods. A combination of these two testing methods provided a relatively complete estimation of *F. virguliforme* sensitivity against the fluopyram fungicide.

At the lower fungicide concentration treatment, a hormetic effect was observed for 20% of the isolates solely in the mycelial growth inhibition assay. The presence of a hormetic effect on isolates in the field indicate that exposure to sublethal doses of fungicide can possibly result in more severe disease symptoms (Garzon et al. 2011). In this study, the hormetic effect was observed at the concentrations of 0.5 and 1 μg/ml (concentration 0.5 μg/ml was tested in the preliminary study, data not shown), so that the application of fluopyram on the seed treatment should ensure an effective concentration above 1 μg/ml.

Multiple non-linear models were selected to fit the fungi growth dose-response curve. The four-parameter log-logistic model (LL.4) was determined to be the best fitting model based on the Akaike's information criteria for most of the isolates (78%). However, the best fitting model

for the isolates showed hormetic effect was the BC.4 model, which was specifically designed for the hormetic effect dose response curve (Cedergreen et al. 2005). The BC.4 model showed a higher estimation of EC_{50} than the LL.4 model, because the hormesis model will lead to higher EC_{50} levels as hormetic effect could possibly delay the onset of toxicity. In reality, most EC50 values (22 out of 29) estimated using the BC.4 fell within the concentration range where 50% growth inhibition was reached (Table 4-3). The LL.4 model underestimated the EC50 for the isolates demonstrating hormesis. Although the BC.4 performs better in predicting EC_{50} for the isolates showed hermetic effect, to achieve the most parsimonious interpretation of the EC_{50} estimations (C. Ritz, personal communication), the LL.4 model was used consistently for all the isolates.

A small fraction (4.8%) of *F. virguliforme* isolates were determined to be less sensitive to fluopyram treatment *in vitro*. Based on the FRAC definition, EC_{50} is the dose that provides 50% inhibition of the isolates as compared to a non-fungicide-amended control, which is also known as absolute EC_{50}. To calculate the EC_{50}, isolates that showed less than 50% growth inhibition at the highest fungicide concentration treatment were filtered out from the data set before using the data for subsequent analysis. In this study, the less sensitive isolates tend to be the slow-growing isolates and secreted melanin-like pigments in the media, even in absence of fluopyram in the medium. Similar results, reduced fungicide sensitivity coupled with slow growth rate and secretion of melanin, were also reported on other plant or human pathogens, such as *Zymoseptoria tritici* (Lendenmann et al. 2015) and *Paracoccidioides brasiliensis* (Taborda et al. 2008). The presence of less sensitive isolates does not always indicate a rapid accumulation of less sensitive isolates in the field. Currently, fluopyram has been mainly applied in seed treatment, which is only applied once per season. Therefore, the selection pressure to accumulate

resistant isolates is not as strong as the foliar fungal disease management, which may require multiple applications of foliar fungicide sprays per season.

Besides *F. virguliforme*, SDS can be caused by three additional *Fusarium* species (*F. tucumaniae, F. brasiliense,* and *F. crassistipitatum*) in South America, which are phylogenetically clustered within the clade-2 *Fusarium solani* species complex (FSSC) with *F. virguliforme* (Aoki et al. 2005; Aoki et al. 2012a). Also, there are additional *Fusarium* species within the clade-2 FSSC causing root rots on dry bean, and these *Fusarium* species are phylogenetically close to *F. virguliforme* (Aoki et al. 2012b). Therefore, it is possible that fluopyram also will be effective in inhibiting mycelial growth or conidia germination for those *Fusarium* species.

Acknowledgement

We thank Dr. Tyre Proffer, Alejandro Rojas, and Janette Jacobs for their suggestions on the design of this experiment. We also thank Zach Noel for his technical suggestions for data analysis. The set of NRRL *F. virguliforme* isolates was kindly provided by ARS culture collection, USDA, Peoria IL. We also thank Dr. Leonor Leandro for sharing some of the *F. virguliforme* isolates. This work was supported by Bayer CropSciences, the North Central Soybean Research Program (NCSRP), and the Michigan Soybean Promotion Committee. Collection of some of the *F. virguliforme* isolates was supported by a grant from the United States Department of Agriculture – National Institute of Food and Agriculture.

APPENDICES

APPENDIX A Supplementary tables

Table S 4-1 EC_{50} estimations for all isolates that were tested in the mycelial growth inhibition assay.

Strain	State	County	Year	EC50	StdErr [a]	Relative growth ratio [b]		
						5ppm	10ppm	50ppm
13Fv163	Illinois	Jackson	2013	2.47	0.17	0.50	0.45	0.38
13Fv182	Illinois	Pope	2013	2.30	0.29	0.46	0.44	0.36
13Fv185	Illinois	Edwards	2013	3.52	0.37	0.61	0.45	0.38
13Fv186	Illinois	Pulaski	2013	2.15	0.23	0.50	0.47	0.41
13Fv193	Illinois	Livingston	2013	3.71	0.48	0.62	0.46	0.41
13Fv196	Illinois	DeKalb	2013	3.18	0.29	0.57	0.50	0.43
14Fv1	Illinois	Clinton	2014	5.24	0.87	0.74	0.66	0.49
14Fv12	Illinois	Adams	2014	2.81	0.23	0.54	0.48	0.41
14Fv14	Illinois	McDonough	2014	2.24	0.17	0.52	0.44	0.41
14Fv21	Illinois	Pike	2014	2.81	0.22	0.54	0.45	0.42
14Fv26	Illinois	Logan	2014	2.62	0.25	0.51	0.44	0.38
14Fv9	Illinois	Mason	2014	2.61	0.26	0.52	0.48	0.42
AL1a	Michigan	Allegan	2009	3.10	0.49	0.45	0.38	0.22
AL1b	Michigan	Allegan	2009	2.48	0.43	0.40	0.34	0.21
ARLE-A1	Arkansas	Lee	2012	3.73	0.98	0.47	0.44	0.18
ARLE-B2	Arkansas	Lee	2012	3.68	0.54	0.50	0.42	0.28
ARLE-B3	Arkansas	Lee	2012	4.07	1.56	0.60	0.47	0.51
ARLE-C1	Arkansas	Lee	2012	3.18	0.82	0.64	0.55	0.37
ARLE-C2	Arkansas	Lee	2012	2.34	0.31	0.39	0.38	0.24
ARLE-C3a	Arkansas	Lee	2012	NA [f]	NA	1.09	1.00	0.70
ARLE-G4	Arkansas	Lee	2012	3.70	1.02	0.59	0.52	0.39
ARLE-G7	Arkansas	Lee	2012	3.22	0.70	0.49	0.37	0.31
Ber1-5	Michigan	Berrien	2009	2.45	0.72	0.35	0.34	0.22
Ber1-9	Michigan	Berrien	2009	3.44	0.39	0.49	0.41	0.26
Ca1a	Michigan	Cass	2009	NA [e]	NA	1.02	0.79	0.81
Ca2a	Michigan	Cass	2009	4.30	1.66	0.87	0.70	0.64
Ca2b	Michigan	Cass	2009	NA [e]	NA	0.87	1.10	0.69
CL-11-1	Michigan	Clinton	2011	3.45	0.64	0.46	0.37	0.27
DBP28R13	Michigan	Van Buren	2013	1.69	0.16	0.38	0.33	0.22
DBP30R5	Michigan	Van Buren	2013	3.02	0.57	0.48	0.44	0.35
DBP30R7	Michigan	Van Buren	2013	1.84	0.27	0.41	0.34	0.29

Table S4-1 (cont'd)

Hu-11-1	Michigan	Huron	2011	2.37	0.29	0.43	0.42	0.34
INMO-A1	Indiana	White	2012	3.06	0.48	0.49	0.40	0.29
INMO-A2	Indiana	White	2012	3.41	1.44	0.41	0.41	0.29
INMO-A3	Indiana	White	2012	2.90	0.40	0.48	0.42	0.32
INMO-A5	Indiana	White	2012	2.22	0.19	0.44	0.37	0.29
INMO-A6	Indiana	White	2012	4.47	0.82	0.70	0.60	0.39
INMO-B2	Indiana	White	2012	2.75	0.48	0.43	0.38	0.31
INMO-B5	Indiana	White	2012	2.37	0.24	0.48	0.44	0.38
INMO-B6	Indiana	White	2012	2.24	0.31	0.39	0.35	0.24
INMO-C1	Indiana	White	2012	3.71	1.07	0.60	0.54	0.54
INMO-C3	Indiana	White	2012	2.48	0.39	0.40	0.38	0.24
INMO-C4	Indiana	White	2012	NA [d]	NA	NA	NA	NA
INMO-D1	Indiana	White	2012	3.25	0.39	0.50	0.42	0.33
INMO-E1	Indiana	White	2012	3.16	0.41	0.47	0.44	0.30
INMO-E5	Indiana	White	2012	3.78	1.22	0.64	0.58	0.51
INMO-F1	Indiana	White	2012	3.62	0.73	0.54	0.32	0.31
INMO-F2	Indiana	White	2012	4.03	0.34	0.57	0.42	0.32
INMO-G3	Indiana	White	2012	3.88	0.50	0.60	0.50	0.36
INMO-G6	Indiana	White	2012	2.62	0.30	0.46	0.37	0.31
KA-11-1	Michigan	Kalamazoo	2011	4.90	0.54	0.83	0.60	0.58
KSSH-A1	Kansas	Shawnee	2012	3.53	0.47	0.53	0.45	0.34
KSSH-A2	Kansas	Shawnee	2012	2.50	0.29	0.42	0.34	0.23
KSSH-A4	Kansas	Shawnee	2012	NA [f]	NA	0.53	0.51	0.38
KSSH-A7	Kansas	Shawnee	2012	1.76	0.40	0.36	0.47	0.35
KSSH-C2	Kansas	Shawnee	2012	1.98	0.19	0.41	0.35	0.27
KSSH-C3	Kansas	Shawnee	2012	3.47	1.28	0.65	0.57	0.40
KSSH-C4	Kansas	Shawnee	2012	3.67	0.85	0.52	0.43	0.34
KSSH-C5	Kansas	Shawnee	2012	3.43	0.53	0.49	0.43	0.25
KSSH-E4	Kansas	Shawnee	2012	3.60	1.00	0.55	0.49	0.35
KSSH-F4	Kansas	Shawnee	2012	NA [f]	NA	0.42	0.59	0.24
KSSH-G2	Kansas	Shawnee	2012	3.73	0.61	0.58	0.52	0.36
LE-11-1	Michigan	Lenawee	2011	NA [e]	NA	1.01	0.92	0.59
MIBer-A1	Michigan	Berrien	2012	3.79	0.47	0.54	0.46	0.30
MIBer-A2	Michigan	Berrien	2012	1.94	0.26	0.46	0.42	0.41
MIBer-A3	Michigan	Berrien	2012	3.68	1.21	0.61	0.56	0.58
MIBer-A5	Michigan	Berrien	2012	NA [f]	NA	0.61	0.51	0.43
MIBer-A6	Michigan	Berrien	2012	3.80	0.81	0.79	0.71	0.52
MIBer-B1	Michigan	Berrien	2012	3.10	1.10	0.62	0.69	0.55
MIBer-B2	Michigan	Berrien	2012	NA [e]	NA	0.88	0.62	0.73
MIBer-B3	Michigan	Berrien	2012	3.83	0.58	0.55	0.45	0.29

Table S4-1 (cont'd)

MIBer-B4	Michigan	Berrien	2012	3.74	0.58	0.50	0.40	0.26
MIBer-B5	Michigan	Berrien	2012	1.75	0.27	0.44	0.41	0.44
MIBer-D1	Michigan	Berrien	2012	NA [f]	NA	NA [c]	0.43	NA [c]
MIBer-E4	Michigan	Berrien	2012	7.70	3.00	1.11	1.00	0.69
MIBer-E6	Michigan	Berrien	2012	3.46	0.62	0.49	0.43	0.23
MIBer-F3	Michigan	Berrien	2012	3.75	0.55	0.57	0.52	0.30
MIBer-F4	Michigan	Berrien	2012	3.49	0.43	0.51	0.44	0.37
MIBer-F6	Michigan	Berrien	2012	3.24	0.59	0.53	0.42	0.22
MIBer-F7	Michigan	Berrien	2012	4.55	1.30	0.56	0.48	0.42
MIBer-out	Michigan	Berrien	2012	NA [e]	NA	1.26	1.19	0.88
MIIN-B7	Michigan	Ingham	2012	2.18	0.20	0.38	0.32	0.20
MISA-A1	Michigan	Saginaw	2012	4.46	1.12	0.64	0.58	0.36
MISA-A3	Michigan	Saginaw	2012	2.96	0.60	0.53	0.49	0.47
MISA-B6	Michigan	Saginaw	2012	3.66	1.63	0.51	0.46	0.33
MISTJ-A1	Michigan	St. Joseph	2012	3.83	0.73	0.55	0.43	0.26
MISTJ-A2	Michigan	St. Joseph	2012	3.55	0.56	0.48	0.39	0.28
MISTJ-A3	Michigan	St. Joseph	2012	2.88	0.38	0.47	0.43	0.30
MISTJ-C6	Michigan	St. Joseph	2012	2.99	0.47	0.49	0.39	0.29
MISTJ-C7	Michigan	St. Joseph	2012	2.71	0.35	0.49	0.47	0.41
MISTJ-D5	Michigan	St. Joseph	2012	7.00	1.97	0.64	0.49	0.27
MISTJ-D6	Michigan	St. Joseph	2012	9.28	2.16	0.38	0.33	0.08
MISTJ-E4	Michigan	St. Joseph	2012	3.15	0.85	0.59	0.54	0.42
MISTJ-E4a	Michigan	St. Joseph	2012	2.27	0.33	0.42	0.39	0.28
MISTJ-F6	Michigan	St. Joseph	2012	4.50	1.06	0.75	0.67	0.43
MITU-A1	Michigan	Tuscola	2012	2.72	0.52	0.47	0.40	0.33
MITU-A2	Michigan	Tuscola	2012	3.69	1.06	0.57	0.52	0.49
MITU-A3	Michigan	Tuscola	2012	2.92	0.41	0.42	0.33	0.21
MITU-A4	Michigan	Tuscola	2012	3.46	0.52	0.49	0.40	0.27
MITU-A5	Michigan	Tuscola	2012	3.41	0.42	0.49	0.42	0.27
MITU-B1	Michigan	Tuscola	2012	4.01	1.46	0.54	0.49	0.32
MITU-C1	Michigan	Tuscola	2012	NA [e]	NA	0.93	0.77	0.59
MITU-C2	Michigan	Tuscola	2012	2.36	0.26	0.45	0.39	0.32
MITU-C3-b	Michigan	Tuscola	2012	5.15	0.86	0.69	0.49	0.35
MITU-C3a	Michigan	Tuscola	2012	3.33	0.91	0.61	0.53	0.41
MIVB-A1	Michigan	Van Buren	2012	3.20	0.37	0.48	0.43	0.25
MIVB-A5	Michigan	Van Buren	2012	2.50	0.28	0.51	0.35	0.25
MIVB-A6	Michigan	Van Buren	2012	4.61	1.58	0.79	0.68	0.47
MIVB-A7	Michigan	Van Buren	2012	3.66	0.41	0.54	0.45	0.29
MIVB-B3	Michigan	Van Buren	2012	2.50	0.39	0.35	0.30	0.19
MIVB-B4	Michigan	Van Buren	2012	2.12	0.613	NA [c]	0.29	NA [c]

Table S4-1 (cont'd)

MIVB-B5	Michigan	Van Buren	2012	NA [e]	NA	0.73	0.71	0.62
MIVB-C1	Michigan	Van Buren	2012	3.79	0.50	0.53	0.43	0.29
MIVB-D5	Michigan	Van Buren	2012	2.05	0.38	0.35	0.32	0.24
MIVB-G7	Michigan	Van Buren	2012	NA [e]	NA	1.26	1.07	0.66
Mo1a	Michigan	Monroe	2009	3.37	0.49	0.46	0.38	0.28
Mo1a-2	Michigan	Monroe	2009	3.71	0.50	0.56	0.51	0.30
Mo1b	Michigan	Monroe	2009	4.33	0.57	0.72	0.54	0.40
Mo2a	Michigan	Monroe	2009	2.43	0.29	0.42	0.34	0.25
Mo3a	Michigan	Monroe	2009	4.38	0.92	0.69	0.59	0.38
Mo4a	Michigan	Monroe	2009	2.91	0.74	0.45	0.38	0.22
Mo4c-2	Michigan	Monroe	2009	3.19	0.47	0.43	0.38	0.26
Mo5a	Michigan	Monroe	2009	2.68	0.37	0.47	0.36	0.23
Mont1	Illinois	Piatt	1991	6.92	1.70	0.77	0.75	0.43
SA-11-2b	Michigan	Saginaw	2011	3.05	0.37	0.68	0.63	0.47
ST-11-1	Michigan	St. Clair	2011	2.54	0.27	0.41	0.37	0.24
STJ-7P2ss	Michigan	St. Joseph	2009	3.59	1.18	0.54	0.47	0.33
STJ3a	Michigan	St. Joseph	2009	3.55	1.00	0.48	0.44	0.30
STJ3b	Michigan	St. Joseph	2009	1.53	0.11	0.38	0.33	0.30
VB1	Michigan	Van Buren	2009	2.98	0.40	0.42	0.38	0.26

[a]: standard error

[b]: relative germination ratio at these concentrations to the 0 μg/ml control

[c]: missing data at these concentrations

[d]: failed at image analysis step possibly due to heavy pigment in the media

[e]: EC_{50} cannot be calculated due to no absolute EC_{50}

[f]: EC_{50} cannot be calculated due to failed at non-linear regression parameter estimation.

Table S 4-2 EC_{50} estimations for isolates that were tested in the conidia germination inhibition assay.

Strain	State	County	Year	EC50	StdErr [a]	Relative growth ratio [c]		
						5ppm	10ppm	20ppm
10Fv680	Illinois	Piatt	2010	2.49	0.49	0.27	0.09	0.01
13C13#1	Unknown	Unknown	2013	1.57	0.14	0.13	0.00	0.00
13C1N	Unknown	Unknown	2013	2.38	0.16	0.20	0.02	0.00
13Clark3#1	Unknown	Unknown	2013	1.30	0.08	0.17	0.06	0.01
13Clinton-N	Iowa	Clinton	2013	2.18	0.20	0.21	0.04	0.00
13Fv163	Illinois	Jackson	2013	1.86	0.18	0.21	0.09	0.02
13Fv165	Illinois	White	2013	2.17	0.16	0.20	0.05	0.00
13Fv167	Illinois	Jasper	2013	3.37	0.62	0.42	0.19	NA
13Fv169	Illinois	Johnson	2013	1.69	0.21	0.28	0.13	NA
13Fv171	Illinois	Union	2013	1.74	0.50	0.36	0.24	0.10
13Fv173	Illinois	Alexander	2013	2.13	0.34	0.38	0.16	NA
13Fv176	Illinois	Saline	2013	2.30	0.34	0.23	0.06	0.09
13Fv179	Illinois	Massac	2013	2.66	0.80	0.26	0.08	0.04
13Fv180	Illinois	Massac	2013	0.81	0.11	0.28	0.10	NA
13Fv182	Illinois	Pope	2013	2.59	0.24	0.26	0.08	0.02
13Fv185	Illinois	Edwards	2013	2.28	0.32	0.25	0.07	0.02
13Fv186	Illinois	Pulaski	2013	1.57	0.15	0.18	0.07	0.00
13Fv188	Illinois	Pulaski	2013	5.58	1.40	0.41	0.15	0.03
13Fv190	Unknown	Unknown	Unknown [b]	NA [d]	NA	0.96	1.00	0.98
13Fv193	Illinois	Livingston	2013	2.57	0.75	0.33	0.08	0.01
13Fv195	Illinois	Grundy	2013	2.44	0.27	0.26	0.12	0.00
13Fv196	Illinois	DeKalb	2013	2.38	0.45	0.30	0.07	0.00
13Fv199	Illinois	Jersey	2013	0.84	0.05	0.00	0.00	0.00
13Fv201	Illinois	Champaign	2013	2.09	0.14	0.20	0.09	0.03
13Fv202	Illinois	Perry	2013	2.25	0.23	0.23	0.06	0.01
13Fv204	Illinois	Monroe	2013	2.35	0.43	0.28	0.12	0.02
13FV206	Illinois	Livingston	2013	1.48	0.28	0.22	0.03	0.00
13Fv207	Illinois	Macoupin	2013	2.31	0.24	0.26	0.07	0.01
13Fv209	Illinois	Warren	2013	4.57	1.38	0.37	0.10	0.02
13Pike1	Unknown	Unknown	2013	1.84	0.15	0.21	0.05	0.00
14Fv1	Illinois	Clinton	2014	2.26	0.15	0.32	0.17	0.02
14Fv12	Illinois	Adams	2014	1.25	0.08	0.10	0.05	0.01
14Fv14	Illinois	McDonough	2014	1.14	0.08	0.08	0.04	0.00
14Fv15	Illinois	Brown	2014	1.16	0.07	0.10	0.02	0.00
14Fv16	Illinois	Brown	2014	2.16	0.12	0.21	0.08	0.00
14Fv17	Illinois	Hancock	2014		0.26	0.18	0.03	0.02

Table S4-2 (cont'd)

14Fv19	Illinois	Henderson	2014	2.30	0.36	0.21	0.04	0.00
14Fv21	Illinois	Pike	2014	1.91	0.41	0.21	0.09	0.02
14Fv22	Illinois	Pike	2014	2.49	0.48	0.28	0.06	0.01
14Fv24	Illinois	Fulton	2014	2.16	0.18	0.20	0.08	0.02
14Fv26	Illinois	Logan	2014	1.41	0.14	0.14	0.07	0.01
14Fv28	Kentucky	Paducah	2014	2.54	0.61	0.23	0.06	0.01
14Fv29	Illinois	LaSalle	2014	1.61	0.20	0.19	0.05	0.01
14Fv3	Illinois	Schuyler	2014	1.84	0.28	0.20	0.12	0.04
14Fv30	Illinois	LaSalle	2014	1.77	0.22	0.24	0.11	0.01
14Fv31	Illinois	Williamson	2014	1.61	0.16	0.14	0.06	0.01
14Fv32	Illinois	Williamson	2014	1.51	0.24	0.19	0.04	0.00
14Fv34	Illinois	Kendall	2014	1.53	0.29	0.22	0.07	0.01
14Fv36	Illinois	Kane	2014	1.67	0.36	0.33	0.09	0.05
14Fv37	Illinois	Lee	2014	4.19	0.54	0.39	0.12	0.02
14Fv6	Illinois	Calhoun	2014	1.62	0.16	0.19	0.05	0.01
14Fv7	Illinois	McLean	2014	1.21	0.09	0.12	0.03	0.00
14Fv9	Illinois	Mason	2014	1.71	0.26	0.17	0.04	0.01
AL1b	Michigan	Allegan	2009	2.28	0.36	0.26	0.08	0.01
AR171	Arkansas	Unknown	Unknown [b]	2.94	0.56	0.40	0.09	0.03
ARLE-C2	Arkansas	Lee	2012	2.41	0.31	0.26	0.07	0.00
Ca1a	Michigan	Cass	2009	4.08	1.12	0.38	0.06	0.01
FAV13	Unknown	Unknown	2013	2.31	0.27	0.22	0.00	0.00
FAYSDS13	Unknown	Unknown	2013	1.24	0.18	0.18	0.04	0.02
FV-LS1-ss1	Minnesota	Unknown	Unknown [b]	3.42	0.77	0.37	0.15	0.04
HU-11-1	Michigan	Huron	2011	1.93	0.16	0.20	0.08	0.00
KSSH-A7	Kansas	Shawnee	2012	3.31	0.71	0.34	0.08	0.01
LE-11-1	Michigan	Lenawee	2011	3.97	1.16	0.39	0.14	0.04
LL0023	Iowa	Unknown	Unknown [b]	2.26	0.34	0.25	0.06	0.01
LL0036	Iowa	Unknown	Unknown [b]	2.49	0.44	0.30	0.09	0.02
LL0039	Iowa	Unknown	Unknown [b]	3.41	0.32	0.35	0.09	0.02
LL0059	Iowa	Unknown	Unknown [b]	4.07	1.03	0.37	0.15	0.01
LL0094	Iowa	Unknown	Unknown [b]	3.49	1.26	0.32	0.10	0.01
MIBer-A5	Michigan	Berrien	2012	2.24	0.41	0.26	0.10	0.01
MIBer-A6	Michigan	Berrien	2012	3.35	0.72	0.30	0.11	0.02
MIBer-F7	Michigan	Berrien	2012	1.34	0.06	0.03	0.00	0.00
Mo1b	Michigan	Monroe	2009	2.35	0.22	0.22	0.05	0.00
Mont-1	Illinois	Piatt	1991	2.02	0.09	0.17	0.03	0.00
VB-2a	Michigan	Van Buren	2009	2.24	0.31	0.27	0.06	0.01
VB1	Michigan	Van Buren	2009	2.81	0.67	0.35	0.12	0.01

Table S4-2 (cont'd)

[a]: indicates standard error

[b]: indicates isolates with unknown year of isolation record

[c]: relative germination ratio at these concentrations to the 0 μg/ml control

[d]: EC_{50} cannot be calculated either due to no absolute EC_{50} or failed at non-linear regression parameter estimation

APPENDIX B Supplementary figures

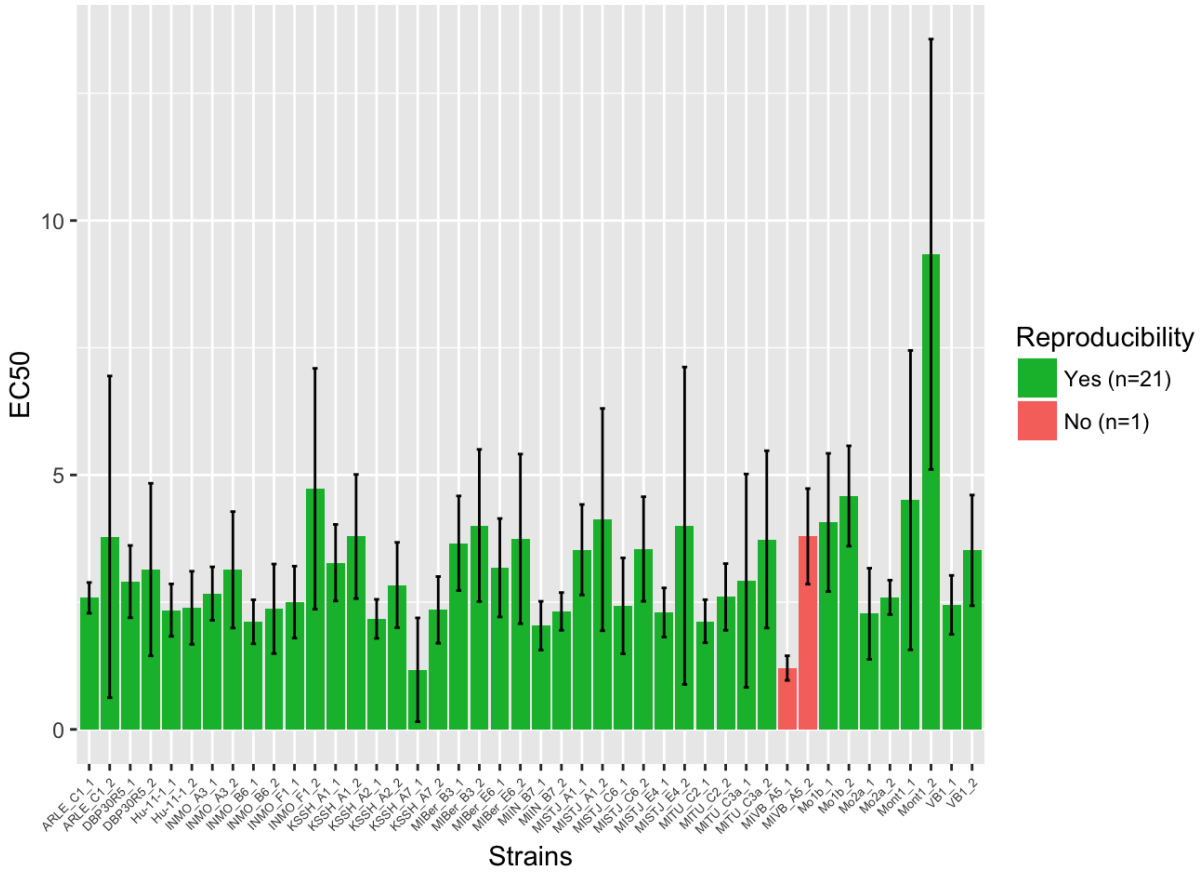

Figure S 4-1 The reproducibility of EC_{50} estimation using mycelial growth inhibition assay. Twenty-two isolates were randomly selected from 11 sets of isolates to evaluate the assay reproducibility between batches. The bar filled with green color indicated a good reproducibility isolates, while the bar filled with red color indicated a poor reproducibility of the isolate. The error bars indicated the 95% confidence interval for the mean EC_{50} estimation.

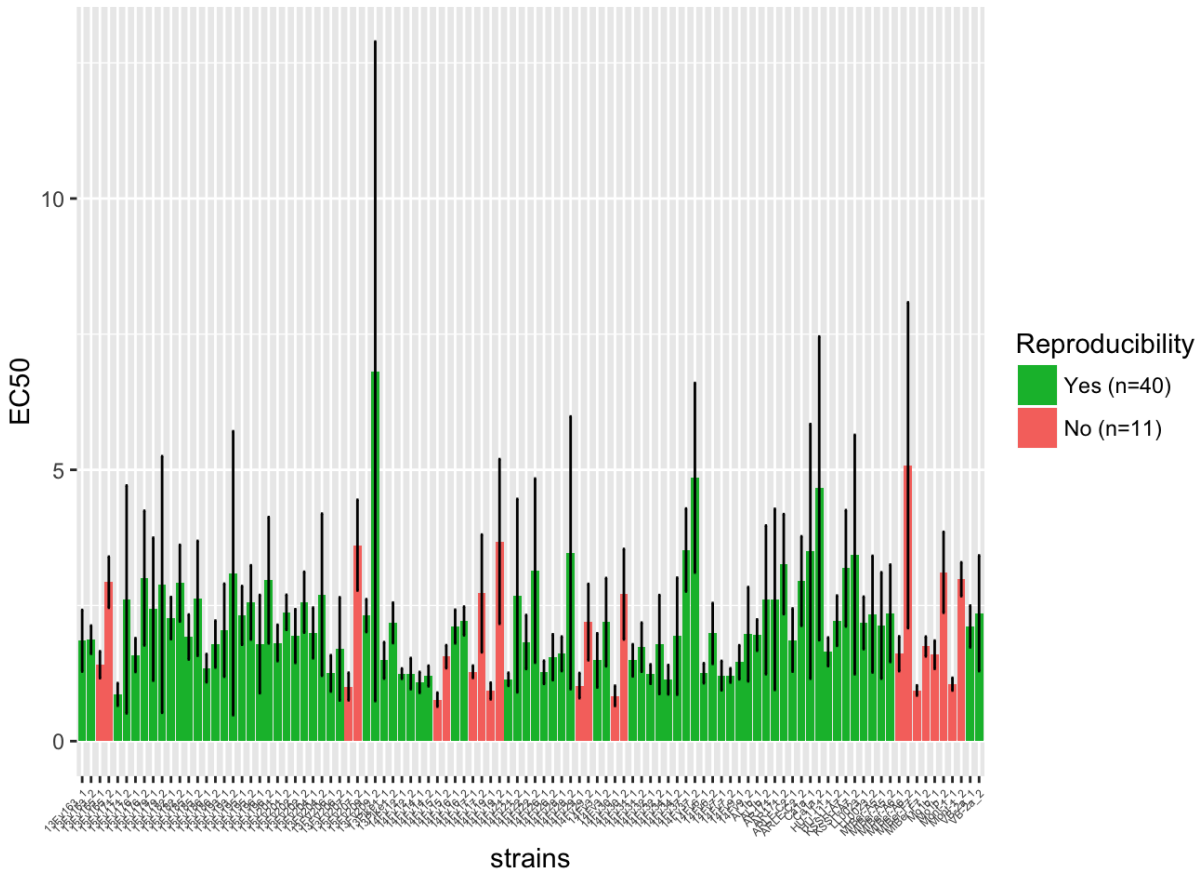

Figure S 4-2 The reproducibility of EC_{50} estimation using conidia germination inhibition assay. Fifty-one isolates were replicated to evaluate reproducibility of this assay. The bar filled with green color indicated a good reproducibility isolates, while the bar filled with red color indicated a poor reproducibility of the isolate. The error bars indicated the 95% confidence interval for the mean EC_{50} estimation.

REFERENCES

REFERENCES

Amiri, A., Heath, S. M., and Peres, N. A. 2014. Resistance to fluopyram, fluxapyroxad, and penthiopyrad in *Botrytis cinerea* from strawberry. Plant Dis 98:532-539.

Aoki, T., O'Donnell, K., and Scandiani, M. M. 2005. Sudden death syndrome of soybean in South America is caused by four species of *Fusarium*: *Fusarium brasiliense* sp. nov., *F. cuneirostrum* sp. nov., *F. tucumaniae*, and *F. virguliforme*. Mycoscience 46:162-183.

Aoki, T., Scandiani, M. M., and O'Donnell, K. 2012a. Phenotypic, molecular phylogenetic, and pathogenetic characterization of *Fusarium crassistipitatum* sp. nov., a novel soybean sudden death syndrome pathogen from Argentina and Brazil. Mycoscience 53:167-186.

Aoki, T., Tanaka, F., Suga, H., Hyakumachi, M., Scandiani, M. M., and O'Donnell, K. 2012b. *Fusarium azukicola* sp nov., an exotic azuki bean root-rot pathogen in Hokkaido, Japan. Mycologia 104:1068-1084.

Avenot, H., Morgan, D. P., and Michailides, T. J. 2008. Resistance to pyraclostrobin, boscalid and multiple resistance to Pristine (R) (pyraclostrobin plus boscalid) fungicide in *Alternaria alternata* causing alternaria late blight of pistachios in California. Plant Pathol 57:135-140.

Avenot, H. F., and Michailides, T. J. 2010. Progress in understanding molecular mechanisms and evolution of resistance to succinate dehydrogenase inhibiting (SDHI) fungicides in phytopathogenic fungi. Crop Protection 29:643-651.

Bradley, C. A., and Pedersen, D. K. 2011. Baseline sensitivity of *Cercospora zeae-maydis* to quinone outside inhibitor fungicides. Plant Dis 95:189-194.

Broomfield, P. L. E., and Hargreaves, J. 1992. A single amino-acid change in the iron-sulphur protein subunit of succinate dehydrogenase confers resistance to carboxin in *Ustilago maydis*. Curr. Genet. 22:117-121.

Cedergreen, N., Ritz, C., and Streibig, J. C. 2005. Improved empirical models describing hormesis. Environ. Toxicol. Chem. 24:3166-3172.

Chiocchio, V., Venedikian, N., Martinez, E. A., Menendez, A., Ocampo, A. J., and Godeas, A. 2000. Effect of the fungicide benomyl on spore germination and hyphal length of the arbuscular mycorrhizal fungus *Glomus mosseae*. Int. Microbiol. 3:173.

Cochrane, V. W., and Cochrane, J. C. 1966. Spore germination and carbon metabolism in *Fusarium solani* V. changes in anaerobic metabolism and related enzyme activities during development. Plant Physiol 41:810-814.

Fraaije, B. A., Bayon, C., Atkins, S., Cools, H. J., Lucas, J. A., and Fraaije, M. W. 2012. Risk assessment studies on succinate dehydrogenase inhibitors, the new weapons in the battle to control Septoria leaf blotch in wheat. Mol. Plant Pathol. 13:263-275.

FRAC. 2015. Fungicide Resistance Action Committee (FRAC) - Fungicides sorted by mode of action., Online publication.

Gao, X., Hartman, G., and Niblack, T. 2006. Early infection of soybean roots by *Fusarium solani* f. sp *glycines*. Phytopathology 96:S38-S38.

Garzon, C. D., Molineros, J. E., Yanez, J. M., Flores, F. J., Jimenez-Gasco, M. D., and Moorman, G. W. 2011. Sublethal doses of mefenoxam enhance *Pythium* damping-off of *Geranium*. Plant Dis 95:1233-1238.

Gougouli, M., and Koutsoumanis, K. P. 2013. Relation between germination and mycelium growth of individual fungal spores. Int J Food Microbiol 161:231-239.

Gunatilleke, I. A. U. N., Arst, H. N., and Scazzocchio, C. 1975. Three genes determine the carboxin sensitivity of mitochondrial succinate oxidation in *Aspergillus nidulans*. Genetics Research 26:297-305.

Hartman, G. L., Chang, H. X., and Leandro, L. F. 2015. Research advances and management of soybean sudden death syndrome. Crop Protection 73:60-66.

Ishii, H., Miyamoto, T., Ushio, S., and Kakishima, M. 2011. Lack of cross-resistance to a novel succinate dehydrogenase inhibitor, fluopyram, in highly boscalid-resistant isolates of *Corynespora cassiicola* and *Podosphaera xanthii*. Pest Manag Sci 67:474-482.

Kandel, Y. R., Wise, K. A., Bradley, C., Chilvers, M. I., Tenuta, A., and Mueller, D. S. 2016. Fungicide and cultivar effects on sudden death syndrome and yield of soybean. Plant Dis *In press*.

Kolander, T. M., Bienapfl, J. C., Kurle, J. E., and Malvick, D. K. 2012. Symptomatic and asymptomatic host range of *Fusarium virguliforme*, the causal agent of soybean sudden death syndrome. Plant Dis 96:1148-1153.

Kuhn, P. 1984. Mode of action of carboxamides. in: Symposium series-British Mycological Society.

Lendenmann, M. H., Croll, D., and McDonald, B. A. 2015. QTL mapping of fungicide sensitivity reveals novel genes and pleiotropy with melanization in the pathogen *Zymoseptoria tritici*. Fungal Genet. Biol. 80:53-67.

Liang, H. J., Di, Y. L., Li, J. L., You, H., and Zhu, F. X. 2015. Baseline sensitivity of pyraclostrobin and toxicity of SHAM to *Sclerotinia sclerotiorum*. Plant Dis 99:267-273.

Liu, H. X., Zhao, X. S., Guo, M. X., Liu, H., and Zheng, Z. M. 2015. Growth and metabolism of *Beauveria bassiana* spores and mycelia. BMC Microbiol. 15:267.

Mueller, D., Wise, K. A., Dufault, N. S., Bradley, C. A., and Chilvers, M. I. 2013. Fungicides for field crops. American Phytopathological Society.

Mueller, T. A., Knake, R. P., and Riggs, J. L. 2011. Control of *Fusarium virguliforme* (sudden death syndrome) with a seed treatment. Phytopathology 101:S124-S124.

Munkvold, G. P. 2009. Seed pathology progress in academia and industry. Annu. Rev. Phytopathol. 47:285-311.

Navi, S. S., and Yang, X. 2008. Foliar symptom expression in association with early infection and xylem colonization by *Fusarium virguliforme* (formerly *F. solani* f. sp. *glycines*), the causal agent of soybean sudden death syndrome. Plant Health Progress 10.

Navi, S. S., and Yang, X. 2016. Impact of Crop Residue and Corn-soybean Rotation on the Survival of *Fusarium virguliforme* a Causal Agent of Sudden Death Syndrome of Soybean. Journal of Plant Pathology & Microbiology 2016.

Njiti, V. N., Suttner, R. J., Gray, L. E., Gibson, P. T., and Lightfoot, D. A. 1997. Rate-reducing resistance to *Fusarium solani* f. sp. *phaseoli* underlies field resistance to soybean sudden death syndrome. Crop Science 37:132-138.

R Core Team. 2015. R: A language and environment for statistical computing. R Foundation for Statistical Computing, Vienna, Austria.

Ritz, C., and Streibig, J. C. 2005. Bioassay analysis using R. J Stat Softw 12:1-22.

Sarkar, D. 2008. Lattice: multivariate data visualization with R. Springer Science & Business Media.

Saville, A., Graham, K., Grunwald, N. J., Myers, K., Fry, W. E., and Ristaino, J. B. 2015. Fungicide sensitivity of us genotypes of *Phytophthora infestans* to six oomycete-targeted compounds. Plant Dis 99:659-666.

Taborda, C. P., da Silva, M. B., Nosanchuk, J. D., and Travassos, L. R. 2008. Melanin as a virulence factor of *Paracoccidioides brasiliensis* and other dimorphic pathogenic fungi: a minireview. Mycopathologia 165:331-339.

Vega, B., and Dewdney, M. M. 2015. Sensitivity of *Alternaria alternata* from citrus to boscalid and polymorphism in iron-sulfur and in anchored membrane subunits of succinate dehydrogenase. Plant Dis 99:231-239.

Vick, C. M., Chong, S. K., Bond, J. P., and Russin, J. S. 2003. Response of soybean sudden death syndrome to subsoil tillage. Plant Dis 87:629-632.

Wang, J., and Chilvers, M. I. 2016. Development and characterization of microsatellite markers for *Fusarium virguliforme* and their utility within clade 2 of the *Fusarium solani* species complex. Fungal Ecology 20:7-14.

Wang, J., Jacobs, J. L., and Chilvers, M. I. 2013. Temporal dynamics of soybean root colonization by *Fusarium virguliforme*. Phytopathology 103:S2.157.

Wang, J., Jacobs, J., and Chilvers, M. 2014. Management of soybean sudden death syndrome by seed treatment with fluopyram. Phytopathology 104 (Suppl.):127-127.

Wang, J., Jacobs, J. L., Byrne, J. M., and Chilvers, M. I. 2015. Improved diagnoses and quantification of *Fusarium virguliforme*, causal agent of soybean sudden death syndrome. Phytopathology 105:378-387.

Weems, J. D., Haudenshield, J. S., Bond, J. P., Hartman, G. L., Ames, K. A., and Bradley, C. A. 2015. Effect of fungicide seed treatments on *Fusarium virguliforme* infection of soybean and development of sudden death syndrome. Canadian Journal of Plant Pathology 37:435-447.

Wickham, H. 2009. ggplot2: elegant graphics for data analysis. Springer Science & Business Media.

CHAPTER 5 DEVELOPMENT AND CHARACTERIZATION OF MICROSATELLITE MARKERS FOR *FUSARIUM VIRGULIFORME* AND THEIR UTILITY WITHIN CLADE 2 OF THE *FUSARIUM SOLANI* SPECIES COMPLEX

This chapter was originally published in *Fungal Ecology*.

Wang, J. and Chilvers, M.I., 2016. Development and characterization of microsatellite markers for *Fusarium virguliforme* and their utility within clade 2 of the *Fusarium solani* species complex *Fungal Ecology*, 20:7-14.

Abstract

Clade 2 of the *Fusarium solani* species complex contains plant pathogens including *F. virguliforme* and closely related species *F. brasiliense*, *F. crassistipitatum*, *F. tucumaniae*, which are the primary causal agents of soybean sudden death syndrome (SDS), a significant threat to soybean production. In this study, we developed microsatellite markers from a *F. virguliforme* genome sequence and applied them to a *F. virguliforme* population collection of 38 isolates from Michigan and four reference strains from other locations. Of the 225 detected microsatellite loci, 108 loci were suitable for primer design, and 12 of the microsatellite markers were determined to be highly polymorphic, amplifying on average 5.7 alleles per locus. Using these markers, *F. virguliforme* isolates were partitioned into three distinct clusters, but isolates were not grouped based on relatedness of sampling sites. In addition, 11 out of 12 markers were demonstrated to be highly transferrable to other closely related species.

Keywords: *Fusarium virguliforme*, marker development, microsatellite, simple sequence repeat (SSR), soybean sudden death syndrome

Introduction

Fusarium species are ascomyceteus filamentous fungi (Class: Sordariomycetes Order: Hypocreales Family: Nectriaceae), including animal and plant pathogens, toxin producers, and debris decomposers. The *F. solani* species complex is one of four major plant pathogenic clades within the genus (Aoki *et al.* 2014). The *Fusarium solani* species complex contains more than 50 phylogenetic species, which comprises three major clades (O'Donnell 2000; Zhang *et al.* 2006). Clade-2 of the *Fusarium solani* species complex contains species that cause soybean (*Glycine max*) sudden death syndrome (SDS) and dry bean (*Phaseolus vulgaris*) root rot (BRR) (O'Donnell *et al.* 2010). In South America, *F. brasiliense*, *F. crassistipitatum*, *F. tucumaniae*, and *F. virguliforme* have been reported to cause soybean sudden death syndrome, while in North America *F. virguliforme* has been reported as the predominant soybean SDS pathogen (Aoki *et al.* 2005; Aoki *et al.* 2012a). In addition to these soybean SDS causing *Fusarium* species, fusaria closely related to the SDS pathogens, *F. azukicola*, *F. phaseoli*, and *F. cuneirostrum*, can cause BRR (Aoki *et al.* 2012a; Aoki *et al.* 2012b).

Symptoms of soybean SDS include interveinal chlorosis and necrosis, premature defoliation, and root rot (Roy *et al.* 1997), which has resulted in considerable yield loss in the U.S. (Wrather & Koenning 2006). Soybean SDS was first observed in Arkansas in 1971, and by the mid-1990s was reported in most U.S. soybean producing states (Roy *et al.* 1997; Chilvers & Brown-Rytlewski 2010; Tande *et al.* 2014; Hartman *et al.* 2015). Recently, *F. virguliforme* was reported from plant and soil samples in South Africa (Tewoldemedhin *et al.* 2013) and Malaysia (Chehri *et al.* 2014), respectively. At this point, very little is known regarding the origin or population structure of *F. virguliforme* or other soybean SDS or BRR causing species.

Various molecular genetic markers have been used in attempt to resolve the genetic diversity of *F. virguliforme*. Sequences of genetic loci, such as the ribosomal DNA internal transcribed

spacer and intergenic spacer, and translation elongation factor 1 alpha, commonly used for resolving phylogenies of fungal species were determined to be identical among *F. virguliforme* isolates (Achenbach *et al.* 1997; Aoki *et al.* 2003; Aoki *et al.* 2005; Malvick & Bussey 2008). Furthermore, multilocus sequence typing studies with five anonymous genetic loci showed that *F. virguliforme* isolates were genetically identical (O'Donnell *et al.* 2010; Aoki *et al.* 2012a). However, differences in aggressiveness of *F. virguliforme* isolates have been observed (Li S. *et al.* 2009), which alluded to possible genetic diversity among *F. virguliforme* isolates. In addition, using RAPD markers and a microsatellite probe, Mbofung et al. (2012) detected 25 genotypes with 72 isolates of *F. virguliforme*. Unfortunately, there are many technical and analytical limitations associated with RAPD markers, especially the poor reproducibility of markers within and between labs (Penner *et al.* 1993; McDonald 1997). Therefore, genetic markers with better reproducibility and precision are needed to improve genotyping of *F. virguliforme*.

Microsatellites have been widely used in genetic mapping, fingerprinting, and population spatiotemporal structure analyses (Yang *et al.* 2001; Varshney *et al.* 2005; Goss *et al.* 2014). High mutation rates and wide distribution in the eukaryotic genome make microsatellites a valuable genetic marker for multilocus genotyping studies (Ellegren 2004). Although the geographical distribution of *F. virguliforme* has been well documented (Hartman *et al.* 2015), there is a distinct lack of knowledge regarding the origin or genetic diversity of *F. virguliforme*. A molecular genetic tool that can effectively and accurately genotype isolates of *F. virguliforme* will greatly aid in the understanding of the ecology, epidemiology and evolution of this pathogen. In Michigan, soybean SDS has become a significant issue for soybean production. In 2009, *F. virguliforme* was documented in six Michigan counties, and has since been confirmed in a total of 22. Given this background, the primary objectives of this study were to i) develop

and characterize microsatellite markers for *F. virguliforme*; ii) determine the genetic diversity of *F. virguliforme* isolated in Michigan; and iii) test the transferability of the microsatellite markers to closely related *Fusarium* species.

Materials and methods

Fungal material and DNA extraction

A total of 42 *F. virguliforme* isolates were included in this study. Among them, 38 isolates were collected from 12 counties in Michigan, and four *F. virguliforme* isolates were obtained from the USDA ARS culture collection, including isolates from Illinois, Indiana and Argentina. Nine isolates collected from Michigan were originally recovered from dry bean (*Phaseolus vulgaris*), and the remaining 29 isolates were collected from soybean (*Glycine max*). In addition, 13 isolates of closely related *Fusarium* species were obtained from the USDA ARS culture collection (Table 5-1). For the Michigan isolates, *F. virguliforme* was recovered from roots of SDS symptomatic soybean plants. Briefly, taproots were split vertically into three pieces and then cut into pieces of 3-4 cm in length. Taproot pieces were surface disinfested with 0.5% sodium hypochlorite for 3 min, rinsed in sterile water for 1 min, and padded dry on sterilized paper towel. Three to four pieces of root tissue were placed on 2% water agar media amended with 300 mg/L of streptomycin and 15 mg/L of metalaxyl in Petri plates to induce formation of *F. virguliforme* sporodochia. Isolation plates were incubated at room temperature in the dark for 7-10 d until white to bluish sporodochia were visible on the root surface. Masses of spores were taken from the sporodochia and spread with a bacterial culturing loop on 3% water agar for monoconidial isolate purification. After overnight incubation germinated single conidia were transferred onto potato dextrose agar (PDA) medium for morphological identification. Putative *F. virguliforme* isolates were cultured on PDA for 14 d at room temperature. A one centimeter

square area from a sporulating part of the colony was cut into small pieces (3 mm^3 cubes) and placed into 2-mL cryogenic vials containing 1 mL of 15% glycerol solution for long-term storage at -80ºC. For DNA extraction, five to six pieces of PDA from the leading edge of a *F. virguliforme* colony were transferred to potato dextrose broth, and still cultured for 7 d at room temperature. Mycelial mats were collected from the surface of the potato dextrose broth, frozen and lyophilized overnight in a 2-mL centrifuge tube. DNA was extracted from 20 mg of freeze-dried mycelia using the Plant DNeasy kit (QIAGEN, Germantown, MD). DNA was eluted from the binding matrix column with 100 µL of AE buffer (QIAGEN), and 1:10 dilutions were used for PCR. A *F. virguliforme* species-specific PCR assay (Wang *et al.* 2015) was used to confirm *F. virguliforme* species identity before microsatellite fragment analysis. The assay was performed in a total volume of 25 µL, which included 2.5 µl of 10× DreamTaq DNA buffer (Thermo Fisher Scientific, Waltham, MA), 0.2 µl of 25 µM dNTPs (Promega Corp., Madison, WI), 1 µl of 10 µM primers (Sigma-Aldrich, St. Louis), 0.2 µl (5 U/µl) of DreamTaq DNA polymerase (Thermo Fisher Scientific), 0.5 µl of BSA at 10 mg/ml, 2 µl of DNA template, and 17.6 µL distilled water. PCR cycling conditions were 1 cycle at 94°C for 3 min; followed by 35 cycles of 30 s at 94°C, 30 s at 65°C, and 30 s at 72°C; and a final extension for 5 min at 72°C. PCR products were separated and visualized on a 1.5% agarose gel at 85 V for 45 min and stained with ethidium bromide at 1 µg/ml. *Fusarium virguliforme* isolates were indicated by amplification of a 375 bp product. Mating types of *F. virguliforme* were also determined using mating type test PCR assays with two degenerate primer sets (fusALPHA and fusHMG), following parameters as described in Kerenyi *et al.* (2004).

Table 5-1 Details of the *Fusarium* species used in this study, including species name, isolate code, year of collection, geographic origin and host.

Species	MLG[a]	Isolate code[b]	Year	Origin	Host/source
Fusarium virguliforme	23	DB_P27R11	2012	Van Buren Co. Michigan, USA	*Phaseolus vulgaris*
F. virguliforme	23	DB_P27R13	2012	Van Buren Co. Michigan, USA	*P. vulgaris*
F. virguliforme	21	DB_P28R13	2012	Van Buren Co. Michigan USA	*P. vulgaris*
F. virguliforme	23	DB_P29R9	2012	Van Buren Co. Michigan USA	*P. vulgaris*
F. virguliforme	19	DB_P30_R3	2012	Van Buren Co. Michigan USA	*P. vulgaris*
F. virguliforme	30	DB_P30_R4	2012	Van Buren Co. Michigan USA	*P. vulgaris*
F. virguliforme	18	DB_P30_R5	2012	Van Buren Co. Michigan USA	*P. vulgaris*
F. virguliforme	24	DB_P30_R6	2012	Van Buren Co. Michigan USA	*P. vulgaris*
F. virguliforme	20	DB_P30R7	2012	Van Buren Co. Michigan USA	*P. vulgaris*
F. virguliforme	23	AL1a[#]	2009	Allegan Co. Michigan USA	*Glycine max*
F. virguliforme	23	AL1b[#]	2009	Allegan Co. Michigan USA	*G. max*
F. virguliforme	22	Ber1-5[#]	2009	Berrien Co. Michigan USA	*G. max*
F. virguliforme	25	Ber1-9[#]	2009	Berrien Co. Michigan USA	*G. max*
F. virguliforme	17	Ca-1a[#]	2009	Cass Co. Michigan USA	*G. max*
F. virguliforme	10	Ca-2a[#]	2009	Cass Co. Michigan USA	*G. max*
F. virguliforme	8	Ca-2b	2009	Cass Co. Michigan USA	*G. max*
F. virguliforme	27	CL-11-1[#]	2011	Clinton Co. Michigan USA	*G. max*
F. virguliforme	25	Hu-11-1[#]	2011	Huron Co. Michigan USA	*G. max*
F. virguliforme	31	KA-11-1	2011	Kalamazoo Co. Michigan USA	*G. max*
F. virguliforme	2	LE-11-1[#]	2011	Lenawee Co. Michigan USA	*G. max*
F. virguliforme	6	Mo1a_2[#]	2009	Monroe Co. Michigan USA	*G. max*
F. virguliforme	29	Mo1a[#]	2009	Monroe Co. Michigan USA	*G. max*
F. virguliforme	13	Mo1b	2009	Monroe Co. Michigan USA	*G. max*
F. virguliforme	26	Mo2a[#]	2009	Monroe Co. Michigan USA	*G. max*
F. virguliforme	15	Mo3a[#]	2009	Monroe Co. Michigan USA	*G. max*
F. virguliforme	23	Mo4a[#]	2009	Monroe Co. Michigan USA	*G. max*
F. virguliforme	23	Mo4c_2	2009	Monroe Co. Michigan USA	*G. max*
F. virguliforme	21	Mo4c[#]	2009	Monroe Co. Michigan USA	*G. max*
F. virguliforme	12	Mo5a[#]	2009	Monroe Co. Michigan USA	*G. max*
F. virguliforme	23	SA-11-2b	2011	Saginaw Co. Michigan USA	*G. max*
F. virguliforme	26	ST-11-1[#]	2011	St. Joseph Co. Michigan USA	*G. max*
F. virguliforme	14	STJ1-7Ps[#]	2009	St. Joseph Co. Michigan USA	*G. max*
F. virguliforme	16	STJ3a[#]	2009	St. Joseph Co. Michigan USA	*G. max*
F. virguliforme	5	STJ3b[#]	2009	St. Joseph Co. Michigan USA	*G. max*
F. virguliforme	7	STJ-7P2ss	2009	St. Joseph Co. Michigan USA	*G. max*
F. virguliforme	28	VB1[#]	2009	VanBuren Co. Michigan USA	*G. max*
F. virguliforme	1	VB-2a[#]	2009	VanBuren Co. Michigan USA	*G. max*
F. virguliforme	23	MIIN-B7	2012	Ingham Co. Michigan USA	*G. max*
F. virguliforme	4	34551[*]	-	San Pedro Buenos Aires Argentina	*G. max*

Table 5-1 (cont'd)

F. virguliforme	9	31041*	1998	Illinois, USA	*G. max*
F. virguliforme	11	22823*	-	Indiana, USA	*G. max*
F. virguliforme	3	Mont1	1991	Monticello, Illinois, USA	*G. max*
F. azukicola	NA	54362*	1996	Obihiro, Hokkaido, Japan	*Vigna angularis*
F. brasiliense	NA	22678*	1993	California, USA	*G. max*
F. brasiliense	NA	22743*	1992	Brasilia, Distrito Federal, Brazil	*G. max*
F. brasiliense	NA	34938*	2003	Brazil, Rio Grande do Sul, Passo Fundo	*G. max*
F. crassistipitatum	NA	31949*	2000	Cristalina, Goiás, Brazil	*G. max*
F. cuneirostrum	NA	31157*	1992	Michigan, USA	*Phaseolus vulgaris*
Fusarium sp.	NA	22574*	-	Guatemala	*Coffea arabica*
Fusarium sp.	NA	22412*	-	French Guiana	bark
Fusarium sp.	NA	22387*	-	French Guiana	bark
F. phaseoli	NA	31156*	-	Michigan, USA	*Phaseolus vulgaris*
F. phaseoli	NA	22276*	-	USA	*Phaseolus vulgaris*
F. phaseoli	NA	22411*	-	California, USA	*Phaseolus vulgaris*
Fusarium sp.	NA	22395*	-	Venezuela	bark
F. tucumaniae	NA	31773*	2000	Ponta Grossa, PR, Brazil	*G. max*
F. tucumaniae	NA	31096*	2001	San Agustín, Tucumán, Argentina	*G. max*
F. tucumaniae	NA	34549*	2000	PérezMillán , Buenos Aires, Argentina	*G. max*

-: Unknown year of isolation

[a]: Multilocus genotype for *F. virguliforme* isolates

[b]: Lab strain code or NRRL (USDA ARS Northern Regional Research Laboratory) numbers

*: Indicates isolates obtained from NRRL

#: Indicates isolates used for the second round screening of polymorphic microsatellites

Development of microsatellite markers and primer design

A genome sequence of *F. virguliforme* strain Mont-1 was obtained from the *F. virguliforme* genome browser site (http://fvgbrowse.agron.iastate.edu/data/) (Srivastava *et al.* 2014). Microsatellite patterns were searched with the perfect microsatellite mode using SciRoKo v3.4 software (Kofler *et al.* 2007). The perfect microsatellite parameters chosen for identifying microsatellite loci were minimum counts of 14, 12, 7, 7, and 7 repeat units for the motifs di-, tri-, tetra-, penta-, and hexa- nucleotides, respectively. Primers were designed to the 200 bp flanking regions of each microsatellite locus using Primer3 software (Koressaar & Remm 2007) with the following parameters: 150-250 bp PCR amplicon size, 20 nt for optimal primer length, and 60ºC for optimal melting temperature. Since a physical genome map is not available for *F. virguliforme,* we estimated microsatellite distribution in the genome by utilizing the closely related species *Nectria haematococca* (also known as *F. solani* f. sp. *pisi*). By aligning flanking regions of the *F. virguliforme* microsatellite motifs with BLASTn (Zhang *et al.* 2000) against the physical map of *N. haematococca* (Figure 5-2) (Coleman *et al.* 2009).

Microsatellite marker screening for polymorphism

To screen for polymorphic microsatellite loci, 92 markers were initially screened against five geographically diverse *F. virguliforme* isolates (Table 5-1, VB-2a, NRRL22292, NRRL31041, NRRL22823, and NRRL34551). Priority marker screening was given to microsatellite markers with longer repeat units and to those located on different *F. virguliforme* genome scaffolds. A subsequent screen was conducted on an additional set of 22 isolates for 18 markers that consistently amplified at least two alleles. Primer sets of 12 selected polymorphic microsatellite loci were modified for fragment analysis. The 5' end of each forward primer was labeled with one of three fluorophores (6-FAM, HEX, or NED) for multiplexing (Applied Biosystems,

Carlsbad, CA). A PIG-tail sequence (GTTT-) was added to the 5' end of each reverse primer to reduce stutter bands in fragment analysis (Brownstein *et al.* 1996). PCR was performed in 25 µL volume reactions, which included 2.5 µL of 10X DreamTaq DNA buffer (Thermo Fisher Scientific, Waltham, MA), 0.2 µL of 25 µM dNTP (Promega, Madison, WI), 1 µL of 10 µM fluorophore labeled forward primer (Applied Biosystems), 1 µL of 10 µM reverse primer (Sigma-Aldrich, St. Louis, MO), 0.2 µL of (5U/µl) DreamTaq DNA polymerase (Thermo Fisher Scientific), 0.5 µL of 10 mg/mL BSA (NEB, Ipswich, MA), 2 µL DNA template (approximately 10 ng total DNA), and molecular grade water. PCR cycling conditions consisted of one cycle at 95ºC for 5 min, followed by 35 cycles at 95ºC for 30 s, 62ºC for 30 s, 72ºC for 25 s and a final extension at 72ºC for 7 min, performed in a Mastercycler nexus PCR thermal cycler (Eppendorf, Hamburg, Germany). Microsatellite alleles were resolved with an ABI 3730XL DNA analyzer (Applied Biosystems) using GENSCAN 400HD ROX size standard, by Macrogen Inc. Fragment analysis was performed twice across 42 isolates and 12 loci with two independent PCRs to determine the reproducibility of allele size calls. Sequence confirmation of microsatellite PCR amplicons was conducted by Sanger sequencing of products from isolate Mont-1 at Macrogen, Inc. USA. Transferability of microsatellite markers to closely related species was conducted using the same PCR conditions and fragment analysis procedures described above.

Data analysis

Allele size within microsatellites was scored using Peak Scanner v1.0 (Applied Biosystems). Allele binning was performed with TANDEM v1.09 by converting haploid data into pseudo-diploid data (Matschiner & Salzburger 2009). The R package 'poppr' (Kamvar *et al.* 2014) was employed to identify unique multi-locus genotypes (MLGs) based on microsatellite allele sizes by isolate and to calculate genetic diversity indices (e.g., Nei's unbiased genotypic diversity and

Shannon-Wiener genetic diversity) for the isolates collected in Michigan. Microsatellite loci summary statistics were calculated using 'locus_table' function within the 'poppr' package (Kamvar *et al.* 2014). In addition, a standardized index of association (Agapow & Burt 2001) was calculated for the isolates collected in Michigan with 1000 permutations using 'ia' function within the 'poppr' package (Kamvar *et al.* 2014). Pairwise genetic distance between isolates was calculated and plotted in a heat map along with a dendrogram based on Bruvo's genetic distance (Bruvo *et al.* 2004). Bootstrap branch support was calculated based on 1000 bootstrap samples; bootstrap branch support values greater than 60% were retained and labeled on the nodes. Population structure was also investigated using the Bayesian clustering software STRUCTURE v2.3 (Pritchard *et al.* 2000). The parameters for each run include 20,000 generations burn-in period and 100,000 iterations for data collection for each K (K = 1-10) replicated for five runs. The lambda was set to 1.0, and an admixture model was assumed. The optimal K was chosen by evaluating dealta K (Evanno *et al.* 2005) calculated with the web-based STRUCTURE-HARVESTER program (Earl & Vonholdt 2012). The five replicated runs of the optimal K were combined using CLUMPP v1.1.2 (Jakobsson & Rosenberg 2007) to generate a single output for direct graphic visualization using DISTRUCT v1.1 (Rosenberg 2004).

Results

Primer development and polymorphism screening

A total of 225 perfect microsatellite loci were identified using the draft genome of *F. virguliforme* (1,386 scaffolds, Ver. 1); microsatellite loci were distributed across 80 scaffolds. The density of microsatellites within the genome given our strict search parameter was 4.42 counts/Mbp. The tri-nucleotide repeat motif was predominant (54%), followed by di-nucleotide (22%) and tetra-nucleotide (13%) motifs. Among all of the microsatellite loci, AAT/ATT was the

most frequent repeat motif, with 96 counts out of 225 microsatellite loci. AC/GT and AG/CT were the two most frequent di-nucleotide repeat motifs with 26 and 21 counts, respectively (Figure 5-1). A total of 108 of the 225 identified microsatellite loci were selected for further evaluation based on primer design criteria.

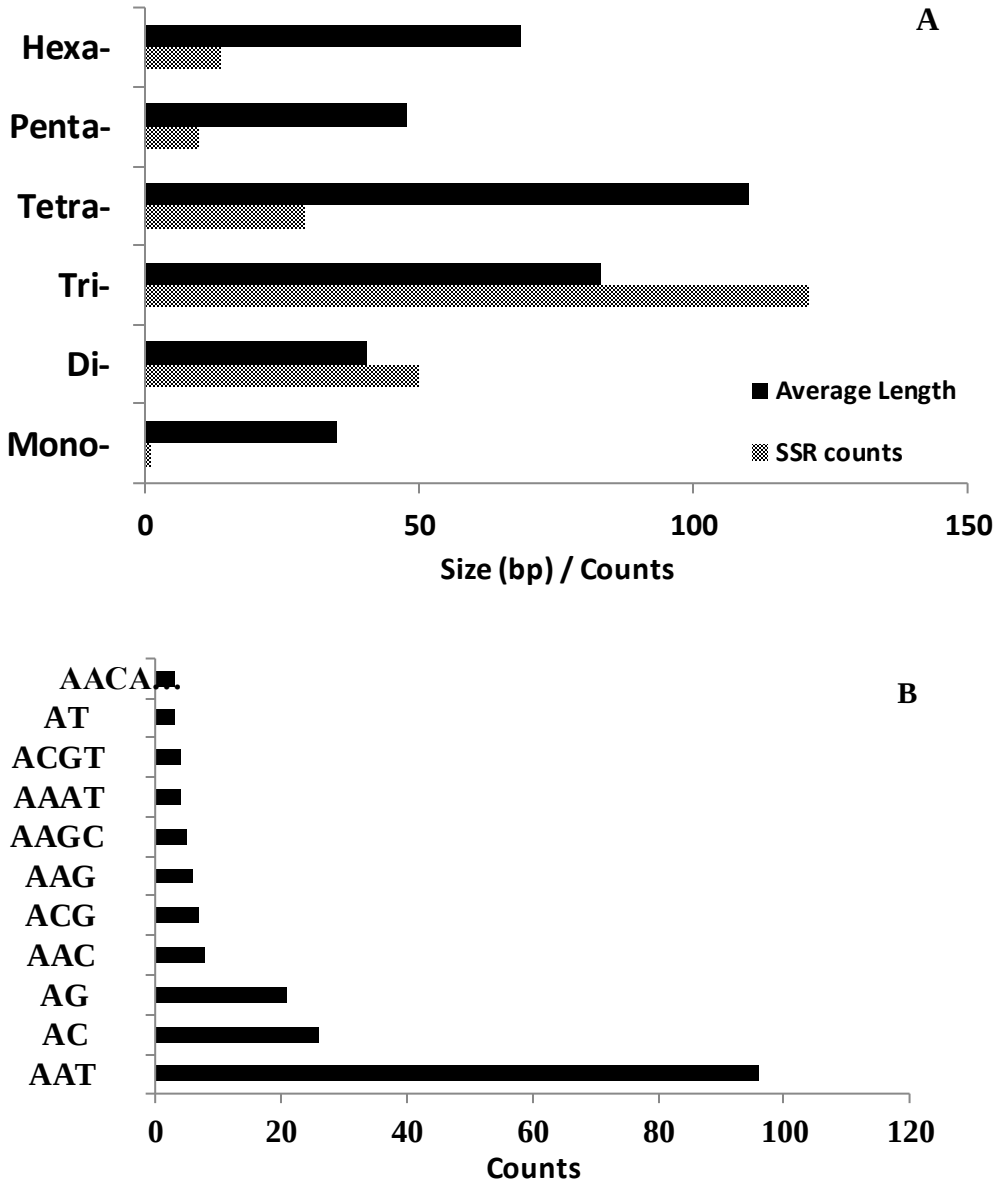

Figure 5-1 Frequencies of repeat motifs in the *F. virguliforme* genome. A, Frequency of di-, tri-, tetra-, penta- and hexa- repeat motifs, and their average length in *F. virguliforme* genome. B, Top ten most frequent repeat motifs in *F. virguliforme* genome

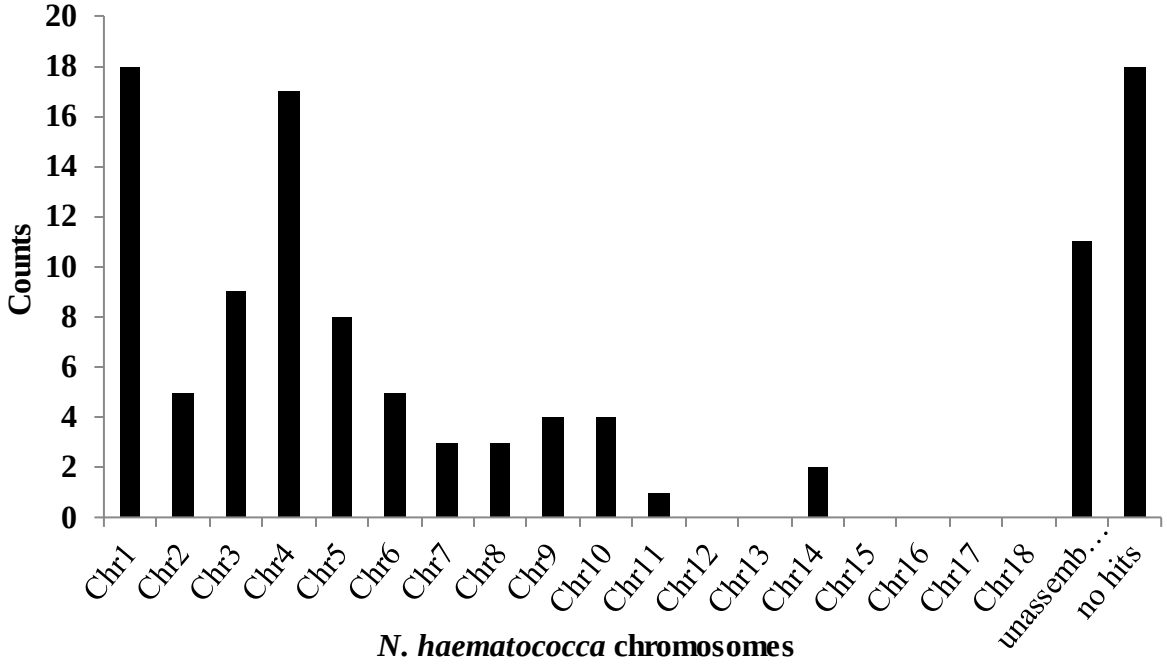

Figure 5-2 Distribution of 108 microsatellite loci in the *Nectria haematococca* genome by chromosome. Chr: Chromosome, unmapped: unassembled sequences, no hits: no matched sequence

Validation of microsatellite polymorphism

Out of 108 microsatellite primer sets identified, we screened 92 of which 80 successfully amplified expected PCR products. Eighteen of the 80 markers tested against the five geographically distant *F. virguliforme* isolates were polymorphic. Further screening of 18 microsatellites across an additional 22 Michigan *F. virguliforme* isolates confirmed 12 of the microsatellite loci to be highly polymorphic. The 12 selected microsatellite loci demonstrated to be highly reproducible with two independent PCR and fragment scoring runs against all 42 *F. virguliforme* isolates. Allele size score errors between two replicate fragments analyses were within ±1.5 bp, which is smaller than the unit size of a dimer repeat motif. Microsatellite allele sizes for 12 loci of all isolates were identical after allele binning. DNA sequences of the 12 highly polymorphic microsatellite loci matched the predicted sequence from the *F. virguliforme*

genome (Srivastava *et al.* 2014). Primer sets for microsatellite markers worked equally well for *F. virguliforme* isolates collected from soybean and dry bean.

Genome location of microsatellites

Ten of the twelve highly polymorphic *F. virguliforme* microsatellite loci mapped to six distinct chromosomes in the *N. haematococca* genome, while no match was found for two of the microsatellites Table 5-2). Of the 12 microsatellite markers, five markers were located within predicted exon regions of the *F. virguliforme* genome, three of them were located at predicted exon and an intron borders, and the remaining four markers were located in predicted intergenic regions (Table 5-2). Allele numbers were not significantly different between the loci residing in predicted coding or non-coding regions (P=0.79).

Table 5-2 *Fusarium virguliforme* microsatellite characteristics, including name, location within the *F. virguliforme* genome, repeat motif, forward and reverse primers, allele number, allele size range, gene location, reference genome location and primer pair combinations, note pigtails on the 5' end of the reverse primers.

ID [a]	Locus [b]	Repeat motif	Forward Primers	Reverse Primers	Allele No.	Allele Size range:	Gene diversity	PIC [c]	Location	Ref. genome [d]	Multiplex set [e]
43	Scaffold1_17	(AAG)13	FAM-GGGCCGTAAGTCGACAGTAA	GTTTATCTTTGGCTTCGCATCATT	5	113-224	0.60	0.58	Intergenic	Chr1	1
12	Scaffold9	(AC)37	HEX-CCTCCGTCATCAAAGATGGT	GTTTTTGCTCTGTGAACCTTGCC	7	173-225	0.35	0.34	Intergenic	Chr2	1
93	Scaffold4_9	(AAC)18	NED-GGGCGAGTCTTCTTCTCTCA	GTTTAAGGCGTTGGTAATGTGGAG	3	166-193	0.22	0.21	Exon	No hit	1
83	Scaffold14	(AACAGC)12	FAM-TACCTACGAGGCCCAGAGAA	GTTTGCCATGATTGCTGAAGTGTT	2	201-219	0.09	0.09	Exon/intron	Chr8	2
4	Scaffold1_22	(AC)22	HEX-TGTGTTGGAGCTGAGGACTG	GTTTTCGTTCGCTACTCCGACTTT	4	185-217	0.56	0.54	Intergenic	Chr1	2
15	Scaffold1_9	(ACG)26	NED-CTGTCGACCTCTCCACCATT	GTTTAAGGTGACGGTGAGGAGATG	7	151-214	0.64	0.62	Exon	Chr4	2
99	Scaffold937	(AAGAGG)18	FAM-CTACAACATACCGCTGCGTG	GTTTTCATCAACCTCCCACTTCCT	7	137-233	0.35	0.34	Exon/intron	No hit	3

Table 5-2 (cont'd)

48	Scaffold1_5	(AATGGC)8	HEX-TTGGCATTGTCCTTGTCATC	GTTTAAGCACTTGGCCGTATCCTA	7	218-290	0.71	0.69	Exon	Chr1	3
38	Scaffold1_7	(ACGGCC)8	NED-GAAATTGGGTTACCGAGCTG	GTTTGAGATCGACAGAGTGGAGGC	5	197-233	0.23	0.22	Exon	Chr1	3
80	Scaffold13_2	(AAC)15	FAM-TGCTGAGACCTTGATCCTCC	GTTTCAACTCGCACGCATCTACTC	7	145-229	0.31	0.30	Intergenic	Chr6	4
59	Scaffold5_3	(ACACAG)10	HEX-GGGATTCCTGTGCTTGTTGT	GTTTGTGCGTGAACGCAGAGATAA	6	155-251	0.53	0.51	Exon/intron	Chr3	4
10	Scaffold18_2	$(AAC)_{30}$	NED-CAGCTCCAGCTTCACCTTTC	GTTTGGACCCGTATGTCGAGTCTG	8	159-279	0.75	0.73	Exon	Chr2	4

[a]: Sequences of microsatellite loci were submitted to GenBank (**KR476359-KR476370**)
[b]: genetic locus of *F. virguliforme* draft genome
[c]: PIC is abbreviated for polymorphic information content
[d]: indicates *N. haematococca* genome
[e]: multiplex set pooled samples in fragment analysis

Genetic diversity and structure

The 12 highly polymorphic microsatellite markers amplified 2 to 8 alleles per locus, with an average allele number of 5.7 when screened against 42 *F. virguliforme* isolates. In total 31 MLGs were detected in the isolate set with 27 genotypes detected as singletons, and four genotypes detected with at least two isolates (Table 5-1). A genotype accumulation curve determined that 90% of the genotypes could be detected with nine or ten of the microsatellite markers (Figure 5-3). Genotype 23 (MLG-23) was the most frequently (9/42 = 21%) detected genotype associated with isolates collected from multiple sites and years. High genetic diversity was found in the isolates collected in Michigan, with a Shannon-Wiener genetic diversity index (which ranges from zero genetic diversity to a maximum of 3.64 for the 38 isolates) of 3.01, and unbiased genotypic diversity index (which ranges from zero genetic diversity to a maximum of one) of 0.95. Cluster analysis, based on Bruvo's genetic distance, revealed three clusters of *F. virguliforme* isolates. The largest cluster (cluster 2, Figure 5-4) was composed of 22 Michigan isolates, which include eight out of nine isolates collected from dry bean. No associations between geographic location and genetic cluster were found in the cluster analysis (Figure 5-4). For example, the isolate from Argentina (NRRL 34551) grouped in the same cluster as the Illinois strain Mont-1 and two Michigan strains (Figure 5-4). Although Bruvo's genetic distance lacked bootstrap support for a partition of three clusters, STRUCTURE analyses also supported three population clusters (K=3) based on the delta K method (Figure S5-1). All of the isolates from outside of Michigan were partitioned to two of the clusters, while isolates from Michigan were separated into all three clusters (Figure 5-4 and Figure S5-1). The index of association deviated significantly ($p<0.01$) from randomly permutated data with a standardized index of association $\bar{r}_d = 0.20$ indicating a lack of recombination, which was supported by the mating

type test, in which only one mating type (*MAT1-1*) was detected across all *F. virguliforme* isolates.

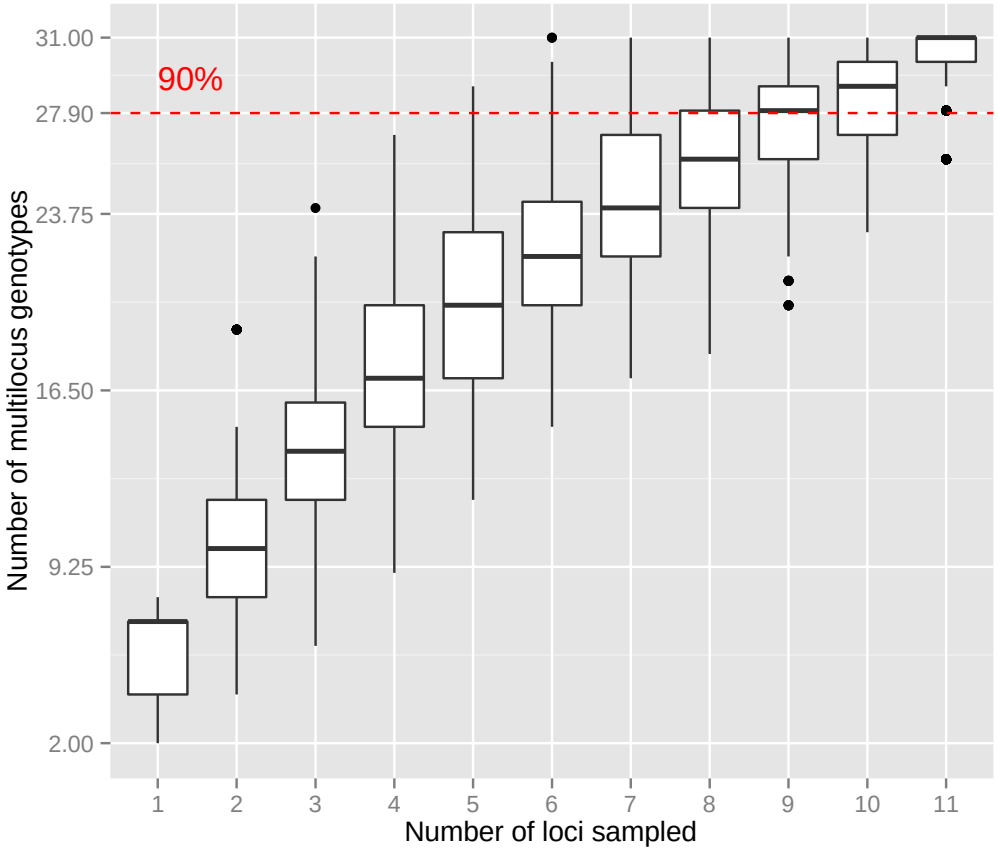

Figure 5-3 Genotype accumulation curve. Unique multilocus genotypes of *F. virguliforme* detected as the number of microsatellite loci sampled. When 9 or 10 microsatellite loci are used in genotyping, 90% of the unique multilocus genotypes can be detected. The 90% unique multilocus genotype level is indicated with dotted red line.

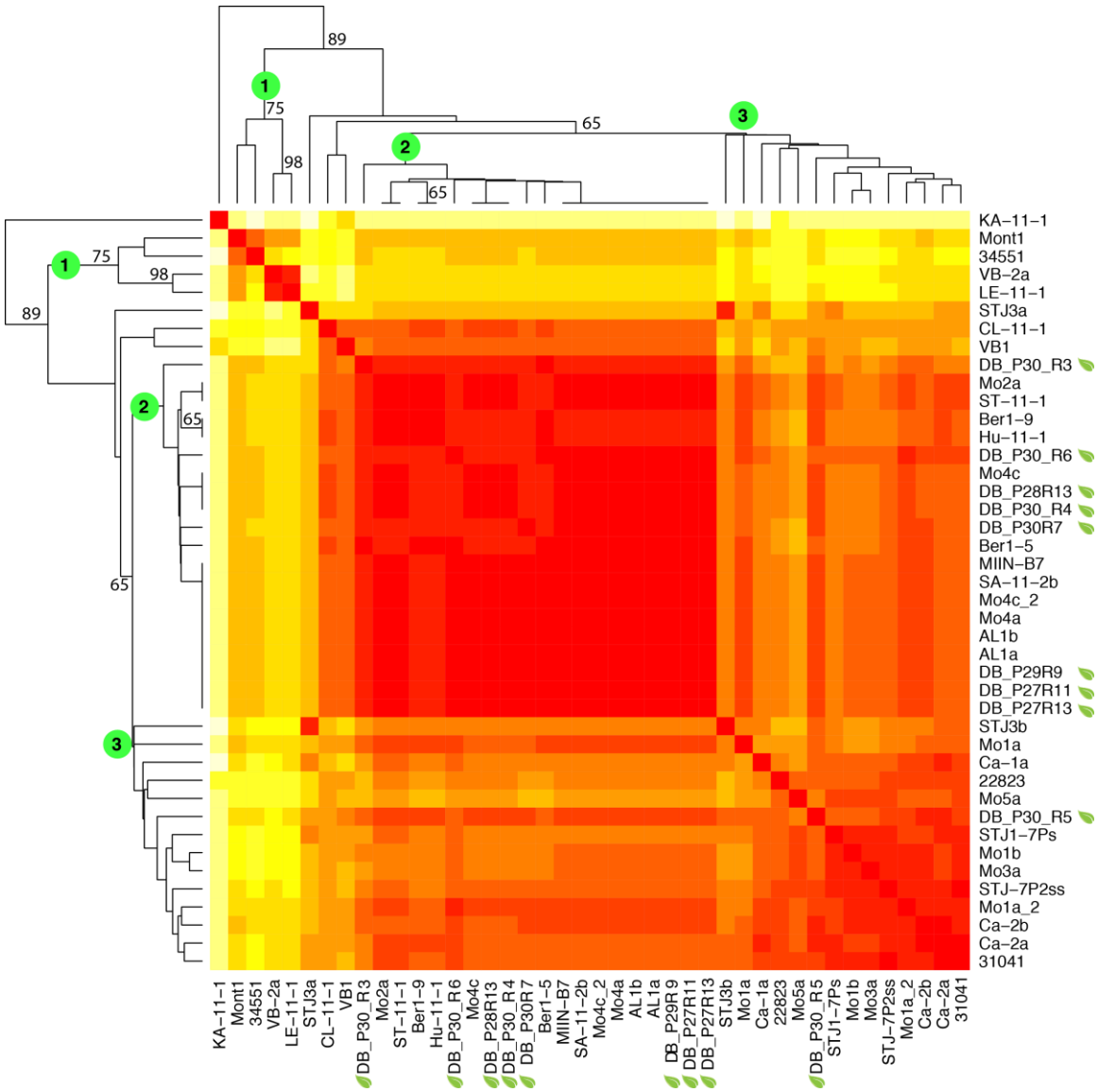

Figure 5-4 Cluster analysis of *F. virguliforme* isolates based on Bruvo's genetic distance. Neighbor-joining trees are plotted on the left and upper margins, and isolates codes are labeled on the right and bottom margins. Color scales in the matrix indicate genetic distance between isolates. Red indicates identical, while light yellow indicates distantly related. Isolates recovered from soybean except those isolates recovered from dry bean as indicated with green leaf symbols. Three main clusters are labeled on the node with a green dot and numbered from 1 to 3.

Cross-species transferability

All of the *F. virguliforme* microsatellite markers successfully transferred to most or some of the closely related species. Microsatellite locus 99 was the poorest performer, with amplification

from only two of the nine species, *F. crassistipitatum* and *Fusarium* sp. (NRRL 22387) (Table 5-3). The remaining 11 microsatellite markers amplified all of the closely related soybean SDS and BRR pathogens (Table 5-3), and at least 10 microsatellite loci were polymorphic (number of alleles ≥ 2) among these species. Allele sizes amplified from non-*F. virguliforme* species were within the range of the allele sizes of *F. virguliforme* isolates. The markers also demonstrated utility for other less closely related species within the *F. solani* species complex with amplification of ten, five and three of the microsatellite loci, respectively from three phylogenetically distinct species within clade 2 (i.e. *Fusarium* species NRRL 22574, 22387, and 22395).

Table 5-3 Transferability of microsatellite markers developed for *F. virguliforme* across isolates in clade 2 of the *Fusarium solani* species complex

		Microsatellite loci allele size range											
Species (n = # of isolates)	Major Hosts /substrate	Locus 43	Locus 12	Locus 93	Locus 83	Locus 4	Locus 15	Locus 99	Locus 48	Locus 38	Locus 80	Locus 59	Locus 10
F. virguliforme (n = 42)	Soybean and Dry bean[a]	113-224	173-225	166-193	201-219	185-217	151-214	137-233	218-290	197-233	145-229	155-251	159-279
Fusarium brasiliense (n=3)	Soybean	123-161	169-171	172-184	184	177-183	151	-	139-207	190-202	145-148	149-155	159-162
Fusarium tucumaniae (n=3)	Soybean	121	171	172-181	181	176	154	-	195-255	196-202	149-161	161-199	171-186
Fusarium crassistipitatum (n=1)	Soybean	138	172	175	201	181	152	227	164	196	145	149	171
Fusarium phaseoli (n=3)	Dry bean[b]	131-152	169-171	181-184	184	151-177	151	-	163-242	196	145-148	155-174	159-168
Fusarium cuneirostrum (n=1)	Dry bean	121	170	181	170	151	151	-	255	196	171	156	174
Fusarium azukicola (n = 1)	Dry bean	-	170	158	177	-	167	-	133	208	133	168	-
Fusarium sp.[c] (n=2)	Bark	-	171-174	-	-	169	157-169	-	-	181-193	-	137	-
Fusarium sp.[d] (n=1)	Bark	138	172	175	-	-	152	227	164	196	145	149	171
Fusarium sp.[e] (n=1)	Bark	-	88	167	-	-	-	-	-	182	-	-	-

[a]: Reported to cause soybean sudden death syndrome
[b]: Reported to cause bean root rot
[c]: represent by NRRL 22574 and 22412
[d]: represent by NRRL 22387
[e]: represent by NRRL 22395; '-': no amplification

Discussion

A total of 225 microsatellite loci were identified in the *F. virguliforme* genome. To increase the chance of identifying polymorphic microsatellite markers, stringent search parameters were used, including a high threshold for the minimum number of repeats (Kelkar *et al.* 2010). As such, a low relative abundance of 4.42 microsatellite counts/Mbp were detected. However, when we adjusted microsatellite search parameters to a minimum repeat length of 10 bp or more as used in other studies, the microsatellite relative abundance of *F. virguliforme* was determined to be 126 counts/Mbp. This value is similar to those reported in other studies but higher than what we found using the same parameters in the *F. graminearum* (Karaoglu *et al.* 2005) and *N. haematococca* (this study, data not shown) genomes with 97 and 106 counts/Mbp, respectively. In the *F. virguliforme* genome, the most frequent microsatellite motif was the trinucleotide motif AAT, which was also the most common motif in *N. haematococca*. While in the more distantly related *F. graminearum*, the most common microsatellite motif was AAG.

After additional *in silico* analysis and wet lab screening, 12 microsatellite markers were identified to be reproducible and highly polymorphic. Out of the 108 microsatellite primer sets designed, 92 primer sets were synthesized and screened for amplification consistency and marker polymorphism. The choice of microsatellite markers for the initial screening was based on two parameters, the length of the repeat unit and distribution within the *F. virguliforme* genome assembly scaffolds. Priority was given to microsatellite loci that had greater number of microsatellite repeats and located on different genome assembly scaffolds. Although additional markers could be developed, the genotype accumulation curve begins to asymptote with nine or ten microsatellite markers, indicating that the 12 microsatellite markers are sufficient to detect most genetic diversity.

To ensure the developed microsatellite markers are representative of variation in the genome and to permit analyses of gametic disequilibrium, it is essential to utilize markers that are not linked (McDonald 1997). *Fusarium virguliforme* is heterothallic and only one mating type (*MAT1-1*) was found in this study and others (Covert *et al.* 2007; Hughes *et al.* 2014), thus it was not possible to conduct an *in vitro* cross to determine linkage between the markers (Ozkilinc *et al.* 2011). Therefore, an alternative method was used to estimate linkage by mapping the microsatellite loci to the most closely related *Fusarium* species (*N. haematococca*) with a high quality reference genome (Coleman *et al.* 2009). We found strong evidence that most of the markers are unlikely to be linked. The final 12 markers were found to be distributed across at least 6 chromosomes of the *N. haematococca* genome, and the markers also mapped to 12 different scaffolds of the *F. virguliforme* draft genome. An index of association (Agapow & Burt 2001) test conducted with the Michigan microsatellite genotype population data indicates the predominance of asexual reproduction, which aligns with the findings of the mating type test.

The Michigan *F. virguliforme* isolate set was revealed to be genetically diverse despite the fact that *F. virguliforme* isolates were collected from a relative small geographical scale (i.e. 12 counties in Michigan). The high genetic diversity observed may be the result of high microsatellite mutation rate which is known in fungi to be higher than that of sequence based markers at 2.50×10^{-5} - 2.80×10^{-6} vs 10^{-9} per generation per site, respectively (Kasuga *et al.* 2002). The observed genetic diversity observed in Michigan may also be the result of multiple introductions. Genetic structure of Michigan *F. virguliforme* isolates was observed in the dendrogram (Figure 5-4 and Figure S5-1), indicating the strong resolution and applicability of this set of markers in population genetic studies of this pathogen. Although three clusters were resolved in the dendrogram using Bruvo's genetic distance, they did not receive significant

bootstrap support (> 60%) (Figure 5-4). However, STRUCTURE analysis was in agreement with the distance based method, with the best number of assumed populations determined to be three (K=3) using the delta K method (Evanno *et al.* 2005). However, no distinct genetic separation between isolates recovered by host or location was observed.

Most of the microsatellite markers successfully amplified species other than *F. virguliforme* within clade 2 of the *Fusarium solani* species complex. It has been suggested that microsatellite markers are conserved among closely related species (Moore *et al.* 1991), and that allele size mutations at the microsatellite loci might be useful for clarifying phylogenetic relationships of recently diverged species (Dawson *et al.* 2010; Moodley *et al.* 2015). The high rate of microsatellite marker transferability supports suggestions that the *Fusarium* species that cause SDS and BRR radiated within the past 0.75 million years (Hughes *et al.* 2014). Non-amplification of microsatellite alleles with more distantly related species within clade 2 of the *F. solani* species complex, such as the phylogenetically distinct species represented by NRRL 22574 and 22387, could be the result of allele loss or mutations in the primer binding regions (Koorey *et al.* 1993). Currently, limited genetic tools are available for this group of important plant pathogens. The microsatellite markers validated in this study should facilitate elucidating genetic diversity of *Fusarium* species in this clade and help explore the many ecological and evolutionary questions that remain for *F. virguliforme*.

Acknowledgement

We thank J. Alejandro Rojas and Janette L. Jacobs for technical and editorial support. We thank the USDA-ARS Culture Collection NRRL for providing isolates of *Fusarium*. This work was supported by grants from Project GREEEN (number GR10-113), the Michigan Soybean Promotion Committee, the A.L. Rogers Endowed Research Scholarship, and the Carter Harrison Endowed Graduate Student Fund. Genome sequence data used in this study were generated from the support of Soybean Research and Development Council and Iowa Soybean Association and available through http://fvgbrowse.agron.iastate.edu/.

Data accessibility

Microsatellite sequence data can be found in NCBI GenBank entries: **KR476359-KR476370**. Microsatellite fragment analysis allele size data reported in this study was submitted to Dryad Digital Repository (http://datadryad.org/review?doi=doi:10.5061/dryad.1sr43).

APPENDICES

APPENDIX A Supplementary tables

Table S 5-1 Microsatellite markers allele sizes (bp) detected for each of the multi-locus genotype

MLG*	Locus 43	Locus 12	Locus 93	Locus 83	Locus 4	Locus 15	Locus 99	Locus 48	Locus 38	Locus 80	Locus 59	Locus 10
1	224	207	193	219	203	184	233	278	233	229	245	198
2	224	207	193	219	203	184	233	272	233	226	251	198
3	209	227	193	219	205	184	233	278	233	163	203	228
4	209	225	193	219	185	211	233	284	233	163	203	228
5	191	213	166	219	217	172	233	272	233	187	203	279
6	191	213	166	219	205	211	233	278	233	187	215	243
7	191	213	166	219	203	208	233	290	233	187	215	243
8	191	213	166	219	203	208	233	278	233	187	209	243
9	191	213	166	219	203	208	233	272	233	187	215	243
10	191	213	166	219	203	208	233	272	233	187	209	243
11	191	213	166	219	203	208	233	218	197	187	215	243
12	191	213	166	219	203	208	209	290	227	190	215	243
13	191	213	166	219	203	208	197	278	233	187	215	243
14	191	213	166	219	203	208	185	272	233	187	215	243
15	191	213	166	219	203	208	137	278	233	187	215	243
16	191	213	166	201	217	172	185	272	233	187	203	279
17	191	213	166	201	203	178	233	272	233	187	209	243
18	191	211	166	219	203	208	233	260	233	187	203	246
19	143	215	166	219	205	211	233	278	233	187	203	249
20	143	213	166	219	205	214	233	278	233	187	203	246
21	143	213	166	219	205	211	233	284	233	187	203	246
22	143	213	166	219	205	211	233	278	233	187	203	249
23	143	213	166	219	205	211	233	278	233	187	203	246
24	143	213	166	219	205	211	233	278	233	187	203	243

Table S 5-1 (cont'd)

25	143	213	166	219	205	211	233	272	233	187	203	249
26	143	213	166	219	205	211	233	272	233	187	203	246
27	143	213	166	219	205	211	209	284	209	187	203	249
28	143	213	166	219	205	211	179	224	203	187	203	246
29	143	213	166	219	203	208	233	272	233	193	203	264
30	143	211	166	219	203	211	233	284	233	187	203	246
31	113	173	178	219	205	151	173	224	203	145	155	159

*: Indicates multi-locus genotype (MLG)

APPENDIX B Supplementary figures

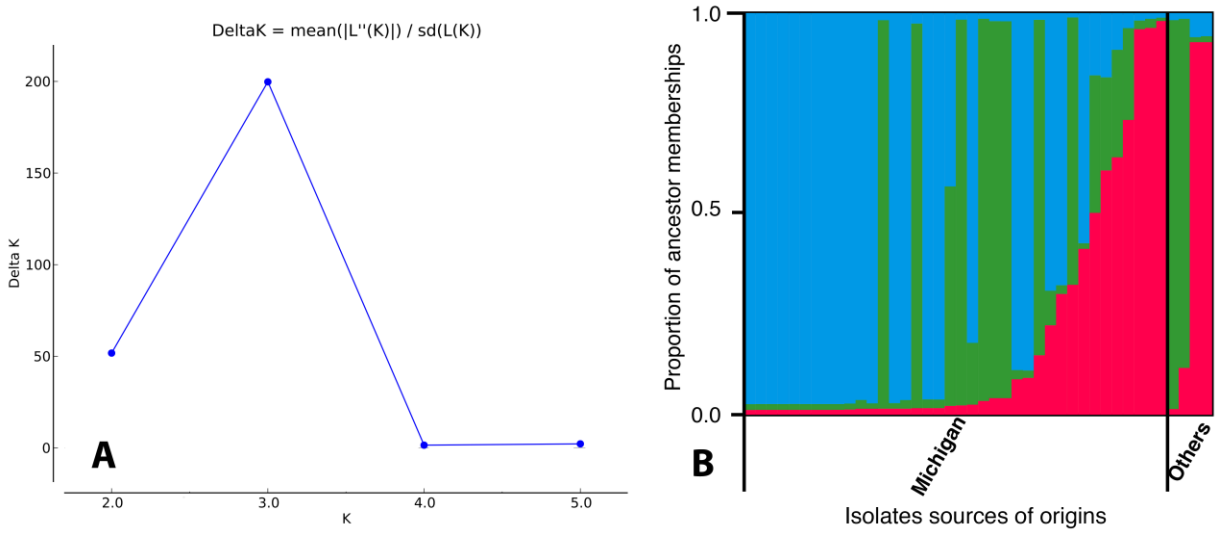

Figure S 5-1 (A) Delta K method to determine the optimal K (assumed ancestors) based on likelihood method (Evanno *et al.* 2005). (B) Assignment of *F. virguliforme* isolates into clusters using the program STRUCTURE. Three ancestor memberships were labeled with three colors (blue, green, and red), the bar height indicates the proportion of ancestor membership compositions. Michigan: isolates were collected from Michigan in this study; others represent four *F. virguliforme* with NRRL codes: 34551, 31041, 22823, and 22292 (Mont1).

REFERENCES

REFERENCES

Achenbach LA, Patrick JA, Gray LE (1997) Genetic homogeneity among isolates of *Fusarium solani* that cause soybean sudden death syndrome. *Theoretical and Applied Genetics* **95**, 474-478.

Agapow PM, Burt A (2001) Indices of multilocus linkage disequilibrium. *Molecular Ecology Notes* **1**, 101-102.

Aoki T, O'Donnell K, Geiser DM (2014) Systematics of key phytopathogenic *Fusarium* species: current status and future challenges. *Journal of General Plant Pathology* **80**, 189-201.

Aoki T, O'Donnell K, Homma Y, Lattanzi AR (2003) Sudden-death syndrome of soybean is caused by two morphologically and phylogenetically distinct species within the *Fusarium solani* species complex— *F. virguliforme* in North America and *F. tucumaniae* in South America. *Mycologia* **95**, 660-684.

Aoki T, O'Donnell K, Scandiani MM (2005) Sudden death syndrome of soybean in South America is caused by four species of *Fusarium*: *Fusarium brasiliense* sp. nov., *F. cuneirostrum* sp. nov., *F. tucumaniae*, and *F. virguliforme*. *Mycoscience* **46**, 162-183.

Aoki T, Scandiani MM, O'Donnell K (2012a) Phenotypic, molecular phylogenetic, and pathogenetic characterization of *Fusarium crassistipitatum* sp. nov., a novel soybean sudden death syndrome pathogen from Argentina and Brazil. *Mycoscience* **53**, 167-186.

Aoki T, Tanaka F, Suga H, *et al.* (2012b) *Fusarium azukicola* sp nov., an exotic azuki bean root-rot pathogen in Hokkaido, Japan. *Mycologia* **104**, 1068-1084.

Brownstein MJ, Carpten JD, Smith JR (1996) Modulation of non-templated nucleotide addition by taq DNA polymerase: Primer modifications that facilitate genotyping. *Biotechniques* **20**, 1004.

Bruvo R, Michiels NK, D'Souza TG, Schulenburg H (2004) A simple method for the calculation of microsatellite genotype distances irrespective of ploidy level. *Molecular Ecology* **13**, 2101-2106.

Chehri K, Salleh B, Zakaria L (2014) *Fusarium virguliforme*, a soybean sudden death syndrome fungus in Malaysian soil. *Australasian Plant Disease Notes* **9**, 1-7.

Chilvers MI, Brown-Rytlewski DE (2010) First report and confirmed distribution of soybean sudden death syndrome caused by *Fusarium virguliforme* in southern Michigan. *Plant Disease* **94**, 1164-1164.

Coleman JJ, Rounsley SD, Rodriguez-Carres M, *et al.* (2009) The genome of *Nectria haematococca*: contribution of supernumerary chromosomes to gene expansion. *Plos Genetics* **5**, e1000618.

Covert SF, Aoki T, O'Donnell K, *et al.* (2007) Sexual reproduction in the soybean sudden death syndrome pathogen *Fusarium tucumaniae*. *Fungal Genet Biol* **44**, 799-807.

Dawson DA, Horsburgh GJ, Kupper C, *et al.* (2010) New methods to identify conserved microsatellite loci and develop primer sets of high cross-species utility - as demonstrated for birds. *Molecular Ecology Resources* **10**, 475-494.

Earl DA, Vonholdt BM (2012) STRUCTURE HARVESTER: a website and program for visualizing STRUCTURE output and implementing the Evanno method. *Conservation Genetics Resources* **4**, 359-361.

Ellegren H (2004) Microsatellites: simple sequences with complex evolution. *Nature Reviews Genetics* **5**, 435-445.

Evanno G, Regnaut S, Goudet J (2005) Detecting the number of clusters of individuals using the software STRUCTURE: a simulation study. *Molecular Ecology* **14**, 2611-2620.

Goss EM, Tabima JF, Cooke DEL, *et al.* (2014) The Irish potato famine pathogen *Phytophthora infestans* originated in central Mexico rather than the Andes. *Proceedings of the National Academy of Sciences of the United States of America* **111**, 8791-8796.

Hartman GL, Chang HX, Leandro LF (2015) Research advances and management of soybean sudden death syndrome. *Crop Protection* **73**, 60-66.

Hughes TJ, O'Donnell K, Sink S, *et al.* (2014) Genetic architecture and evolution of the mating type locus in fusaria that cause soybean sudden death syndrome and bean root rot. *Mycologia* **106**, 686-697.

Jakobsson M, Rosenberg NA (2007) CLUMPP: a cluster matching and permutation program for dealing with label switching and multimodality in analysis of population structure. *Bioinformatics* **23**, 1801-1806.

Kamvar ZN, Tabima JF, Grünwald NJ (2014) Poppr: an R package for genetic analysis of populations with clonal, partially clonal, and/or sexual reproduction. *PeerJ* **2**, e281.

Karaoglu H, Lee CMY, Meyer W (2005) Survey of simple sequence repeats in completed fungal genomes. *Molecular Biology and Evolution* **22**, 639-649.

Kasuga T, White TJ, Taylor JW (2002) Estimation of nucleotide substitution rates in eurotiomycete fungi. *Molecular Biology and Evolution* **19**, 2318-2324.

Kelkar YD, Strubczewski N, Hile SE, *et al.* (2010) What is a microsatellite: A computational and experimental definition based upon repeat mutational behavior at A/T and GT/AC repeats. *Genome Biology and Evolution* **2**, 620-635.

Kerenyi Z, Moretti A, Waalwijk C, Olah B, Hornok L (2004) Mating type sequences in asexually reproducing *Fusarium* species. *Applied and Environmental Microbiology* **70**, 4419-4423.

Kofler R, Schlotterer C, Lelley T (2007) SciRoKo: a new tool for whole genome microsatellite search and investigation. *Bioinformatics* **23**, 1683-1685.

Koorey DJ, Bishop GA, Mccaughan GW (1993) Allele non-amplification - a source of confusion in linkage studies employing microsatellite polymorphisms. *Human Molecular Genetics* **2**, 289-291.

Koressaar T, Remm M (2007) Enhancements and modifications of primer design program Primer3. *Bioinformatics* **23**, 1289-1291.

Li S., Hartman G.L., Chen Y. (2009) Evaluation of aggressiveness of *Fusarium virguliforme* isolates that cause soybean sudden death. *Journal of Plant Pathology* **91**, 77-86.

Malvick DK, Bussey KE (2008) Comparative analysis and characterization of the soybean sudden death syndrome pathogen *Fusarium virguliforme* in the northern United States. *Canadian Journal of Plant Pathology* **30**, 467-476.

Matschiner M, Salzburger W (2009) TANDEM: integrating automated allele binning into genetics and genomics workflows. *Bioinformatics* **25**, 1982-1983.

Mbofung G, Harrington TC, Steimel JT, *et al.* (2012) Genetic structure and variation in aggressiveness in *Fusarium virguliforme* in the Midwest United States. *Canadian Journal of Plant Pathology* **34**, 83-97.

McDonald BA (1997) The population genetics of fungi: tools and techniques. *Phytopathology* **87**, 448-453.

Moodley Y, Masello JF, Cole TL, *et al.* (2015) Evolutionary factors affecting the cross-species utility of newly developed microsatellite markers in seabirds. *Molecular Ecology Resources* **15**, 1046-1058.

Moore SS, Sargeant LL, King TJ, *et al.* (1991) The conservation of dinucleotide microsatellites among mammalian genomes allows the use of heterologous PCR primer pairs in closely related species. *Genomics* **10**, 654-660.

O'Donnell K (2000) Molecular phylogeny of the *Nectria haematococca-Fusarium solani* species complex. *Mycologia* **92**, 919-938.

O'Donnell K, Sink S, Scandiani MM, *et al.* (2010) Soybean sudden death syndrome species diversity within North and South america revealed by multilocus genotyping. *Phytopathology* **100**, 58-71.

Ozkilinc H, Akamatsu H, Abang M, *et al.* (2011) Development, characterization and linkage analysis of microsatellite loci for the *Ascochyta* blight pathogen of faba bean, *Didymella fabae*. *Journal of Microbiological Methods* **87**, 128-130.

Penner G, Bush A, Wise R, *et al.* (1993) Reproducibility of random amplified polymorphic DNA (RAPD) analysis among laboratories. *Genome Research* **2**, 341-345.

Pritchard JK, Stephens M, Donnelly P (2000) Inference of population structure using multilocus genotype data. *Genetics* **155**, 945-959.

Rosenberg NA (2004) DISTRUCT: a program for the graphical display of population structure. *Molecular Ecology Notes* **4**, 137-138.

Roy KW, Hershman DE, Rupe JC, Abney TS (1997) Sudden death syndrome of soybean. *Plant Disease* **81**, 1100-1111.

Srivastava SK, Huang X, Brar HK, *et al.* (2014) The genome sequence of the fungal pathogen *Fusarium virguliforme* that causes sudden death syndrome in soybean. *PLoS One* **9**, e81832.

Tande C, Hadi B, Chowdhury R, Subramanian S, Byamukama E (2014) First report of sudden death syndrome of soybean caused by *Fusarium virguliforme* in South Dakota. *Plant Disease* **98**, 1012-1012.

Tewoldemedhin YT, Lamprecht SC, Geldenhuys JJ, Kloppers FJ (2013) First report of soybean sudden death syndrome caused by *Fusarium virguliforme* in South Africa. *Plant Disease* **98**, 569-569.

Varshney RK, Graner A, Sorrells ME (2005) Genic microsatellite markers in plants: features and applications. *Trends in Biotechnology* **23**, 48-55.

Wang J, Jacobs JL, Byrne JM, Chilvers MI (2015) Improved diagnoses and quantification of *Fusarium virguliforme*, causal agent of soybean sudden death syndrome. *Phytopathology* **105**, 378-387.

Wrather J, Koenning S (2006) Estimates of disease effects on soybean yields in the United States 2003 to 2005. *Journal of nematology* **38**, 173-180.

Yang H, Sweetingham MW, Cowling WA, Smith PM (2001) DNA fingerprinting based on microsatellite-anchored fragment length polymorphisms, and isolation of sequence-specific PCR markers in lupin (*Lupinus angustifolius* L.). *Molecular Breeding* **7**, 203-209.

Zhang N, O'Donnell K, Sutton DA, *et al.* (2006) Members of the *Fusarium solani* species complex that cause infections in both humans and plants are common in the environment. *Journal of clinical microbiology* **44**, 2186-2190.

Zhang Z, Schwartz S, Wagner L, Miller W (2000) A greedy algorithm for aligning DNA sequences. *Journal of Computational Biology* **7**, 203-214.

CHAPTER 6 POPULATION GENETICS OF THE FILAMENTOUS FUNGUS *FUSARIUM VIRGULIFORME* CAUSING SUDDEN DEATH SYNDROME ON SOYBEAN

Abstract

Soybean sudden death syndrome (SDS), caused by the fungus *Fusarium virguliforme*, is one of the top five diseases threatening soybean production in the US. Since SDS was first reported in 1971 in Arkansas, SDS has been reported in the surrounding states in the following years with an apparent pattern of dispersal. To date, most soybean producing states were confirmed with SDS caused *F. virguliforme* in US. Contrary to wide distribution of *F. virguliforme* in the US, SDS caused by *F. virguliforme* is less common in South America, and primarily distributed in Argentina. Given the wide distribution in the American continents, little is known about the center of origin or population structure of *F. virguliforme*. Although previous studies proposed the South American center of origin hypothesis for *F. virguliforme*, no direct analysis of *F. virguliforme* population biology to support this hypothesis. In this study, we used multilocus microsatellite typing, population genetics tools, and a collection of 539 *F. virguliforme* isolates from both South and North America to test the center of origin hypotheses within the US and intercontinentally. High genotypic diversity and diverse population structure composition of the Arkansas population supported the hypothesis that Arkansas is the center of origin in the US. The distribution of *F. virguliforme* in the US is not in isolation by distance as detected in Mantel test, suggesting a rapid and recent expansion of this pathogen in the US. The hypothesis that South America is the center of origin was supported by the coalescence based migrate analysis; however, genotypic diversity and population structure of the Argentinean populations were less diverse than the Arkansas population. The Argentinean population cannot explain the genotypic diversity and population structure composition detected in the US, and therefore the hypothesis that South America is the center of origin is not supported in this study.

Introduction

Fusarium is a diverse and ubiquitous genus of filamentous fungi (Ascomycetes: Sordariomycetes: Hypocreales: Nectriaceae) that are widely distributed in soil and associated with plants as pathogens or endophytes (Aoki *et al.* 2014; Ma *et al.* 2013). *Fusarium virguliforme* causes sudden death syndrome of soybean and is one of the most devastating soybean diseases (Roy *et al.* 1997; Wrather & Koenning 2009). Yield losses caused by *F. virguliforme* ranged from 20 - 46% in SDS symptomatic fields (Brzostowski *et al.* 2014; Hartman *et al.* 1995). *F. virguliforme* is a soilborne fungus that completes most of its life cycle within soil or plant roots (Rupe 1989). To date, only one mating type (*MAT1-1*) has been found and no sexual structure was formed in the field or in the lab, thus the only known mode of reproduction for *F, virguliforme* is asexual reproduction through production of conidia and chlamydospores (Covert *et al.* 2007; Hughes *et al.* 2014). The lack of aboveground structure or production of aerial spores is thought to limit the mobility of this pathogen, therefore it is thought that the dispersal of *F. virguliforme* is associated with the movement of infested plant material or soil.

Since the first report of SDS in 1971 in Arkansas (Hirrel 1983), SDS has been reported in most soybean producing areas in North America, with an apparent dispersive pattern (Figure 6-1) (Bernstein *et al.* 2007; Chilvers & Brown-Rytlewski 2010; Hartman *et al.* 1999; Kurle *et al.* 2003; Pennypacker 1999; Roy *et al.* 1997; Tande *et al.* 2014; Ziems *et al.* 2006). To date, although SDS is reported in most soybean producing areas, little research has been conducted to study the population biology of *F. virguliforme*, and thus the center of origin responsible for the dispersal of *F. virguliforme* is still unknown. Besides North America, SDS has also been reported in South America in the early 1990s (Nakajima *et al.* 1993; Ploper 1993). In North America, *F. virguliforme* is the only known SDS pathogen. However, SDS is caused by four

Fusarium species in South America, including *F. brasiliense, F. crassistipitatum, F. virguliforme*, and *F. tucumaniae* the predominant SDS pathogen in South America (Aoki *et al.* 2003; Aoki *et al.* 2005; Aoki *et al.* 2012; Scandiani *et al.* 2004). In a survey of SDS causing *Fusarium* species in South America, *F. virguliforme* was only identified in several provinces in Argentina, and not in any other soybean producing countries in South America (O'Donnell *et al.* 2010). To date, the US and Argentina are the only two countries confirmed to have *F. virguliforme* in the Americas. In recent years, SDS and *F. virguliforme* were reported in the areas outside of American continents, including South Africa, Malaysia, and Iran (Chehri 2015; Chehri *et al.* 2014; Tewoldemedhin *et al.* 2013). Although this pathogen has been reported in a wide range of geographical area, little is known about the dispersal method or center of origin for *F. virguliforme*, which raises concerns about the imminent epidemic of SDS in other soybean producing countries in Asia and Africa.

Previous studies examining genetic variations among *F. virguliforme* isolates have resolved little or no within species genetic diversity. The rDNA intergenic spacer region and translation elongation factors 1 alpha DNA sequences were determined to be identical among *F. virguliforme* isolates (Aoki *et al.* 2003; Aoki *et al.* 2005; Malvick & Bussey 2008). Five anonymous regions of *F. virguliforme* genome were sequenced, and their sequences were determined to be identical within *F. virguliforme* species, and thus suggested that a highly clonal population of *F. virguliforme* is present in the US (Aoki *et al.* 2012; O'Donnell *et al.* 2010). Though none of the DNA sequence markers demonstrated within species polymorphism, varied aggressiveness of *F. virguliforme* to soybean was observed with the isolates collected from North and South America (Li S. *et al.* 2009), which may indicate genetic diversity among *F. virguliforme* isolates. Using RAPD markers combined with microsatellite probes, 25 unique

genotypes were revealed out of 72 isolates and these isolates were clustered into 4 subgroups, but there was no association between virulence and genotypic data (Mbofung *et al.* 2012). The poor between-lab reproducibility of RAPD markers may limit the use of RAPD-based genotyping method for *F. virguliforme* (McDonald 1997; Penner *et al.* 1993). To further the study of *F. virguliforme*, we developed a set of polymorphic microsatellite markers that are locus-specific and highly polymorphic. This set of microsatellite markers has been validated and demonstrated to resolve the genetic diversity for *F. virguliforme* isolates (Wang & Chilvers 2016).

Several previous studies proposed South America as the center of origin of *F. virguliforme* (Aoki *et al.* 2003; Aoki *et al.* 2012; Covert *et al.* 2007; Hughes *et al.* 2014; O'Donnell 2000). Evidence supporting this hypothesis is based on phylogeny and mating type gene characterization for the *Fusarium* species located within the clade2 *Fusarium solani* species complex (FSSC). The evolution and radiation of clade2 FSSC has been dated back to the mid-Pleistocene, approximately 0.75 Mya (Hughes *et al.* 2014; O'Donnell *et al.* 2013), which is well before the domestication of common bean and soybean (Gaut 2014; Hymowitz 2004). Furthermore, phylogenetic analysis of clade2 FSSC species suggests that the evolutionary origin of *F. virguliforme* was on the South American continent (Aoki *et al.* 2003; O'Donnell 2000). With this evidence, it was proposed that the evolution of SDS causing *Fusarium* species involved several independent host jumps after soybean was introduced to South America roughly a century ago (Aoki *et al.* 2012). Only the *MAT1-1 F. virguliforme* adapted to soybean, was introduced to the US, and spread to the rest of the North America (Covert *et al.* 2007; Hughes *et al.* 2014). Both phylogenetic and mating type gene profiling provided indirect evidence to form this South America as the center of origin hypothesis; however, no direct measurement of

population diversity and structure of *F. virguliforme* in the US or Argentina, and thus left the hypothesis not tested.

Population structure of plant pathogens differs between natural habitats and agro-ecosystems. In the agro-ecosystems, the high-density crops of genetically homogeneous plants, and the anthropogenic activities that may facilitate propagation and distribution of plant pathogens favor the emergence and spread of plant pathogens (McDonald & Linde 2002; Stukenbrock & McDonald 2008). For instance, movement of farm equipment could possibility create the population spatial pattern that differs from the natural habitat, such as absence of isolation by distance (Njambere *et al.* 2014; Travadon *et al.* 2011). In addition, if the host adaptation in South America and introduction to the US hypothesis is true, signs of newly established populations, such as losses in genetic diversity (founder effect) and strong reduction in sexual recombination (Stukenbrock & Bataillon 2012), are expected in the US populations. In this study, we collected or obtained 539 *F. virguliforme* isolates from more than 46 field sites located in both North and South America for a population genetic study. Specifically, we have tested three hypotheses: (i) whether Arkansas is the center of origin for *F. virguliforme* spread in the US; (ii) is there founder effect in the area where SDS was recently reported; (iii) Is *F. virguliforme* introduced from South America to North America?

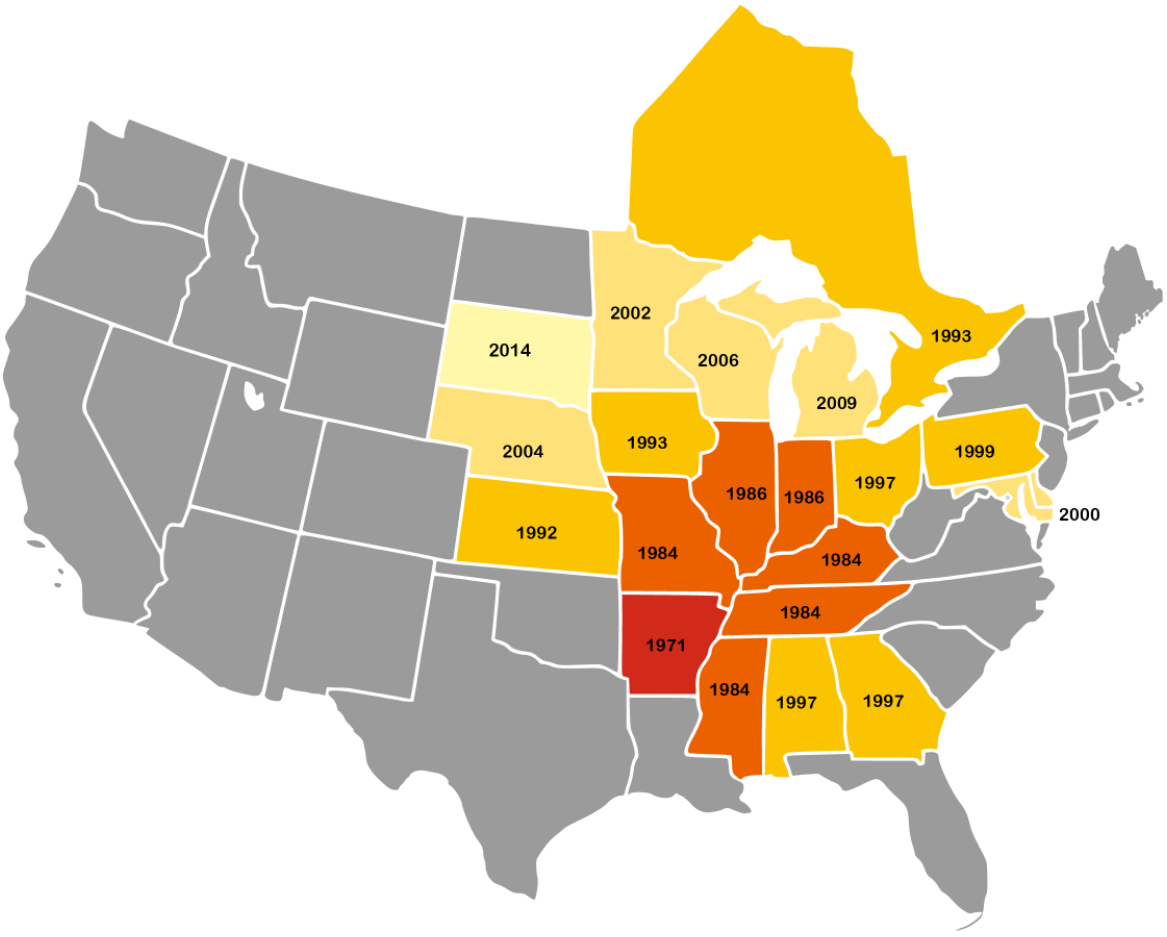

Figure 6-1 Distribution of soybean sudden death syndrome (SDS) in the US and Canada based on the year of first report in journal articles. Since the first report of SDS in 1971 in Arkansas, SDS has been reported in the surrounding states in the following years with apparent pattern of spreading. By 2014, SDS has been confirmed in most soybean producing areas in the US and Canada, thus to continuing threat soybean production.

Materials and methods

Sampling, fungal isolation, and DNA extraction

A total of 539 isolates were included in this study. Among them, 389 isolates were collected using the grid sampling method from 12 sampling sites located in Michigan, Indiana, Kansas, and Arkansas in 2012 and 2014. At each sampling site, a 7-by-7 square grid (10 m between sampling points for a total area of 70 m x 70 m area) containing 49 sample points located in a SDS symptomatic soybean field. For each sampling point, 2-3 SDS symptomatic plants were

collected, and stems were removed from the plant and roots were transported to the lab for recovery of *F. virguliforme* isolates. Fungal isolation to obtain monosporic culture of *F. virguliforme* were processed as described in Wang and Chilvers (2016). Briefly, soybean roots were washed, trimmed into 3-4 cm pieces, surface sterilized, and placed on semi-selective media (2% water agar, 1ml of 300 mg/ml streptomycin, and 1 ml of 15mg.ml metalaxyl in 1 liter of dH_2O) to induce formation of sporodochia on the root surface. Macroconidium collected from sporodochium was used to culture monosporic *F. virguliforme* isolates. Besides the isolates collected from grid sampling, 150 *F. virguliforme* isolates were obtained from lab collection, or provided by collaborators and USDA ARS Northern Regional Research Laboratory (NRRL) (Table 6-1). All isolates were confirmed to be *F. virguliforme* using the *F. virguliforme* specific PCR assay (Wang *et al.* 2015). All the isolates included in this study were stored in three different ways: on SNA slants at room temperature, on filter paper at -20ºC, and in 30% glycerol solution at -80ºC, as described in Wang and Chilvers (2016).

Pure fungal cultures grown on potato dextrose agar (Acumedia, Lansing, MI) for 7-10 d were transferred to a 150-ml flask containing 50 ml potato dextrose broth (Acumedia) and incubated at room temperature without shaking for 7-10 d. The fungal mycelial mat formed on the surface of the broth was collected into a 2-ml Eppendorf tube. Mycelia were frozen and lyophilized over night. Dried mycelia were stored at -20ºC until DNA extraction. Dried mycelia (20-50 mg) were measured into a 6-tube sample rack, and 1 ml plant lysis solution (AutoGen) was added to each tube to lyse the cells. Sample racks were sealed with aluminum foil and incubated in a water bath at 75ºC for 1 h. Samples were submitted to the Michigan State University genomics core for automated phenol-chloroform DNA purification steps on the AutoGenprep 850 Alpha system (AutoGen). DNA pellets precipitated in the bottom of the tube were suspended in 150 µl 1X Tris-

EDTA buffer. DNA concentrations were measured using a NanoDrop-1000 spectrophotometer (Thermo Scientific, Wilmington, Delaware).

Haplotype identification

Fusarium virguliforme genotypes were determined at 12 microsatellite loci including FvSSR_43, FvSSR_12, FvSSR_93, FvSSR_83, FvSSR_4, FvSSR_15, FvSSR_99, FvSSR_48, FvSSR_38, FvSSR_80, FvSSR_59, and FvSSR_10 (Wang & Chilvers 2016). A 4-nucleotide long oligo pigtail was added to the 5' to decrease allele drift effect at the capillary electrophoresis. Polymerase chain reactions (PCR) were carried out in a total volume of 25 µl and contained 5 - 20 ng genomic DNA template, 1 U DreamTaq DNA polymerase (Thermal Fisher Scientific, Waltham, MA), 1X PCR buffer containing 2 mmol/L $MgCl_2$, 0.2 mmol/L of dNTP (Promega Corp., Madison, WI), 200 nmol/L of forward and reverse primers, the forward primers (Applied Biosystems, Carlsbad, CA) were labeled with one of the three fluorophores (6-FAM, HEX, or NED) as described in Wang and Chilvers (2016), 200 ng/µl of BSA, and filled to 25 µl with distilled water. The PCR conditions consisted of an initial denaturation step at 95ºC for 5 min, followed by 35 cycles of 95ºC for 30 s, 62ºC for 30s, and 72ºC for 25s, and a final extension step at 72ºC for 7 min. To check the PCR product quality, PCR products were separated and visualized in a 1.5% agarose gel at 85 volts for 45 min and stained with 1 mg/ml ethidium bromide. To multiplex PCR products for fragment analysis, PCR products were combined according to the type of fluorescent label attached to the forward primer. The premixed samples were resolved with an ABI 3730XL DNA analyzer (Applied Biosystems) using GENSCAN 400HD ROX size standard by Macrogen Inc. Microsatellite allele assignments were determined using Peak Scanner v1.0 software (Applied Biosystems). To compensate for the allelic drift effect in microsatellite allele size assignment (Amos *et al.* 2007), automated binning

of alleles in TANDEM software v1.09 (Matschiner & Salzburger 2009) was used to increase allele size assignment accuracy.

Data analyses

Genotypic diversity

For the population genetic analyses that assume sexual reproduction, *F. virguliforme* microsatellite genotypic data were clone corrected to keep only one isolate per multilocus genotype (MLG) per hierarchical level. Population clone correction was performed using the 'clonecorrect' function in the R package 'poppr' (Kamvar *et al.* 2014) with the population strata setting to '~Year/Country/State/Loc'.

Genotypic diversity was calculated with the regional populations at the level of states or provinces using R package 'poppr'. The Shannon-Wiener index (H) and Stoddart and Taylor's index (G) that estimated both genotypic richness and evenness were calculated to determine the genotypic diversity for each population. Genotypic evenness was calculated using E5 index, which gives a ratio of abundant genotypes to the rare genotypes and is less sensitive to sample size (Grunwald *et al.* 2003). The corrected genotypic richness, expected number of MLGs (eMLG), is a rarefied measurement for genotypic richness for correction of varied sample sizes as implemented in R package 'vegan' (OHara *et al.* 2012) and 'poppr'.

Test for population clonality

To assess the probability that two isolates with the same MLG are parts of the same clonal lineage and therefore not derived from a distinct sexual reproductive event, the P_{gen} and P_{sex} were calculated for all isolates (Arnaud-Haond *et al.* 2007). By calculating P_{gen} and P_{sex} indices, the observed genotypic diversity contributed by possible sexual reproduction was partitioned. Additionally, the standardized index of association ($\bar{r}_D$) was calculated to test the linkage

disequilibrium among 12 microsatellite markers (Agapow & Burt 2001). The $\bar{r}_D$ index ranged from 0 to 1, with 0 indicating no association of alleles at unlinks loci, which is a sign for random mating. The level of significance for the $\bar{r}_D$ index is obtained through 1,000 resampling of permutation test in the R package 'poppr', and the null hypothesis is the population under random mating.

Analysis of molecular variance

A hierarchical analysis of molecular variance (AMOVA) (Excoffier *et al.* 1992) was conducted using 'amova' function in ade4 package (Dray & Dufour 2007) to test for significant variation among sampling locations. To determine the level of significance for the explained variations by each hierarchical level, 10, 000 permutations were performed to calculate the *P*-value.

Index of population differentiation

To determine the extent of pairwise population differentiations, the Hedrick's G'_{st} index of population differentiation (Hedrick 2005) was calculated among populations using the R package 'mmod' (Winter 2012). Hedrick's G'_{st} is a standardized analog to the F_{st} or Nei's G_{st} population differentiation index, but G'_{st} is a ratio between the observed G_{st} and the maximum of G_{st} can be, so that G'_{st} can reach to a maximum of 1 if no allele overlaps between subpopulations. Regional populations with less than five isolates were excluded in the pairwise population differentiation index calculation. The significance levels of the observed *P* values were determined by running 10,000 permutations. The 'heatmap.2' function in 'gplots' R package (Warnes *et al.* 2009) was used to generate the graphical display of the pairwise G'_{st} matrix, and the populations were clustered using the UPGMA dendrogram based on G'_{st} values.

Mantel test and isolation by distance

In addition, three tests were performed to test the isolation by distance (IBD) for the populations in the US, Argentina, and combined. The genetic distances among populations were calculated using the linearized Hedrick's G'_{st} (i.e., $G'_{st}/(1-G'_{st})$). Geographic distances between each pair of sampling locations were calculated using 'Geosphere' R package (https://cran.r-project.org/web/packages/geosphere) based on the Haversine direct distance method. Both genetic distance and geographical distance were converted to Euclidean distance for Mantel test. The first Mantel test was performed using all pairwise comparisons combined with both US and Argentina populations, whereas the other two Mantel tests were performed against US and Argentinean population, respectively. The Mantel test was performed using the 'ade4' R package (Dray & Dufour 2007), and levels of significance was calculated using 10,000 permutations.

STRUCTURE analysis

To examine genetic structure within the populations, an individual-based analysis of population structure was conducted using the Bayesian assignment approach with the program STRUCTURE v. 2.3.4 (Pritchard *et al.* 2000). Both admixture and non-admixture models were used in two runs, but no significant difference was detected in membership assignment between two methods. The non-admixture model was used in the STRUCTURE analysis, because *F. virguliforme* appears to be very clonal based on the index of association test. Lambda was set to 1.0 and 1,000,000 Monte Carlo Markov chain steps were used after a burn-in of 100,000. The number of clusters (K) was varied from 1 to 13 and replicated 12 times to validate for convergence. The optimal K was determined by the highest rate of change in the log probability of data between successive K values, which was implemented in Structure Harvester known as ΔK method (Earl & Vonholdt 2012; Evanno *et al.* 2005). The 12 replicated STRUCTURE runs

were aligned using the software CLUMPP v1.1.2 using greedy algorithm (Jakobsson & Rosenberg 2007). Software Distruct v.1.1 (Rosenberg 2004) was used to plot the results of membership coefficient assignment for each isolate.

Clustering based on individual genetic distances

The Bruvo's genetic distance utilizing the step-wise mutation model was calculated to elucidate the relationship among MLGs with 'dist.burvo' function in R package 'poppr'. These genetic distance relationships among individuals were visualized in minimum spanning network and in a UPGMA tree with the R packages 'ape' (Paradis *et al.* 2004) and 'ggtree' (Yu & Lam 2016).

Multivariate analysis

The model-free multivariate method, discriminant analysis of principle components (DAPC), was used to detect the clusters of *F. virguliforme* isolates based on prior population information (Jombart *et al.* 2010). DAPC method is sensitive to the number of principle components (PC) included in the analysis, so that cross validation was used to determine the optimal number of PCs in the discriminant analysis. The number of PCs was chosen based on the PC number that can reach the highest average percentage of successful reassignment and the lowest root mean squared error with 1,000 replicates using a training set of 90% of the data.

Multilocus inference of migration

Directional migration of *F. virguliforme* was estimated using the Bayesian coalescent approach implemented in an MPI version Migrate-n v. 3.6.11 (Beerli 2006; Beerli & Felsenstein 2001). The Argentina, Arkansas, Michigan and Indiana populations were grouped into three regional populations: 1, Argentina; 2, Arkansas; and 3, Michigan and Indiana. The groupings of these populations were based on their geographical distribution. To standardize the varied

population sampling sizes, a subsample of 85 isolates were used for model selection. For the population with less than 85 individuals (Argentina population), all isolates from Argentina population were used for migration analysis. Five replicated runs with different initial seeds were used to test the convergence of model selection results. Twelve migration models were compared as listed in Table 6-3, and the most supported model was determined based on the highest Bezier marginal likelihood (Beerli & Palczewski 2010). The Brownian mutation model was utilized to estimate the mutation rate of each microsatellite locus, and the starting estimate of the mutation scaled migration rates were derived from the F_{st} calculated for every possible migration route in each migration model. At the model selection step, six million simulation steps along with 200,000 burn-in steps were sampled to obtain the Bezier log marginal likelihood for model selection with three replicates for each run. For the parameter estimation, runs with thirty million steps along with one million burn-in steps were used for migration model parameters estimation. The mutation scaled population size (Θ) and mutation scaled migration rates (M) were estimated over three replicates. The migrate-n analysis was run in parallel on the institute for Cyber-Enabled Research (iCER) cluster at Michigan State University.

Results

Genotyping results

Based on 12 microsatellite loci, 286 unique multilocus genotypes (MLG) were identified from 539 individual isolates. A total of 192 different alleles were resolved from 12 loci with an average 16 allele (±6.63 SD) per locus. Each locus ranged from 8 alleles at locus 4 and locus 93 to 32 alleles at locus 10. The genotype accumulation curve showed that 90% of the MLG can be resolved using 11 microsatellites, which indicated that this set of microsatellite markers have enough power to describe the genotypic diversity of *F. virguliforme*.

High genotypic diversity was observed across the populations in the US and Argentina, with exception of the Kansas population, which showed relatively low genotypic diversity. The genotypic diversity indices (H and G) were particularly high in the Arkansas, Michigan, Indiana, and Buenos Aires populations (Table 6-1). Genotypic richness (eMLG) was also determined to be in a range between 4.7 and 9.3 for the populations with more than 5 isolates. High genotypic diversity and richness were not expected for *F. virguliforme*, since variation can only accumulate via spontaneous mutations.

In the US populations, 247 unique MLGs have been identified, and the top three most abundant genotypes are MLG202, MLG115, and MLG110. MLG202 (n=38) was the most abundant genotype, and was only found in the Indiana and Michigan populations. The second most abundant genotype is MLG115 (n=37) that has been found in four states, and a majority of this genotype (n=28) was found in the Kansas population (Figure S6-1). The third most abundant genotype is MLG110, which has been detected in five states in the US. Additionally, one of the historical isolates collected from Arkansas in 1985 was genotyped to be MLG110, which is the only historical isolate that has been detected in high abundance and with wide distribution in current populations (Table S6-1).

In total, 26 MLGs shared across the populations in the US (Figure S 6-1). In Argentina, MLG202 (n=6) and MLG231 (n=3) were the two most abundant genotypes, and were the only genotypes shared among provinces. The MLG202 has been found in both Argentina and US, and it is the most abundant genotype in both countries. The minimum spanning network showed that MLGs 202, 110, and 115 were located in two main clusters in the network and most of the US isolates are connected closely to one of these three genotypes with a genetic distance of 0.042 or less, which is approximately equivalent to one step mutation under the stepwise mutation model.

Clonality in populations

The standardized index of association ($\bar{r}_D$) to test the multilocus linkage disequilibrium on the clone-corrected data populations rejected the null hypothesis of random mating ($P < 0.01$) in all state/province populations, except the Cordoba population ($P = 0.933$, sample size n = 4). Asexual reproduction should be the only or major mode of reproduction for *F. virguliforme*. The genotype probability (P_{gen}) of two isolates at the same or different locations can evolve to the same genotype was detected to be very low, the P_{gen} for 513/539 isolates were detected to be lower than 0.05. The probability of encountering a genotype more than once by chance (P_{sex}) for most of the genotypes (504 /539) were determined to be lower than 0.05. Both P_{gen} and P_{sex} demonstrated that *F. virguliforme* populations in the US and Argentina were clonal in reproduction or at least clonal reproduction was a main means of reproduction for *F. virguliforme*.

Table 6-1 Genotypic and genetic diversity of *F. virguliforme* populations collected in both South and North America in this study.

ID	Countries	State/Province	Years	N	MLG	eMLG	SE	H	G	E.5	Ia	$\bar{r}_D$
1	Argentina	Buenos Aires	1999, 2002, 2012, 2013	40	31	9.39	0.71	3.35	25.81	0.90	2.97	0.31
2	Argentina	Santa Fe	2004, 2012, 2013	12	10	8.50	0.58	2.21	8.00	0.86	2.59	0.26
3	Argentina	Entre Rios	2012	2	2	2.00	0.00	0.69	2.00	1.00	NA	NA
4	Argentina	Cordoba	2012, 2013	6	4	4.00	0.00	1.33	3.60	0.94	-0.54	-0.14
5	USA	Arkansas	1985, 1986, 2001, 2012, 2014	120	82	9.26	0.85	4.10	36.18	0.59	3.38	0.31
6	USA	Illinois	1991, 2001, 2006	8	8	8.00	0.00	2.08	8.00	1.00	5.26	0.48
7	USA	Indiana	2000, 2012	50	36	9.17	0.85	3.43	24.51	0.79	1.43	0.14
8	USA	Iowa	2006	16	13	8.85	0.80	2.56	11.56	0.89	3.95	0.36
9	USA	Kansas	2012	46	17	4.79	1.34	1.73	2.62	0.35	1.03	0.12
10	USA	Michigan	2009, 2011, 2012, 2013, 2014	235	127	8.89	1.03	4.25	27.30	0.38	2.14	0.20
11	USA	Wisconsin	Unknown	2	1	1	0	0	1	NaN	NA	NA
12	USA	Missouri	2002	1	1	1	0	0	1	NaN	NA	NA
13	Canada	Ontario	2014	1	1	1	0	0	1	NaN	NA	NA
				539	333							

N, number of isolates; **MLG**, number of unique multilocus genotypes; **eMLG**, expected number of MLG, which was calculated using rarefaction; **SE**, standard error for eMLG; **H**, Shannon-Wiener index; **G**, Stoddard and Taylor's index; $\mathbf{E_5}$, MLG evenness; $\bar{r}_D$, corrected index of association.

*: Genetic summary statistic calculated using the clone-corrected data was indicated with an astrisk (*)
[a]: Statistical values that cannot be calculated given the population

Table 6-2 Analysis of molecular variance (AMOVA) of *F. virguliforme* within populations, among populations, and between continents. Sampling fields and states/provinces were labeled as populations and regions, respectively.

Dataset	Number of populations	Number of regions	% Variation						ϕ_{ST}	*P*-value [a]
			Among regions	df	Among Pops	df	Within pops	df		
US	36	8	2.17	7	7.76	27	90.07	261	0.10	0.001
Argentina	15	4	4.26	3	-[b]	-	95.74	41	0.04	0.162
Intercontinent	51	12	13.75	11	8.88	38	77.37	292	0.23	0.001

[a] *P*-value based on 1000 random sampling replicates, α=0.01
[b] Variations cannot be calculated due to lack of enough sample size for each sampling population

Population structure

The AMOVA results showed that at a continental scale, with the states/provinces representing regions, most of the variation was distributed within populations (Table 6-2, 77.37%), but a significant portion of variations were distributed among regions (13.75%, P < 0.001) and sampled fields within regions (8.88%, *P*<0.001). Within the US, 2.17% (*P*=0.186) of variation was distributed among states, 7.76% (*P*<0.001) variation was distributed among sampling sites within states, and 90.07% variation were within populations. In Argentina, most of the variations (95.74%) were distributed within populations, while a small portion of variation (4.26%, P = 0.125) was distributed among provinces. At the intercontinental scale and among US populations, high population differentiations were detected (Table 6-2, $\phi_{ST} > 0.1$, $P < 0.001$); however, no population structure was detected within Argentinean populations ($\phi_{ST} = 0.04$, $P = 0.162$).

Genetic structure and SDS spread in the United States

F-statistics results showed that the majority of sampling locations were genetically differentiated. The average G'st was 0.75 across all 12 microsatellites, and the pairwise G'st among eight states or provinces ranged from 0.05 (Michigan vs. Indiana) to 0.83 (Santa Fe vs. Indiana), which demonstrated a diverse range of population differentiation levels. UPGMA tree was constructed to group sampling populations by state or provinces based on the pairwise G'st, which resolved two major branches: US populations and Argentinean populations (Figure 6-2). The populations between two countries were significantly differentiated with G'st ranging between 0.32 and 0.83. The high G'st values estimated between US and Argentinean populations suggested a strong geographical barrier that prevents intercontinental movement of *F. virguliforme*. Within the US populations, two subgroups were revealed with the between

subgroup pairwise G'st ranged between 0.12 and 0.43, which suggested limited population movement between those two subgroups. Population differentiation within each subgroup ranged between 0.04 and 0.11, which indicated less differentiation between populations within each subgroup. However, the grouping of populations is not always based on their geographical distances. For example, the Kansas population was grouped with Indiana and Michigan populations with low pairwise population differentiation (G'st = [0.07, 0.11]).

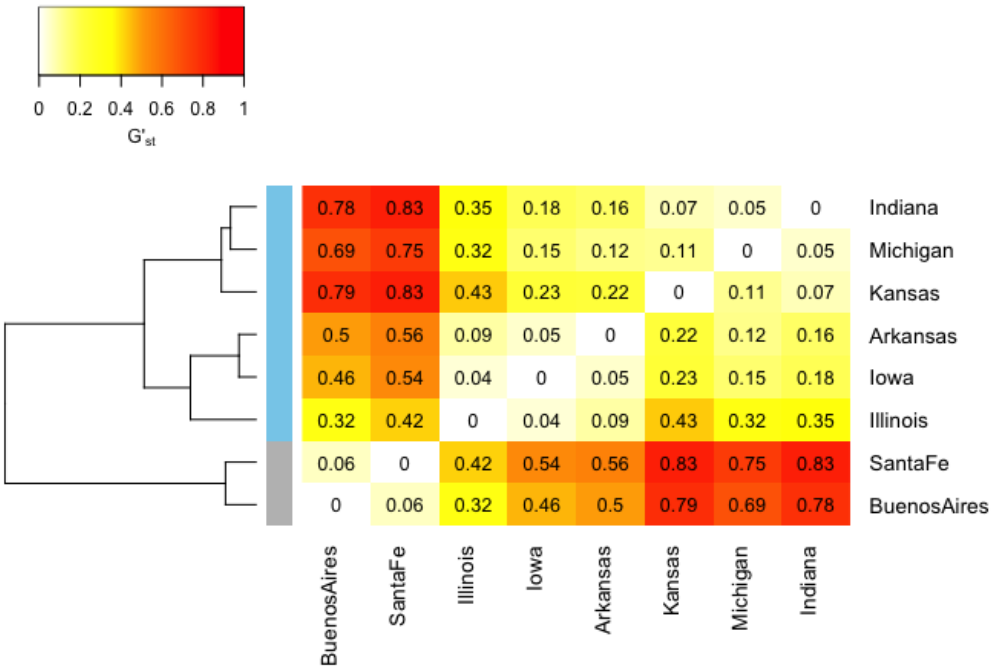

Figure 6-2 *F. virguliforme* population dendrogram and heatmap based on the pairwise G'st values among the eight *F. virguliforme* populations by state or provinces. The heatmap color gradients and dendrogram delineate two main clusters of *F. virguliforme* populations, as the US and Argentina branches. Within the US branch, two subgroups were divided based on their relative geographical locations, except for the Kansas population.

Bayesian method – STRUCTURE analysis

Population structure was investigated using the Bayesian method as implemented in STRUCTURE software. A range of clusters (K) were used to assign the ancestor memberships

using the multilocus genotypic data, there was a constant increase in the likelihood Ln(Pr(X|K)) as the number of cluster K increased from K=2 to K=7; however, after K=4, the rate of probability increase became smaller and gradually approached plateau (Figure S 6-2). The ancestor membership bar plots from K=2 to K=7 demonstrated that each new cluster added at K>4, more admixed individuals would appear in the bar plots and therefore did not correspond to the most parsimonious population structure cluster assignment. In addition, the ad hoc statistic ΔK method indicated that K=4 has the highest support (Figure S 6-2). Taken together, K=4 was the optimal cluster number that could detect the finest population structure with *F. virguliforme* multilocus genotypic data.

At K=4, a clear separation was observed between the US and Argentinean populations as most of the US isolates were assigned to three color clusters (i.e., red, green, and purple) and all Argentinean isolates were assigned to two color clusters (i.e., blue and green), except the for the Arkansas and Michigan populations that were assigned with all four color clusters (Figure 6-3). Between Michigan and Arkansas populations, Arkansas was composed of all cluster colors in a relative equal ratio of all color clusters, but Michigan population was mainly composed with green, red, and purple clusters with only a few isolates assigned to the blue cluster (Figure 6-3 and Figure S6-4). The population structure analysis showed a distinct population composition between US and Argentinean populations, and Arkansas appears to be the most diverse in population composition.

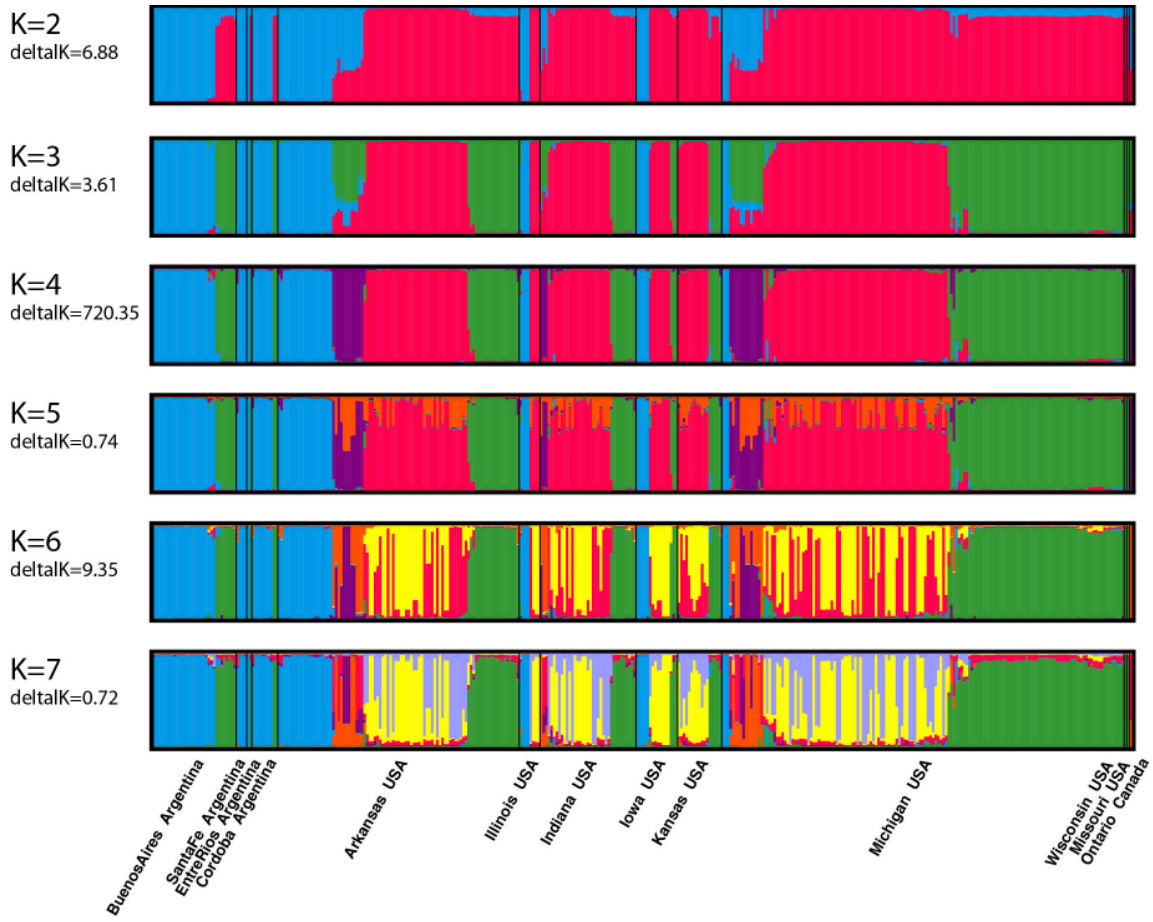

Figure 6-3 Population structure of *F. virguliforme* ancestry proportion from K=2 to K=7 clusters inferred from the STRUCTURE software. *F. virguliforme* isolates were grouped based on the source of origin to the hierarchical level of state or provinces. Each vertical bar represents an individual isolate that was partitioned into K segments indicating the proportion of assignment to the K clusters. For K=2, isolates from four provinces in Argentina, shown in blue, are distinct from most of the isolates collected in the United States, which are shown in red. For K=3, isolates from Argentina are mainly composed with two cluster, as shown in blue and green. In the US, Arkansas population has more similar population composition with the Argentinean populations, while the rest of the populations were primarily clustered into two clusters, shown as green and red. For K=4, which was the optimal K cluster as chosen based on deltaK method (Evano, 2005), isolates from Argentina still remained with two clusters composition, whereas the isolates from the US populations are mainly composed with three clusters, shown as green, red and purple. Admixed isolates are less common at K=4 clusters. With the increase of K clusters from K=5 to K=7, more admixed individuals started to appear in the US populations, but not in the Argentinean populations.

At K=7, the Argentinean populations were mainly assigned to two color clusters (blue and green) and almost none of the Argentinean isolates were in admixture, while a majority of US isolates were assigned to multiple clusters in admixed individuals. The blue cluster isolates found both in Argentina and US remained non-admixed even at K=7, which may represent a non-admixed clonal lineage of *F. virguliforme* shared between US and Argentinean populations. In addition, the green cluster appears to be non-admixed across populations from K=3 to K=5, and these green cluster individuals became admixed gradually at K>5.

The Arkansas population showed the most diverse population structure composition. The STRUCTURE analysis demonstrated a diverse population structure composition in the US and Argentina populations, suggesting that movement of *F. virguliforme* was more frequent within the US, but intercontinental movement was rare. Intercontinental movement of *F. virguliforme* was less common than pathogen movement the within the US populations, as the Argentina population possessed the most unique population composition than the US populations (Figure S6-4).

Relationships among genotypes

The minimum spanning network revealed two main groups between US and Argentinean populations, with one group mainly composed of Argentinean isolates and the other group predominantly US isolates. Within the US cluster, three subgroups were resolved into two big groups and one smaller group (Figure 6-4). Each of the two big subgroups include two of the four most abundant genotypes in the US, MLG202, MLG115, MLG110, and MLG200. Besides the US isolates, some Argentinean isolates were clustered within the subgroup containing MLG202 and MLG200 as well. Within the Argentinean cluster, no predominant MLG was found, and isolates were connected with a short genetic distance. In the whole network, the

Arkansas isolates spanned all branches in the minimum spanning network, which indicated a very high genetic diversity and composition of the Arkansas population.

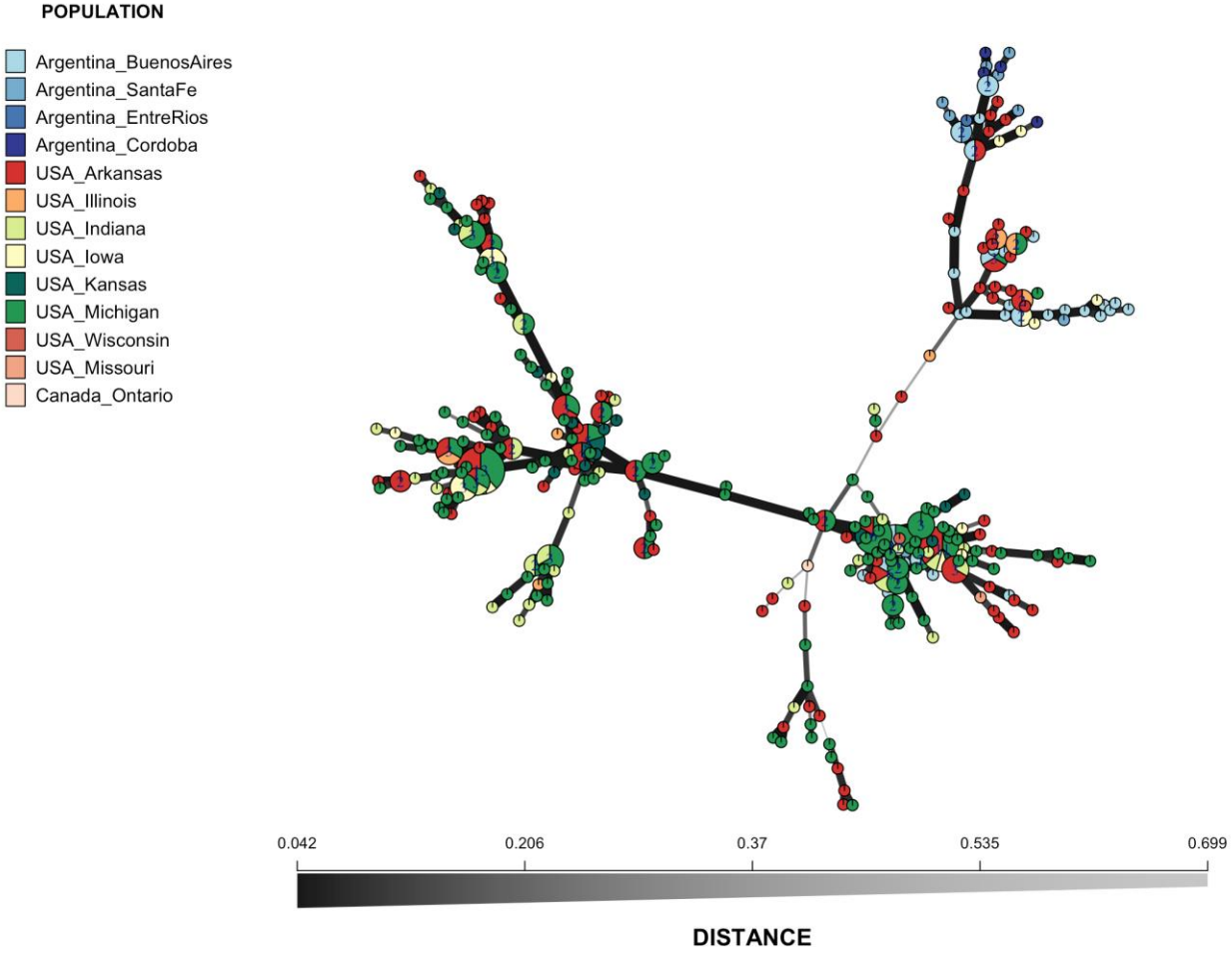

Figure 6-4 minimum spanning networks of *F. virguliforme* multilocus genotypes (MLG) based on microsatellite data. Distance between each MLG was calculated using Bruvo's genetic distance. Each node in the network represents a unique MLG. Line thickness indicates the genetic distance between MLGs, with thicker line represents closer distance, *vice versa*. MLG from different populations were labeled with different colors.

In the DAPC analysis, *F. virguliforme* isolates were colored based on their source of origin (Figure 6-5). The US and Argentinean populations were mainly separated by the first axis (X axis) in the DAPC scatter plot, and the second axis separated the different state or provincial populations within the US or Argentina. Although Argentina population cluster was differentiated from the US population clusters by the first axis, there was overlap among the Buenos Aires,

Santa Fe, Arkansas, Iowa, and Illinois populations. Furthermore, within the US cluster, the Indiana and Michigan populations were closely connected, and with small overlaps with the Kansas population. These results aligned with the finding in the population differentiation results (Figure 6-2), the placement of population clusters are the same with the pairwise population differentiation tree cluster results.

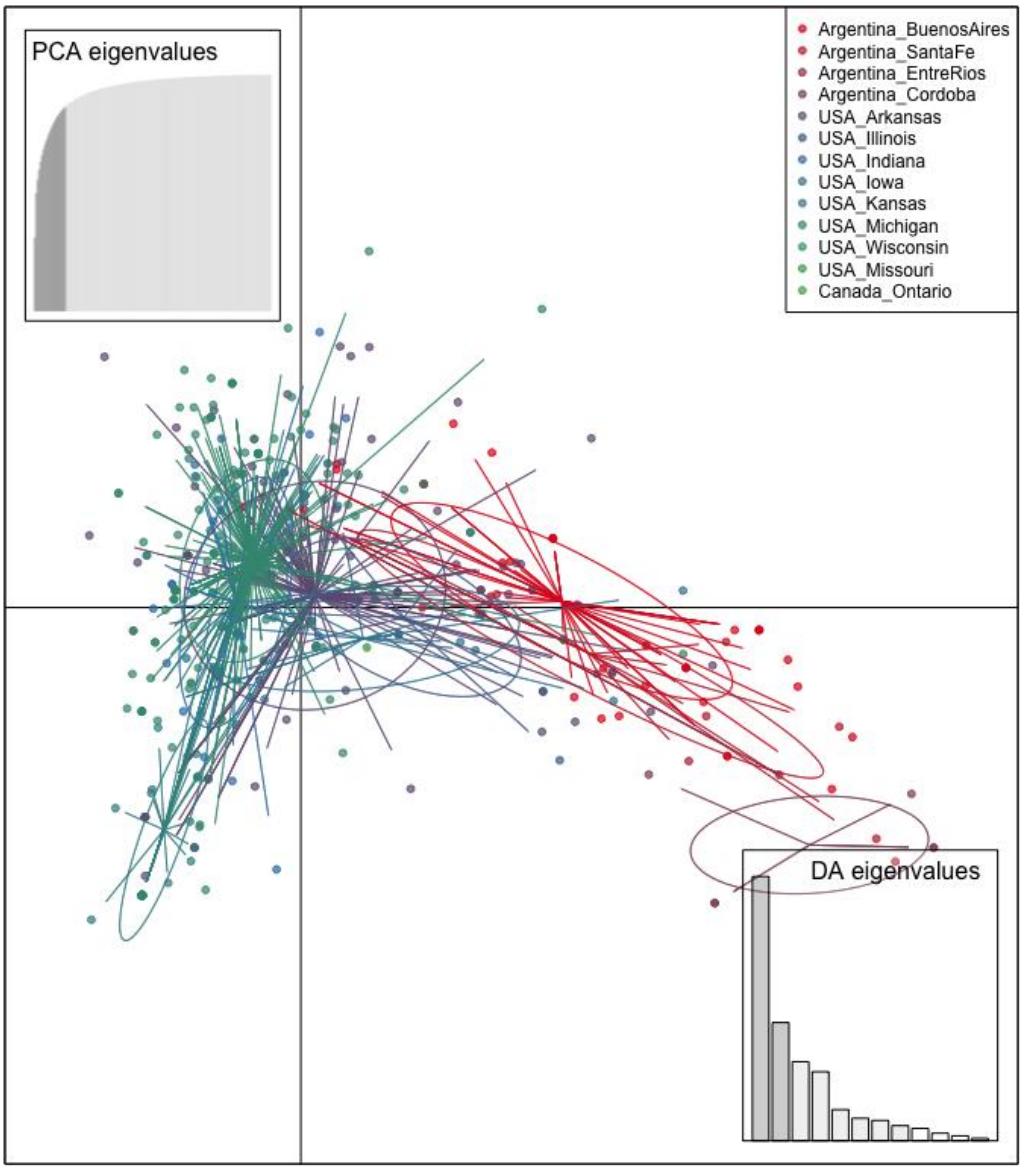

Figure 6-5 Scatter plot of the discriminant analysis of principal components of *F. virguliforme* microsatellite multilocus genotypic data. Each point represents one individual, and individual points were colored based on their source of origin as states or provinces.

Spatial correlations - isolation by distance

The Mantel test revealed non-significant correlation between geographic distance and genetic distance G'st/(1-G'st) for most of the samples collected in 2012 and 2014 in the US (Simulated *P*=0.069), although a positive correlation has been detected (y = 0.478 + 1.7*10-4, r2=0.01, Figure 6-6). Due to limited sampling size in each sampling site in Argentina, no meaningful genetic distance can be calculated among samples, thus Mantel test was not performed with Argentinean populations.

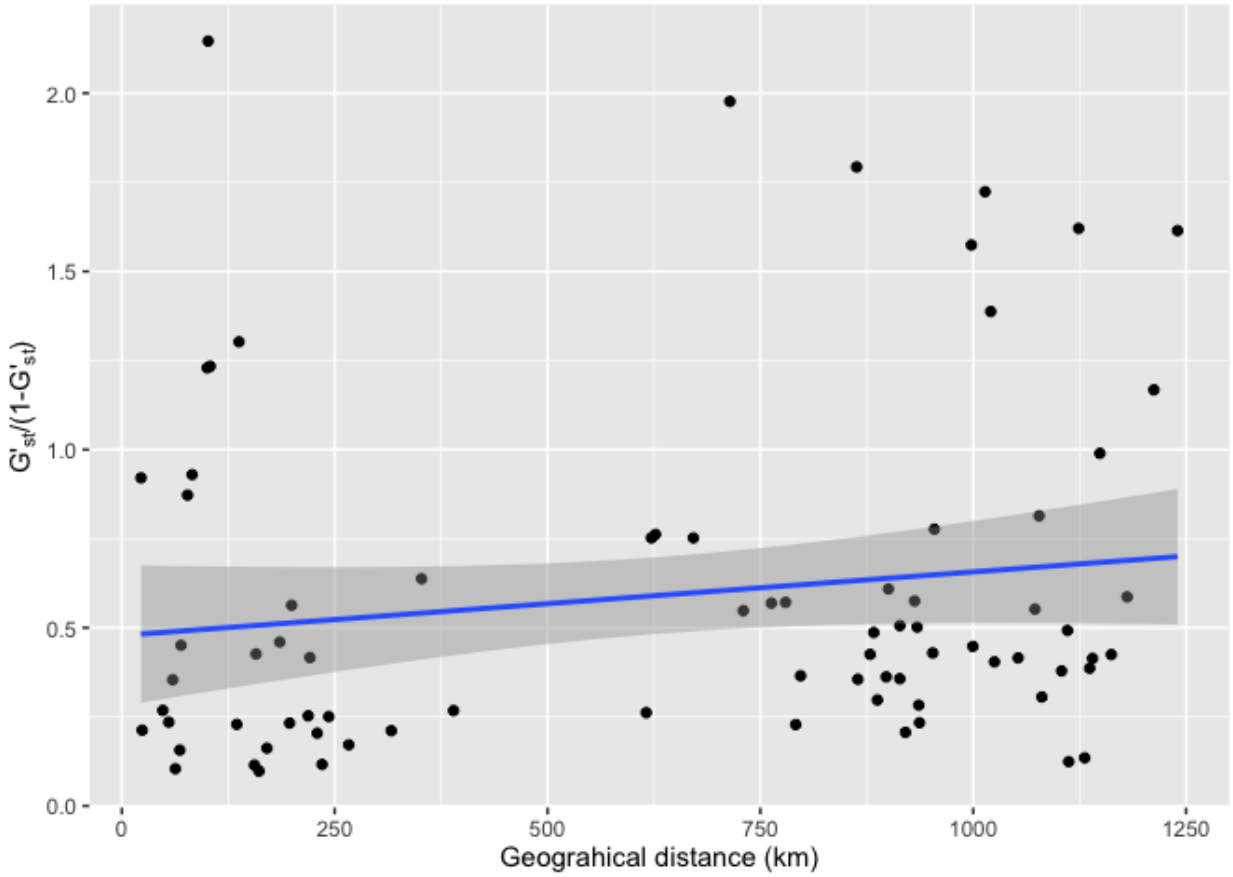

Figure 6-6 Correlation between pairwise population genetic distance (linearized Hedrick's G'st) and geographic distance (km) with linear regression line fitting, and 95% confidence interval was plot in grey. No significant correlation between genetic distance and geographical distances (*P*=0.065).

Migrate analysis

The coalescence based method implemented in software Migrate-n was used to compare different migration models (Table 6-4) and predict the parameters in migration models. Five replicated short runs with five different initial seed were used to compare different migration models listed in Table 6-3. Four out of five runs supported the model-12 that *F. virguliforme* was introduced from the Argentina to Arkansas and bidirectional movements within the US populations (i.e., migration among Arkansas, Michigan, and Indiana populations) (log marginal likelihood = -28356.55, rank=1,Table 6-3). The other one run supported the model-10 that *F. virguliforme* was introduced from the Argentina to Arkansas with unidirectional migration from Arkansas to Michigan and Indianan population, and model 12 was the second best model in the model selection. Together, the best-supported model in five replicated runs supported the unidirectional migration from Argentina to Arkansas, and uni- or bidirectional migration within the US. Consistent patterns across multiple runs provided evidences that estimations of migration models between regions were valid.

At the migration model parameter estimation, one long run (30 million sampled steps) with three replicates was sampled to predict the migration parameters: mutation scaled population size (Θ) and migration rates (M). The acceptance ratio for each predicted parameter was in a range between 0.44 and 0.49 and the single peak at all posterior distribution histograms (Figure S 6-3), suggesting that the length of chain was enough. The population size of the Argentina population was determined to be the highest (Θ = 6.730), and the population size for the Michigan and Indiana population (Θ = 1.84) was determined to be the second highest. The mutation scaled population size Θ was estimated to be 1.06 for the Arkansas population. The three migration rates (M) were determined to be: $M_{1->2}$=0.83, $M_{2->3}$=1.37, and $M_{3->2}$= 1.83 migrants per

generation, indicating long distance movements of *F. virguliforme* were less frequent for *F. virguliforme*, and it was particularly infrequent for the intercontinental migrations (Figure 6-7).

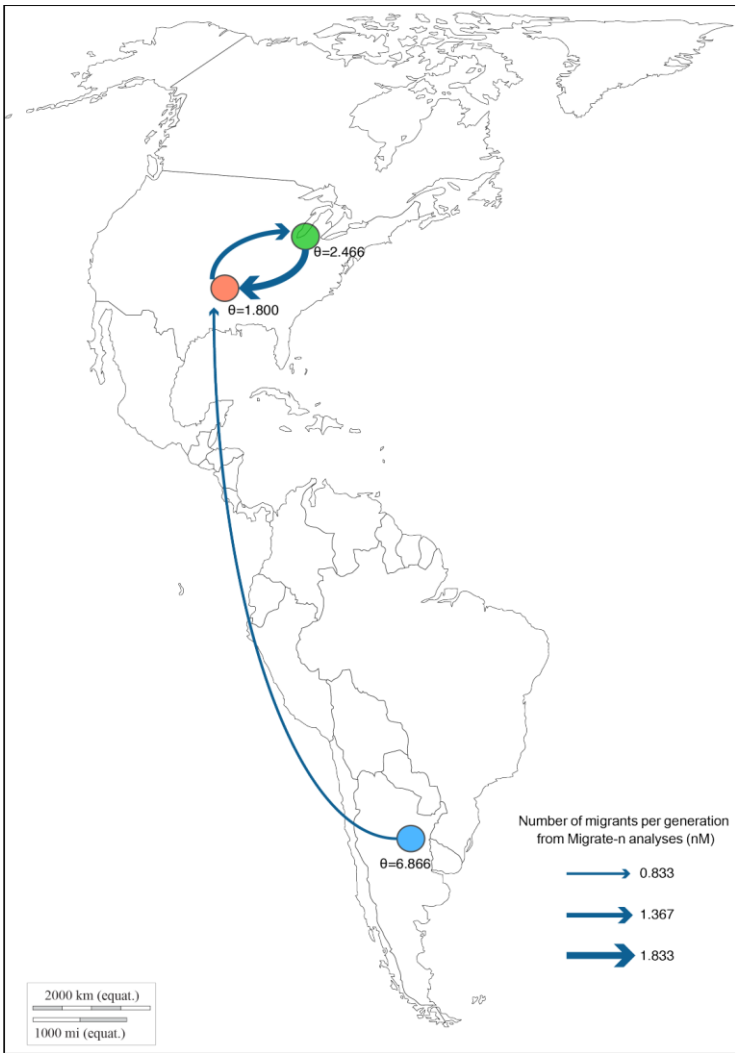

Figure 6-7 Migrate analysis with three pooled populations: 1) Argentina, 2) Arkansas, and 3) Indiana and Michigan. Arrows connecting between locations showed directional migration model as supported in the Migrate-n analysis. The line thickness represents the number of migrants per generation as descried in the legends.

Table 6-3 Migration models selection using marginal log-likelihood calculated in the coalescence method Migrate-n.

Model	Migration Model [a]	Model description	Number of parameters	Marginal log-likelihood [b]	Rank
10	N-US <-> S-US <- Arg	Argentina migrate to the US, unidirectional from Arkansas to Michigan	6	-28356.55	1
12	N-US <- S-US <- Arg	Argentina migrate to the US, bidirection migration within the US	5	-35355.2	2
9	N-US <-> S-US -> Arg	US migrate to Argentina	6	-69960.51	3
7	N-US <-> S-US <-> Arg	Stepping stone I	7	-83037.33	4
8	S-US <-> N-US <-> Arg	Stepping stone II	7	-92220.71	5
2	Full migration	N-US migrate to S-US, but isolate with Argentina	9	-145591.91	6
11	N-US -> S-US <- Arg	US migrate to the Argentina, unidirection migration from Michigan to Arkansas	5	-738770.71	7
4	N-US <- S-US | Arg	Migration within US, but isolate with Argentina	5	-1299050.74	8
3	N-US <-> S-US | Arg	N-US migrate to S-US, but isolate with Argentina	5	-1406090.29	9
5	N-US -> S-US | Arg	S-US migrate to N-US, but isolate with Argentina	4	-1510248.35	10
6	N-US | S-US | Arg	Full isolation	3	-1764858.37	11
1	Panmixia	Panmixia	1	-4890524.81	12

[a] migration scenario models. N-US represents the *F. virguliforme* populations located in Indiana and Michigan; S-US represents the *F. virguliforme* populations located in Arkansas; Arg represents the *F. virguliforme* populations located in Argentina. Dash arrow symbol (->) represents migration event and direction from one population to the other.

[b] Bezier log marginal likelihood was calculated for migration model selection. The higher likelihood, the better the model is.

Discussion

The primary goal of this study was to determine the genotypic diversity and population structure of *F. virguliforme* and to test the center of origin hypotheses. We found support for Arkansas as the origin of *F. virguliforme* within the US. Bayesian structure analysis revealed four clusters within *F. virguliforme* populations. Arkansas was the only population by state composed of all four clusters with a relatively even ratio of each cluster, demonstrating the highest population composition diversity among the US populations (Figure 6-3). Coalescence based analysis supported directional migration from Arkansas to Michigan and Indiana populations (Figure 6-7), which is consistent with the reported epidemic origin in Arkansas and spread to subsequent states (Figure 6-1). In addition, isolation by distance was not detected in the US populations, which may suggest a recent expansion of *F. virguliforme* in the US. We did not find strong support for South America as the center of origin between the North and South American continents. Although unidirectional migration from the Argentina to Arkansas population was supported in coalescence based migrate analysis, the Argentinean populations cannot explain the genotypic diversity, population structure, and genotype relationships observed in the Arkansas populations.

Arkansas is center of origin in the US

Several lines of evidence support Arkansas as the center of origin in the US. First, SDS was first reported in Arkansas in 1971, with subsequent published reports of SDS in adjacent states and continued radiation (Figure 6-1). Secondly, founder effect predicts that the newly established population should have lower genetic diversity than the population that has been stable in a given locality (Hartl *et al.* 1997). The Arkansas population demonstrated the highest genotypic diversity among populations in the US, particularly Arkansas has the highest adjusted genotypic

richness (eMLG, Table 6-1). In the population STRUCTURE analysis, four clusters were used to delineate the population structure in the US populations, and Arkansas was demonstrated to be the most diverse with assignment to all four clusters with roughly equal ratios.

Furthermore, shared genotypes across populations reveal genotype flows among populations in the US, which suggests that *F. virguliforme* populations are not isolated and migrations between populations are frequent. We detected 26 MLG shared between at least two populations in the US. The Arkansas and Michigan populations are the most distantly related populations, but 15 MLGs were shared between them. One historical isolate collected from Arkansas in 1985 genotyped to be MLG110, which is one of the top-3 most abundant genotypes in the US, and has been found in all the US populations except Kansas population. The wide distribution and historical presence of MLG110 in Arkansas may indicate that this genotype could be involved into the historical expansion of *F. virguliforme* in the US, and possibly MLG110 is one of the successful genotype adapted to multiple locations in the US. In 1985, when the Arkansas historical MLG110 isolates was collected, SDS has only been reported in the four Southern states in the US. In current populations, MLG110 has been detected in five out of six states in this study, which indicating Arkansas was the source for this genotype.

Coalescence based migrate analysis supports a bidirectional migration between Arkansas to Michigan and Indiana population using the three-population model (Pop1: Argentina, Pop2: Arkansas, and Pop3: Michigan and Indiana) (Table 6-3). The second best supported model was a uni-directional migration from Arkansas to the Michigan and Indiana population. The bidirectional migration within the US suggested the movement of *F. virguliforme* is not only from one center spread to the rest of the area, but also back movement is also possible. To simplify the migration model, we exclude the Argentinean population in the migrate analysis.

The model with one directional migration from Arkansas to the Michigan and Indiana population got the best support (Table S6-2). The mutation scaled population size of Michigan and Indiana population was determined to be higher than Arkansas, so that a higher mutation scaled migration rate from Michigan and Indiana to Arkansas was expected. This result could be caused by pooling of the Michigan and Indiana populations in the migrate analysis. The reason to pool Michigan and Indiana population was that the sampling sites in Indiana were close the south border of Michigan, so that they were merged with the Michigan population for migrate analysis. Given the evidences discussed above, the center of origin of *F. virguliforme* in the US appears to be located in Arkansas.

South America is the center of origin

Between the American continents, South America as the center of origin hypothesis was proposed and supported by through mating type gene characterization and phylogeny of the FSSC. Based on previous surveys of the SDS causing *Fusarium* species in Argentina and Brazil, the Pampas region of Argentina is the main area, where *F. virguliforme* is distributed in South America (O'Donnell *et al.* 2010; Scandiani *et al.* 2004). One *F. virguliforme* isolate used in Li et al. (2009) labeled as a Brazilian sourced isolate was proved to be erroneous (K. O'Donnell, personal communication). We included 60 Argentinean *F. virguliforme* isolates in our analysis which should provide good representation of *F. virguliforme* diversity in South America based on current knowledge of *F. virguliforme* distribution.

In our analyses, to place the center of origin in South America was supported by the coalescence based migrate analysis. The top two best-supported models both suggested a directional migration from Argentina to the Arkansas population, but the third best-supported migration model suggested an Arkansas as the center of origin migration model (Table 6-3). The

mutation scaled population size of Argentina population was significantly higher than the two US populations, but a smaller migration rates was predicted from Argentina to the Arkansas population (Figure 6-7).

STRUCTURE analysis grouped *F. virguliforme* population into four clusters. The Argentinean population showed very distinct population compositions with all the individuals assigned to either green or blue non-admixed ancestor memberships even assumed number of clusters (K) increased to K=7 (Figure 6-3). Among the US populations, the Arkansas populations demonstrated the most diverse population composition with their individual assigned with all four cluster, and the rest of the US populations were mainly composed with red, green, and purple clusters. Apart from the Arkansas and part of Michigan isolates shared the blue cluster with the Argentinean populations, no purple or red clusters were present in the Argentina populations. If the South America center of origin hypothesis is true, it cannot explain the genetic structure composition of the red and purple clusters.

Furthermore, the relationship among genotypes in the minimum spanning network demonstrated a clear separation between the Argentinean genotypes with the US population genotypes, with almost all Argentinean genotypes grouped within one branch. The Arkansas population genotypes have been found in all four branches in the network, indicating a diverse distribution of Arkansas genotypes. MLG202 was determined to the most abundant genotype in both Argentina and US populations, and this genotype is located in the center of the minimum spanning network connecting to the Argentina population. Also lots of similar genotypes with short genetic distance were clustered next to MLG202, suggesting this genotype and its associated genotypes may represent a distinct lineage of *F. virguliforme* shared between US and

Argentina. No genotypes from the other two branches of the US populations shared genotypes with the Argentinean population.

In conclusion, Argentina as the center or origin hypothesis is merely supported by the coalescence based migrate analysis, but the genotypic diversity and population structure detected in the US populations cannot be explained by this hypothesis. Also, the sampling efforts in North America and South America were not equal, which could limit the power to test the South America as the center of origin hypothesis.

Means of pathogen dispersal

Mixed patterns of pathogen dispersal have been observed with *F. virguliforme* populations in the US. The soilborne pathogen *F. virguliforme* was thought to have limited dispersal range, and movement of the pathogen been associated with the movement of infested soil or plant materials. However, shipment of plant materials or transportation of farm equipment may facilitate the long distance movement of plant pathogens. The population pairwise G'st analysis indicates that geographically distant populations tend to be more differentiated (Figure 6-2); however, exception was observed with the Kansas population that was grouped with the Michigan and Indiana populations. This exception in the pairwise population differentiation index and geographical distance suggested a rapid and recent expansion of *F. virguliforme* in the Kansas population (Excoffier *et al.* 2009). This result aligns with the low genotypic diversity and high clonal rate (1-MLG/N) detected in the Kansas population, due to founder effect (Table 6-1). In addition, a weak correlation between genetic distance and geographic distance was determined in a Mantel test, suggesting the population structure cannot be explained by isolation by distance (Figure 6-6). Albeit the correlation between genetic dissimilarity and geographical distance was not significant, a positive slope for the linear regression was obtained and some of the data points

fall within the confidence interval of the regression line (Figure 6-6), which indicate that population expansions among some populations can be explained using isolation by distance. Therefore, a mixed means of population expansion was detected for *F. virguliforme* in the US.

Acknowledgement

We gratefully acknowledge Kerry O'Donnell from USDA-ARS for providing isolates from Argentina, John Rupe from University of Arkansas for assisting with sample collections and provided historical isolates, Doug Jardine of Kansas State University, Kiersten Wise and Nolan Anderson of Purdue University for helping with sample collections, Leandro Leonor from Iowa State University for providing Iowa isolates, and NRRL for providing isolates.

Data accessibility

All data and R script for population genetic analysis are accessible on github (https://github.com/wjidea/PopGenFvSSR). All 12 microsatellite sequences were submitted to NCBI Genbank with reference numbers: KR476359-KR476370.

APPENDICES

APPENDIX A Supplementary tables

Table S 6-1 Shared genotypes between historical *F. virguliforme* isolates from Arkansas and current isolates. Of 13 historical *F. virguliforme* isolates, 13 unique MLGs were identified. In current populations, three MLGs were found to be identical with the historical isolates recovered from year 1985. MLG 110 was the most predominant shared genotype across a wide range of current geographic distributions.

Historical isolates					Current populations (from 2012-2014)						
ID	Year of collection	Sources	Field locations	MLG [a]	Arkansas	Kansas	Illinois	Indiana	Iowa	Michigan	Total
JR-4	1985	Arkansas	Pine Tree	4	-	-	-	-	-	-	-
JR-8	1985	Arkansas	Pine Tree	13	-	-	-	-	-	-	-
JR-16	1985	Arkansas	Pine Tree	37	-	-	-	-	-	-	-
JR-18	1985	Arkansas	Pine Tree	51	1	1	-	-	-	-	2
JR-7	1985	Arkansas	Pine Tree	52	-	-	-	-	-	1	1
JR-12	1985	Arkansas	Pine Tree	53	-	-	-	-	-	-	-
JR-1b	1985	Arkansas	St. Charles	110	12	-	1	6	1	16	36
JR-9	1985	Arkansas	Pine Tree	118	-	-	-	-	-	-	-
JR-14	1985	Arkansas	Pine Tree	122	-	-	-	-	-	-	-
JR-11	1985	Arkansas	Pine Tree	147	-	-	-	-	-	-	-
JR-10	1985	Arkansas	Pine Tree	155	-	-	-	-	-	-	-
JR-13	1985	Arkansas	Pine Tree	233	-	-	-	-	-	-	-
JR-197	1986	Arkansas	Pine Tree	269	-	-	-	-	-	-	-

[a] MLG, Multilocus genotypes.

Table S 6-2 Simplified migration models selection using marginal log-likelihood calculated in the coalescence method Migrate-n.

Migration Model [a]	Model description	Number of parameters	Marginal log-likelihood [b]	Rank
N-US <- S-US	S-US migrate to N-US	3	-45357.21	1
N-US -> S-US	N-US migrate to S-US	3	-47125.66	2
Panmix	Panmixia	1	-72551.19	3
N-US <-> S-US	Full Migration	4	-164591.91	4

APPENDIX B Supplementary figures

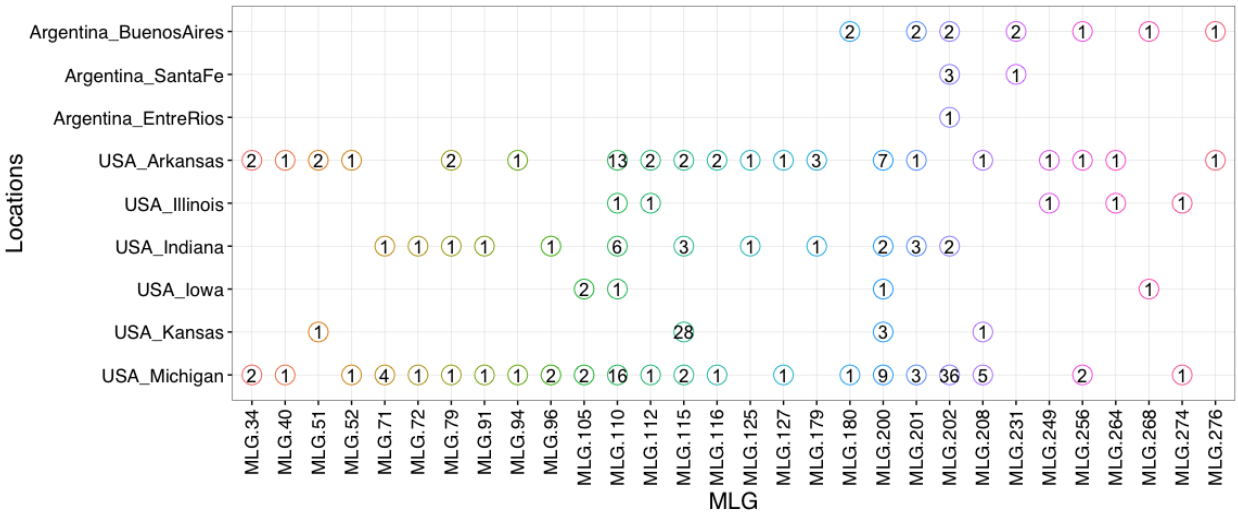

Figure S 6-1 Shared multilocus genotypes (MLG) among populations by state/provinces within countries.

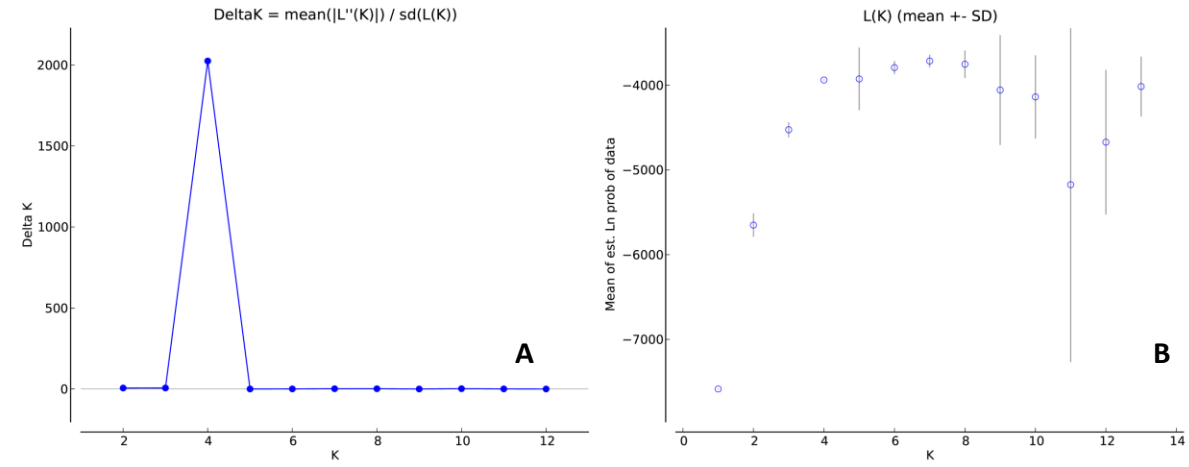

Figure S 6-2 In STRUCTURE analysis, determination of optimal K for clustering individuals for each assigned populations. (A) log likelihood values of delta K against a range of K values. (B) The mean likelihood values calculated under varying K values, from K=2 to K=13.

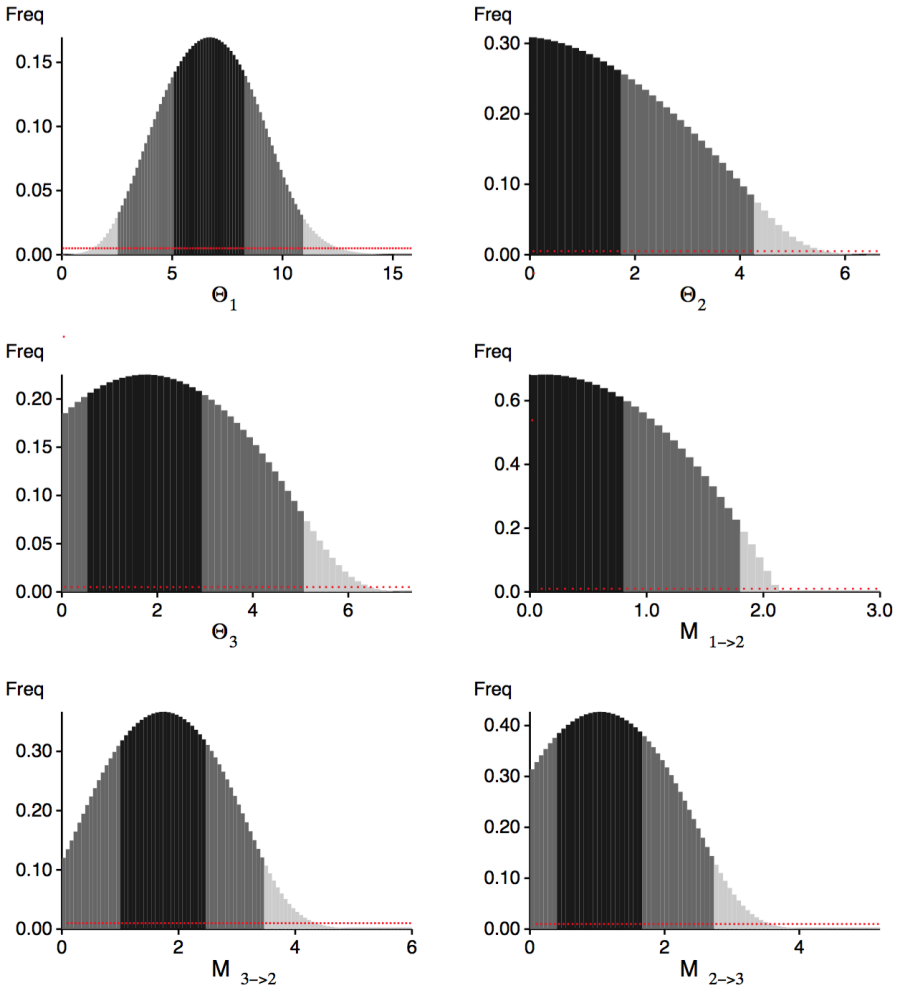

Figure S 6-3 Histogram of posterior distribution of parameter estimation in migrate analysis. Θ is the mutation scaled population size and M is mutation scale migration rates (migrants per generation).

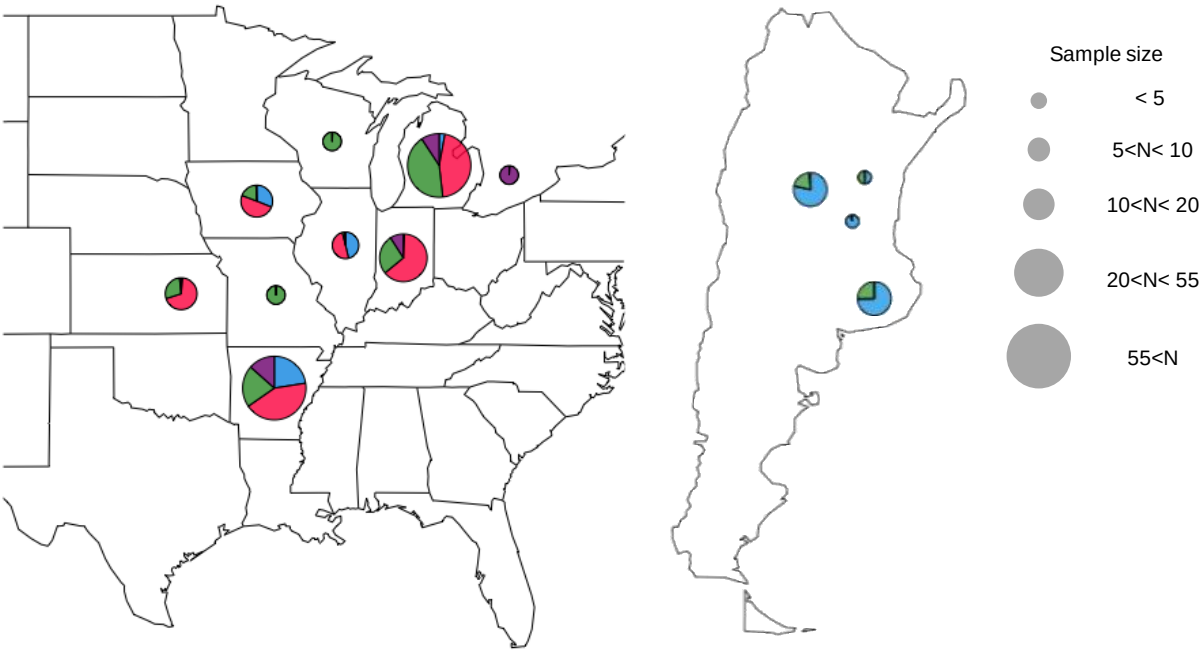

Figure S 6-4 Geographical distribution of *F. virguliforme* sample locations in Midwest - United States, Ontario - Canada, and Pampas area in Argentina. Pie chart on the map represents the population composition based on STRUCTURE analysis ancestry membership assignment (K=4). Argentinean populations are mainly composed with blue and green clusters, while the US and Canadian populations were primarily composed of red and green clusters. The Arkansas population composed with four color-clusters, with each cluster contains at least 10%.

REFERENCES

REFERENCES

Agapow PM, Burt A (2001) Indices of multilocus linkage disequilibrium. *Molecular Ecology Notes* **1**, 101-102.

Amos W, Hoffman JI, Frodsham A, *et al.* (2007) Automated binning of microsatellite alleles: problems and solutions. *Molecular Ecology Notes* **7**, 10-14.

Aoki T, O'Donnell K, Geiser DM (2014) Systematics of key phytopathogenic *Fusarium* species: current status and future challenges. *Journal of General Plant Pathology* **80**, 189-201.

Aoki T, O'Donnell K, Homma Y, Lattanzi AR (2003) Sudden-death syndrome of soybean is caused by two morphologically and phylogenetically distinct species within the *Fusarium solani* species complex— *F. virguliforme* in North America and *F. tucumaniae* in South America. *Mycologia* **95**, 660-684.

Aoki T, O'Donnell K, Scandiani MM (2005) Sudden death syndrome of soybean in South America is caused by four species of *Fusarium*: *Fusarium brasiliense* sp. nov., *F. cuneirostrum* sp. nov., *F. tucumaniae*, and *F. virguliforme*. *Mycoscience* **46**, 162-183.

Aoki T, Scandiani MM, O'Donnell K (2012) Phenotypic, molecular phylogenetic, and pathogenetic characterization of *Fusarium crassistipitatum* sp. nov., a novel soybean sudden death syndrome pathogen from Argentina and Brazil. *Mycoscience* **53**, 167-186.

Arnaud-Haond S, Duarte CM, Alberto F, Serrao EA (2007) Standardizing methods to address clonality in population studies. *Molecular Ecology* **16**, 5115-5139.

Beerli P (2006) Comparison of Bayesian and maximum-likelihood inference of population genetic parameters. *Bioinformatics* **22**, 341-345.

Beerli P, Felsenstein J (2001) Maximum likelihood estimation of a migration matrix and effective population sizes in n subpopulations by using a coalescent approach. *Proceedings of the National Academy of Sciences of the United States of America* **98**, 4563-4568.

Beerli P, Palczewski M (2010) Unified framework to evaluate panmixia and migration direction among multiple sampling locations. *Genetics* **185**, 313-U463.

Bernstein ER, Atallah ZK, Koval NC, Hudelson BD, Grau CR (2007) First report of sudden death syndrome of soybean in Wisconsin. *Plant Disease* **91**, 1201-1201.

Brzostowski L, Schapaugh W, Rzodkiewicz P, Todd T, Little C (2014) Effect of host resistance to *Fusarium virguliforme* and *Heterodera glycines* on sudden death syndrome disease severity and soybean yield. *Plant Health Progress* **15**, 1.

Chehri K (2015) First report on *Fusarium virguliforme* in Persian Gulf Beach soils. *Journal of Mycology Research* **2**, 55-61.

Chehri K, Salleh B, Zakaria L (2014) *Fusarium virguliforme*, a soybean sudden death syndrome fungus in Malaysian soil. *Australasian Plant Disease Notes* **9**, 1-7.

Chilvers MI, Brown-Rytlewski DE (2010) First report and confirmed distribution of soybean sudden death syndrome caused by *Fusarium virguliforme* in southern Michigan. *Plant Disease* **94**, 1164-1164.

Covert SF, Aoki T, O'Donnell K, *et al.* (2007) Sexual reproduction in the soybean sudden death syndrome pathogen *Fusarium tucumaniae*. *Fungal Genet Biol* **44**, 799-807.

Dray S, Dufour AB (2007) The ade4 package: Implementing the duality diagram for ecologists. *Journal of Statistical Software* **22**, 1-20.

Earl DA, Vonholdt BM (2012) STRUCTURE HARVESTER: a website and program for visualizing STRUCTURE output and implementing the Evanno method. *Conservation Genetics Resources* **4**, 359-361.

Evanno G, Regnaut S, Goudet J (2005) Detecting the number of clusters of individuals using the software STRUCTURE: a simulation study. *Molecular Ecology* **14**, 2611-2620.

Excoffier L, Foll M, Petit RJ (2009) Genetic Consequences of Range Expansions. *Annual Review of Ecology, Evolution, and Systematics* **40**, 481-501.

Excoffier L, Smouse PE, Quattro JM (1992) Analysis of molecular variance inferred from metric distances among dna haplotypes - application to human mitochondrial-DNA restriction data. *Genetics* **131**, 479-491.

Gaut BS (2014) The complex domestication history of the common bean. *Nature Genetics* **46**, 663-664.

Grunwald NJ, Goodwin SB, Milgroom MG, Fry WE (2003) Analysis of genotypic diversity data for populations of microorganisms. *Phytopathology* **93**, 738-746.

Hartl DL, Clark AG, Clark AG (1997) *Principles of population genetics* Sinauer associates Sunderland.

Hartman GL, Noel GR, Gray LE (1995) Occurrence of soybean sudden-death syndrome in east-central Illinois and associated yield losses. *Plant Disease* **79**, 314-318.

Hartman GL, Sinclair JB, Rupe JC (1999) *Compendium of soybean diseases* American Phytopathological Society (APS Press).

Hedrick PW (2005) A standardized genetic differentiation measure. *Evolution* **59**, 1633-1638.

Hirrel M (1983) Sudden-death syndrome of soybean-a disease of unknown etiology. *Phytopathology* **73**, 501-502.

Hughes TJ, O'Donnell K, Sink S, *et al.* (2014) Genetic architecture and evolution of the mating type locus in fusaria that cause soybean sudden death syndrome and bean root rot. *Mycologia* **106**, 686-697.

Hymowitz T (2004) Speciation and cytogenetics. *Soybeans: Improvement, production, and uses*, 97-136.

Jakobsson M, Rosenberg NA (2007) CLUMPP: a cluster matching and permutation program for dealing with label switching and multimodality in analysis of population structure. *Bioinformatics* **23**, 1801-1806.

Jombart T, Devillard S, Balloux F (2010) Discriminant analysis of principal components: a new method for the analysis of genetically structured populations. *Bmc Genetics* **11**.

Kamvar ZN, Tabima JF, Grünwald NJ (2014) Poppr: an R package for genetic analysis of populations with clonal, partially clonal, and/or sexual reproduction. *PeerJ* **2**, e281.

Kurle J, Gould S, Lewandowski S, Li S, Yang X (2003) First report of sudden death syndrome (*Fusarium solani* f. sp. *glycines*) of soybean in Minnesota. *Plant Disease* **87**, 449-449.

Li S., Hartman G.L., Chen Y. (2009) Evaluation of aggressiveness of *Fusarium virguliforme* isolates that cause soybean sudden death. *Journal of Plant Pathology* **91**, 77-86.

Ma LJ, Geiser DM, Proctor RH, *et al.* (2013) Fusarium pathogenomics. *Annu Rev Microbiol* **67**, 399-416.

Malvick DK, Bussey KE (2008) Comparative analysis and characterization of the soybean sudden death syndrome pathogen *Fusarium virguliforme* in the northern United States. *Canadian Journal of Plant Pathology* **30**, 467-476.

Matschiner M, Salzburger W (2009) TANDEM: integrating automated allele binning into genetics and genomics workflows. *Bioinformatics* **25**, 1982-1983.

Mbofung G, Harrington TC, Steimel JT, *et al.* (2012) Genetic structure and variation in aggressiveness in *Fusarium virguliforme* in the Midwest United States. *Canadian Journal of Plant Pathology* **34**, 83-97.

McDonald BA (1997) The population genetics of fungi: tools and techniques. *Phytopathology* **87**, 448-453.

McDonald BA, Linde C (2002) The population genetics of plant pathogens and breeding strategies for durable resistance. *Euphytica* **124**, 163-180.

Nakajima T, Mitsueda T, Charchar M (1993) Occurrence of soybean sudden-death syndrome caused by Fusarium solani in Brazil, P79.

Njambere EN, Peever TL, Vandemark G, Chen W (2014) Genotypic variation and population structure of *Sclerotinia trifoliorum* infecting chickpea in California. *Plant Pathology* **63**, 994-1004.

O'Donnell K (2000) Molecular phylogeny of the *Nectria haematococca-Fusarium solani* species complex. *Mycologia* **92**, 919-938.

O'Donnell K, Rooney AP, Proctor RH, *et al.* (2013) Phylogenetic analyses of RPB1 and RPB2 support a middle Cretaceous origin for a clade comprising all agriculturally and medically important fusaria. *Fungal Genet Biol* **52**, 20-31.

O'Donnell K, Sink S, Scandiani MM, *et al.* (2010) Soybean sudden death syndrome species diversity within North and South america revealed by multilocus genotyping. *Phytopathology* **100**, 58-71.

OHara R, Simpson G, Solymos P, Stevens M, Wagner H (2012) Vegan: community ecology package. R package version 2.0-2.

Paradis E, Claude J, Strimmer K (2004) APE: analyses of phylogenetics and evolution in R language. *Bioinformatics* **20**, 289-290.

Penner G, Bush A, Wise R, *et al.* (1993) Reproducibility of random amplified polymorphic DNA (RAPD) analysis among laboratories. *Genome Research* **2**, 341-345.

Pennypacker BW (1999) First report of sudden death syndrome caused by *Fusarium solani* f. sp. *glycines* on soybean in Pennsylvania. *Plant Disease* **83**, 879-879.

Ploper D (1993) Síndrome de la muerte súbita: Nueva enfermedad de la soja en el noroeste argentino. *Avance Agroindustrial* **13**, 5-9.

Pritchard JK, Stephens M, Donnelly P (2000) Inference of population structure using multilocus genotype data. *Genetics* **155**, 945-959.

Rosenberg NA (2004) DISTRUCT: a program for the graphical display of population structure. *Molecular Ecology Notes* **4**, 137-138.

Roy KW, Hershman DE, Rupe JC, Abney TS (1997) Sudden death syndrome of soybean. *Plant Disease* **81**, 1100-1111.

Rupe JC (1989) Frequency and pathogenicity of *Fusarium solani* recovered from soybeans with sudden death syndrome. *Plant Disease* **73**, 581-584.

Scandiani M, Ruberti D, O'Donnell K, *et al.* (2004) Recent outbreak of soybean sudden death syndrome caused by *Fusarium virguliforme* and *F. tucumaniae* in Argentina. *Plant Disease* **88**, 1044-1044.

Stukenbrock EH, Bataillon T (2012) A population genomics perspective on the emergence and adaptation of new plant pathogens in agro-ecosystems. *PLoS Pathogens* **8**.

Stukenbrock EH, McDonald BA (2008) The origins of plant pathogens in agro-ecosystems. *Annual Review of Phytopathology* **46**, 75-100.

Tande C, Hadi B, Chowdhury R, Subramanian S, Byamukama E (2014) First report of sudden death syndrome of soybean caused by *Fusarium virguliforme* in South Dakota. *Plant Disease* **98**, 1012-1012.

Tewoldemedhin YT, Lamprecht SC, Geldenhuys JJ, Kloppers FJ (2013) First report of soybean sudden death syndrome caused by *Fusarium virguliforme* in South Africa. *Plant Disease* **98**, 569-569.

Travadon R, Sache I, Dutech C, *et al.* (2011) Absence of isolation by distance patterns at the regional scale in the fungal plant pathogen *Leptosphaeria maculans*. *Fungal biology* **115**, 649-659.

Wang J, Chilvers MI (2016) Development and characterization of microsatellite markers for *Fusarium virguliforme* and their utility within clade 2 of the *Fusarium solani* species complex. *Fungal Ecology* **20**, 7-14.

Wang J, Jacobs JL, Byrne JM, Chilvers MI (2015) Improved diagnoses and quantification of *Fusarium virguliforme*, causal agent of soybean sudden death syndrome. *Phytopathology* **105**, 378-387.

Warnes GR, Bolker B, Bonebakker L, *et al.* (2009) gplots: Various R programming tools for plotting data. *R package version* **2**.

Winter DJ (2012) MMOD: an R library for the calculation of population differentiation statistics. *Molecular Ecology Resources* **12**, 1158-1160.

Wrather J, Koenning S (2009) Effects of diseases on soybean yields in the United States 1996 to 2007. *Plant Health Progress*.

Yu G, Lam TT-Y (2016) ggtree: a phylogenetic tree viewer for different types of tree annotations. *Methods in Ecology and Evolution* **Submitted**.

Ziems AD, Giesler LJ, Yuen GY (2006) First report of sudden death syndrome of soybean caused by *Fusarium solani* f. sp *glycines* in Nebraska. *Plant Disease* **90**, 109-109.

CONCLUSION AND FUTURE DIRECTIONS

Summary of dissertation

Soybean sudden death syndrome (SDS) is one of the biggest concerns for American soybean growers. *Fusarium virguliforme* is the only known SDS causal pathogen in the US, however there are multiple closely causal species identified in South America. The surviving propagules of *F. virguliforme*, macroconidia and chlamydospores, can be viable in soil for an extended period of time. In addition, *F. virguliforme* can colonize several plant species that are commonly present or rotated in soybean fields, including corn. Therefore, it is very difficult to reduce *F. virguliforme* inoculum, once a field is infested. The primary SDS disease management strategy is the use of soybean cultivars that are partially resistant to SDS foliar symptoms. **Chapter 1** is a review of the literature with respect to *Fusarium virguliforme*.

In **chapter 2**, a quantitate real-time (qPCR) assay is described for the detection and quantification of *F. virguliforme* from plant and soil samples. The assay was designed to target the rDNA IGS region, which has been demonstrated to differentiate *F. virguliforme* from closely related *Fusarium* species in a phylogenetic study. The target of this qPCR assay contains multiple copies in the *F. virguliforme* genome, which significantly increases assay detection sensitivity, when compared to a single copy target. The assay was validated on two real-time PCR thermal cycler platforms, demonstrating similar detection sensitivity and specificity. The qPCR assay has been adopted by multiple labs and applied in routine SDS disease diagnostics and research projects. In the future, the qPCR assay may be used to make association between *F. virguliforme* propagule density in soil prior to planting, so that soybean growers can make timely SDS disease management decisions.

In **chapter 3**, the qPCR assay was utilized to study the temporal dynamics of *F. virguliforme* colonization of soybean roots. Previously the association between SDS foliar symptom severity

and *F. virguliforme* root colonization was not clear. To address this issue, soybean roots from four soybean cultivars were sampled at nine time points throughout the season to quantify *F. virguliforme* quantity in soybean root. Despite significant differences in SDS foliar symptoms among cultivars, the quantities of *F. virguliforme* in roots were not significantly different. Indicating that SDS foliar symptom severity is not only driven by *F. virguliforme* quantities in roots, and suggests the planting partially resistant varieties that demonstrate no foliar symptoms may not be managing *F. virguliforme* inoculum levels in the field. In addition, quantification of *F. virguliforme* in soybean roots provided a quantitative phenotype to screen soybean lines for resistance to *F. virguliforme* root colonization.

In **chapter 4**, the in-vitro sensitivity of *F. virguliforme* isolates to the SDHI fungicide fluopyram was investigated. Fluopyram has demonstrated in reducing SDS foliar symptoms in field trials, but the *in vitro* efficacy to inhibit mycelia growth had not been evaluated. In this study, 185 *F. virguliforme* isolates collected from multiple locations in the US were tested against the fungicide fluopyram in a poison plate assay. Most *F. virguliforme* isolates (>95%) appear to be sensitive to fluopyram, but eight isolates were determined to be less sensitive to fluopyram in the poison plate assay.

In **chapter 5**, a set of microsatellite markers were developed to detect genetic diversity within *F. virguliforme*. Previous studies using standard loci for phylogeny studies could not resolve genetic diversity within *F. virguliforme*, and they proposed *F. virguliforme* in the US belong to one clonal lineage. In this study, a set of robust microsatellite markers were developed to measure genetic diversity within *F. virguliforme*. The markers were demonstrated to be polymorphic and informative through validation with a set of *F. virguliforme* isolates collected from Michigan.

After the first report of SDS in Arkansas in 1971, SDS has subsequently been confirmed in surrounding states with an apparent spread from Arkansas. It had also been proposed that the center of origin for *F. virguliforme* was South America, given that *F. virguliforme* and multiple closely related species causing SDS had been found in the continent. However, the hypothesis of *F. virguliforme* origin in the US and inter-continental had not been tested. In **chapter 6**, *F. virguliforme* isolates were collected from multiple states in the US and from Argentina in South American to test the center of *F. virguliforme* center of origin hypothesis. A total of 539 *F. virguliforme* isolates were recovered and genotyped. High genotypic diversity and diverse population structure was observed in Arkansas, which supported the hypothesis that Arkansas is the center of origin in the US. The distribution of *F. virguliforme* in the US was not in isolation by distance as detected in a Mantel test, suggesting a rapid and recent expansion of *F. virguliforme* in the US. The hypothesis of South America as the center was supported by the coalescence based migrate analysis; however, the highest genotypic diversity and population structure diversity was detected in Arkansas. Therefore, the South America as the center of origin hypothesis is not clear. Additional sampling effort in South America particularly outside of Argentina is needed to further test South America as the center of origin hypothesis.